Bechtel Nevada

DOE/NV/11718-160

ANALYSIS OF FRACTURES IN VOLCANIC CORES FROM PAHUTE MESA, NEVADA TEST SITE

by

Sigmund L. Drellack, Jr. and Lance B. Prothro, Bechtel Nevada
Keith E. Roberson, IT Corportation
Brad A. Schier, Daniel B. Stevens and Associates
Edwin H. Price, HSI GeoTrans, Inc.

September 1997

Prepared for the
U. S. Department of Energy, Nevada Operations Office
Under Contract No. DE-AC08-96NV11718

DISCLAIMER

Table of Contents

Table of Contents (Continued)

Table of Contents (Continued)

Table of Contents *(Continued)*

List of Figures

List of Figures *(Continued)*

List of Figures *(Continued)*

List of Tables

List of Acronyms and Abbreviations

BAQ	Basal Aquifer
BCU	Basal Confining Unit
BHTV	Borehole televiewer
BN	Bechtel Nevada
CAU	Corrective Action Unit
DOE/NV	U.S. Department of Energy, Nevada Operations Office
Fe/Mn	Iron and Manganese oxides
FMS	Formation MicroScanner™
ft	Foot (feet)
gpm	Gallon(s) per minute
gpm/ft	Gallon(s) per minute per foot
HGU	Hydrogeologic unit(s)
HRMP	Hydrologic Radionuclide Monitoring Program
HSU	Hydrostratigraphic unit(s)
ID	Identify
in.	Inch(es)
IT	International Technology Corporation
km	Kilometer(s)
LFA	Lava-flow aquifer
m	Meter(s)
mm	millimeter(s)
NTS	Nevada Test Site
TBA	Belted Range Aquifer
TC	Tuff Cone
TCB	Bullfrog Confining Unit
TCU	Tuff confining unit
TD	Total depth
TMA	Timber Mountain Aquifer
UGTA	Underground Test Area
USGS	U.S. Geological Survey
VTA	Vitric-tuff aquifer
WTA	Welded-tuff aquifer
YMP	Yucca Mountain Project

This Page Intentionally Left Blank.

1.0 Introduction

The Nevada Test Site (NTS), located in Nye County, southern Nevada, was the location of 828 announced underground nuclear tests, conducted between 1951 and 1992 (DOE, 1994). Approximately one-third of these tests were detonated near or below the water table (Laczniak *et al.*, 1996). An unavoidable consequence of these testing activities was introducing radionuclides into the subsurface environment, impacting groundwater. Groundwater flows beneath the NTS almost exclusively through interconnected natural fractures in carbonate and volcanic rocks (Blankennagle and Weir, 1973; GeoTrans, 1995). Information about these fractures is necessary to determine hydrologic parameters for future Corrective Action Unit (CAU)-specific flow and transport models which will be used to support risk assessment calculations for the U.S. Department of Energy, Nevada Operations Office (DOE/NV) Underground Test Area (UGTA) remedial investigation. Fracture data are critical in reducing the uncertainty of the predictive capabilities of CAU-specific models because of their usefulness in generating hydraulic conductivity values and dispersion characteristics used in transport modeling. Specifically, fracture aperture and density (spacing) are needed to calculate the permeability anisotropy of the formations. Fracture mineralogy information is used qualitatively to evaluate diffusion and radionuclide retardation potential in transport modeling. All these data can best be collected through examination of core samples.

1.1 Project Description

1.1.1 Scope of Investigation

Fracture data from cores collected from eight drill holes in the Pahute Mesa/Timber Mountain area are presented in this report. Fracture analyses were performed on two continuous cores from drill holes UE-18t and UE-19x and core segments from six other drill holes (UE-18r, U-20c, UE-20c, UE-20e#1, UE-20f, and UE-20bh#1). Also, fracture analyses using borehole televiewer (BHTV) and Formation MicroScanner™ (FMS) data were performed on four wells (UE-18r, UE-20bh#1, ER-20-2#1, and ER-20-5#1), two of which (ER-20-2#1 and ER-20-5#1) were not cored. The locations of these wells on the NTS is shown in Figure 1-1. The data analyzed relate to several attributes of the fractures, including distribution, density, aperture, openness, roughness, orientation, and fracture-lining mineralogy. These attributes have been compared against hydrogeology and hydrostratigraphy, and the resulting information can be used to generate values for hydrologic model inputs such as hydraulic conductivity and radionuclide retardation.

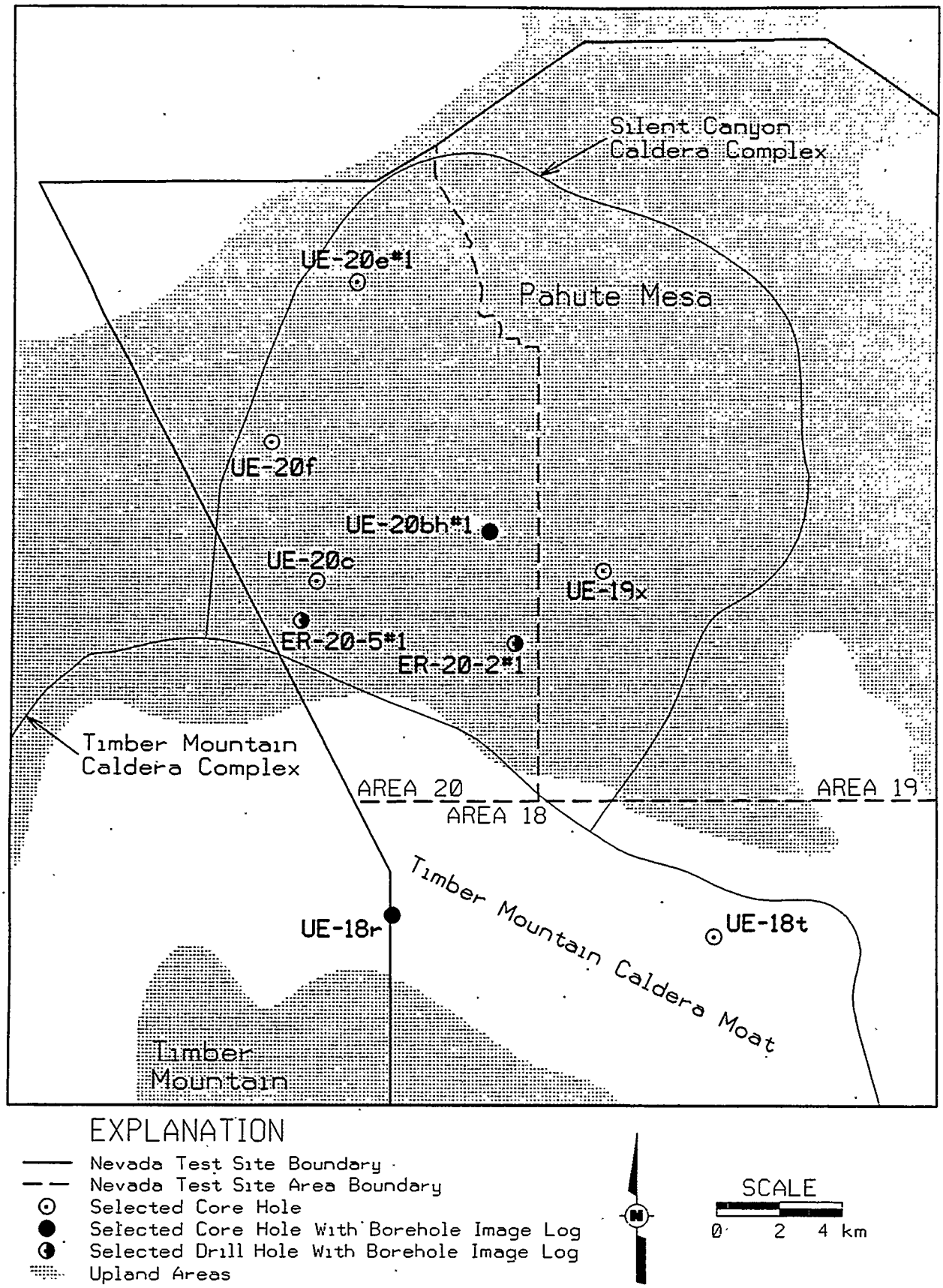

Figure 1-1
Location Map for Drill Holes Used in This Report

This report is presented as a compilation of data and is intended to be used for future CAU-specific flow and transport models.

1.1.2 Project History

This report is an account of work accomplished in late 1995 and early 1996, which was documented in a draft report distributed by IT Corporation (IT) for limited external review in April 1996 (IT, 1996a). Reviewers' comments have been addressed in this final report, but the scope and conclusions have not changed significantly from those presented in the IT draft publication.

The hydrostratigraphic nomenclature used in this report follows that used for the UGTA Phase I regional groundwater modeling efforts (IT, 1996b). However, hydrogeologic characterization of the NTS area is a continuing process, and changes in the definitions of some hydrostratigraphic units have occurred as a result of work conducted after publication of the draft report that forms the basis of this document (IT, 1996a). These changes have not been incorporated into this final report.

Conclusions from the data presented in this fracture analysis report have, however, been assimilated into subsequent reports. For a more in-depth look at the hydrostratigraphy of the Pahute Mesa study area, the reader is directed to these recent works, which include Drellack and Prothro (1997) and Prothro and Drellack (1997).

1.2 Objectives

The objective of this study was to obtain information about fractures in volcanic hydrogeologic and hydrostratigraphic units at Pahute Mesa to determine important hydrologic parameters for future CAU-specific flow and transport models. Critical fracture information gathered during this study included:

- Fracture density
- Aperture
- Orientation
- Secondary mineral coatings

1.3 Methodology

1.3.1 Core Fracture Analysis

A core fracture analysis was performed on conventional core samples from eight drill holes on or in the vicinity of Pahute Mesa. The drill holes were UE-18r, UE-18t, UE-19x, UE-20bh #1, U-20c, UE-20c, UE-20e #1, and UE-20f. A summary of pertinent information about these wells is presented in Table 1-1. These drill holes were selected because cummulatively they provide representative core through five of the six hydrostratigraphic units (HSUs) defined in the Phase I regional groundwater flow model, and they provide the opportunity to compare fractures in core to the BHTV and/or FMS borehole fracture logs.

A total of 1,578 meters (m) (5,177 feet [ft]) of core was examined from December 1995 to February 1996 by geologists from Bechtel Nevada Corporation (BN), IT Corporation, Daniel B. Stephens and Associates, and GeoTrans, Inc. This study was conducted at the U. S. Geological Survey's (USGS) Geologic Data Center and Core Library in Mercury, Nevada. Typically, core was examined megascopically; however, 10x- to 40x-zoom binocular microscopes were used routinely for more detailed examination. The fracture data collected during the fracture analysis as well as stratigraphic, lithologic, hydrogeologic, hydrostratigraphic, and geophysical information were entered into a StratiFact® database for graphical presentations and an Excel® spreadsheet for statistical analysis. The data are on file at BN Geology/Hydrology in Mercury, Nevada, and at the IT office in Las Vegas, Nevada.

During this analysis, the lithology and stratigraphy of the cores were compared to available published logs. Relevant observations, such as degree of welding and alteration, were added as necessary. Stratigraphic nomenclature was also revised and updated as necessary to conform to the new southwestern Nevada volcanic field stratigraphic nomenclature (Ferguson *et al.*, 1994).

A total of 2,851 natural fractures was examined during the analysis. Because only natural fractures were described, it was necessary to differentiate between natural fractures and breaks induced during coring or handling. The presence of secondary mineral coatings on fracture surfaces is generally indicative of a natural fracture; therefore, all breaks in the cores were carefully examined for the presence of secondary minerals. In addition, natural fractures are usually more planar and have smoother surfaces that commonly appear weathered or stained. Faults (as indicated by the presence of slickensides, gouge, or apparent relative displacement)

Table 1-1
Hydrogeologic Information for Selected Boreholes in the Pahute Mesa Fracture Study

Hole Name	Core Available (feet)	Stratigraphy Penetrated by Borehole[1]	Lithologies Represented in Core[2]	Hydrostratigraphy Represented in Core[3]	Structural Block[4]	Comments
UE-19x	2,488 (Continuous)	Tf, Tm, Tp, Ta	B, L, WT, ZT	TMA, TC	Southern Area 19	Unsaturated and saturated zones included.
UE-18t	2,480 (Continuous) 1,490 saturated	QTa, Tt, Tf, Tm	TB, WT	TMA	Northeastern Timber Mountain Bench	TMA at this location may be anomalous. Only the saturated portion below 278.9 m (915 ft) depth was included in this study.
UE-18r	117 (Intermittent) mostly saturated	Tt, Tf, Tm	L, TB, WT	TMA	Northern Timber Mountain Moat	FMS log. TMA at this location may be anomalous (i.e., significant TB confining units).
UE-20e #1	264.5	Tt, Tm, Ta, Tc, Tb	B, WT, L, ZT, FB	TMA, TC, TBA	Southeastern Gold Flat	Only the lower most TC and TBA were studied.
UE-20bh #1	61.5	Tm, Tp, Ta	ZT, L, FB	TC	Central Area 19	FMS and BHTV available.
UE-20c and U-20c	278 (Intermittent) 120 (Intermittent)	Tt, Tm, Tp, Ta	L, WT, B, ZT ZT	TMA, TC TC	Western Area 20	Related to the BENHAM event. Proximity to ER-20-5.
UE-20f	394 (Intermittent)	Tt, Tm, Tp, Ta, Tc, Tb, Tu, To	B, L, WT, FB, ZT	TMA, TC, TCB, TBA, BAQ	Western Area 20	Deepest drill hole on the NTS.
ER-20-5 #1	None	Tm, Tp, Ta	No core	No core	Western Area 20	BHTV log.
ER-20-2 #1	None	Tm, Tp, Ta, Tc	No core	No core	Central Area 19	BHTV log.

1 Stratigraphic symbols from Ferguson *et al.*, 1994; also defined in Table C-22

2 Lithology nomenclature:
- B Bedded tuff
- FB Flow breccia
- L Lava
- NWT Nonwelded tuff
- TB Tuff breccia
- WT Welded tuff
- ZT Zeolitized tuff

3 Hydrostratigraphic nomenclature from the simplified UGTA Phase I hydrogeologic model (Pahute Mesa units only)
- TMA Timber Mountain Aquifer
- TC Tuff Cone
- TCB Bullfrog Confining Unit
- TBA Belted Range Aquifer
- BCU Basal Confining Unit
- BAQ Basal Aquifer

4 Structural block convention by Warren (1994)

and cooling joints are defined as fractures in this data set. Faults were, however, noted on the data sheets so they can easily be separated from the larger data set if desired.

Both open and closed natural fractures were examined during the analysis; however, particular attention was given to open fractures because of their hydrologic significance. In the case of open fractures, the location of each fracture was typically recorded to the next whole foot. However, due to high total fracture density open fractures examined in drill hole UE-18t were recorded in five-foot intervals. All the fracture characteristics were recorded, including surface texture, the type of secondary mineral coating(s) present, an estimate of the percent of the fracture surfaces coated with secondary minerals, the measured dip of the fracture, an estimate of the representative aperture, an estimate of the percent of the fracture open, and any additional characteristics such as the shape of the fracture.

Closed fractures were recorded in either one- or five-foot (0.3- or 1.5-m) intervals, depending on the drill hole and the abundance of fractures. At UE-18t, for example, fractures are very abundant (particularly closed fractures), so a five-foot (1.5-m) recording interval was used for convenience. The attributes noted include the averaged measured dip, the secondary mineral(s) filling the fractures, and any additional characteristics. Table 1-2 summarizes the criteria used for defining fracture attributes that were analyzed in the study.

Twenty samples of secondary mineral coatings were collected and sent to Analytical Materials Laboratory, Santa Barbara, California, for mineralogical analysis. Field descriptions of the samples submitted are provided in Table A-1 in Appendix A. Samples were collected in accordance with the appropriate UGTA and/or DOE-approved procedures (BN, 1996; IT, 1995a and b; DOE, 1995). The methodology and results of the analysis are provided by Iyengar (1996) and included in Appendix A. In addition, select x-ray diffraction data reported by the USGS for drill holes UE-18t (Byers *et al.*, 1981) and UE-19x (Blackmon, 1978) were also incorporated into the study. Results from these analyses provided detailed and precise mineralogy impossible to obtain from visual observation alone. Forty-nine photographs were taken of select features and fractures, including the samples collected for mineralogical analysis. The photos serve as documentation for this study, but perhaps more importantly, they may be used as a visual reference in future studies. The photos are on file at the IT office in Las Vegas, Nevada.

Table 1-2
Definitions of Terms Used in the Core Fracture Analyses

Term	Definition Used in Study
Fracture	A break or crack in a rock core.
Natural Fracture	A fracture resulting from natural geologic processes, including faults and cooling joints. Natural fractures are usually coated or filled with secondary minerals. They are usually high- to medium-angle (but seldom vertical and running down the center of the core), relatively smooth and planar, and have a weathered or stained appearance.
Coring and Handling-Induced Fracture	A fracture resulting from stresses created during coring or handling. Coring and handling-induced fractures will not have secondary mineral coatings and usually have rough textures, curved to irregular shapes, and "fresh" appearances.
Open Fracture	A natural fracture that has open space between the sides of the fracture.
Closed Fracture	A natural fracture that is completely filled with secondary minerals and, thus, has no open space along the fracture trace in the core.
Depth of Fracture	The bottom of the one-foot or five-foot interval in which the fracture occurs (i.e., the depth of the fracture recorded to the next whole foot or five-foot depth).
Fracture Density	The number of fractures per vertical foot.
Fracture Orientation	The dip of the fracture (i.e., the acute angle formed by the fracture and a horizontal plane normal to the long axis of the core).
High-angle	A fracture with a dip greater than 60 degrees and less than or equal to 90 degrees.
Medium-angle	A fracture with a dip greater than 30 degrees and less than or equal to 60 degrees.
Low-angle	A fracture with a dip greater than or equal to 0 degrees and less than or equal to 30 degrees.
Aperture	A representative open distance in millimeters between the sides of the fracture, visually estimated as representative for the portion of the fracture exposed in the core.
Percent Open	The estimated percent of the open space (i.e., aperture) along the entire visible portion of the fracture. When only a single fracture surface was available for examination, estimate of percent open was based on the abundance, distribution, and crystal size of the minerals observed on the surface.
Secondary Mineral Coatings	Naturally occurring minerals that coat the surface of a fracture. Secondary mineralization occurs after the formation of natural fractures, and, therefore, is indicative of natural fractures.
Percent Coated	The estimated percent of the fracture surface that is coated with secondary minerals.
Texture	The feel and appearance of the sides (i.e., surfaces) of a fracture. Texture was described as either very smooth, smooth, intermediate, or rough.
Very Smooth	A fracture surface that is polished. The surface feels slick and appears glossy and shiny.
Smooth	A fracture surface that has a very minor coarse feel and appearance.
Intermediate	A fracture surface that has a coarse and somewhat jagged feel and appearance.
Rough	A fracture surface that has a very coarse and jagged feel and appearance.
Fracture Shape	The general shape of the fracture plane. Fracture shape was described as either planar, curved, or irregular.

1.3.2 Borehole Image Log Analysis

Oriented borehole image logs are tools for identifying and determining the *in situ* orientation of fractures that were penetrated by a borehole and are used when the strike of fractures is desired. There are two types of borehole image logs: the BHTV is an acoustic device operated by most logging companies, and the FMS is a micro-resistivity measuring tool, operated by Schlumberger. Both types have been used at the NTS.

Four drill holes used in this study had borehole image logs. Well UE-18r has an FMS log. Wells ER-20-2#1 and ER-20-5-#1 have BHTV logs, and Well UE-20bh#1 has both BHTV and FMS logs available. Wells UE-18r and UE-20bh#1 both have intermittent core for comparison with the image logs.

1.3.3 Comparison of Geophysical Logs and Hydrologic Data with Fracture Data

In addition to the borehole image logs, other geophysical logs for the drill holes selected for this study were collected and evaluated. Because most of the holes were drilled more than twenty years ago, complete suites of logs were unavailable. However, most of the holes had a caliper log available that was used for comparison against the fracture data and the hydrologic test data. The results of these comparisons are reported in Section 2.0 and summarized in Section 4.4 of this report.

Available hydrologic test data were assembled and evaluated for the study wells. Comparisons were made between well hydrologic data and the fracture data derived from core fracture analysis, as reported in Section 2.0 and summarized in Section 4.5.

1.3.4 Literature Search

An extensive literature search of existing data about fractures at the NTS and vicinity was performed. An annotated bibliography of documents found during the search is provided in Appendix B. An effort was made to compare data from these other studies, and they are included and cited, where appropriate.

1.4 Summary of Pahute Mesa and Timber Mountain Hydrogeology

Pahute Mesa and Timber Mountain are physiographic features within the southwestern Nevada volcanic field. The rocks that underlie these areas consist chiefly of Miocene rhyolitic volcanic rocks that were erupted from several local nested and/or overlapping calderas that include the Silent Canyon and Timber Mountain caldera complexes (*Figure 1-1*). The Silent Canyon caldera complex underlies Pahute Mesa, which is bounded and truncated on its southern margin by the

younger Timber Mountain caldera complex (Ferguson *et al.*, 1994). Six of the wells used in this study (NTS Area 20 and Area 19 wells) were drilled on Pahute Mesa through extra-caldera ash flows that erupted from the Timber Mountain caldera onto older rocks of the Silent Canyon caldera complex. The other two wells (NTS Area 18 wells) were drilled into the Timber Mountain moat, a ring-shaped topographic depression filled with intra-caldera lava flows and ash flows erupted from the Timber Mountain caldera. The thickness of the lava flows and ash flows in these calderas approaches 5 kilometers (km) (Ferguson *et al.*, 1994).

The Pahute Mesa/Timber Mountain area lies within the Alkali Flat-Furnace Creek Ranch sub-basin (as defined by Waddell *et al.*, 1984) of the regional Death Valley groundwater flow system. Groundwater flow within this regional system is generally to the south-southwest, from recharge occurring on Pahute Mesa and areas in central Nevada and intervening uplands to surface discharge areas at Oasis Valley, Alkali Flat, Death Valley, and Ash Meadows. Throughout the Pahute Mesa/Timber Mountain caldera complex area, volcanic rocks are interpreted to extend downward to the regional hydrologic "basement" (IT, 1996). Paleozoic carbonate rocks, which underlie much of the area and serve as the primary regional aquifer for the Death Valley groundwater flow system, are probably not present beneath the caldera complex. In the caldera complex, groundwater flows primarily through volcanic aquifers.

The volcanic rocks of the Pahute Mesa/Timber Mountain area have been subdivided, following two different classification schemes, into hydrogeologic units (HGUs) and hydrostratigraphic units. Both of these units are used throughout this report. HGUs are lithologic units defined on the basis of primary lithologic properties, degree of fracturing, and secondary mineral alteration, and are used to categorize lithologies about their ability to transmit groundwater. Four HGUs have been defined for the area and include the welded-tuff aquifer (WTA), the lava-flow aquifer (LFA), the vitric-tuff aquifer (VTA), and the tuff confining unit (TCU) (Blankennagle and Weir, 1973; Winograd and Thordarson, 1975; Laczniak *et al.*, 1996; IT, 1996). More information about these HGUs is provided in Table 1-3.

HSUs are stratigraphic units formed by combining stratigraphic groups and formations on the basis of similar hydrogeologic properties. An HSU may consist of several HGUs, but is usually dominated by a single type of HGU (for example, mostly WTA and LFA, or mostly TCU). HSUs were defined to serve as layers for the regional (Phase I) groundwater modeling (IT, 1996). The volcanic strata in the Pahute Mesa/Timber Mountain area were subdivided into six HSUs: the Timber Mountain Aquifer (TMA), the Tuff Cone (TC), the Bullfrog Confining Unit

Table 1-3
Hydrogeologic Nomenclature Used in this Report

Hydrogeologic Unit	Typical Lithologies	Hydrologic Significance
Vitric-Tuff Aquifer (VTA)	Bedded tuffs; air-fall and reworked tuffs; unaltered, vitric to devitrified	Constitutes a volumetrically minor hydrogeologic unit. Generally does not extend far below the static water level due to tendency to become zeolitized (which drastically reduces permeability) under saturated conditions. Significant interstitial porosity (20 to 40 percent). Generally insignificant fracture permeability.
Welded-Tuff Aquifer (WTA)	Welded ash-flow tuff; vitric to devitrified	Either intra- or extra-caldera. Degree of welding greatly affects interstitial porosity (less porosity as degree of welding increases) and permeability (greater fracture permeability as degree of welding increases). Welded zones typically intercalated between nonwelded zones.
Tuff Confining Unit (TCU)	Zeolitized bedded tuffs; with interbedded, but less significant, zeolitized, nonwelded to partially welded ash-flow tuffs	May be saturated but measured transmissivities are very low. Responsible for perched and/or semiperched water in overlying units.
Lava-Flow Aquifer (LFA)	Rhyolite lava flows; includes flow breccias (commonly at base) and pumiceous zones (commonly at top)	Generally a caldera-filling unit. Hydrologically complex: wide range of transmissivities; fracture density and interstitial porosity differ with lithologic variations. Lateral and vertical continuity uncertain, especially where intercalated with thick zeolitized nonwelded tuffs (TCUs).

Source: Adapted from Blankennagle and Weir (1973); Winograd and Thordarson (1973); IT (1996); and Laczniak *et al.* (1996).

(TCB), the Belted Range Aquifer (TBA), the Basal Confining Unit (BCU), and the Basal Aquifer (BAQ), as shown in Table 1-4. The TC exhibits the greatest lithologic heterogeneity and constitutes a large proportion of the saturated section of the caldera complex. Drill holes were selected to maximize coverage of the TC HSU. Tables 1-5 and 1-6 show the amounts of core examined in this study, grouped by HSU and HGU, respectively.

Table 1-4
Hydrostratigraphy of the Pahute Mesa/Timber Mountain Area

Hydrostratigraphic Unit (HSU) [1]	Properties	Stratigraphic Units [2]
Timber Mountain Aquifer (TMA)	Uppermost welded tuffs	Tt, Tf, Tm, Tp
Tuff Cone (TC)	Laterally variable tuffs and lava flows	Tp, Ta, Tc
Bullfrog Confining Unit (TCB)	Nonwelded tuff	Tcb
Belted Range Aquifer (TBA)	Welded tuffs above BCU	Tcbs, Tr, Tb, Tub
Basal Confining Unit (BCU)	Mostly nonwelded tuffs	Tr, Tq, Tn, Tub, To
Basal Aquifer (BAQ)	Mostly welded tuffs	Tqm, To, Tlt

1 UGTA Phase I nomenclature. See IT (1996b).
2 Refer to Table C-22 in Appendix C for explanation of stratigraphic nomenclature.

Table 1-5
Amount of Core Examined for this Fracture Study Grouped by Hydrostratigraphic Units

Hydrostratigraphic Unit[1] (HSU)	UE-18r meters (feet)	UE-18t meters (feet)	UE-19x meters (feet)	UE-20bh#1 meters (feet)	U-20c, UE-20c meters (feet)	UE-20e#1 meters (feet)	UE-20f meters (feet)
TMA	35.7 (117)	513.6 (1,685)	295.0 (968)	—	—	—	—
TC	—	—	467.9 (1,535)	18.7 (61.5)	109.4 (359)	38.7 (127)	53.6 (176)
TCB	—	—	—	—	—	—	33.2 (109)
TBA	—	—	—	—	—	7.8 (25.5)	4.0 (13)
BCU	—	—	—	—	—	—	
BAQ	—	—	—	—	—	—	4.9 (16)
Total 578 (5,177 ft)	35.7 (117)	513.6 (1,685)	158.3 (2,488)	18.7 (61.5)	109.4 (359)	46.5 (152.5)	95.7 (314)

1 Refer to *Table 1-4* for explanation of hydrostratigraphic nomenclature.
— Unit not represented in borehole or in logged core from borehole.

Table 1-6
Amount of Core Examined for This Fracture Study
Grouped by Hydrogeologic Unit

Hydrogeologic Unit [1]	UE-18r meters (feet)	UE-18t meters (feet)	UE-19x meters (feet)	UE-20bh#1 meters (feet)	U-20c, UE-20c meters (feet)	UE-20e#1 meters (feet)	UE-20f meters (feet)
VTA	11.9 (39)	121.3 (398)	100.6 (330)	—	—	—	3.0 (10)
WTA	3.0 (10)	392.2 (1,287)	265.5 (871)	—	27.7 (91)	—	7.9 (26)
LFA	6.7 (22)	—	207.6 (681)	1.2 (4)	4.6 (15)	9.6 (31.5)	16.5 (54)
TCU	14.0 (46)	—	184.7 (606)	17.5 (57.5)	77.1 (253)	36.9 (121)	68.3 (224)
Total	35.7 (117)	513.6 (1,685)	158.3 (2,488)	18.7 (61.5)	109.4 (359)	46.5 (152.5)	95.7 (314)

1 Refer to *Table 1-3* for explanation of hydrogeologic nomenclature.

The correlation between HGUs and HSUs is indirect because HGUs are formed on the basis of lithology, and HSUs are groups of HGUs defined on the basis on stratigraphic position. For example, the WTA HGU for a given core consists of all the welded tuff lithologies in that core, regardless of their stratigraphic position. Some of those welded tuffs might occur within a formation that has been assigned to the TMA HSU, while other welded tuffs might occur within a formation that is assigned to the TC HSU. Observations regarding various fracture attributes are analyzed relative to both HGUs and HSUs in this study.

2.0 Fracture Analysis for Selected Drill Holes

Several attributes of fractures were analyzed, including vertical distribution of closed and open fractures, distribution relative to fracture orientation, density within the various HGUs and HSUs, aperture and openness within HGUs and HSUs, and fracture-coating minerals within HGUs and HSUs. These fracture attributes are discussed below for each of the drill holes examined. In Section 4.0 of this report, data regarding these attributes are summarized for the entire study area.

In the discussions that follow, two terms are used to quantify the relative abundances of open and closed fractures. The term "fracture distribution" is used to refer to the numbers or relative proportions of open and closed fractures in a certain portion of a given hole. "Fracture density" is defined as the number of observed natural fractures per vertical foot of core. Because the amounts of core footage vary tremendously from drill hole to drill hole, fracture density is considered here to be a more reliable indicator of the degree of fracturing in a certain HGU or HSU. Similarly, different terms are used to subjectively evaluate the attributes that affect the ability of a fracture to transmit water. Two components of relative openness, "aperture" and "percent openness," were estimated for fractures in each sampling interval. "Aperture" is defined as the average width of the void space between fracture surfaces, with the "average" being a visual estimate of the representative width that falls between the minimum and maximum widths measured with a feeler gauge. "Percent openness" is a visual estimate of the percentage of the length of a fracture that is open and was categorized as 0 percent (i.e., closed), 1 - 10 percent, 10 - 50 percent, 50 - 90 percent, 90 - 99 percent, and 100 percent (i.e., completely open). Both components considered together are valuable in estimating the ability of the fracture to transmit water. Aperture and percent openness of open fractures have been analyzed relative to the HGUs and HSUs in which the fractures occur.

Virtually all of the natural fractures quantified in this study were coated or filled with mineral coatings. The presence of a mineral coating was the primary line of evidence used to differentiate between natural fractures and coring- or handling-induced breaks. In a few isolated instances, natural fractures were identified without a visible secondary mineral coating. Closed fractures were those completely filled with one or more secondary minerals, whereas open fractures were typically partially to completely "coated" with precipitated minerals, but not completely filled. For the remainder of this report, the term "fracture-coating minerals" will refer to secondary minerals that coat open fractures or fill closed fractures. Secondary fracture-coating minerals observed in this study include zeolites, clays, quartz, chalcedony, calcite, iron

and manganese oxides, vapor-phase silicate minerals (primarily cristobalite, tridymite, and feldspars), and in some cases, pulverized host rock (fault gouge). Mineral coatings, as identified during fracture examination, are summarized in Table A-1 (Appendix A).

2.1 Exploratory Hole UE-19x

2.1.1 Hole History

Exploratory Hole UE-19x is located on southeastern Pahute Mesa in the southwestern part of Area 19 of the NTS (*Figure 1-1*). The hole was drilled in 1977 to obtain subsurface structural information and physical properties data for the BACKBEACH underground nuclear test which was to be conducted in nearby Emplacement Hole U-19x (DOE, 1994). Exploratory Hole UE-19x was continuously cored from 4.6 m (15 ft) to its total depth (TD) of 762.9 m (2,503 ft). Table C-1 (Appendix C) provides a summary of drill hole data for UE-19x.

Exploratory Hole UE-19x was selected for this fracture study because it was continuously cored to TD allowing a comparison of fracture characteristics above and below the water table. All core available, approximately 758.3 m (2,488 ft), was logged for this study.

2.1.2 Hydrogeology

Exploratory Hole UE-19x is located within the Silent Canyon caldera complex. The hole is situated on a north-south-trending structural block bounded on the west by the West Greeley fault and on the east by the Almendro fault. This block is included in the larger Southern Area 19 structural block as defined by Warren (1994).

Exploratory Hole UE-19x penetrated 696.2 m (2,284 ft) of caldera-burying rocks. These include, from the surface down: 5.3 m (18 ft) of nonwelded tuff related to the rhyolite of Beatty Wash; 294 m (965 ft) of ash-flow tuffs related to the Timber Mountain Group; and 396.5 m (1,301 ft) of rhyolite lavas, ash-flow tuffs, and bedded tuffs related to the Paintbrush Group. The underlying caldera-filling units include 66.8 m (219 ft) of bedded tuff, nonwelded tuff, and flow breccia related to the Volcanics of Area 20. A condensed stratigraphic and lithologic log for this hole is provided in Table C-2 (Appendix C).

Two HSUs are represented in this stratigraphic sequence, the TMA and the TC. All four HGUs (VTA, WTA, LFA, and TCU) are also well-represented in the core. The static water level is at the depth of approximately 695 m (2,280 ft). However, a local perched water table was

encountered at 674.8 m (2,214 ft) within a zeolitzed pumiceous lava. No hydrologic tests were conducted in this hole.

2.1.3 Fracture Analysis

2.1.3.1 Density and Distribution

The density of fractures in the continuous core from Exploratory Hole UE-19x has been analyzed relative to occurrence within various HGUs and HSUs and relative to fracture orientation. In UE-19x, fracture density has also been examined relative to position above or below the water table. In these analyses, the distribution of fractures has been examined separately for open and closed fractures. These relationships are shown in Figures 2-1 and 2-2a-d and discussed below.

Vertical Distribution of Open and Closed Fractures

Figure 2-1 shows the vertical distribution of all open and closed fractures within the HGUs and HSUs in the UE-19x core. The figure also summarizes the aperture, openness, and density of fractures at high, medium, and low angles, as well as the relationship of fracture distribution to the caliper log.

Density of Open and Closed Fractures in Hydrostratigraphic Units

The UE-19x corehole penetrated two HSUs: the TMA, and the TC. Fracture density was approximately three times higher in the TC. The density of open fractures exceeded that of closed fractures in both HSUs (*Figure 2-2a*).

Density of Open and Closed Fractures in Hydrogeologic Units

Total fracture density is highest in LFA units, followed by WTA units (*Figure 2-2b*). Most of the variation in fracture density between different HGUs is due to variation in the numbers of open fractures since there is little variation in the density of closed fractures between the different units. No fractures were identified in the VTA.

Density of Open and Closed Fractures Relative to the Water Table

There is little difference in the density of total fractures above and below the water table in the UE-19x core. However, the density of open fractures is twice that of closed fractures above the water table, whereas below the water table, the density of closed fractures exceeds that of open fractures (*Figure 2-2c*).

This page intentionally left blank.

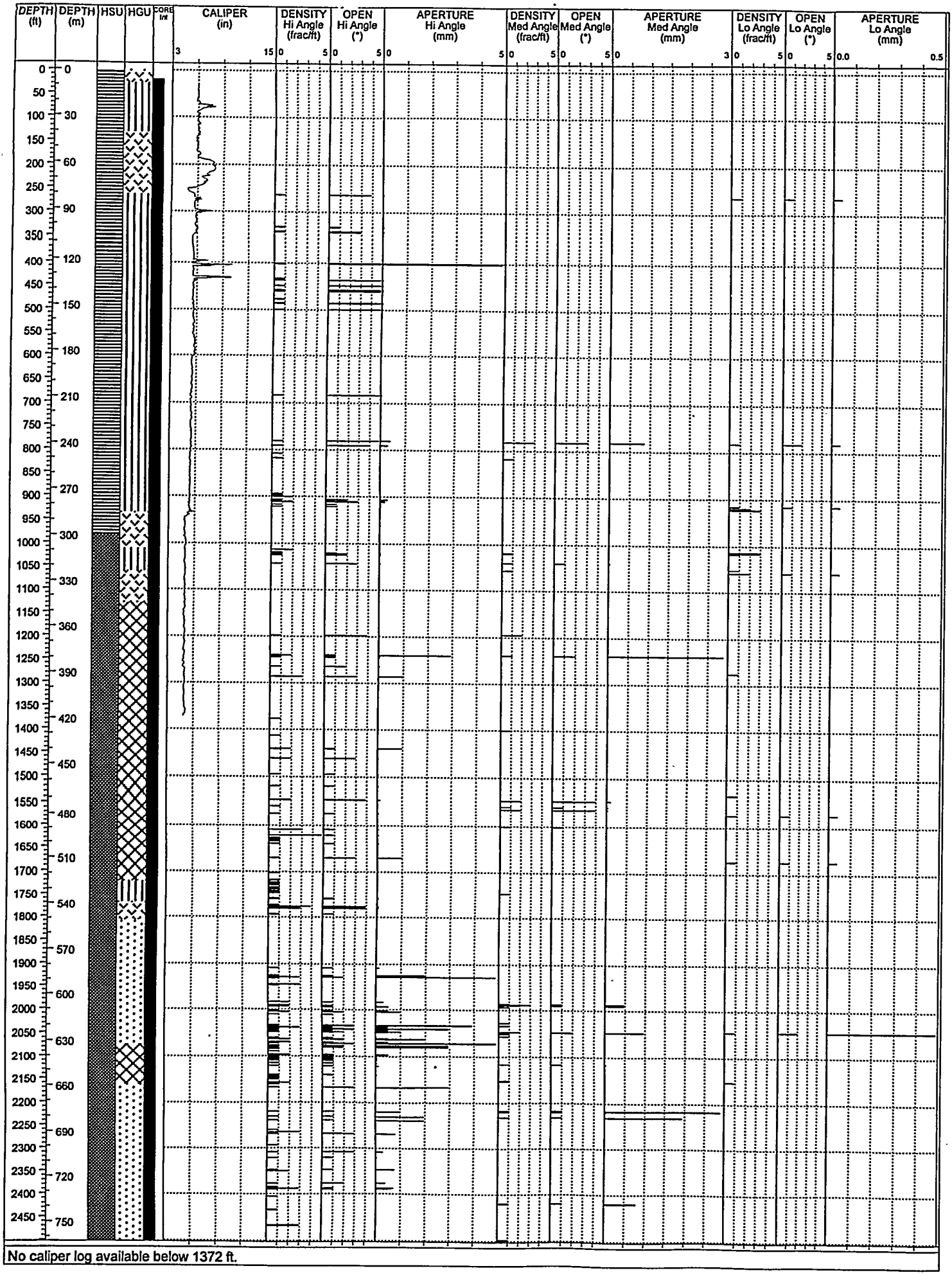

No caliper log available below 1372 ft.

LEGEND

Hydrostratigraphic Unit (HSU)

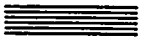
Timber Mountain Aquifer (TMA)


Tuff Cone (TC)


Bullfrog Confining Unit (TCB)


Belted Range Aquifer (TBA)


Basal Aquifer (BAQ)

Hydrogeologic Unit (HGU)


Welded–tuff aquifer (WTA)

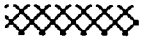
Lava–flow aquifer (LFA)


Vitric–tuff aquifer (VTA)


Tuff confining unit (TCU)

(•) OPEN
(for all angles)

Number	Estimated Range of Percent Openness
0	0%
1	1 – 10%
2	10 – 50%
3	50 – 90%
4	90 – 99%
5	100%

Figure 2-1
UE-19x: Composite Log of Open and Closed Fracture Data, 4.6 Meters - TD

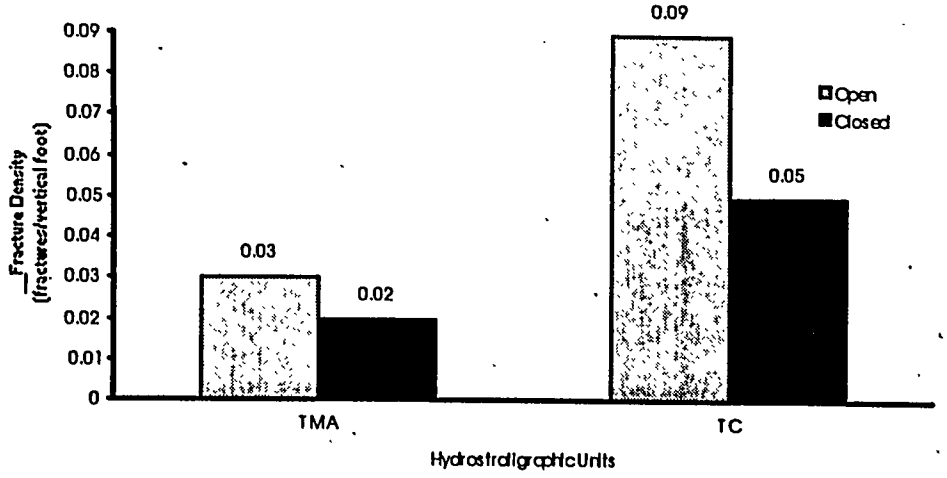

Figure 2-2a
Density of Open and Closed Fractures Relative to Hydrostratigraphy at UE-19x

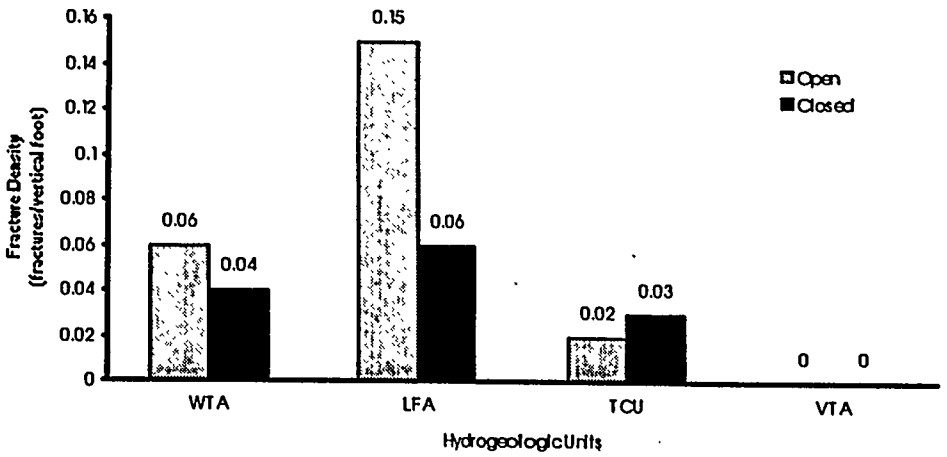

Figure 2-2b
Density of Open and Closed Fractures Relative to Hydrogeology at UE-19x

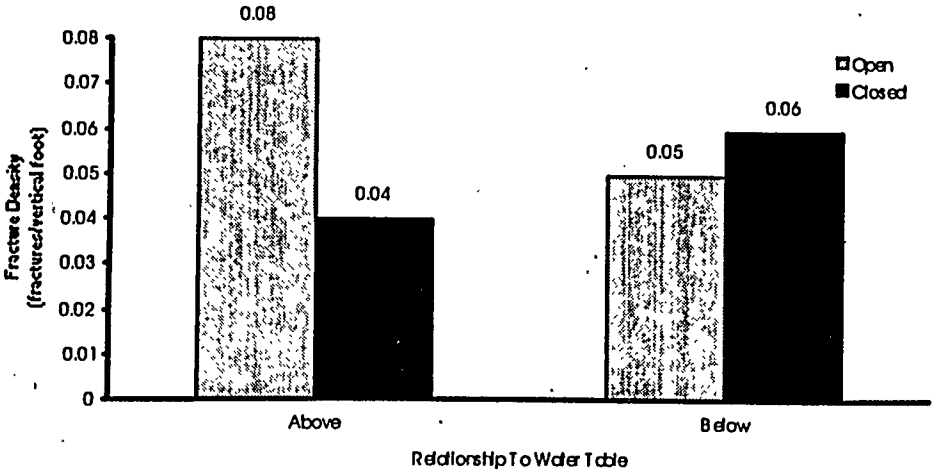

Figure 2-2c
Density of Open and Closed Fractures Relative to the Water Table at UE-19x

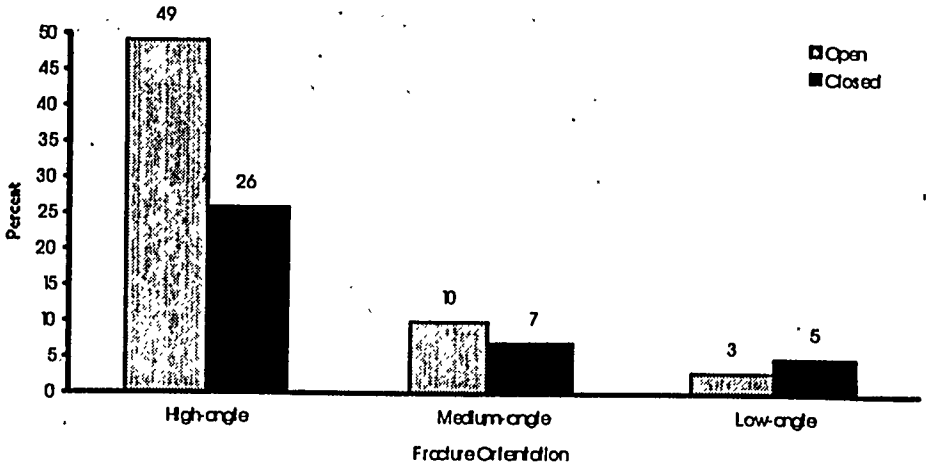

Figure 2-2d
Distribution of Open and Closed Fractures Relative to Orientation at UE-19x

Figure 2-2a-d
Density and Distribution of Fractures at UE-19x

Distribution of Open and Closed Fractures Relative to Orientation

Seventy-five percent of the fractures in the UE-19x core are high-angle. At high-angle and medium-angle orientations, the density of open fractures exceeds that of closed fractures, whereas at low-angle orientations, closed fractures are more abundant (*Figure 2-2d*).

2.1.3.2 Aperture and Fracture Openness

The aperture and openness relationships observed in the UE-19x core are shown in Table 2-1 and discussed below.

Aperture and Openness Relative to Hydrostratigraphic Units

Fractures within the TC have an average aperture twice that of fractures within the TMA, however the fractures within the TMA are more open (*Table 2-1*).

Table 2-1
UE-19x Fracture Aperture and Percent Open Data

Data Grouped by Hydrostratigraphic Units

Hydrostratigraphic Units	Average Aperture (millimeters)	Percent Open
Timber Mountain Aquifer (TMA)	0.4	50 - 100 percent
Tuff Cone (TC)	0.8	1 - 50 percent

Data Grouped by Hydrogeologic Units

Hydrogeologic Unit	Aperture (millimeters)	Percent Open
Vitric-tuff aquifer (VTA)	*[1]	*
Welded-tuff aquifer (WTA)	0.2	50 - 100 percent
Lava-flow aquifer (LFA)	1.0	1 - 50 percent[2]
Tuff confining unit (TCU)	0.6	1 - 50 percent[3]

1 No open fractures logged.
2 Typical range as presented; however, data set is skewed toward the 10 - 50 percent category.
3 Typical range as presented; however, data set is skewed toward the 1 - 10 percent category.

Aperture and Openness Relative to Hydrogeologic Units

The LFA contains fractures with the largest average aperture at 1.0 mm (0.04 in.), followed by fractures within the TCU at 0.6 mm (0.02 in.), and finally by fractures within the WTA at 0.20 mm (0.008 in.) (*Table 2-1*). Although the fractures within the WTA have the lowest average aperture, they are the most open, averaging 50 - 100 percent open.

2.1.3.3 Mineralogy of Fracture Coatings

Distribution of Fracture-Coating Minerals in Hydrostratigraphic Units

Figure 2-3a shows the distribution of fracture-coating minerals in the two HSUs represented in the UE-19x core: the TMA and the TC. Overall, zeolites (specifically clinoptilolite/heulandite and mordenite) were the most commonly occurring mineral coating. Chalcedony was the second most abundant fracture-coating mineral in the core. In the TMA, which is positioned primarily above the water table in this well, vapor-phase silicate minerals are the most abundant fracture-coating minerals. Chalcedony, clay, and calcite are also abundant in the TMA with euhedral quartz, zeolites, oxides, and fault gouge present. In the TC, zeolites (clinoptilolite and mordenite) and chalcedony, in that order, are the dominant fracture-coating minerals.

Distribution of Fracture-Coating Minerals in Hydrogeologic Units

Three HGUs (the WTA, the LFA, and the TCU) were found to contain fractures in the UE-19x core. The distribution of minerals lining or filling fractures varied significantly between the different HGUs as illustrated in Figure 2-3b. In the WTA, a fairly even distribution between several mineral types (zeolites, clays, calcite, chalcedony, and vapor-phase silicate minerals) was observed with quartz, iron and manganese (Fe/Mn) oxides, and fault gouge also observed but in lesser abundances. In the LFA, zeolites and chalcedony were distinctly more abundant as fracture-coating materials than the other mineral types. In the TCU, the same relationship was more pronounced, with zeolites accounting for 60 percent of the occurrences of mineral coatings counted, chalcedony accounting for an additional 31 percent, and clay minerals and oxides representing the remaining 9 percent of the mineral coatings. Euhedral quartz, calcite, vapor-phase minerals, and fault gouge were not observed in the TCU.

Distribution of Fracture-Coating Minerals Relative to the Water Table

In the UE-19x core, zeolites and chalcedony are the predominant mineral fracture coatings both above and below the water table (Figure 2-3c). Below the water table, zeolites and chalcedony

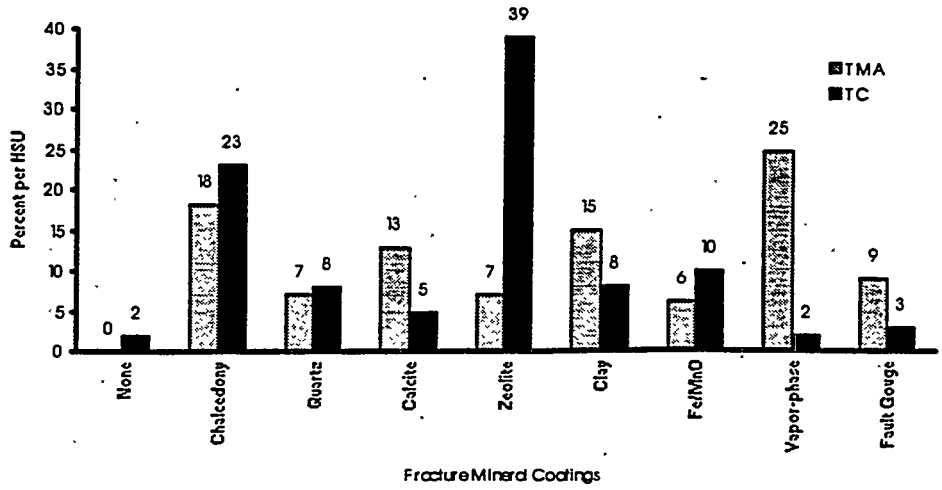

Figure 2-3a
Distribution of Fracture Mineral Coatings Relative to Hydrostratigraphy at UE-19x

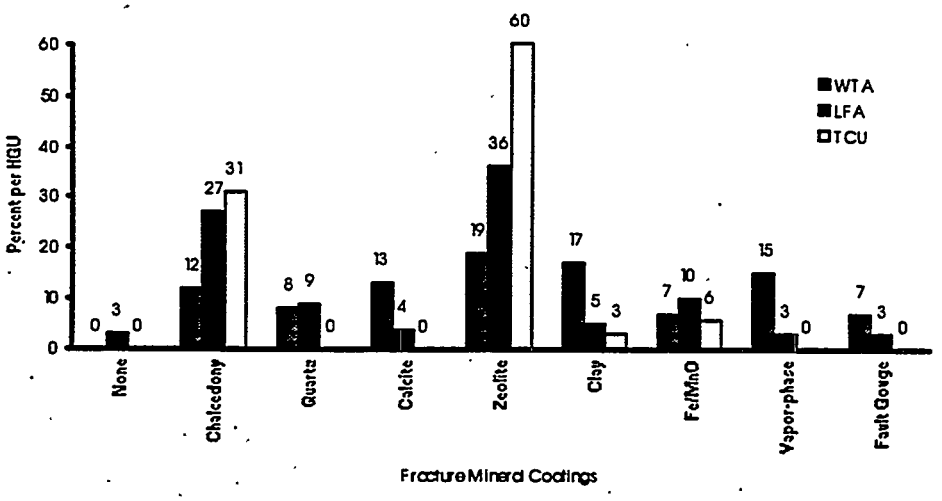

Figure 2-3b
Distribution of Fracture Mineral Coatings Relative to Hydrogeology at UE-19x

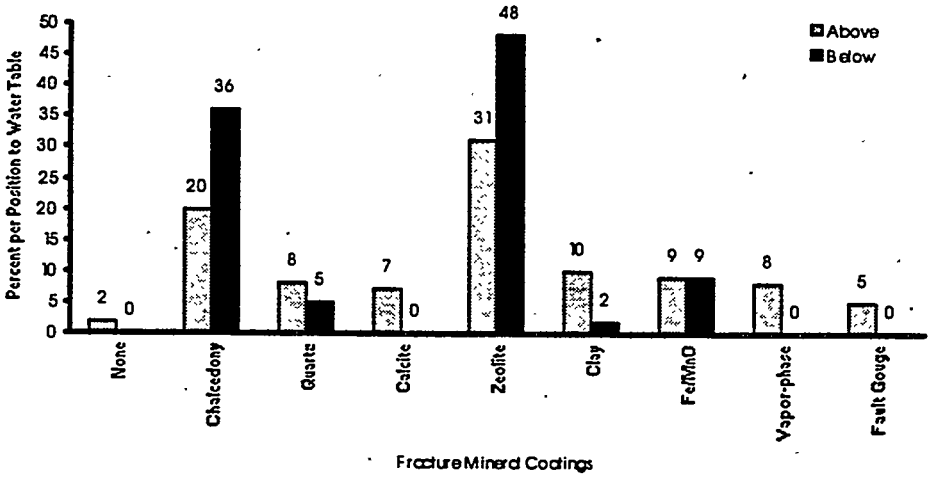

Figure 2-3c
Distribution of Fracture Mineral Coatings Relative to the Water Table at UE-19x

Figure 2-3a-c
Distribution of Fracture-Coating Minerals at Exploratory Hole UE-19x

are strongly dominant, with other mineral species only rarely observed. Above the water table, the predominance of zeolite and chalcedony is less pronounced, and minerals such as clay minerals, Fe/Mn oxides, euhedral quartz, calcite, and vapor-phase silicates (combined) account for a significant portion (42 percent) of the mineral coatings observed. Calcite, vapor-phase silicates, and fault-gouge coatings were observed only above the water table.

2.2 Exploratory Hole UE-18t

2.2.1 Hole History

Exploratory hole UE-18t is located immediately southeast of Pahute Mesa in the northeastern part of the Timber Mountain caldera moat in Area 18 of the Nevada Test Site (*Figure 1-1*). The hole was drilled in 1978 to evaluate the suitability of the Timber Mountain moat area for underground nuclear tests (Byers *et al.*, 1981). UE-18t was continuously cored from 36.6 m (120.1 ft) to its total depth of 792.5 m (2,600 ft). Drill hole statistics for this hole are summarized in Table C-3 in Appendix C. A more thorough account of the UE-18t drill hole is provided in Byers *et al.* (1981).

Exploratory Hole UE-18t was selected for this fracture study because it provides a significant interval of continuous core below the static water level. Also, and of equal importance, its location affords the possibility to yield significant hydrogeologic information about the Timber Mountain caldera and its influence upon the groundwater flow at the NTS.

2.2.2 Hydrogeology

The Timber Mountain caldera complex consists of two nested calderas formed by the collapse of pre-Rainier Mesa rocks over a magma chamber following eruptions of two major ash-flow tuff units: the older Rainier Mesa Tuff (which formed the larger Rainier Mesa caldera) and the younger Ammonia Tanks Tuff (which resulted in the smaller Ammonia Tanks caldera).

The Timber Mountain caldera moat is a structural and geomorphic feature defined by the outermost caldera wall and the Timber Mountain resurgent dome. Drill hole UE-18t is located in the northeastern moat area within the northeastern Timber Mountain Bench structural block as defined by Warren (1994). Additionally, geophysical data (aeromagnetic and gravity) and lithologic details from UE-18t indicate that this site lies within the outer collapse zone of the (larger) Rainier Mesa caldera (Warren, 1994; Byers *et al.*, 1981).

The UE-18t drill hole penetrated tuffaceous alluvium to a depth of 91.7 m (301 ft); caldera-filling ash-flow and bedded tuffs related to the Thirsty Canyon Group, Volcanics of Fourtymile Canyon, and the Ammonia Tanks Tuff to a depth of 498.4 m (1,635 ft); and reached total depth within an intracaldera facies of the Rainier Mesa Tuff. A condensed stratigraphic and lithologic log for drill hole UE-18t is provided in Table C-4 in Appendix C.

Based on the above stratigraphy, the volcanic rocks encountered at UE-18t are assigned to the TMA. Initially, the two dominant lithologies, welded ash-flow tuffs and nonwelded/bedded tuffs, can be subdivided hydrogeologically into VTA and WTA, respectively. However, proximity of this site to the caldera ring fracture zone has resulted in sporadic hydrothermal alteration. In the more porous rocks, massive clay alteration is common, mostly to montmorillonite, with minor illite and lesser kaolinite. For the welded ash-flow tuffs, discrete argillized zones and/or clay and calcite filled fractures are common. Such alteration has significant hydrologic ramifications. See the following subsections and Section 4.0 for additional details and discussion.

The static water level at UE-18t is reported at depth of 278.9 m (915 ft) (Reiner *et al.*, 1995). No hydrologic tests were conducted in the borehole.

2.2.3 Fracture Analysis

2.2.3.1 Density and Distribution

Examination of fractures in this core was limited to those that occur below the water table. The density of fractures within the TMA has been analyzed relative to occurrence within various HGUs and relative to fracture orientation. In these analyses, the distribution of fractures has been examined separately for open and closed fractures. These relationships are shown in Figures 2-4 and 2-5a-c and discussed in the following text.

Vertical Distribution of Fractures

Figure 2-4 shows the vertical distribution of open fractures in the HGUs in the UE-18t core. The figure also presents data on the aperture, openness, and density of fractures at high, medium, and low angles as well as the relationship of fracture distribution to the caliper log.

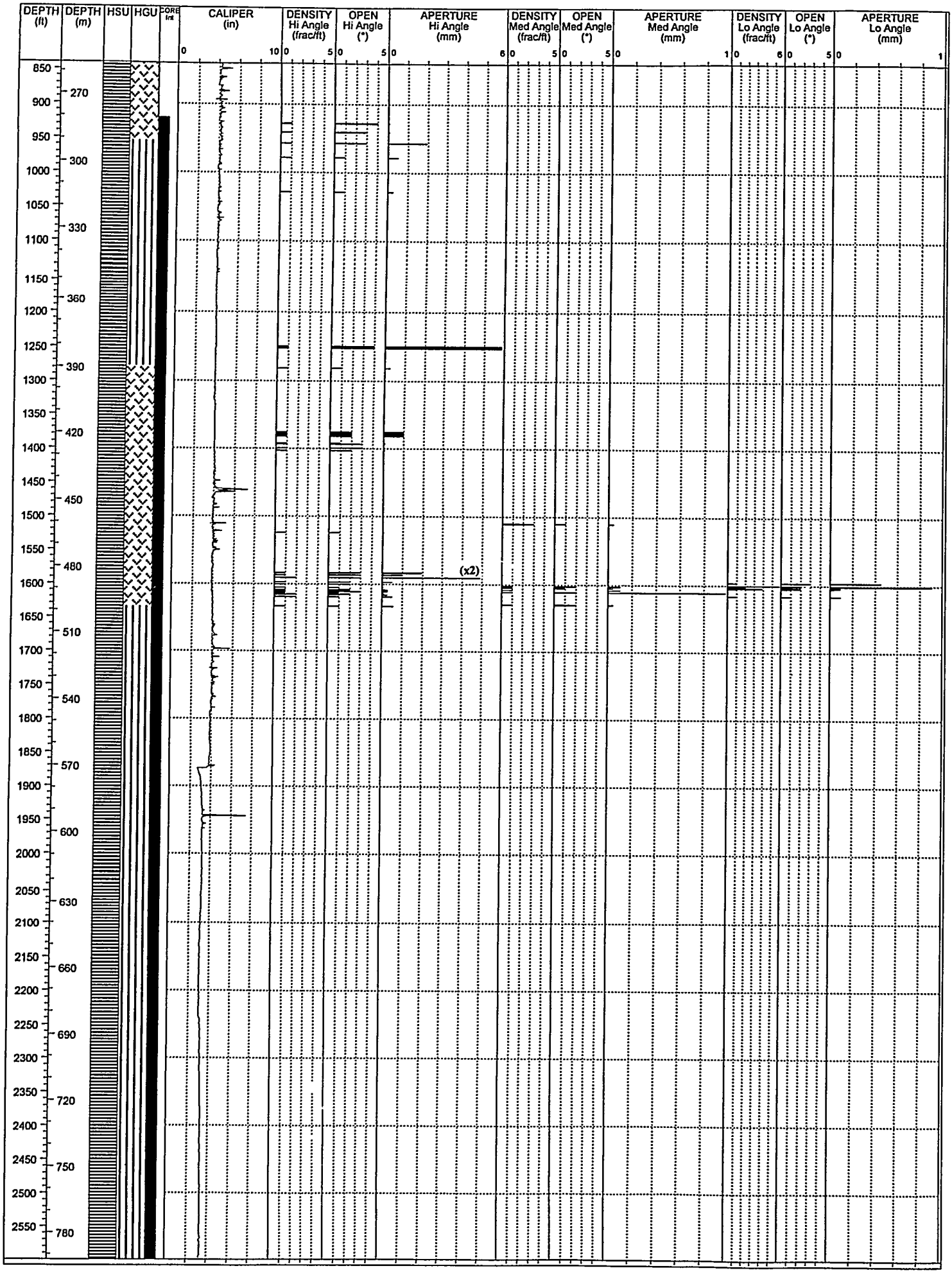
DEPTH (ft)
DEPTH (m)
HSU
HGU
CORE Int
CALIPER (in)
0
10
DENSITY Hi Angle (frac/ft)
0
5
OPEN Hi Angle (°)
0
5
APERTURE Hi Angle (mm)
0
6
DENSITY Med Angle (frac/ft)
0
5
OPEN Med Angle (°)
0
5
APERTURE Med Angle (mm)
0
1
DENSITY Lo Angle (frac/ft)
0
6
OPEN Lo Angle (°)
0
5
APERTURE Lo Angle (mm)
0
1
850
900
950
1000
1050
1100
1150
1200
1250
1300
1350
1400
1450
1500
1550
1600
1650
1700
1750
1800
1850
1900
1950
2000
2050
2100
2150
2200
2250
2300
2350
2400
2450
2500
2550
270
300
330
360
390
420
450
480
510
540
570
600
630
660
690
720
750
780
(x2)

LEGEND

Hydrostratigraphic Unit (HSU)

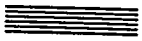
Timber Mountain Aquifer (TMA)


Tuff Cone (TC)


Bullfrog Confining Unit (TCB)


Belted Range Aquifer (TBA)


Basal Aquifer (BAQ)

Hydrogeologic Unit (HGU)


Welded–tuff aquifer (WTA)


Lava–flow aquifer (LFA)


Vitric–tuff aquifer (VTA)


Tuff confining unit (TCU)

(•)OPEN
(for all angles)

Number	Estimated Range of Percent Openness
0	0%
1	1 – 10%
2	10 – 50%
3	50 – 90%
4	90 – 99%
5	100%

Figure 2-4
UE-18t: Composite Log of Open Fracture Data, 256 Meters - TD

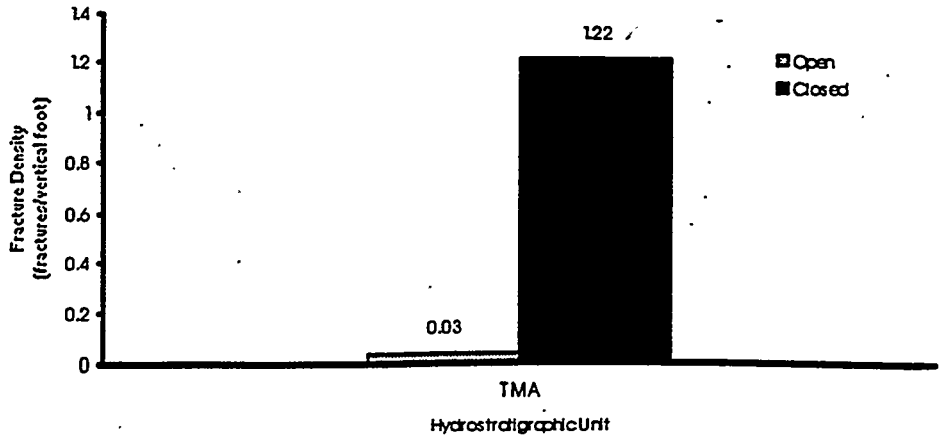

Figure 2-5a
Density of Open and Closed Fractures Relative to Hydrostratigraphy at UE-18t

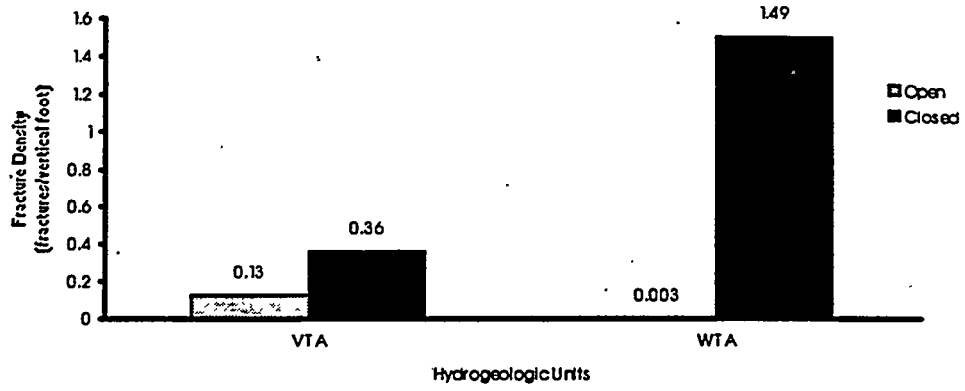

Figure 2-5b
Density of Open and Closed Fractures Relative to Hydrogeology at UE-18t

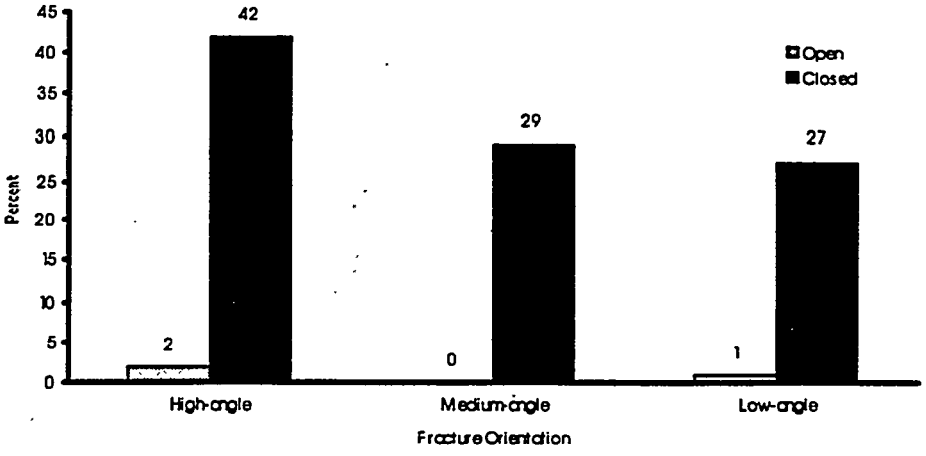

Figure 2-5c
Distribution of Open and Closed Fractures Relative to Orientation at UE-18t

Figure 2-5a-c
Density and Distribution of Fractures at Exploratory Hole UE-18t

Density of Open and Closed Fractures in Hydrostratigraphic Units

The UE-18t corehole penetrated only one HSU, the TMA. In this core, the density of closed fractures greatly exceeds that of open fractures (*Figure 2-5a*). A total of 2,108 fractures were counted in the core, 2,051 of which (97 percent) were closed, and only 57 (three percent) were open.

Density of Open and Closed Fractures in Hydrogeologic Units

The WTA has a higher fracture density than the VTA; however, essentially all the fractures observed in the WTA are closed (*Figure 2-5b*). The density of closed fractures is twice that for open fractures within the VTA.

Distribution of Open and Closed Fractures Relative to Orientation

In UE-18t, fractures oriented at high angles are more abundant than medium- and low-angle fractures. Sixty-six percent of the open fractures are high-angle, while 43 percent of the closed fractures are high-angle (*Figure 2-5c*).

2.2.3.2 Aperture and Fracture Openness

Aperture and percent openness of open fractures in the UE-18t core have been analyzed relative to the HGUs and the HSUs in which the fractures occur. These relationships are shown in Table 2-2 and outlined below.

Aperture and Openness Relative to Hydrostratigraphic Units

At UE-18t the TMA contains fractures that have an average aperture of 0.8 mm (0.03 in.) and are 10 - 50 percent open (Table 2-2).

Aperture and Openness Relative to Hydrogeologic Units

Fractures within the WTA have a relatively large average aperture of 2.2 mm (0.09 in.) which is over twice that of fractures within the VTA, which have an average aperture of 1.0 mm (.04 in.) (Table 2-2). However, the fractures within the VTA have a higher average percent open.

2.2.3.3 Mineralogy of Fracture Coatings

Distribution of Fracture-Coating Minerals in Hydrostratigraphic Units

The distribution of fracture-coating minerals in the UE-18t core, all of which is assigned to the TMA, is presented in Figure 2-6a. Clay minerals are the most abundant fracture-coating or –filling mineral in the core, followed by calcite, and iron and manganese oxides. Occurrences of

Table 2-2
UE-18t Fracture Aperture and Percent Open Data

Data Grouped by Hydrostratigraphic Units

Hydrogeologic Unit	Average Aperture (millimeters)	Percent Open
Timber Mountain Aquifer (TMA)	0.8	10 - 50 percent

Data Grouped by Hydrogeologic Units

Hydrogeologic Unit	Average Aperture (millimeters)	Percent Open
Vitric-tuff aquifer (VTA)	1.0	10 - 50 percent
Welded-tuff aquifer (WTA)	2.2	1 - 10 percent

chalcedony, quartz, and zeolites are conspicuously low in core from UE-18t compared to the cores from other holes examined in this study.

Distribution of Fracture-Coating Minerals in Hydrogeologic Units

Because the majority of total fractures in the UE-18t core occur in the WTA, the relationships mentioned previously regarding the distribution of fracture-filling minerals in the TMA also apply to the WTA. Clay minerals, calcite, and iron and manganese oxides are the most commonly observed mineral fillings in fractures in the WTA (Figure 2-6b). The distribution of fracture-filling minerals in the VTA, however, is markedly different from that in the WTA. In the VTA, zeolites are the significant fracture-filling material, followed by clay minerals, Fe/Mn oxides, and quartz are also relatively abundant. Clay minerals and calcite are significantly less common in the VTA than in the WTA.

2.3 Exploratory Hole UE-18r

2.3.1 Hole History

Exploratory hole UE-18r is located in northwestern Area 18 near the western boundary of the NTS. This location is within the northern part of the Timber Mountain caldera moat south of Pahute Mesa (*Figure 1-1*). UE-18r, drilled in late 1967 and early 1968, was the first deep exploratory hole in the Timber Mountain caldera. Its purpose was to obtain stratigraphic, structural, and hydrologic information for this part of the caldera and to evaluate the area for

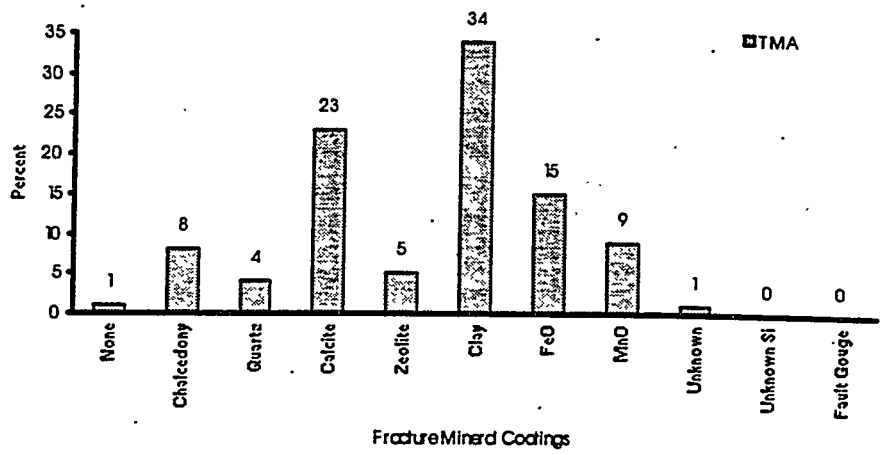

Figure 2-6a
Distribution of Fracture Mineral Coatings Relative to Hydrostratigraphy at UE-18t

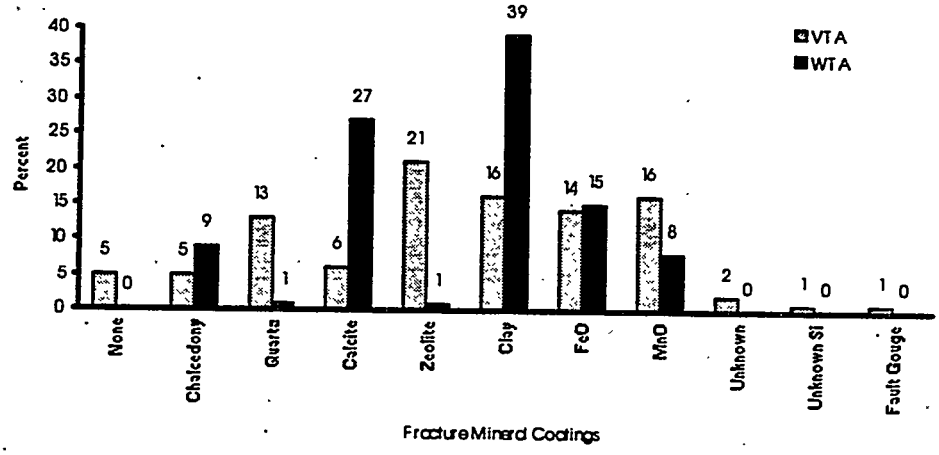

Figure 2-6b
Distribution of Fracture Mineral Coatings Relative to Hydrogeology at UE-18t

Figure 2-6a-b
Distribution of Fracture Mineral Coatings at UE-18t

underground nuclear testing (Carr *et al.*, 1968, 1981). The borehole was rotary drilled to a total depth of 1,525.2 m (5,004 ft). Fifteen cores were taken at various depths during drilling. A summary of drill hole statistics is provided in Table C-5 in Appendix C, and coring data is given in Table C-6 in Appendix C.

Exploratory Hole UE-18r was selected for this study because of the availability of a televiewer log with intermittent core and because of its hydrogeologically important location within the Timber Mountain caldera. All available core from this hole, approximately 35.7 m (117 ft), was logged for this fracture study.

2.3.2 Hydrogeology

Exploratory Hole UE-18r is located within the Northern Timber Mountain Moat structural block (Warren, 1994). Intracaldera facies of the Ammonia Tanks Tuff and the Rainier Mesa Tuff were penetrated, suggesting this location lies within both the Ammonia Tanks and the Rainier Mesa calderas (Warren, 1994). Major units penetrated by the borehole include: 324.6 m (1,065 ft) of welded ash-flow tuffs related to the Thirsty Canyon Group and Volcanics of Forty Mile Canyon; 860 m (2,821 ft) of intracaldera welded ash-flow tuff and lava related to the Ammonia Tanks Tuff and rhyolite of Tannenbaum Hill, respectively; and 74.7 m (245.1 ft) of intracaldera welded ash-flow tuff sandwiched between two fairly thick (182.5 and >83.5 m), landslide or eruptive breccia deposits all related to the Rainier Mesa Tuff. The debris flows and breccias result from the erosion and collapse of the caldera walls. They are a mixture of dense, hard rhyolite lava and welded tuff blocks derived from the caldera wall in a matrix of soft nonwelded tuff. At UE-18r, these debris flows intertongue with the Rainier Mesa ash-flow tuff. A condensed stratigraphic and lithologic log for Exploratory Hole UE-18r is provided in Table C-7 in Appendix C.

The volcanic units previously described are categorized hydrostratigraphically as the TMA. This sequence can be further subdivided into the four hydrogeologic units based on lithology and alteration (Figure 2-7). The static water level at UE-18r is reported at 416 m (1,365 ft) depth (Reiner *et al.*, 1995). Aquifer tests were conducted in 1968 and are summarized in Blankennagel and Weir (1973) and Carr *et al.* (1968, 1981). FMS and flow logs were run in recent years as part of a recompletion effort for the UGTA program. The results of hydrologic tests are presented in Section 2.3.4.

This page intentionally left blank.

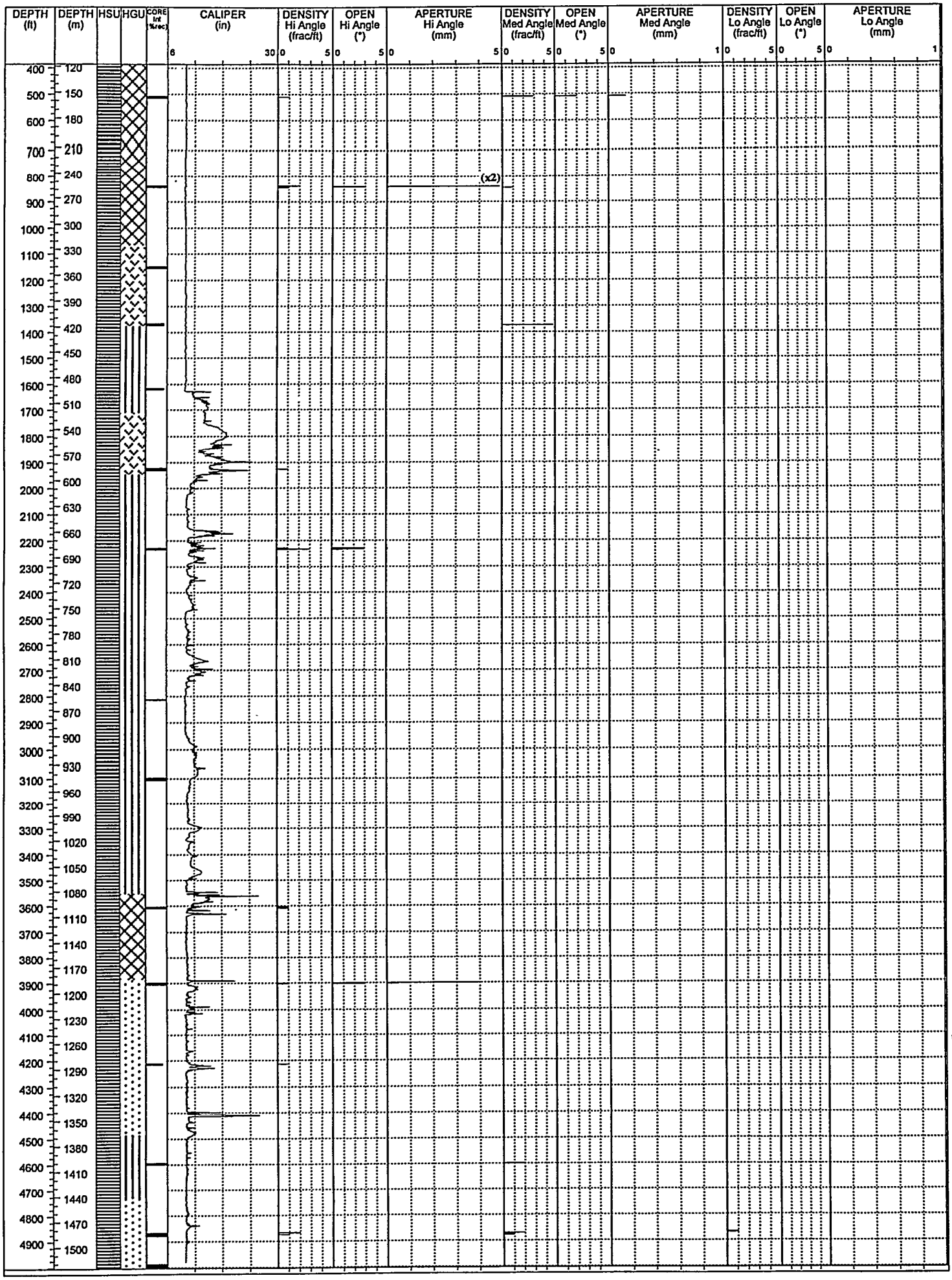
DEPTH (ft)
DEPTH (m)
HSU
HGU
CORE Int %rec
CALIPER (in)
6
30
DENSITY Hi Angle (frac/ft)
OPEN Hi Angle (°)
APERTURE Hi Angle (mm)
(x2)
DENSITY Med Angle (frac/ft)
OPEN Med Angle (°)
APERTURE Med Angle (mm)
DENSITY Lo Angle (frac/ft)
OPEN Lo Angle (°)
APERTURE Lo Angle (mm)
0
5
1
400 120
500 150
600 180
700 210
800 240
900 270
1000 300
1100 330
1200 360
1300 390
1400 420
1500 450
1600 480
1700 510
1800 540
1900 570
2000 600
2100 630
2200 660
2300 690
2400 720
2500 750
2600 780
2700 810
2800 840
2900 870
3000 900
3100 930
3200 960
3300 990
3400 1020
3500 1050
3600 1080
3700 1110
3800 1140
3900 1170
4000 1200
4100 1230
4200 1260
4300 1290
4400 1320
4500 1350
4600 1380
4700 1410
4800 1440
4900 1470
1500

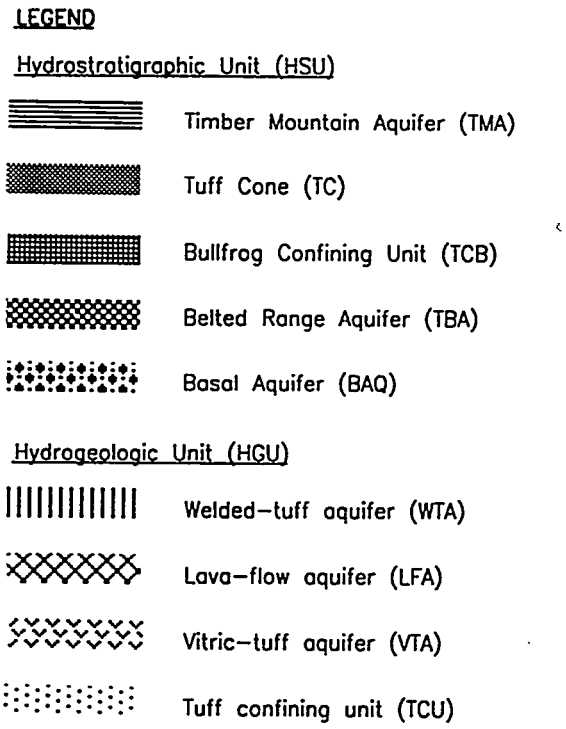

(•) OPEN
(for all angles)

Number	Estimated Range of Percent Openness
0	0%
1	1 – 10%
2	10 – 50%
3	50 – 90%
4	90 – 99%
5	100%

Figure 2-7
UE-18r: Composite Log of Open and Closed Fracture Data, 117.3 Meters - TD

2.3.3 Fracture Analysis

2.3.3.1 Density and Distribution

The density of fractures in the core sections from UE-18r has been analyzed relative to occurrence within the TMA HSU, various HGUs, and relative to fracture orientation. In these analyses, the distribution of fractures has been examined separately for open and closed fractures. These relationships are shown in *Figure 2-7* and Figure 2-8a-d and discussed below.

Vertical Distribution of Open and Closed Fractures

Figure 2-7 shows the core intervals examined and the vertical distribution of open and closed fractures within the TMA in the UE-18r core. The figure also presents data on the aperture, openness, and density of fractures at high, medium, and low angles. The figure also shows the relationship of fracture distribution to the caliper log.

Density of Open and Closed Fractures in Hydrostratigraphic Units

The cored intervals in Exploratory Hole UE-18r represent strata that have been assigned to the TMA. The density of closed fractures in the TMA is twice that of open fractures (*Figure 2-8a*). Sixty-seven percent of the fractures examined in the core sections are closed, while 33 percent are open.

Density of Open and Closed Fractures in Hydrogeologic Units

Four HGUs (the LFA, the VTA, the WTA, and the TCU) are represented in the UE-18r core. In the WTA, the density of open fractures exceeds that of closed fractures, whereas in the other HGUs, closed fractures outnumber the open fractures (*Figure 2-8b*).

Density of Open and Closed Fractures Relative to the Water Table

The density of closed fractures exceeds that for open fractures both above and below the water table at UE-18r (*Figure 2-8c*). Closed fractures are only slightly more abundant than open fractures above the water table, whereas below the water table, closed fractures are more than twice as abundant than open fractures. The density of closed fractures is approximately equal above and below the water table. In contrast, the density of open fractures above the water table is over twice the density of open fractures below the water table.

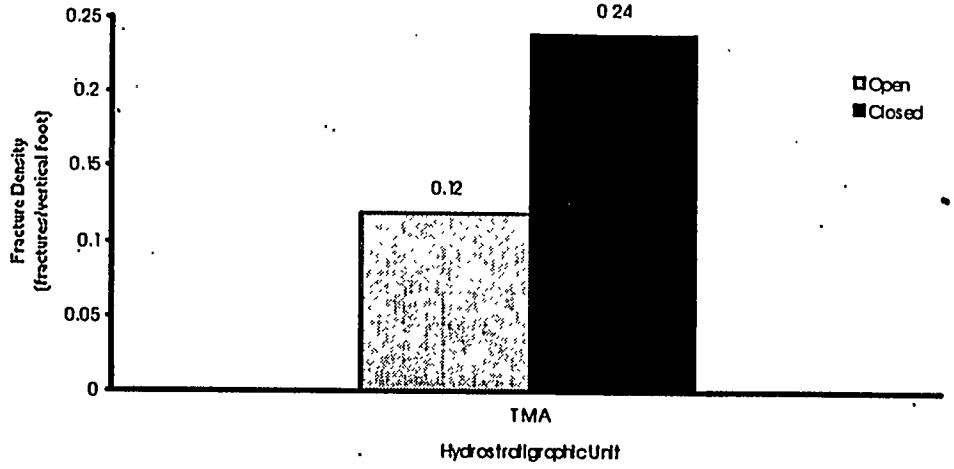

Figure 2-8a
Density of Open and Closed Fractures Relative to Hydrostratigraphy at UE-18r

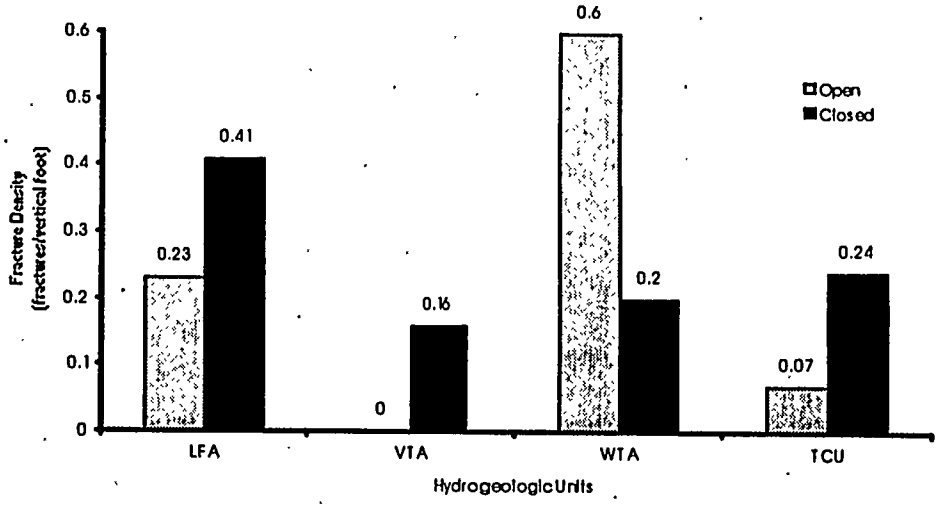

Figure 2-8b
Density of Open and Closed Fractures Relative to Hydrogeology at UE-18r

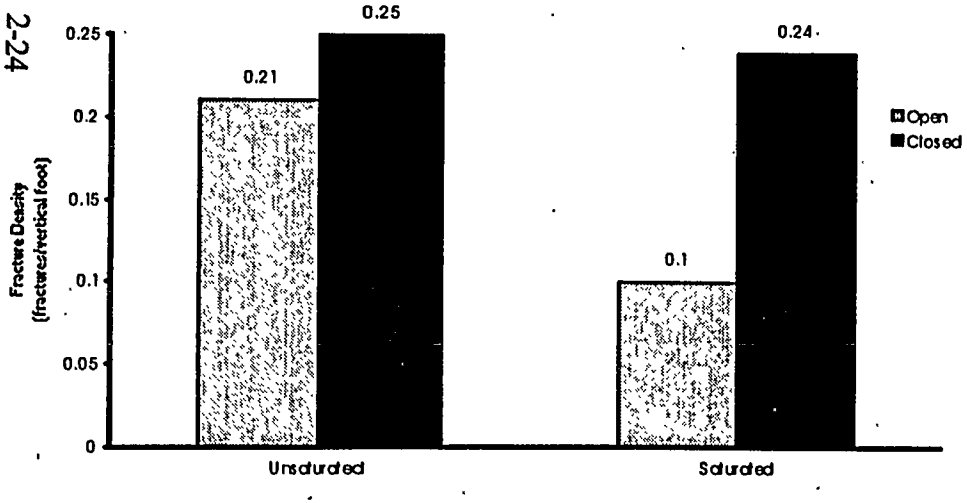

Figure 2-8c
Density of Open and Closed Fractures Relative to the Water Table at UE-18r

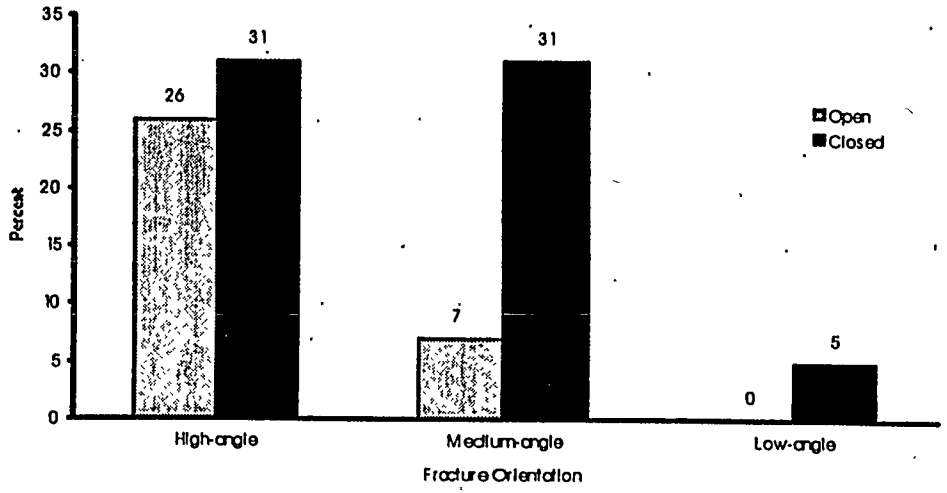

Figure 2-8d
Distribution of Open and Closed Fractures Relative to Orientation at UE-18r

Figure 2-8a-d
Density and Distribution of Fractures at Exploratory Hole UE-18r

Distribution of Open and Closed Fractures Relative to Orientation

In UE-18r, 79 percent of the open fractures are at high angles, and the remainder of open fractures are medium-angle; no low-angle open fractures were observed. The closed fractures are evenly distributed between high- and medium-angle orientations, with only two low-angle closed fractures observed (*Figure 2-8d*).

2.3.3.2 Aperture and Fracture Openness

Aperture and percent openness of open fractures in the UE-18r core have been analyzed relative to the HGUs and the HSU in which the fractures occur. These relationships are shown in Table 2-3 and outlined below.

Table 2-3
UE-18r Fracture Aperture and Percent Open Data

Data Grouped by Hydrostratigraphic Units

Hydrostratigraphic Units	Average Aperture (millimeters)	Percent Open
Timber Mountain Aquifer (TMA)	1.1	50 - 90 percent[1]

Data Grouped by Hydrogeologic Units

Hydrogeologic Unit	Average Aperture (millimeters)	Percent Open
Vitric-tuff aquifer (VTA)	*[2]	*[2]
Welded-tuff aquifer (WTA)	0.04	1 - 10 and 50 - 90 percent[3]
Lava-flow aquifer (LFA)	2.1[4]	50 - 90 percent
Tuff confining unit (TCU)	1.5	50 - 90 and 1 - 10 percent[5]

1 Percent open data collected is bimodal. The most popular group is 50 - 90 percent as shown; however, a lesser group of fractures fell into the 1 - 10 percent open category.

2 11.9 m (39.ft) of VTA core logged, but no open fractures observed.

3 Percent open data collected is bimodal; 66 percent of the fractures fell into the 1 - 10 percent open category, while 33 percent fell into the 50 - 90 percent category.

4 Average aperture is skewed by a single, 10 mm wide fracture in this relatively small data set (N=5).

5 Percent open data collected is bimodal; 66 percent of the fractures fell into the 50 - 90 percent category and 33 percent fell into the 1 - 10 percent category.

Aperture and Openness Relative to Hydrostratigraphic Units

The average aperture for fractures within the TMA is relatively large at 1.1 mm (0.04 in.) (*Table 2-3*). The average percent open for the fractures is 50 - 90 percent.

Aperture and Openness Relative to Hydrogeologic Units

Both the LFA and TCU contain fractures with relatively large average apertures of 2.1 mm (0.08 in.) and 1.5 mm (0.06 in.), respectively. In contrast, fractures within the WTA have a very small average aperture of 0.04 mm (0.002 in.). Most of the fractures within the LFA and TCU average greater than 50 percent open, whereas most of the fractures within the WTA average less than 10 percent open.

2.3.3.3 Mineralogy of Fracture Coatings

The distribution of fracture-coating minerals in core from UE-18r is illustrated by hydrostratigraphic unit, hydrogeologic unit, and relative to the water table in Figure 2-9a-c.

Distribution of Fracture-Coating Minerals in Hydrostratigraphic Units

The distribution of fracture-coating minerals in the UE-18r core, all of which is assigned to the TMA, is presented in *Figure 2-9a.* Zeolites (clinoptilolite and mordenite) are the most abundant fracture-coating or -filling minerals in the core, followed by iron/manganese oxides and chalcedony.

Distribution of Fracture-Coating Minerals in Hydrogeologic Units

Marked variation exists in the distribution of fracture-coating minerals between the four HGUs represented in the UE-18r core sections. The following relationships are shown in *Figure 2-9b*:

- LFA - dominant zeolites, common chalcedony, minor clay, unknown silicates, and Fe/Mn oxides
- VTA - even distribution between zeolites Fe/Mn oxides, and fault gouge
- WTA - common chalcedony and Fe/Mn oxides; all others absent
- TCU - strongly dominant zeolites, minor quartz Fe/Mn oxides, and clay

Zeolites are the predominant fracture-coating mineral in the TCU and the LFA and very common in the VTA, but not observed in the WTA. Conversely, Fe/Mn oxides are very common in the WTA, but not observed at all in the other HGUs. Chalcedony is common in the WTA and the LFA, but not present in the VTA or TCU. Euhedral quartz is observed only in the TCU.

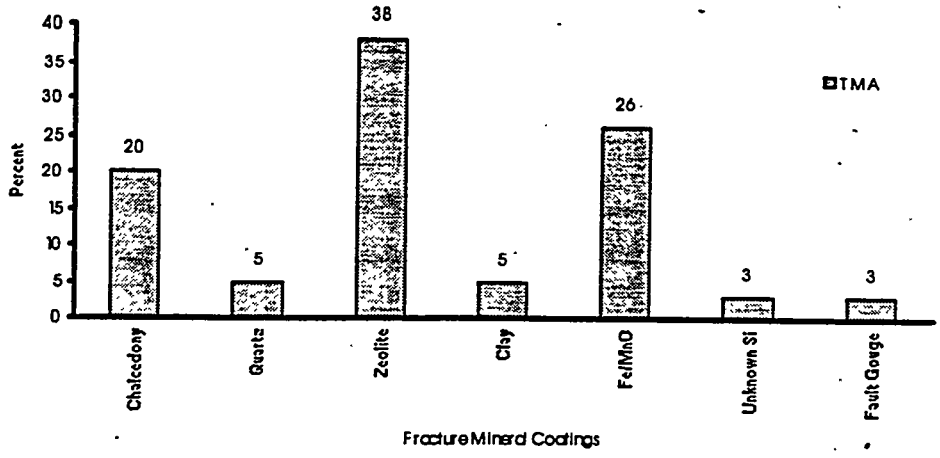

Figure 2-9a
Distribution of Fracture Mineral Coatings Relative to Hydrostratigraphy at UE-18r

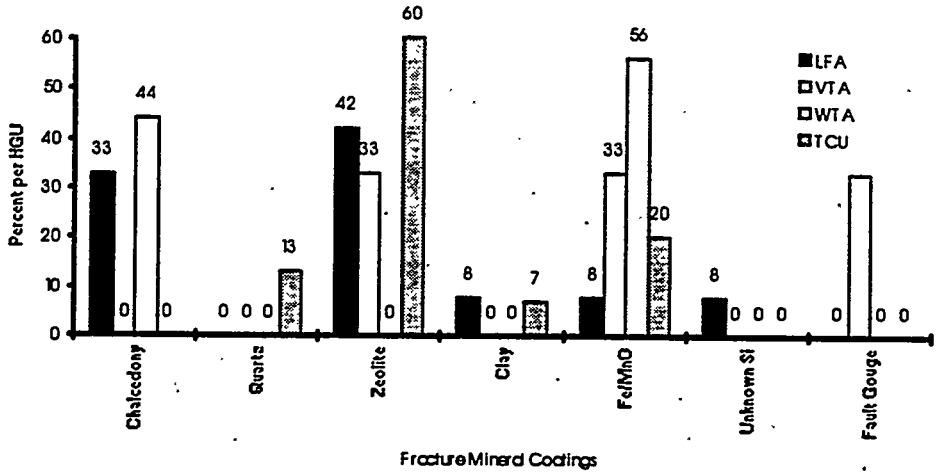

Figure 2-9b
Distribution of Fracture Mineral Coatings Relative to Hydrogeology at UE-18r

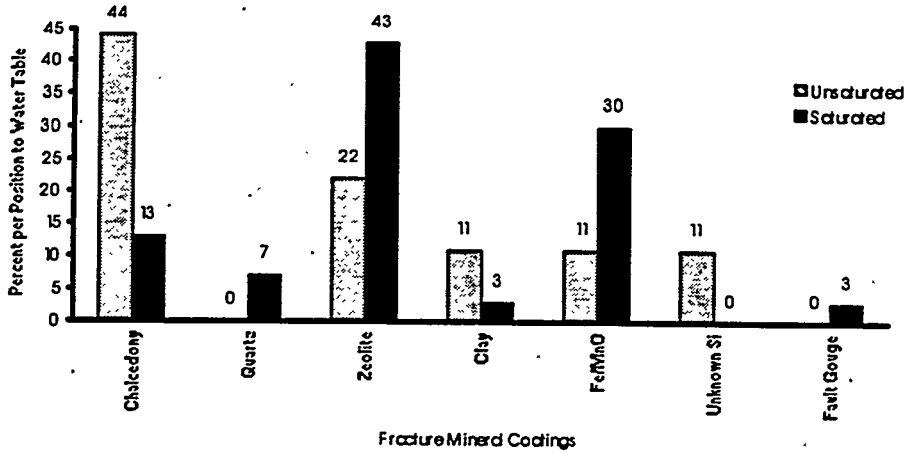

Figure 2-9c
Distribution of Fracture Mineral Coatings Relative to the Water Table at UE-18r

Figure 2-9a-c
Distribution of Fracture Mineral Coatings at UE-18r

Distribution of Fracture-Coating Minerals Relative to the Water Table

The distribution of fracture-coating minerals relative to the water table in UE-18r is illustrated in *Figure 2-9c*. Chalcedony is the primary fracture-coating mineral present above the water table, followed by zeolites, with clay minerals, Fe/Mn oxides, and unidentified silicate minerals also present. Below the water table, zeolites are the most abundant fracture-coating material, followed by Fe/Mn oxides with all other mineral species relatively uncommon.

2.3.4 Comparisons of Fracture Data, Available Hydraulic Test Data, and Caliper Log

Direct comparison between aquifer hydraulic tests conducted in the UE-18r wellbore and core fracture data is not straightforward. Only a small percentage (2.4 percent) of the borehole was cored; furthermore, the short intermittent cores do not always correlate to the much longer borehole hydrologic test intervals.

In general, given the above caveats, core fracture data correlates well with the hydraulic properties derived from tests conducted in 1968. The most transmissive intervals identified by borehole hydrologic tests correspond to fractured LFAs and WTAs. The impermeable zones correspond to less fractured zeolitized units classified hydrogeologically as TCUs. For example, one of the more permeable intervals, 676.7 to 681.2 m (2,220 to 2,235 ft) noted in Carr, *et al.* (1968, 1981) corresponds to a cored interval 679.1 to 680.9 m (2,228 to 2,234 ft), where a high number of open fractures are observed. Two cores from 492.3 to 494.4 m (1,615 to 1,622 ft) and 943.7 to 946.7 (3,096 to 3,106 ft) had no open fractures correspond to intervals having the lowest relative specific capacity values in the borehole (Figure 2-10). Note also that there is a fair correlation between borehole rugosity, as indicated by the caliper log and relative specific capacity values.

Analysis of more recent flow meter data indicate that a complex hydrologic flow regime may exist within the UE-18r borehole (Paillet, 1991). However, there is some question regarding the quality of this data and the validity of the flow meter tests under the existing borehole conditions (Paillet, 1994 and Adams, 1994). Because of this uncertainty, the flow meter results were not included in this fracture study.

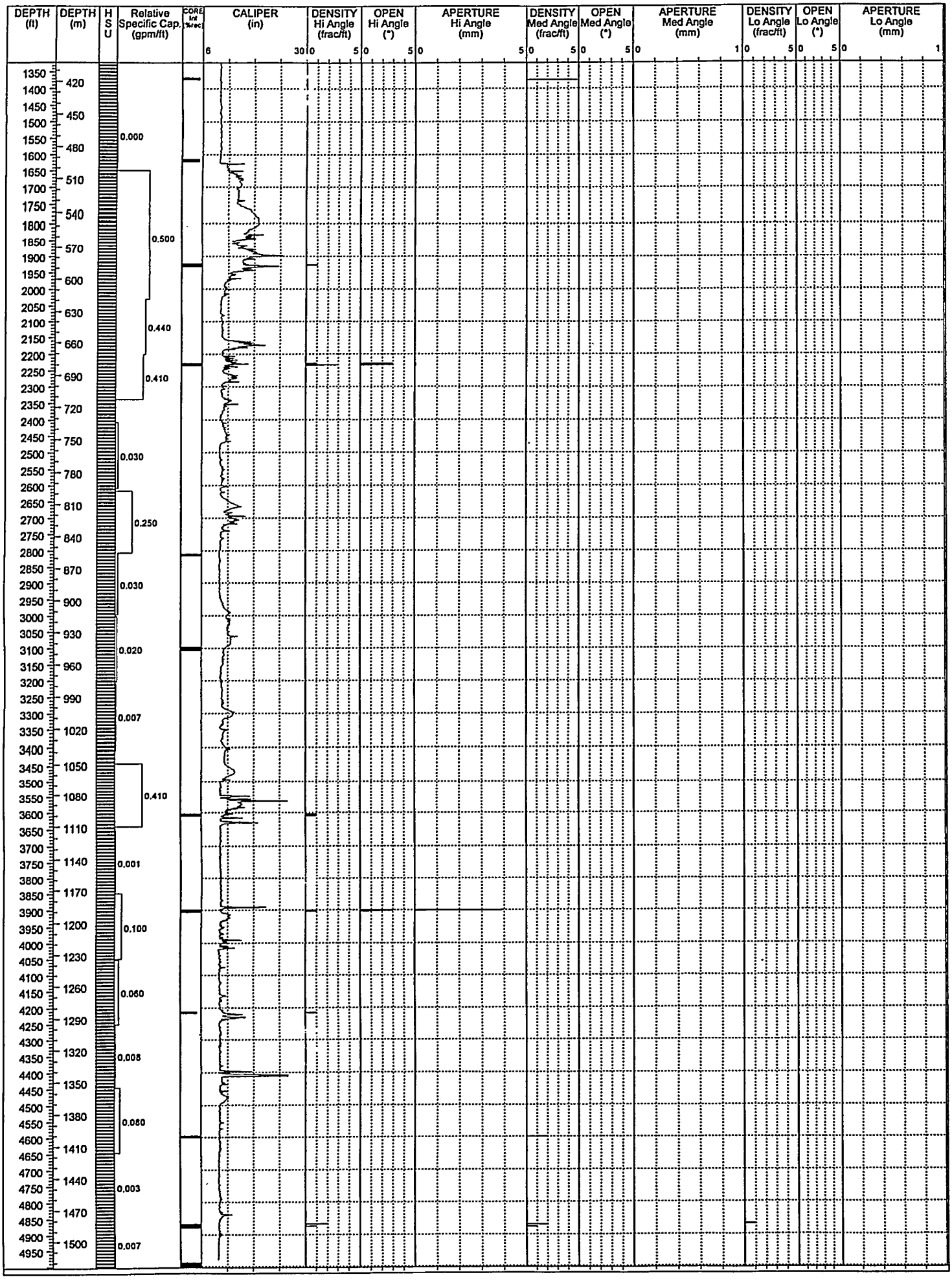
DEPTH (ft)
DEPTH (m)
H S U
Relative Specific Cap. (gpm/ft)
CORE Int %rec
CALIPER (in)
6
30
DENSITY Hi Angle (frac/ft)
OPEN Hi Angle (°)
APERTURE Hi Angle (mm)
DENSITY Med Angle (frac/ft)
OPEN Med Angle (°)
APERTURE Med Angle (mm)
DENSITY Lo Angle (frac/ft)
OPEN Lo Angle (°)
APERTURE Lo Angle (mm)
0
5
1
1350
1400
1450
1500
1550
1600
1650
1700
1750
1800
1850
1900
1950
2000
2050
2100
2150
2200
2250
2300
2350
2400
2450
2500
2550
2600
2650
2700
2750
2800
2850
2900
2950
3000
3050
3100
3150
3200
3250
3300
3350
3400
3450
3500
3550
3600
3650
3700
3750
3800
3850
3900
3950
4000
4050
4100
4150
4200
4250
4300
4350
4400
4450
4500
4550
4600
4650
4700
4750
4800
4850
4900
4950
420
450
480
510
540
570
600
630
660
690
720
750
780
810
840
870
900
930
960
990
1020
1050
1080
1110
1140
1170
1200
1230
1260
1290
1320
1350
1380
1410
1440
1470
1500
0.000
0.500
0.440
0.410
0.030
0.250
0.030
0.020
0.007
0.410
0.001
0.100
0.060
0.008
0.060
0.003
0.007

LEGEND

Hydrostratigraphic Unit (HSU)


Timber Mountain Aquifer (TMA)


Tuff Cone (TC)


Bullfrog Confining Unit (TCB)


Belted Range Aquifer (TBA)


Basal Aquifer (BAQ)

(•) OPEN
(for all angles)

Number	Estimated Range of Percent Openness
0	0%
1	1 – 10%
2	10 – 50%
3	50 – 90%
4	90 – 99%
5	100%

Figure 2-10
UE-18r: Composite Log of Hydrologic Test Data, Caliper Log, and Fracture Data, 402.3 Meters - TD

2.4 Exploratory Hole UE-20e#1

2.4.1 Hole History

The UE-20e#1 drill hole is located near the north flank of Pahute Mesa in northern Area 20 of the NTS at an elevation of 1,919.3 m (6,297 ft) (*Figure 1-1*). The hole was drilled to a TD of 1,949.2 m (6,395 ft) as part of an exploratory program conducted in 1964 to investigate sites prior to drilling emplacement holes (Hoover, 1964). Drill hole UE-20e#1 replaced the UE-20e drill hole that was prematurely abandoned at a depth of 737.6 m (2,420 ft) (Hoover, 1964). Table C-8 in Appendix C is an abridged summary of the drill hole statistics for the hole. The UE-20e#1 drill hole was intermittently cored during the drilling operation, and the core intervals are included in Table C-9 in Appendix C.

2.4.2 Hydrogeology

The UE-20e#1 drill hole is located in a north-south trending structural block within the buried, Silent Canyon caldera complex. The structural block is bound on the west side by the west-dipping, high-angle Purse fault, and on the east side by the Boxcar fault that has similar structural kinematics. The surface geology near the drill hole includes flat-lying, volcanic strata of the Trail Ridge Tuff (Ekren *et al.*, 1966).

This area is also included in the Southeastern Gold Flat structural block, as defined by Warren (1994). The TMA, TC, and TBA comprise the primary HSUs associated with this block as defined by area drill holes. The following HSUs were encountered in the UE-20e#1 drill hole:

- The TMA from the surface to 424.6 m (1,393 ft), which includes bedded tuff and partially welded to densely welded ash-flow tuff of the Thirsty Canyon Group and Timber Mountain Group
- The TC from 424.6 m (1,393 ft) to 1,558.7 m (5,114 ft), which consists primarily of lavas and zeolitized bedded tuffs of the Volcanics of Area 20
- The TBA from 1,558.7 m (5,114 ft) to TD, which includes mostly devitrified to zeolitized lava flows and bedded tuffs of the Belted Range Group.

The condensed lithologic log and the stratigraphic record for UE-20e#1 are included in Table C-10 in Appendix C.

Hydrologic tests conducted in UE-20e#1 are discussed in Section 2.4.4.

The UE-20e#1 drill hole was included in the study to provide fracture characteristics in the saturated section of the lower part of the TC and the TBA HSUs. Only the core intervals that contain these HSU intervals from 1,188.7 m (3,900 ft) to TD were analyzed for fracture characteristics.

2.4.3 Fracture Analysis

2.4.3.1 Density and Distribution

The density of fractures in the core sections from UE-20e#1 has been analyzed relative to occurrence within various HSUs and HGUs and relative to fracture orientation. In these analyses, the distribution of fractures has been examined separately for open and closed fractures. These relationships are shown in Figures 2-11 and 2-12a-c and discussed below.

Vertical Distribution of Open and Closed Fractures

Figure 2-11 shows the cored intervals examined and the vertical distribution of open and closed fractures within HGUs and HSUs in the UE-20e#1 core. The figure also presents data about the aperture, openness, and density of fractures at high, medium, and low angles. The figure also illustrates the relationship of fracture distribution to the caliper log.

Density of Open and Closed Fractures in Hydrostratigraphic Units

The cored intervals examined from Exploratory Hole UE-20e#1 represent strata that have been assigned to the TC and the TBA. The density of closed and open fractures is significantly higher in the TBA than in the TC. The density of closed fractures in the TBA is twice that of open fractures and even greater in the TC (*Figure 2-12a*).

Density of Open and Closed Fractures in Hydrogeologic Units

Two HGUs (the LFA and the TCU) are represented in the UE-20e#1 core. The density of open and closed fractures is significantly higher in the LFA than in the TCU. In both HGUs, the density of closed fractures exceeds that of open fractures (*Figure 2-12b*).

Distribution of Fractures Relative to Orientation

In UE-20e#1, the density of open and closed fractures are greatest at high-angle orientations. Closed fractures were also abundant at medium angles, but rare at low angles. The density of open fractures is negligible at medium and low angles (*Figure 2-12c*).

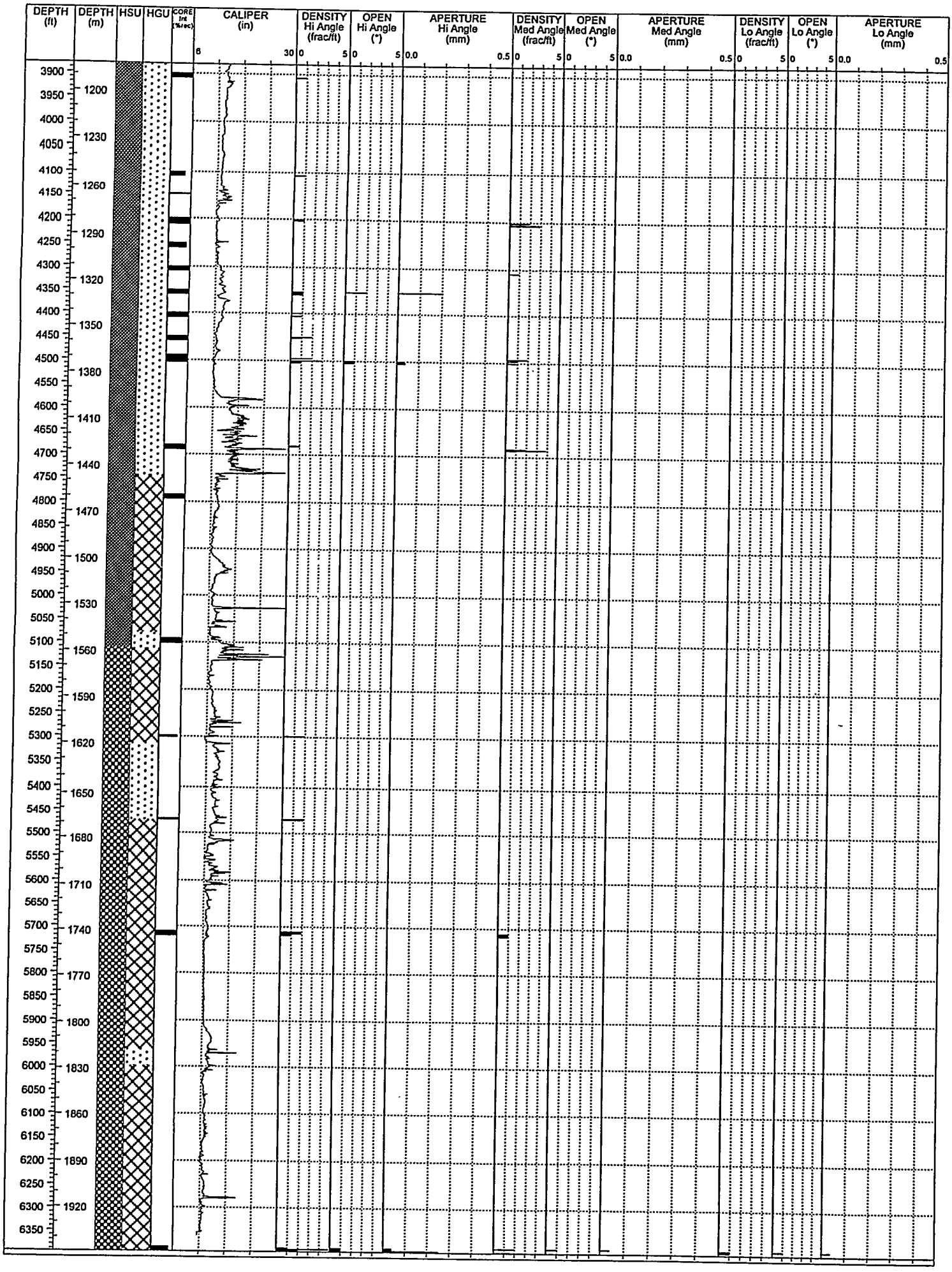
DEPTH (ft)
DEPTH (m)
HSU
HGU
CORE Int (%rec)
CALIPER (in)
6
30
DENSITY Hi Angle (frac/ft)
OPEN Hi Angle (°)
APERTURE Hi Angle (mm)
DENSITY Med Angle (frac/ft)
OPEN Med Angle (°)
APERTURE Med Angle (mm)
DENSITY Lo Angle (frac/ft)
OPEN Lo Angle (°)
APERTURE Lo Angle (mm)
0
5
0.0
0.5
3900
3950
4000
4050
4100
4150
4200
4250
4300
4350
4400
4450
4500
4550
4600
4650
4700
4750
4800
4850
4900
4950
5000
5050
5100
5150
5200
5250
5300
5350
5400
5450
5500
5550
5600
5650
5700
5750
5800
5850
5900
5950
6000
6050
6100
6150
6200
6250
6300
6350
1200
1230
1260
1290
1320
1350
1380
1410
1440
1470
1500
1530
1560
1590
1620
1650
1680
1710
1740
1770
1800
1830
1860
1890
1920

LEGEND

Hydrostratigraphic Unit (HSU)

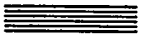
Timber Mountain Aquifer (TMA)


Tuff Cone (TC)


Bullfrog Confining Unit (TCB)


Belted Range Aquifer (TBA)


Basal Aquifer (BAQ)

Hydrogeologic Unit (HGU)


Welded–tuff aquifer (WTA)


Lava–flow aquifer (LFA)


Vitric–tuff aquifer (VTA)


Tuff confining unit (TCU)

(•) OPEN
(for all angles)

Number	Estimated Range of Percent Openness
0	0%
1	1 – 10%
2	10 – 50%
3	50 – 90%
4	90 – 99%
5	100%

Figure 2-11
UE-20e #1: Composite Log of Open and Closed Fracture Data, 1,182.6 Meters - TD

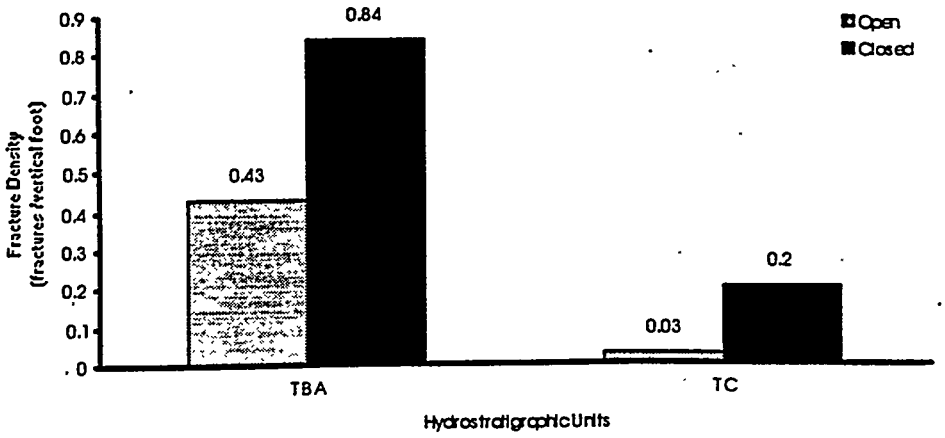

Figure 2-12a
Distribution of Open and Closed Fractures Relative to Hydrostratigraphy at UE-20e #1

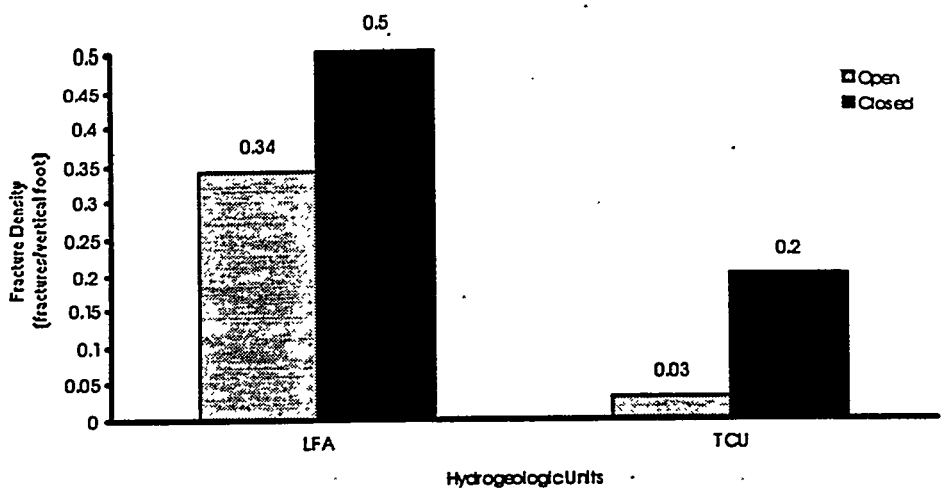

Figure 2-12b
Density of Open and Closed Fractures Relative to Hydrogeology at UE-20e #1

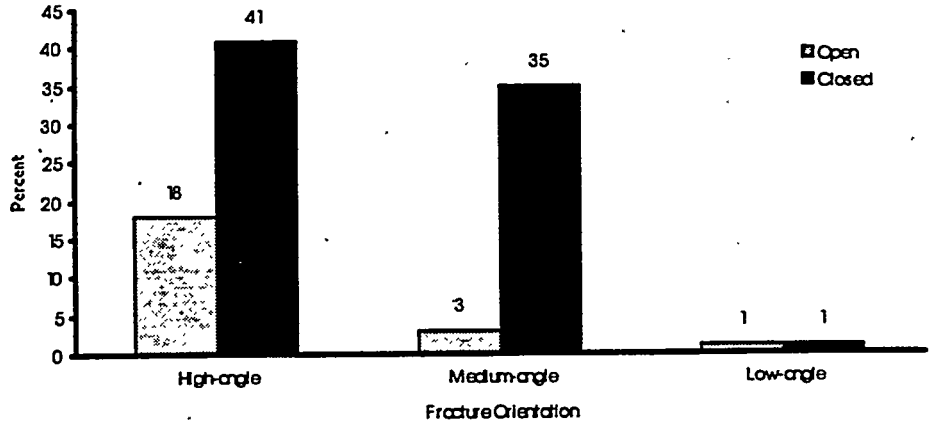

Figure 2-12c
Distribution of Open and Closed Fractures Relative to Orientation at UE-20e #1

Figure 2-12a-c
Density and Distribution of Fractures at UE-20e#1

2.4.3.2 Aperture and Fracture Openness

Aperture and percent openness of open fractures in the UE-20e#1 core have been analyzed relative to the HGUs and HSUs in which the fractures occur. These relationships are shown in Table 2-4 and discussed in the following text.

Aperture and Openness Relative to Hydrostratigraphic Units

Average apertures for fractures within both the TBA and TC are relatively small at 0.08 mm (0.003 in.) and 0.03 mm (0.001 in.), respectively (Table 2-4). Fractures within both HSU average 1 - 10 percent open.

Aperture and Openness Relative to Hydrogeologic Units

The average aperture and percent open for fractures within the LFA is the same as that for TBA (*Table 2-4*). This same relationship also holds true with regard to the TCU and the TC.

Table 2-4
UE-20e#1 Fracture Aperture and Percent Open Data

Data Grouped by Hydrostratigraphic Units

Hydrostratigraphic Units	Average Aperture (millimeters)	Percent Open
Tuff Cone (TC)	0.03	1 - 10 percent
Belted Range Aquifer (TBA)	0.08	1 - 10 percent

Data Grouped by Hydrogeologic Units

Hydrogeologic Unit	Average Aperture (millimeters)	Percent Open
Lava-flow aquifer (LFA)	0.08	1 - 10 percent
Tuff confining unit (TCU)	0.03	1 - 10 percent

2.4.3.3 Mineralogy of Fracture Coatings

Distribution of Fracture-Coating Minerals in Hydrostratigraphic Units

The distribution of fracture-coating minerals in the two HSUs present in the UE-20e#1 core (the TBA and the TC) is presented in Figure 2-13a. Zeolites (clinoptilolite and mordenite) are the predominant fracture-coating or -filling minerals in the TC, with other minerals (clays, chalcedony, quartz, vapor-phase silicates, and Fe/Mn oxides) being relatively rare. In contrast, Fe/Mn oxides are the dominant fracture-coating mineral in the TBA, followed by zeolites and clays.

Distribution of Fracture-Coating Minerals in Hydrogeologic Units

The distribution of fracture-coating minerals in the two HGUs present in the UE-20e#1 core (the LFA and the TCU) is presented in Figure 2-13b. Because the LFA is essentially equivalent to the TBA HSU and the TCU is equivalent to the TC HSU in this core, the distribution of mineral coatings is essentially the same for HGUs as for the HSUs.

2.4.4 Comparison of Fracture Data, Available Hydraulic Test Data, and Caliper Logs

Hydrologic tests were conducted in UE-20e#1 in 1964 (Hoover, 1964) to determine the water-yielding potential of the volcanic rock and to ascertain whether the site is suitable for an emplacement hole. In most cases, the tests were intentionally limited to low permeable zones that would be favorable to the development of mined chambers.

When the hydrologic data from the test intervals are compared to the fracture data derived from the analyzed core, only limited qualitative conclusions can be reached. The very small ratio of available core to the hydrologic test interval precludes a useful comparison.

The hydrologic tests included isolating six 60.4-m (198-ft) intervals and one 565.4-m (1,855-ft) interval with packers and conducting either injection or swab tests. The test results indicate very low relative specific capacities in the 60.4-m (198-ft) intervals (ranging from 0.014 - 0.130 gallons per minute per foot of drawdown). The relative specific capacity in the 565.4-m (1,855-ft) interval was not recorded because there was no measurable drawdown five minutes after swabbing ceased (Hoover, 1964). Only three test intervals with data correspond with core examined in this study, and they are presented on Figure 2-14 as they compare to fracture distribution and caliper logs.

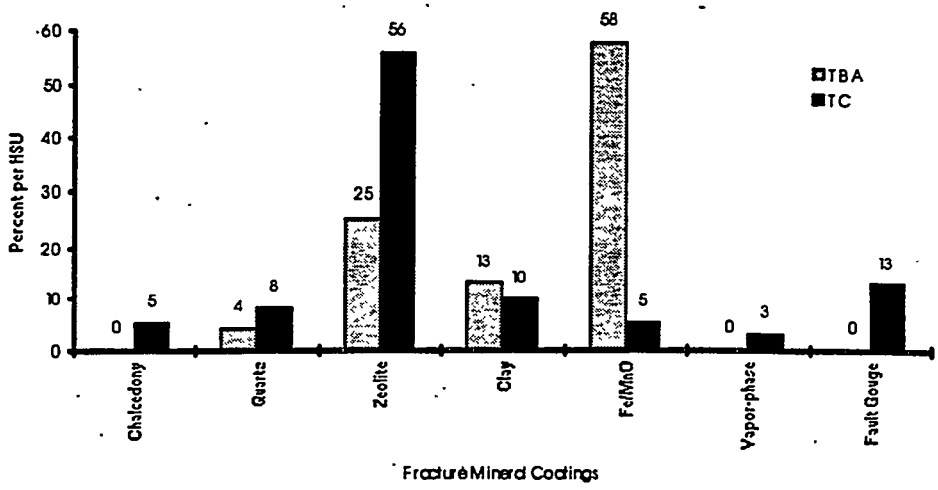

Figure 2-13a
Distribution of Fracture Mineral Coatings Relative to Hydrostratigraphy at UE-20e #1

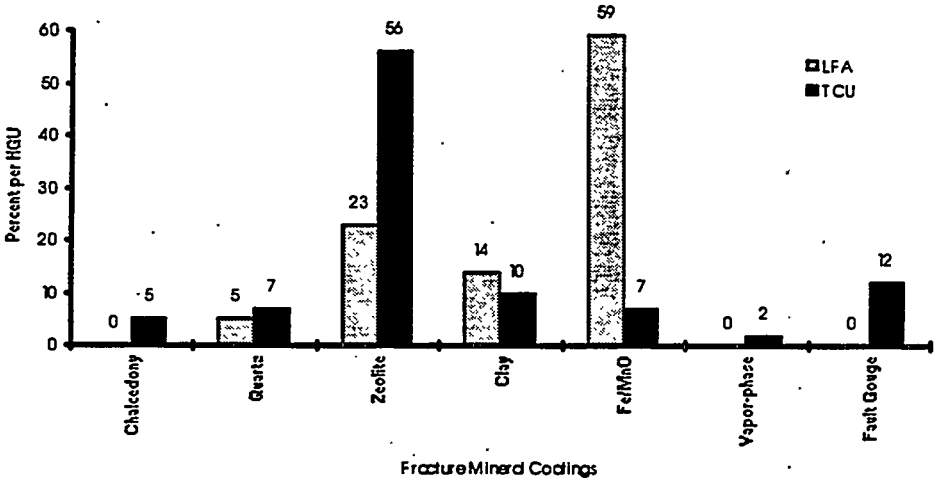

Figure 2-13b
Distribution of Fracture Mineral Coatings Relative to Hydrogeology at UE-20e #1

Figure 2-13a-b
Distribution of Fracture Mineral Coatings at UE-20e #1

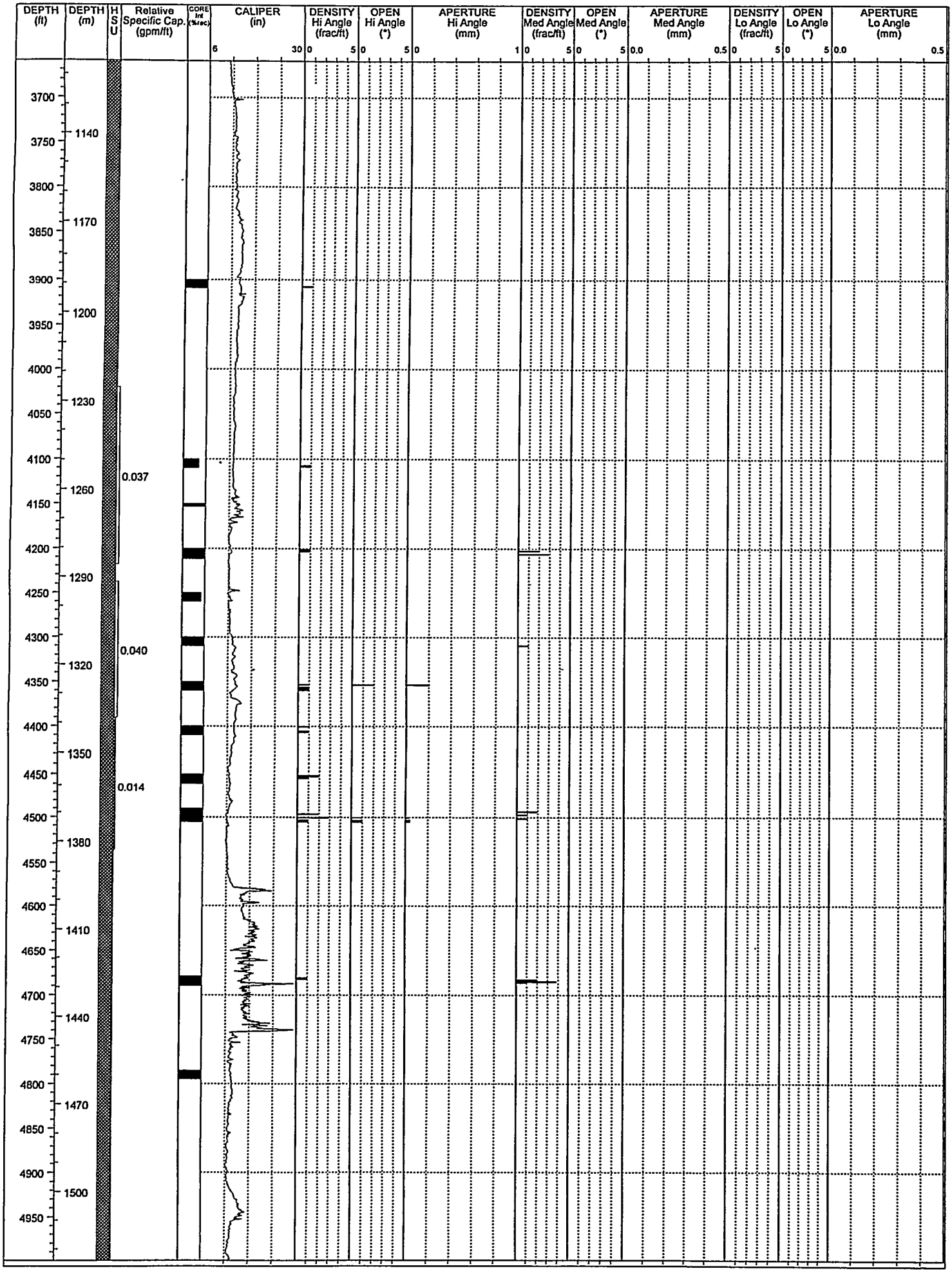
DEPTH (ft)
DEPTH (m)
H S U
Relative Specific Cap. (gpm/ft)
CORE Int (%rec)
CALIPER (in)
DENSITY Hi Angle (frac/ft)
OPEN Hi Angle (°)
APERTURE Hi Angle (mm)
DENSITY Med Angle (frac/ft)
OPEN Med Angle (°)
APERTURE Med Angle (mm)
DENSITY Lo Angle (frac/ft)
OPEN Lo Angle (°)
APERTURE Lo Angle (mm)
6
30
0
5
0
5
0
1
0
5
0
5
0.0
0.5
0
5
0
5
0.0
0.5
3700
3750
3800
3850
3900
3950
4000
4050
4100
4150
4200
4250
4300
4350
4400
4450
4500
4550
4600
4650
4700
4750
4800
4850
4900
4950
1140
1170
1200
1230
1260
1290
1320
1350
1380
1410
1440
1470
1500
0.037
0.040
0.014

LEGEND

Hydrostratigraphic Unit (HSU)


Timber Mountain Aquifer (TMA)


Tuff Cone (TC)


Bullfrog Confining Unit (TCB)


Belted Range Aquifer (TBA)


Basal Aquifer (BAQ)

(•)OPEN
(for all angles)

Number	Estimated Range of Percent Openness
0	0%
1	1 – 10%
2	10 – 50%
3	50 – 90%
4	90 – 99%
5	100%

Figure 2-14
UE-20e #1: Composite Log of Hydrologic Test Data, Caliper Log, and Fracture Data, 1,115.6 - 1,524 Meters

In each of the 60.4-m (198-ft) intervals, the low relative specific capacities compared favorably with the low fracture densities that ranged from 0-3 fractures per interval with less than 10 percent openness. Although the fracture data agree with the results of the tests from a qualitative standpoint, it is important to note that on average, less than 18 percent of the hydrologic test interval had core available for fracture analysis.

The caliper log on *Figure 2-14* indicates some degree of borehole rugosity through the 60.4-m (198-ft) test zones. The rugosity does not appear to be directly associated with fractured intervals or flow zones as indicated by the hydrologic test results and limited fracture data.

2.5 Monitoring Well UE-20bh#1

2.5.1 Hole History

The UE-20bh#1 drill hole is located on Pahute Mesa in eastern Area 20 of the NTS at an elevation of 2,022.8 m (6,636.6 ft) (see *Figure 1-1*). The hole was drilled in 1991 to a total depth of 856.5 m (2,810 ft) as part of the Hydrologic Radionuclide Migration Program (HRMP) to investigate and characterize groundwater flow in southeast Pahute Mesa (Boyd *et al.*, 1992). The hole was intermittently cored during the drilling operation at three separate intervals. Table C-11 in Appendix C is an abridged summary of the drill hole statistics for UE-20bh#1, and Table C-12 in Appendix C includes the core intervals.

The primary purpose for including UE-20bh#1 in the fracture study was to compare fracture characteristics derived from the core to characteristics interpreted from the BHTV and FMS logs. A secondary objective was to collect additional fracture data to expand the TC data set.

2.5.2 Hydrogeology

The UE-20bh#1 drill hole is located in a north-south trending structural block within the Silent Canyon caldera complex. The structural block is bound on the west side by the west-dipping, West Greely fault, and on the east side by the west-dipping, East Greely fault system. The surface geology in the area includes gentle, east dipping, volcanic strata of the Timber Mountain group and a local, thin veneer of alluvium. This area is also included in the Central Area 19 structural block (Warren, 1994).

The TMA, TC, TCB, and TBA comprise the primary HSUs associated with this block as defined by drill holes in the area. UE-20bh#1 penetrated only volcanic rocks of the TMA and TC HSUs. From below 169.2 m (955 ft) to total depth, the drill hole penetrated approximately 687.3 m

(209 ft) of caldera-filling rock types representing the TC. These include various lavas and tuffs of the Calico Hills Formation. From the surface to the top of the Calico Hills Formation, the drill hole encountered caldera-burying units consisting of ash-flow and bedded tuffs of the Rainier Mesa Tuff that are included in the TMA. The lithology and the stratigraphic record for the hole are provided in Table C-13 in Appendix C.

The static water level at UE-20bh#1 is reported at 674.7 m (2,214 ft) depth. Open-hole pumping tests were conducted in 1991 as part of the HRMP characterization effort at this site (Boyd *et al.*, 1992). These test results are discussed in Section 2.5.4.

2.5.3 Fracture Analysis

2.5.3.1 Density and Distribution

The density of fractures in the core sections from UE-20bh#1 has been analyzed relative to occurrence within the HSU and HGUs and relative to fracture orientation. In these analyses, the distribution of fractures has been examined separately for open and closed fractures. These relationships are shown in Figures 2-15 and 2-16a-c and discussed in the following text.

Vertical Distribution of Open and Closed Fractures

Figure 2-15 shows the cored intervals examined and the vertical distribution of open and closed fractures within HGUs and HSU in the UE-20bh#1 core. The figure also presents data on the aperture, openness, and density of fractures at high, medium, and low angles. The figure also shows the relationship of fracture distribution to the caliper log.

Density of Open and Closed Fractures in Hydrostratigraphic Units

All strata represented in the cored intervals from Monitoring Well UE-20bh#1 have been assigned to the TC. The density of closed fractures is significantly higher than the density of open fractures in the TC (*Figure 2-16a*).

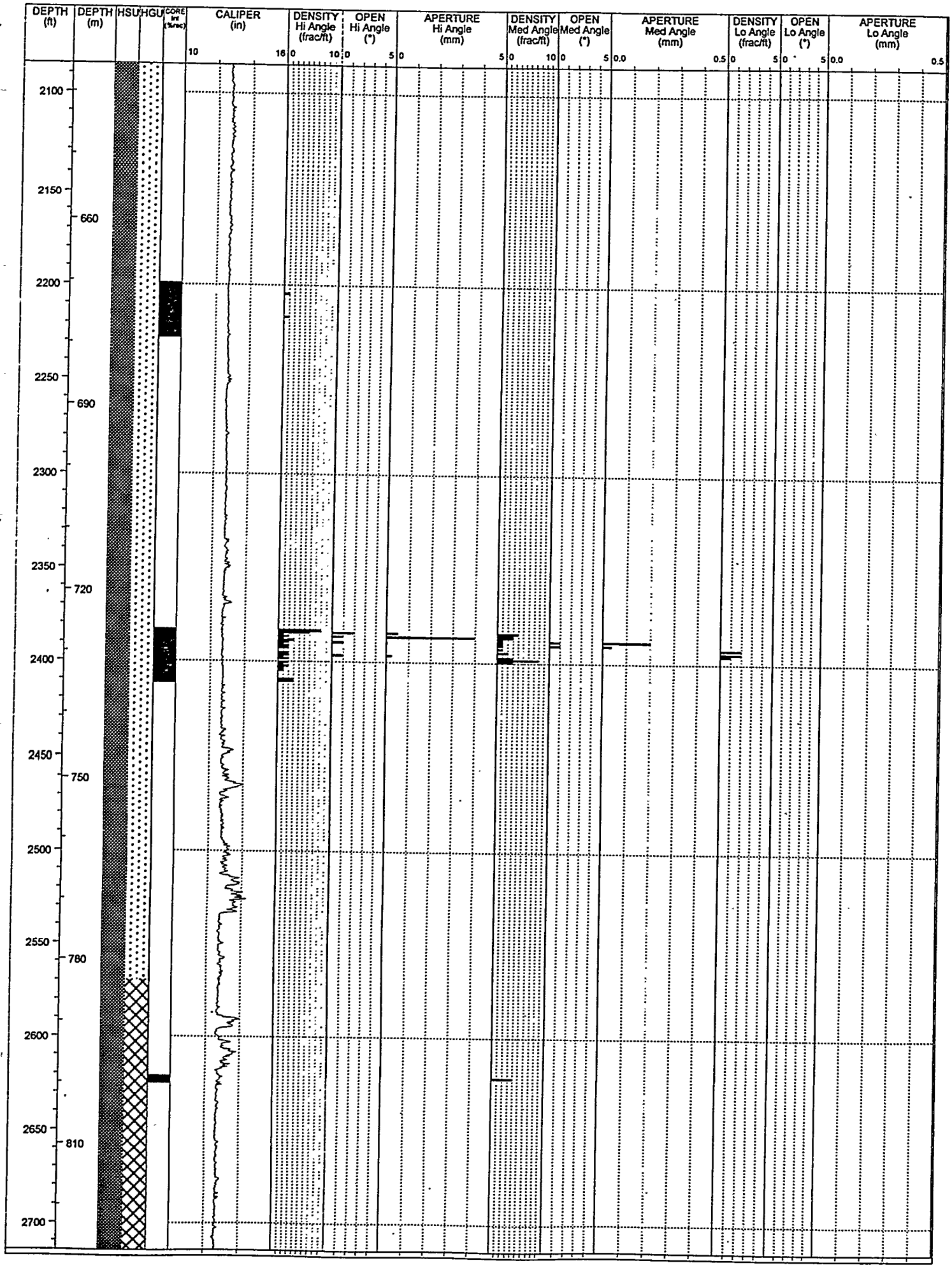
DEPTH (ft)
DEPTH (m)
HSU
HGU
CORE Int (%rec)
CALIPER (in)
10
16
DENSITY Hi Angle (frac/ft)
0
10
OPEN Hi Angle (°)
0
5
APERTURE Hi Angle (mm)
0
5
DENSITY Med Angle (frac/ft)
0
10
OPEN Med Angle (°)
0
5
APERTURE Med Angle (mm)
0.0
0.5
DENSITY Lo Angle (frac/ft)
0
5
OPEN Lo Angle (°)
0
5
APERTURE Lo Angle (mm)
0.0
0.5
2100
2150
660
2200
2250
690
2300
2350
720
2400
2450
750
2500
2550
780
2600
2650
810
2700

LEGEND

Hydrostratigraphic Unit (HSU)

Timber Mountain Aquifer (TMA)

Tuff Cone (TC)

Bullfrog Confining Unit (TCB)

Belted Range Aquifer (TBA)

Basal Aquifer (BAQ)

Hydrogeologic Unit (HGU)

Welded–tuff aquifer (WTA)

Lava–flow aquifer (LFA)

Vitric–tuff aquifer (VTA)

Tuff confining unit (TCU)

(•)OPEN
(for all angles)

Number	Estimated Range of Percent Openness
0	0%
1	1 – 10%
2	10 – 50%
3	50 – 90%
4	90 – 99%
5	100%

Figure 2-15
UE-20bh #1: Composite Log of Open and Closed Fracture Data, 635.5 - 827.5 Meters

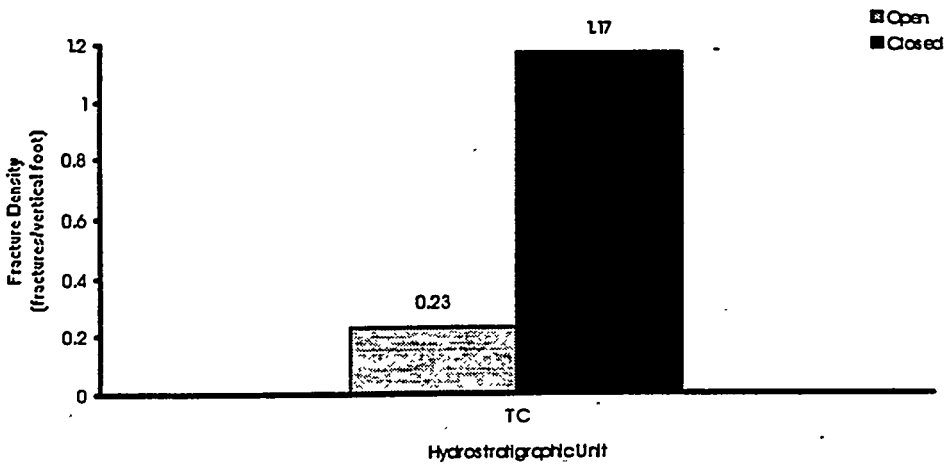

Figure 2-16a
Density of Open and Closed Fractures Relative to Hydrostratigraphy at UE-20bh #1

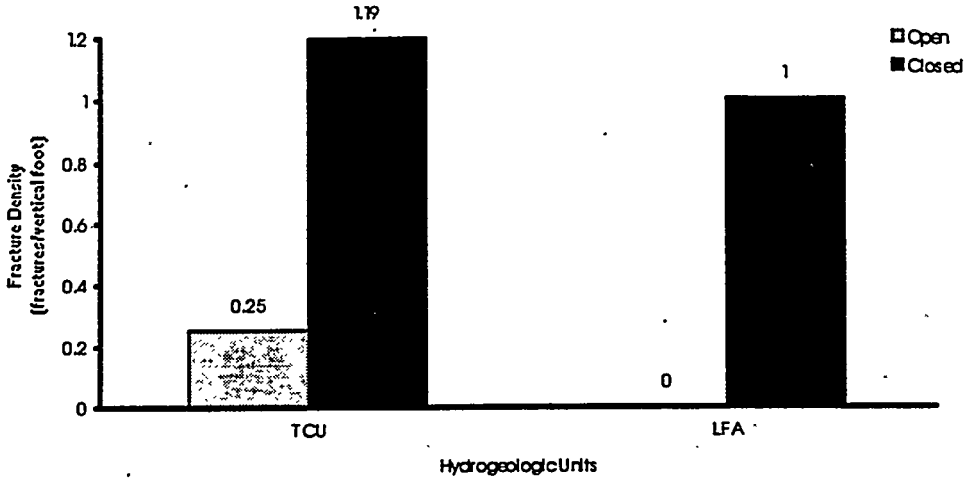

Figure 2-16b
Density of Open and Closed Fractures Relative to Hydrogeology at UE-20bh #1

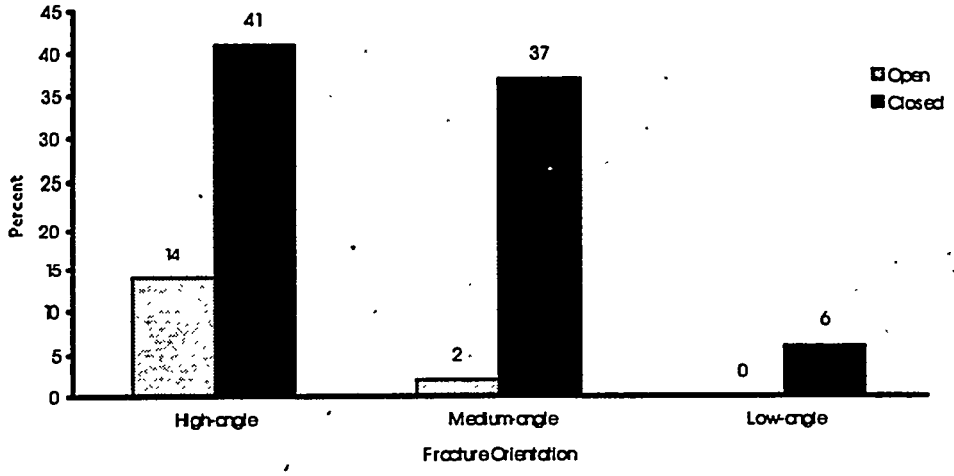

Figure 2-16c
Distribution of Open and Closed Fractures Relative to Orientation at UE-20bh #1

Figure 2-16a-c
Density and Distribution of Fractures at UE-20bh #1

Density of Open and Closed Fractures in Hydrogeologic Units

Two HGUs (the LFA and the TCU) are represented in the UE-20bh#1 core. In the TCU, the density of closed fractures greatly exceeds that of open fractures; in the LFA, all fractures were closed (*Figure 2-16b*). Note, however, that only 1.2 m (4 ft) of LFA was cored.

Distribution of Open and Closed Fractures Relative to Orientation

In UE-20bh#1, the percentage of open and closed fractures are greatest at high-angle orientations. Closed fractures were also abundant at medium angles, but rare at low angles. The percentage of open fractures is negligible at medium and low angles (*Figure 2-16c*).

2.5.3.2 Aperture and Fracture Openness

Aperture and percent openness of open fractures in the UE-20bh#1 core have been analyzed relative to the HGUs and the HSU in which the fractures occur. These relationships are shown in Table 2-5 and discussed in the following text.

Aperture and Openness Relative to Hydrostratigraphic Units

The average aperture for fractures within the TC, the only HSU cored at UE-20bh#1, is 0.8 mm (0.03 in.) (*Table 2-5*). The fractures average 1 - 50 percent open.

Table 2-5
UE-20bh #1 Fracture Aperture and Percent Open Data

Data Grouped by Hydrostratigraphic Units

Hydrostratigraphic Units	Average Aperture (millimeters)	Percent Open
Tuff Cone (TC)	0.8	1 - 50 percent

Data Grouped by Hydrogeologic Units

Hydrogeologic Unit	Average Aperture (millimeters)	Percent Open
Lava-flow aquifer (LFA)	*[1]	*[1]
Tuff confining unit[2] (TCU)	0.8	1 - 50 percent

1 Only 1.2 m (4 ft) of LFA logged; no open fractures.
2 Mostly zeolitized lava.

Aperture and Openness Relative to Hydrogeologic Units

Fracture aperture within the TCU averages 0.8 mm (0.03 in.) (*Table 2-5*). The average percent open for the fractures is 1 - 50 percent. No open fractures were observed within the LFA.

2.5.3.3 Mineralogy of Fracture Coatings

Distribution of Fracture-Coating Minerals in Hydrostratigraphic Units

The distribution of fracture-coating minerals in the TC in the UE-20bh#1 core is presented in Figure 2-17a. Zeolites, Fe/Mn oxides, and chalcedony occur in approximately equivalent abundances and are the dominant fracture-coating or -filling minerals in the core. Euhedral quartz and calcite occur in some fractures. Clay minerals were not observed in UE-20bh#1.

Distribution of Fracture-Coating Minerals in Hydrogeologic Units

The distribution of fracture-coating minerals in the two HGUs present in the UE-20bh#1 core (the LFA and the TCU) is presented in Figure 2-17b. The differences between the two HGUs are noteworthy. In the LFA, all fractures are coated with chalcedony; no other minerals were observed. In the TCU, zeolites, Fe/Mn oxides, and chalcedony occur in roughly equal amounts with quartz and calcite present in minor amounts.

2.5.4 Comparison of Fracture Data, Available Hydrologic Test Data, and Caliper Log

Rudimentary step drawdown pumping tests were conducted in the open borehole as part of the HRMP (Allen, 1993). Preliminary evaluation of these largely unprocessed and unpublished data indicate the presence of an aquifer of only moderate transmissivity. This is consistent with the hydrogeology of the saturated section; roughly 40 percent LFA (the bottom 73.2 m [240 ft] of the borehole) and 60 percent TCU. This ratio is not uncommon for the TC HSU.

The comparison between the fracture data and hydrologic test data is inconclusive, due to the limited amount of core and the nature of the tests. Furthermore, the caliper log provides no indication of the fractured interval at 726.3 to 735.2 m (2,383 -2,412 ft) (*Figure 2-15*).

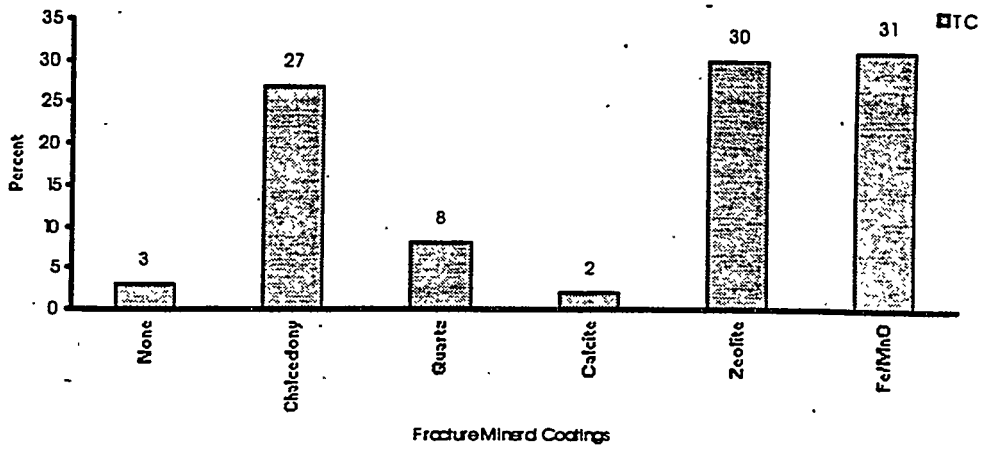

Figure 2-17a
Distribution of Fracture Mineral Coatings Relative to Hydrostratigraphy at UE-20bh #1

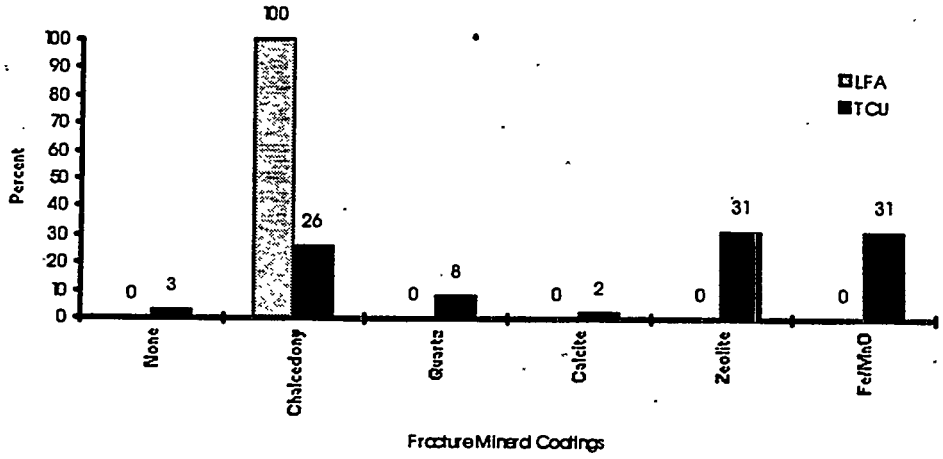

Figure 2-17b
Distribution of Fracture Mineral Coatings Relative to Hydrogeology at UE-20bh #1

Figure 2-17a-b
Distribution of Fracture Mineral Coatings at UE-20bh#1

2.6 Emplacement Hole U-20c and Exploratory Hole UE-20c

2.6.1 Well Histories

Exploratory Hole UE-20c is located in south central Pahute Mesa in Area 20 of the NTS (*Figure 1-1*). The hole was drilled in 1964 to characterize the subsurface geology prior to drilling nearby Emplacement Hole U-20c. UE-20c was rotary-drilled to a TD of 1,630.1 m (5,348 ft), short of the planned TD of 1,828.8 m (6,000 ft) because of severe hole sloughing problems (Santos, 1964). Thirty-five intermittent cores were obtained at various intervals between the depth of 137.2 and 1,573.1 m (450-5,161 ft). A summary of drill hole data for UE-20c is provided in Table C-14 in Appendix C. Coring data are provided in Table C-15 in Appendix C. Additional details regarding the UE-20c drill hole are included in Santos (1964).

Emplacement Hole U-20c is located 169.4 m (555.7 ft) west-northwest of UE-20c. This 1.83-m (72-in.) diameter emplacement hole was rotary-drilled in 1964 using dual-string, reverse circulation with air-foam to a TD of 1,463 m (4,800 ft). Six conventional cores were center-punched at various depths between 1,386.5 to 1,463.0 m (4,549 to 4,800 ft). Table C-16 in Appendix C is a summary of drill hole data for Emplacement Hole U-20c; core data is provided in Table C-17 in Appendix C.

Core data from these two holes were included in this fracture study for two reasons: 1) The core represents important hydrogeologic units associated with the BENHAM event; and 2) These holes are close to the UGTA near-field drilling site, Well Cluster ER-20-5. The BENHAM event was a relatively large-yield (1.15 Megaton) underground nuclear test conducted in December, 1968 in Emplacement Hole U-20c (DOE, 1994). Subsequently, the site of this test has been the subject of several hydrologic and radionuclide migration studies (Brikowski, 1991). This existing body of data, along with work planned at Well Cluster ER-20-5, has a potentional to influence CAU near-field experiments and modeling.

The extra core from U-20c was added to supplement the core available from UE-20c. All core from U-20c, 36.6 m (120 ft), and core below the static water level from UE-20c, approximately 72.8 m (239 ft), were logged for this study.

2.6.2 Hydrogeology

The UE-20c drill hole is located within the Silent Canyon caldera complex. The hole is situated on a north-south trending structural block bounded on the west by the Purse fault and on the east

by the West Boxcar fault. This block is included in the Western Area 20 structural block (Warren, 1994).

Exploratory Hole UE-20c penetrated 67.1 m (220 ft) of welded ash-flow and bedded tuffs related to the Thirsty Canyon Group and Volcanics at Fortymile Canyon; 222.5 m (730 ft) of welded ash-flow tuffs and minor bedded tuffs related to the Timber Mountain Group; and 640 m (2,100 ft) of rhyolite lavas, welded ash-flow tuffs and bedded tuffs related to the Paintbrush Group; and 700.4 m (2,298 ft) of interbedded lavas and bedded tuffs related to the Volcanics of Area 20. For simplicity, the stratigraphic and lithologic logs for both holes have been combined and referenced as the deeper hole, UE-20c, in Table C-18, in Appendix C.

All core examined is from the TC HSU. HGUs represented include the WTA, LFA, and the TCU. The static water level is about 648 m (2,126 ft) deep. Limited hydrogeologic tests (injection and swabbing) were conducted in 1964 within the center-punched portion of the U-20c drill hole, 1,390 to 1,463 m (4,560 to 4,800 ft) depth (Santos, 1964). These tests will be discussed in Section 2.6.4.

2.6.3 Fracture Analysis

2.6.3.1 Density and Distribution

The density of fractures in the core sections from U-20c/UE-20c has been analyzed relative to occurrence within the HSU and HGUs and relative to fracture orientation. In these analyses, the distribution of fractures has been examined separately for open and closed fractures. These relationships are shown in Figures 2-18 and 2-19a-c and discussed in the following text.

Vertical Distribution of Open and Closed Fractures

Figure 2-18 shows the cored intervals examined and the vertical distribution of open fractures in the HGUs and the TC HSU in the U-20c/UE-20c core. The figure also summarizes data on the aperture, openness, and density of fractures at high, medium, and low angles.

Density of Open and Closed Fractures in Hydrostratigraphic Units

All strata represented in the cored intervals from boreholes U-20c/UE-20c have been assigned to the TC. The density of open fractures is slightly higher than the density of closed fractures in the TC (*Figure 2-19a*).

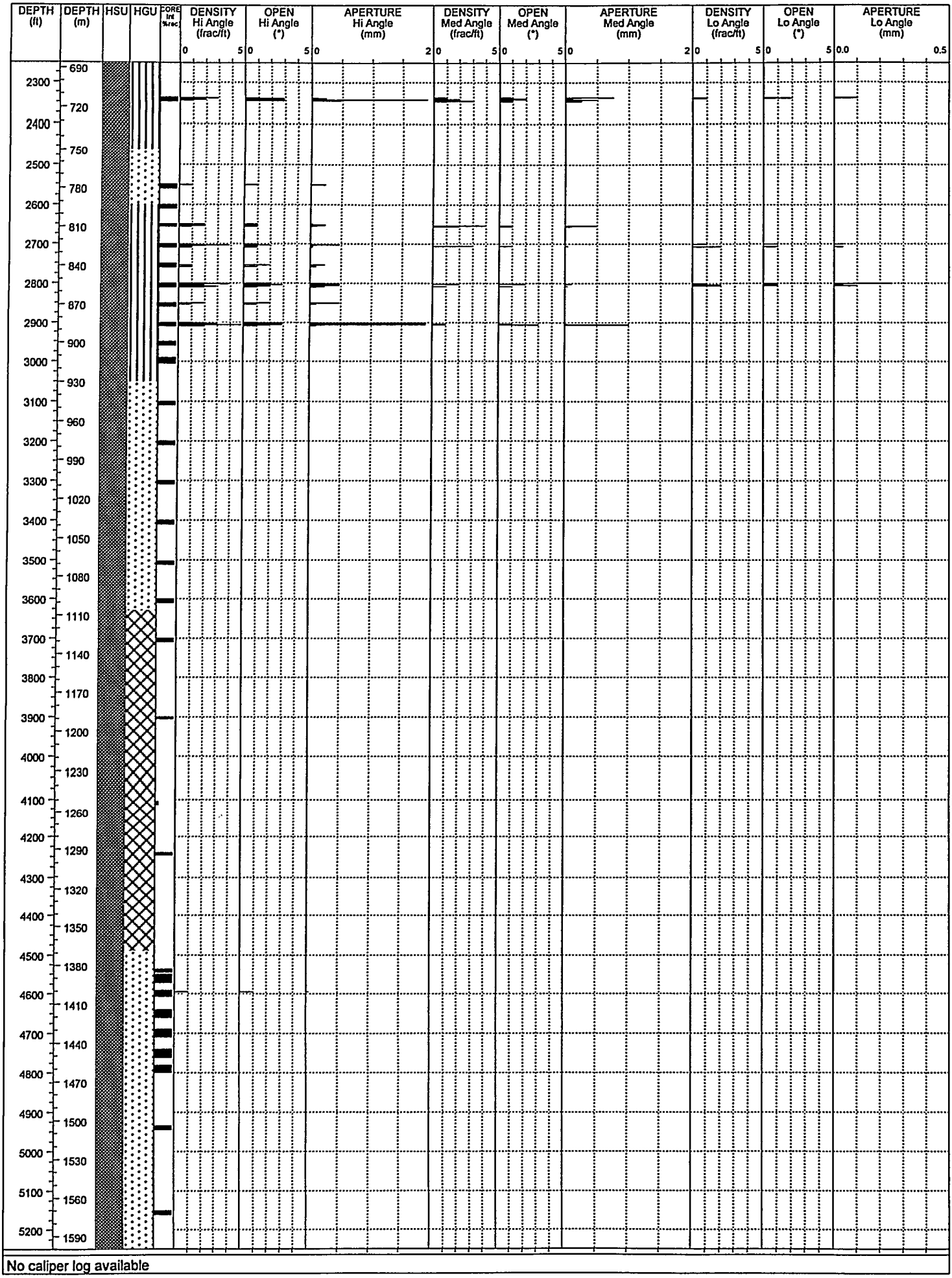

No caliper log available

LEGEND

Hydrostratigraphic Unit (HSU)


Timber Mountain Aquifer (TMA)


Tuff Cone (TC)


Bullfrog Confining Unit (TCB)


Belted Range Aquifer (TBA)


Basal Aquifer (BAQ)

Hydrogeologic Unit (HGU)


Welded–tuff aquifer (WTA)


Lava–flow aquifer (LFA)


Vitric–tuff aquifer (VTA)


Tuff confining unit (TCU)

(•) OPEN
(for all angles)

Number	Estimated Range of Percent Openness
0	0%
1	1 – 10%
2	10 – 50%
3	50 – 90%
4	90 – 99%
5	100%

Figure 2-18
UE-20c: Composite Log of Open Fracture Data, 685.8 Meters - TD

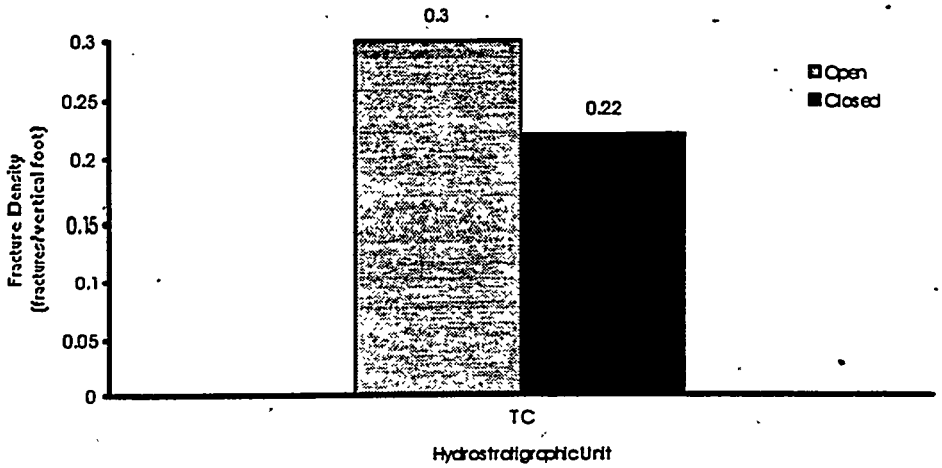

Figure 2-19a
Density of Open and Closed Fractures Relative to Hydrostratigraphy at U-20c/UE-20c

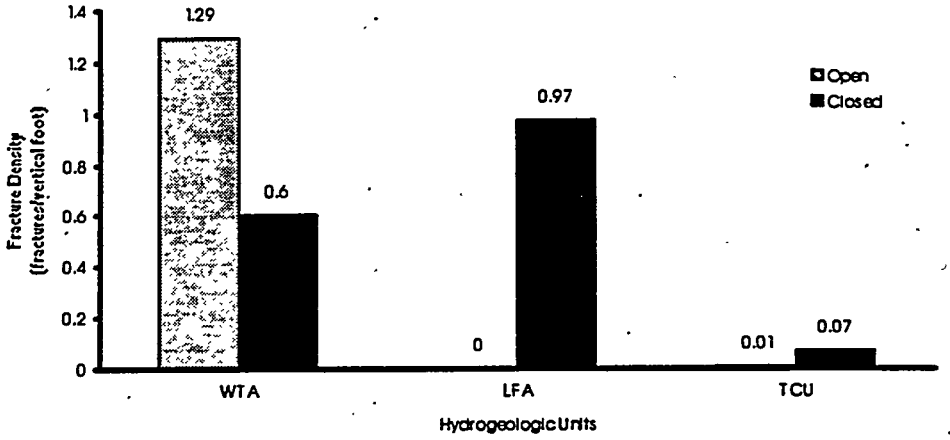

Figure 2-19b
Density of Open and Closed Fractures in Hydrogeologic Units at U-20c/UE-20c

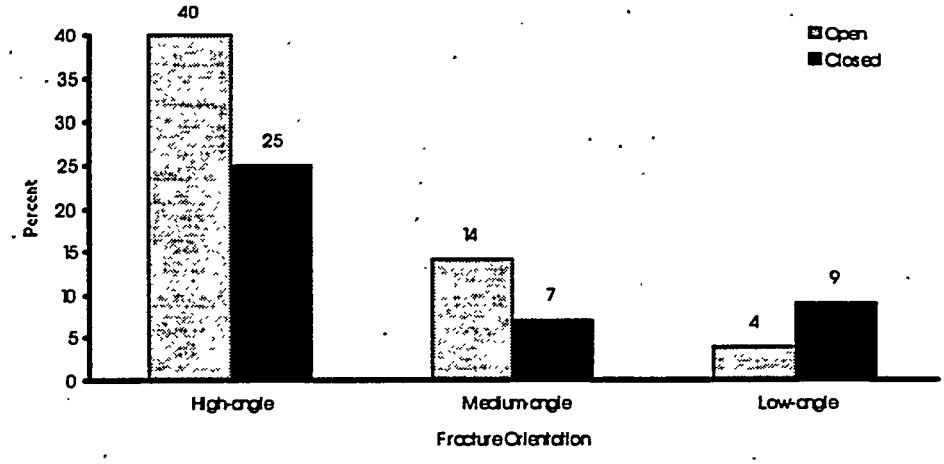

Figure 2-19c
Distribution of Open and Closed Fractures Relative to Orientation at U-20c/UE-20c

Figure 2-19a-c
Density and Distribution of Fractures at U-20c/UE-20c

Density of Open and Closed Fractures in Hydrogeologic Units

Three HGUs--the WTA, the LFA and the TCU--are represented in the U-20c/UE-20c cores. The density of open fractures is approximately twice that of closed fractures in the WTA. With the exception of two open fractures in the TCU, all other open fractures are in the WTA (*Figure 2-19b*).

Distribution of Open and Closed Fractures Relative to Orientation

In U-20c/UE-20c, the percentages of open and closed fractures are greatest at high-angle orientations. Closed fractures were more abundant than open fractures at low angles (*Figure 2-19c*).

2.6.3.2 Aperture and Fracture Openness

Aperture and percent openness of open fractures in the U-20c/UE-20c cores have been analyzed relative to the HGUs and the HSU in which the fractures occur. These relationships are shown in Table 2-6 and discussed below.

Table 2-6
U-20c/UE-20c Fracture Aperture and Percent Open Data

Data Grouped by Hydrostratigraphic Units

Hydrostratigraphic Units	Average Aperture (millimeters)	Percent Open
Tuff Cone (TC)	0.4	1 - 50 percent[1]

Data Grouped by Hydrogeologic Units

Hydrogeologic Unit	Average Aperture (millimeters)	Percent Open
Welded-tuff aquifer (WTA)	0.4	1 - 50 percent[1]
Lava-flow aquifer (LFA)	*[2]	*[2]
Tuff confining unit (TCU)	0.1	0 - 10 percent

1 Typical range (1 - 50 percent) is presented; however, the data set is skewed toward the low end (1 - 10 percent).
2 4.6 m (15 ft) of LFA core logged, but no open fractures observed.

Aperture and Openness Relative to Hydrostratigraphic Units

The average aperture for fractures within the TC is 0.4 mm (0.02 in.) (*Table 2-6*). Fractures were observed to average 1 - 50 percent open.

Aperture and Openness Relative to Hydrogeologic Units

Apertures for fractures within the WTA average 0.4 mm (0.02 in.), whereas fractures within the TCU have apertures that average considerably less at 0.1 mm (.004 in.) (*Table 2-6*). In addition to having a larger average aperture than those within the TCU, fractures within the WTA are also more open, averaging 1 - 50 percent versus 0 - 10 percent for TCU.

2.6.3.3 Mineralogy of Fracture Coatings

Distribution of Fracture-Coating Minerals in Hydrostratigraphic Units

The distribution of fracture-coating minerals in the TC in the U-20c/UE-20c cores is presented in Figure 2-20a. Fe/Mn oxides and chalcedony are the dominant mineral coatings in the cores, followed closely by clay minerals. Zeolites were conspicuously rare in these cores. Calcite and vapor-phase silicate minerals were observed in very low abundances.

Distribution of Fracture-Coating Minerals in Hydrogeologic Units

The distribution of fracture-coating minerals in the three HGUs present in the U-20c/UE-20c cores (the WTA, the LFA and the TCU) is presented in Figure 2-20b. Significant differences were found between the dominant mineral coatings in the three HGUs. In the WTA, chalcedony, Fe/Mn oxides, and clays are the dominant minerals, occurring in approximately equivalent proportions. In the LFA, calcite is the most abundant fracture-coating mineral, followed by chalcedony and Fe/Mn oxides in equal abundances. In fractures in the TCU, zeolites are the dominant mineral, with Fe/Mn oxides and chalcedony also abundant.

2.6.4 Fracture Data Comparisons with Available Hydrologic Test Data

Injection and swabbing tests were conducted in the 24.4-cm (9 5/8-in) diameter center-punched hole between 1,390 to 1,463 m (4,560 to 4,800 ft) depth. These data indicate that the interval has a very low relative specific capacity, on the order of 0.002 gallons per minute (gpm) per foot of drawdown (Blankennagel and Weir, 1966). This is consistent with its zeolitized bedded tuff lithology and its TCU assignment. Low fracture density (only one open fracture logged) and other attributes obtained from the cores recovered over the test interval are also consistent with

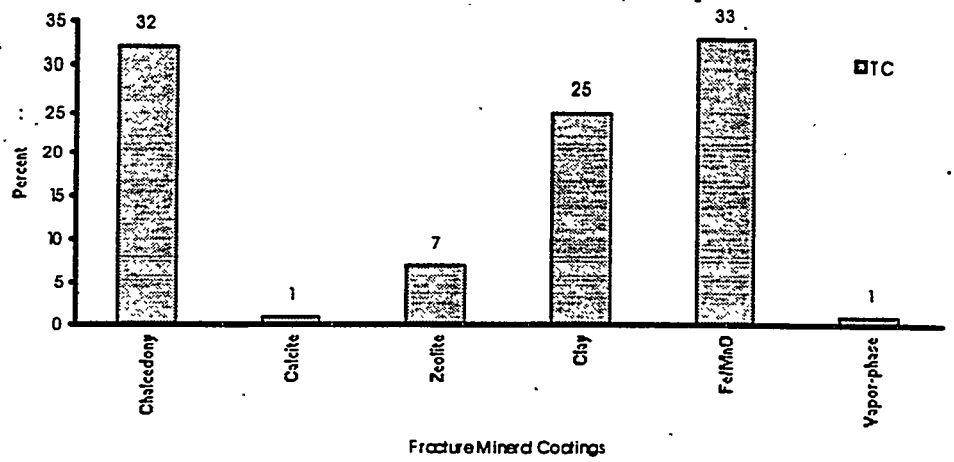

Figure 2-20a
Distribution of Fracture Mineral Coatings Relative to Hydrostratigraphy at U-20c/UE-20c

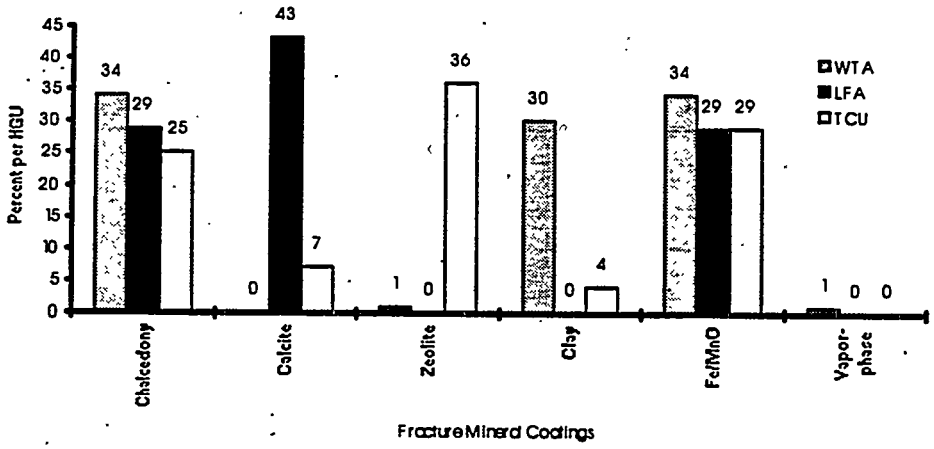

Figure 2-20b
Distribution of Fracture Mineral Coatings Relative to Hydrogeology at U-20c/UE-20c

Figure 2-20a-b
Distribution of Fracture Mineral Coatings at U-20c/UE-20c

the apparently poor hydraulic properties (Figure 2-21). No caliper log is available for the center-punched portion of the borehole in which the hydrologic tests were conducted.

2.7 Exploratory Hole UE-20f

2.7.1 Hole History

The UE-20f drill hole is located on Pahute Mesa in central Area 20 of the NTS at an elevation of 1,864.2 m (6,116 ft) (*Figure 1-1*). The hole was drilled in 1964 to a TD of 4,171.5 m (13,686 ft) as part of a program to explore individual sites on Pahute Mesa prior to drilling emplacement holes (Carroll, 1966). UE-20f is currently the deepest drill hole on the NTS and the intermittent cores that were cut during the drilling operation provide valuable lithologic and fracture information. Table C-19 in Appendix C is an abridged summary of the drill-hole statistics for UE-20f, and Table C-20 in Appendix C includes the core intervals.

2.7.2 Hydrogeology

Exploratory hole UE-20f is located in a north-south trending-structural block within the buried, Silent Canyon caldera complex. The structural block is bound on the west side by the high-angle, west-dipping Purse fault and on the east side by the West Boxcar fault that has similar structural kinematics. The surface geology in the area includes nearly horizontal, volcanic strata of the Trail Ridge Tuff (Ekren *et al.*, 1966).

This structural block is also included in the Western Area 20 structural block (Warren, 1994). Six HSUs are associated with this block and include the TMA, TC, TCB, TBA, BCU, and BAQ. Only the following five HSUs were encountered in the UE-20f drill hole. The HSUs are:

- TMA from the surface to 752.9 m (2,470 ft) depth, which includes bedded tuff and nonwelded to densely welded ash-flow tuff of the Thirsty Canyon Group and Timber Mountain Group
- TC from 752.9 m (2,470 ft) to 1,859.3 m (6,100 ft), which consists of lava flows, flow breccia, bedded tuff, and nonwelded to densely welded ash-flow tuff of the Paintbrush Group, Volcanics of Area 20, and the Crater Flat Group
- TCB from 1,859.3 m (6,100 ft) to 2,521.6 m (8,273 ft), which include the zeolitized, nonwelded ash-flow tuff of the mafic-poor, lithic-rich Bullfrog Tuff (Crater Flat Group)

This page intentionally left blank.

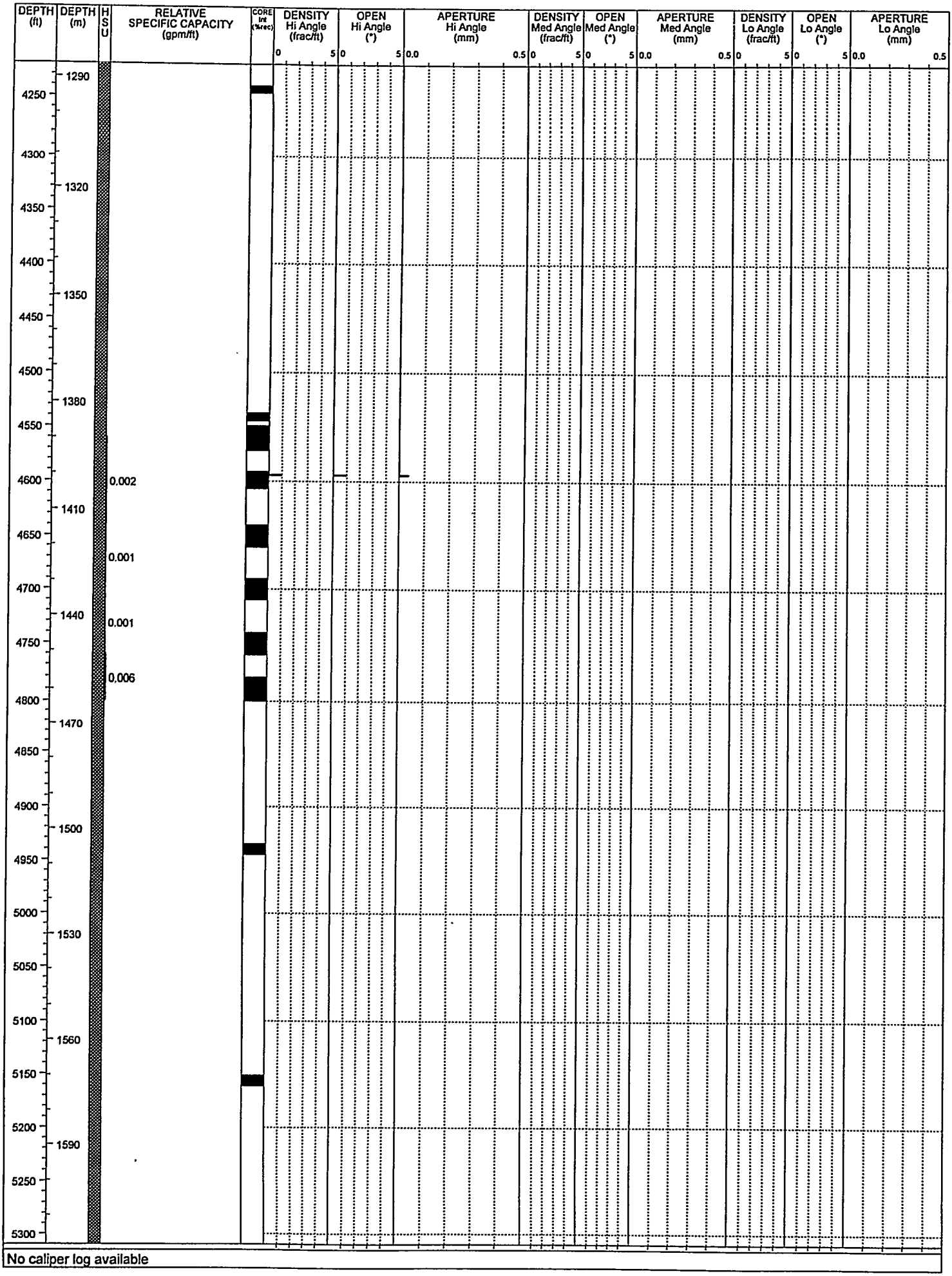

No caliper log available

LEGEND

Hydrostratigraphic Unit (HSU)

Timber Mountain Aquifer (TMA)

Tuff Cone (TC)

Bullfrog Confining Unit (TCB)

Belted Range Aquifer (TBA)

Basal Aquifer (BAQ)

(•) OPEN
(for all angles)

Number	Estimated Range of Percent Openness
0	0%
1	1 – 10%
2	10 – 50%
3	50 – 90%
4	90 – 99%
5	100%

Figure 2-21
UE-20c: Composite Log of Hydrologic Test Data and Fracture Data, 1,286.3 - 1,618.5 Meters

- TBA from 2,521.6 m (8,273 ft) to 3,378.7 m (11,085 ft), which consists of lava flows, flow breccia, and nonwelded to densely welded ash-flow tuff of the Belted Range Group and Volcanics of Big Dome

- BAQ from 3,378.7 m (11,085 ft) to TD, which includes lava flows and nonwelded to moderately welded ash-flow tuff of the Volcanics of Oak Spring Butte.

The lithologic characteristics that define the remaining HSU for this block, the BCU, were not encountered in the deepest stratigraphic interval of UE-20f, thus, precluding characterization. The condensed lithologic and stratigraphic log for the hole are outlined in Table C-21 in Appendix C.

The UE-20f drill hole was included in the fracture study to examine the HSUs present at depth in the caldera complex (TCB and BAQ). Additional data were collected from the TC and TBA to expand their respective datasets.

Hydrologic tests conducted in UE-20f are discussed in Section 2.7.4. The static water level was recorded at 595.6 m (1,954 ft).

2.7.3 Fracture Analysis

2.7.3.1 Density and Distribution

The density of fractures in the core sections from UE-20f has been analyzed relative to occurrence within various HSUs and HGUs, and relative to fracture orientation. In these analyses, the distribution of fractures has been examined separately for open and closed fractures. These relationships are shown in Figures 2-22, 2-23, and 2-24a-c and discussed in the following text.

Vertical Distribution of Open and Closed Fractures

Figures 2-22 and 2-23 show the core intervals examined and the vertical distribution of open fractures in the UE-20f core. The figures also present data on the aperture, openness, and density of fractures at high, medium, and low angles. The figures also show the relationship of fracture density and the caliper log.

This page intentionally left blank.

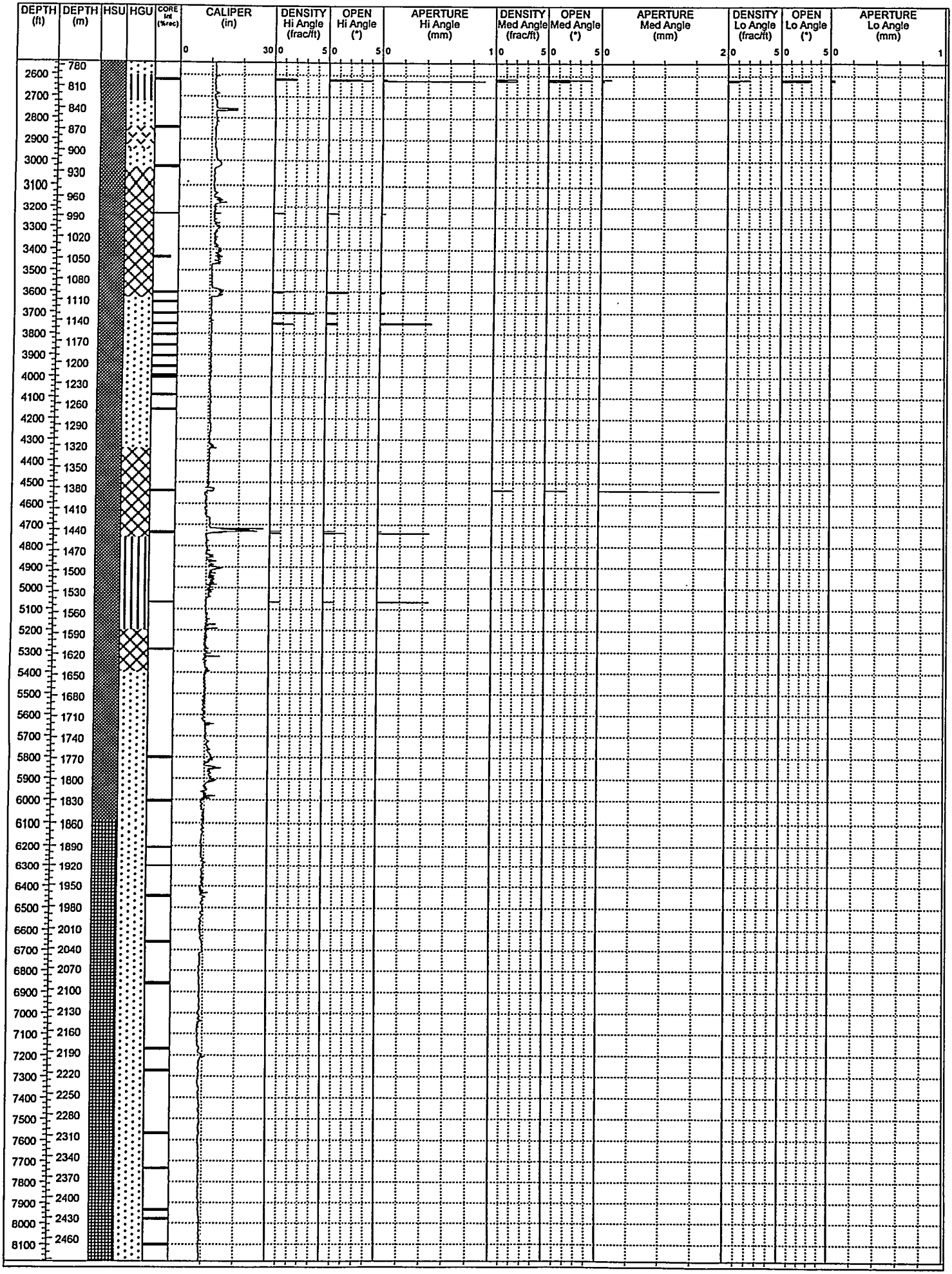
DEPTH (ft)
DEPTH (m)
HSU
HGU
CORE (in) (%rec)
CALIPER (in)
0
30
DENSITY Hi Angle (frac/ft)
OPEN Hi Angle (°)
APERTURE Hi Angle (mm)
DENSITY Med Angle (frac/ft)
OPEN Med Angle (°)
APERTURE Med Angle (mm)
DENSITY Lo Angle (frac/ft)
OPEN Lo Angle (°)
APERTURE Lo Angle (mm)
2600 780
2700 810
2800 840
2900 870
3000 900
3100 930
3200 960
3300 990
3400 1020
3500 1050
3600 1080
3700 1110
3800 1140
3900 1170
4000 1200
4100 1230
4200 1260
4300 1290
4400 1320
4500 1350
4600 1380
4700 1410
4800 1440
4900 1470
5000 1500
5100 1530
5200 1560
5300 1590
5400 1620
5500 1650
5600 1680
5700 1710
5800 1740
5900 1770
6000 1800
6100 1830
6200 1860
6300 1890
6400 1920
6500 1950
6600 1980
6700 2010
6800 2040
6900 2070
7000 2100
7100 2130
7200 2160
7300 2190
7400 2220
7500 2250
7600 2280
7700 2310
7800 2340
7900 2370
8000 2400
8100 2430
2460

LEGEND

Hydrostratigraphic Unit (HSU)


Timber Mountain Aquifer (TMA)


Tuff Cone (TC)


Bullfrog Confining Unit (TCB)


Belted Range Aquifer (TBA)


Basal Aquifer (BAQ)

Hydrogeologic Unit (HGU)

Welded–tuff aquifer (WTA)


Lava–flow aquifer (LFA)


Vitric–tuff aquifer (VTA)


Tuff confining unit (TCU)

(•)OPEN
(for all angles)

Number	Estimated Range of Percent Openness
0	0%
1	1 – 10%
2	10 – 50%
3	50 – 90%
4	90 – 99%
5	100%

Figure 2-22
UE-20f: Composite Log of Open Fracture Data, 774.2 - 2,493.3 Meters

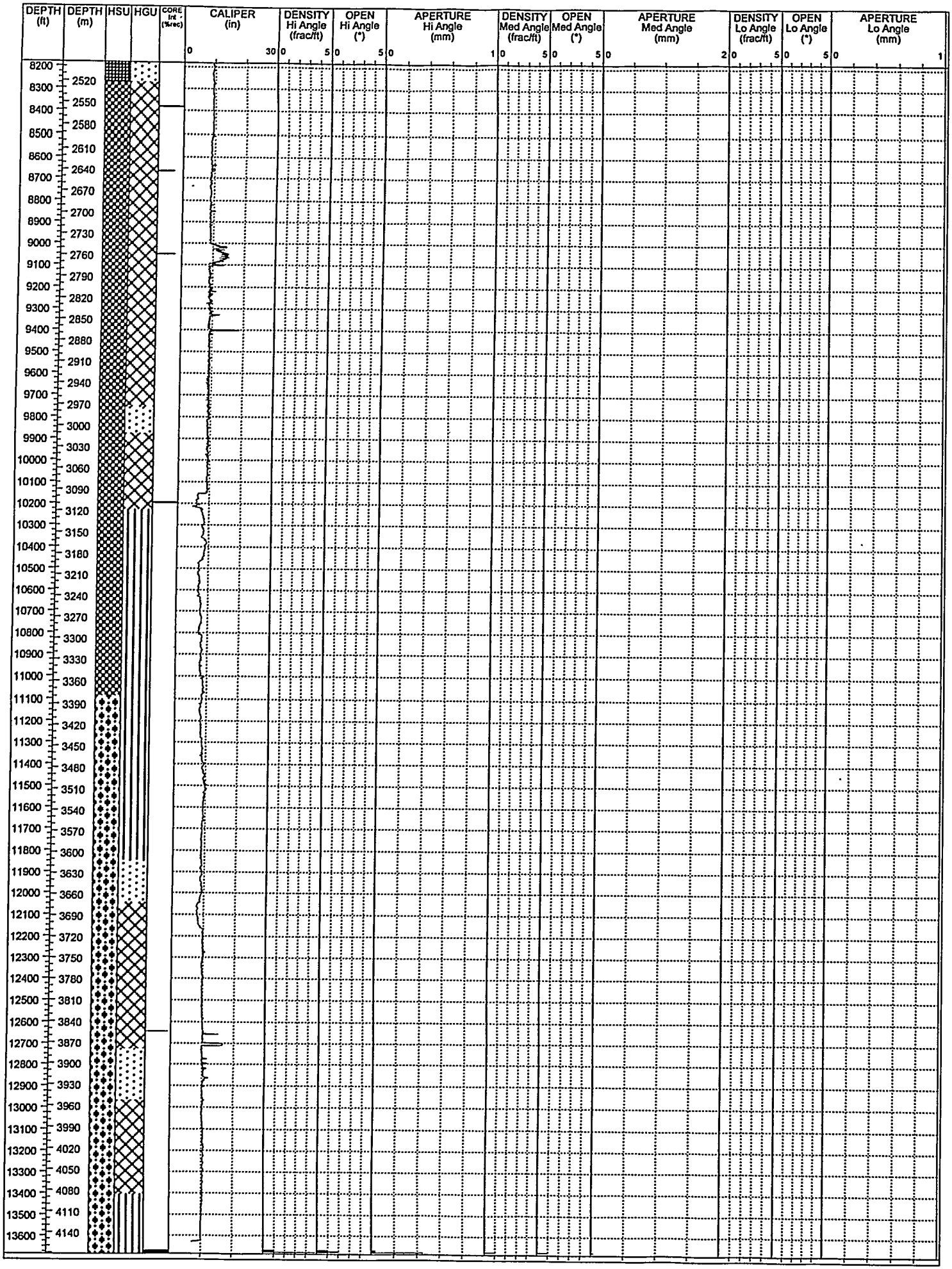
DEPTH (ft)
DEPTH (m)
HSU
HGU
CORE Int. (%rec)
CALIPER (in)
0
30
DENSITY Hi Angle (frac/ft)
OPEN Hi Angle (°)
APERTURE Hi Angle (mm)
DENSITY Med Angle (frac/ft)
OPEN Med Angle (°)
APERTURE Med Angle (mm)
DENSITY Lo Angle (frac/ft)
OPEN Lo Angle (°)
APERTURE Lo Angle (mm)
8200 2520
8300 2550
8400 2580
8500 2610
8600 2640
8700 2670
8800 2700
8900 2730
9000 2760
9100 2790
9200 2820
9300 2850
9400 2880
9500 2910
9600 2940
9700 2970
9800 3000
9900 3030
10000 3060
10100 3090
10200 3120
10300 3150
10400 3180
10500 3210
10600 3240
10700 3270
10800 3300
10900 3330
11000 3360
11100 3390
11200 3420
11300 3450
11400 3480
11500 3510
11600 3540
11700 3570
11800 3600
11900 3630
12000 3660
12100 3690
12200 3720
12300 3750
12400 3780
12500 3810
12600 3840
12700 3870
12800 3900
12900 3930
13000 3960
13100 3990
13200 4020
13300 4050
13400 4080
13500 4110
13600 4140

LEGEND

Hydrostratigraphic Unit (HSU)

Timber Mountain-Aquifer (TMA)

Tuff Cone (TC)

Bullfrog Confining Unit (TCB)

Belted Range Aquifer (TBA)

Basal Aquifer (BAQ)

Hydrogeologic Unit (HGU)

Welded–tuff aquifer (WTA)

Lava–flow aquifer (LFA)

Vitric–tuff aquifer (VTA)

Tuff confining unit (TCU)

(•)OPEN
(for all angles)

Number	Estimated Range of Percent Openness
0	0%
1	1 – 10%
2	10 – 50%
3	50 – 90%
4	90 – 99%
5	100%

Figure 2-23
UE-20f: Composite Log of Open Fracture Data, 2,493.3 - 4,171.5 Meters

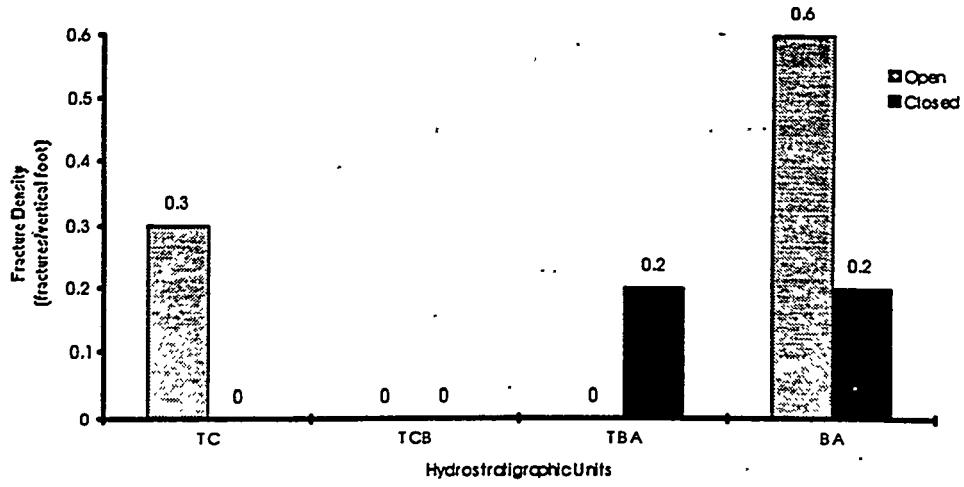

Figure 2-24a
Density of Open and Closed Fractures Relative to Hydrostratigraphy at UE-20f

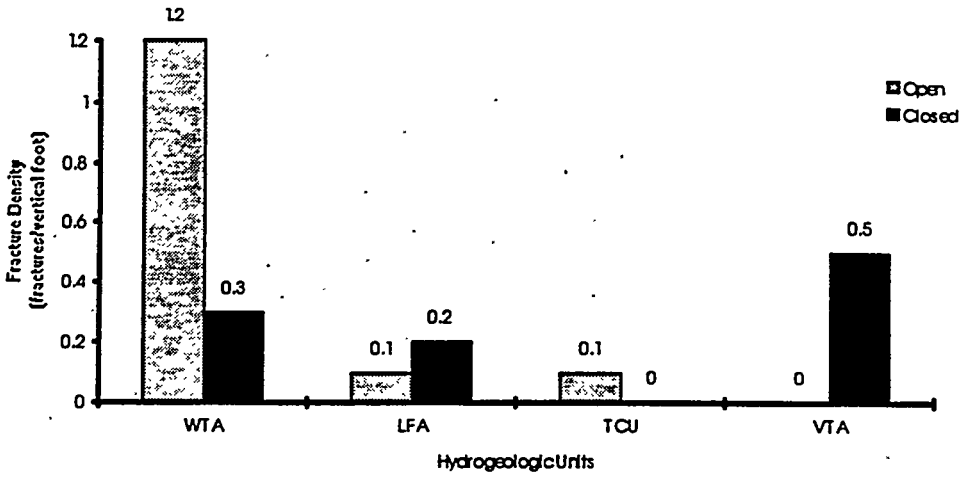

Figure 2-24b
Density of Open and Closed Fractures Relative to Hydrogeology at UE-20f

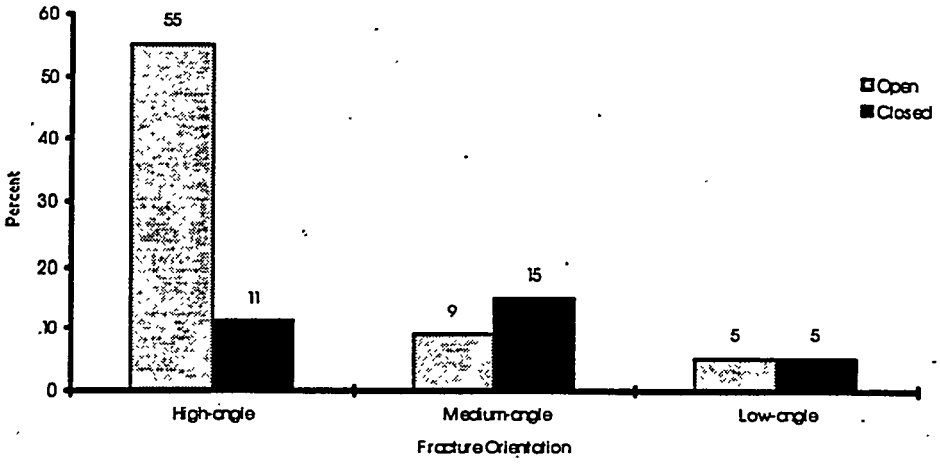

Figure 2-24c
Distribution of Open and Closed Fractures Relative to Orientation at UE-20f

Figure 2-24a-c
Density and Distribution of Fractures at UE-20f

Density of Open and Closed Fractures in Hydrostratigraphic Units

The five HSUs represented in the cored strata in Exploratory Hole UE-20f are the TMA, the TC, the TBA, the TCB, and the BAQ. Fractures were analyzed in all HSUs except the TMA. In the TC, all observed fractures were open, whereas in the TBA, all observed fractures were closed. In the BAQ, the density of open fractures is three times that of closed fractures. No fractures were observed in the TCB (*Figure 2-24a*).

Density of Open and Closed Fractures in Hydrogeologic Units

Four HGUs (the WTA, the LFA, the TCU, and the VTA) are represented in the UE-20f cores. The greatest density of fractures occurs in the WTA, where open fractures are approximately four times more abundant than closed fractures. Closed fractures are twice as abundant as open fractures in the LFA. All fractures observed in the TCU were open, while all fractures in the VTA were closed (*Figure 2-24b*).

Distribution of Open and Closed Fractures Relative to Orientation

In the UE-20f core, the percentage of open fractures is greatest at high-angle orientations. Fifty-five percent of all observed fractures in the core are high-angle open fractures. The percentage of closed fractures is greatest at medium orientations (*Figure 2-24c*).

2.7.3.2 Aperture and Fracture Openness

Aperture and percent openness of open fractures in the UE-20f cores have been analyzed relative to the HGUs and HSUs in which the fractures occur. These relationships are shown in Table 2-7 and in the following text.

Aperture and Openness Relative to Hydrostratigraphic Units

Fractures within the BAQ have the largest apertures observed averaging 0.3 mm (0.01 in.) (*Table 2-7*). Average apertures of fractures within the TC were observed to be somewhat less, at 0.2 mm (0.008 in.). Fractures within both of these HSUs average 0 - 10 percent open. No open fractures were observed within the TCB and TBA.

Table 2-7
UE-20f Fracture Aperture and Percent Open Data

Data Grouped by Hydrostratigraphic Units

Hydrostratigraphic Units	Average Aperture (millimeters)	Percent Open
Tuff Cone (TC)	0.2	1 - 10 percent[1]
Bullfrog Confining Unit (TCB)	*[2]	*[2]
Belted Range Aquifer (TBA)	*[3]	*[3]
Basal Aquifer (BAQ)	0.3	1-10 percent

Data Grouped by Hydrogeologic Units

Hydrogeologic Unit	Average Aperture (millimeters)	Percent Open
Vitric-tuff aquifer (VTA)	*[4]	*[4]
Welded-tuff aquifer (WTA)	0.2	50 - 99 percent
Lava-flow aquifer (LFA)	0.5	1 - 50 percent
Tuff confining unit (TCU)	0.1	1 - 10 percent

1 The 1 - 10 percent open category was most commonly observed; however, the data spans the full range of.1 - 99 percent open.
2 33.2 m (109 ft) of TCB logged, but no open fractures observed.
3 4.0 m (13 ft) of TBA logged, but no open fractures observed.
4 3 m (10 ft) of VTA core logged, but no open fractures observed.

Aperture and Openness Relative to Hydrogeologic Units

Fractures within the LFA have the largest average apertures observed at 0.5 mm (0.02 in.) (*Table 2-7*). Average apertures of fractures in the WTA are considerably less at 0.2 mm (0.008 in.). However, fractures appeared more open in the WTA averaging 50 - 99 percent open versus 1 - 50 percent open for LFA. The TCU had the smallest apertures, averaging 0.1 mm (0.004 in.), as well as the least percent open, at 1 - 10 percent.

2.7.3.3 Mineralogy of Fracture Coatings

Distribution of Fracture-Coating Minerals in Hydrostratigraphic Units

The distribution of fracture-coating minerals in the four HSUs represented in the UE-20f core is presented in Figure 2-25a. Overall, zeolites and Fe/Mn oxides are the most important fracture-lining minerals in the core, but significant differences exist between the dominant mineral coatings in the different HSUs. In the TC, zeolites and Fe/Mn oxides are the dominant mineral coatings, with chalcedony, quartz, calcite, clay, vapor-phase silicates, and fault gouge also

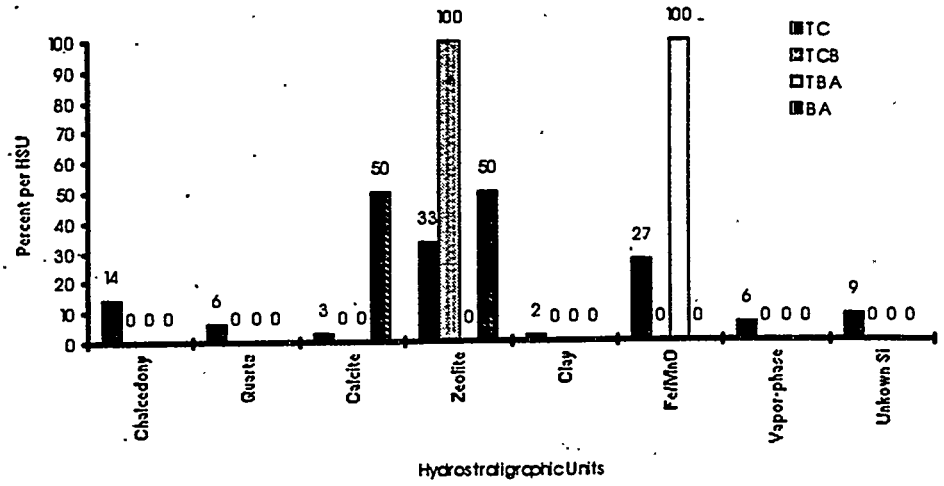

Figure 2-25a
Distribution of Fracture Mineral Coatings Relative to Hydrostratigraphy at UE-20f

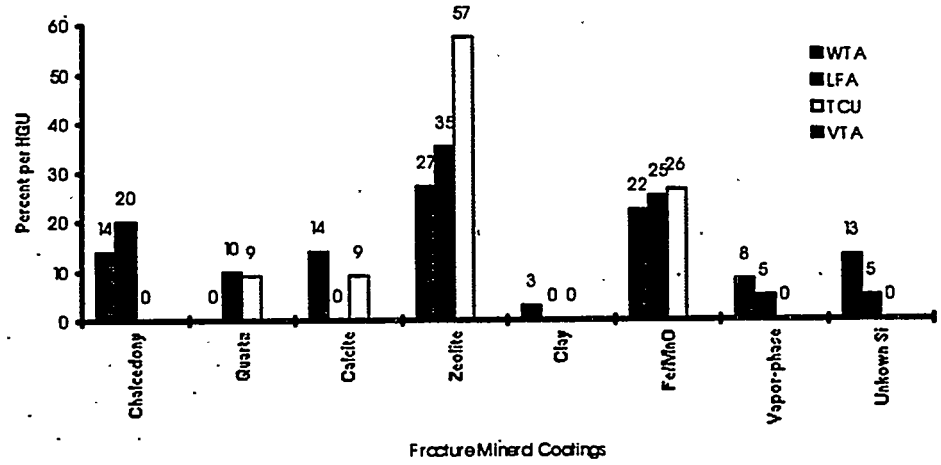

Figure 2-25b
Distribution of Fracture Mineral Coatings Relative to Hydrogeology at UE-20f

Figure 2-25a-b
Distribution of Fracture Mineral Coatings at UE-20f

present. In contrast, all fractures in the TCB are coated or filled with zeolites; no other mineral coatings were observed. In the TBA, all fractures were coated or filled with Fe/Mn oxides. In the BAQ, fractures were coated with calcite and/or zeolites, in equivalent abundances.

Distribution of Fracture-Coating Minerals in Hydrogeologic Units

The distribution of fracture-coating minerals in the four HGUs represented in the UE-20f cores is presented in *Figure 2-25b*. In the WTA, the LFA, and the TCU, zeolites and Fe/Mn oxides are the most common mineral coatings. In the WTA, chalcedony, calcite, and fault gouge are also important. In the LFA, chalcedony and quartz are fairly abundant fracture-coating minerals.

2.7.4 Comparison of Fracture Data, Available Hydrologic Test Data, and Caliper Log

Hydrologic testing was conducted in UE-20f in 1964 to determine the water yielding potential of the volcanic rock and to ascertain whether the site is suitable for an emplacement hole (Blankennagel *et al.*, 1964). The tests were intentionally limited to the low permeability zones within the first 2,795 m (9,170 ft) of the hole. Figure 2-26 presents the hydrologic test intervals and test data as they compare to the fracture data and caliper log.

When the hydrologic data from the test intervals are compared to the fracture data derived from the analyzed core, only limited qualitative conclusions can be reached. The very small ratio of available core to the hydrologic test interval precludes a useful comparison.

The hydrologic tests included isolating 23 separate, 60.4-m (198-ft) intervals with packers and conducting either injection or swab tests to determine relative specific capacity. The results from the valid tests (19 of the 23 intervals maintained packer integrity) varied from 0.00-0.39 gallons per minute per foot (gpm/ft) with an average of 0.04 gpm/ft (Blankennagel *et al.*, 1964). Overall, the low relative specific capacities compare favorably with the low fracture densities and low openness recorded in the core associated with the test intervals. Although from a qualitative standpoint the fracture data agree with the hydrologic test data, it is important to note that on the average, core was available for fracture analysis from less than 5 percent of the hydrologic test interval.

The interval with the highest relative specific capacity (3.9 gpm/ft) compares favorably with fracture data derived from core and a conspicuous washout indicated on the caliper log (*Figure 2-26*).

This page intentionally left blank.

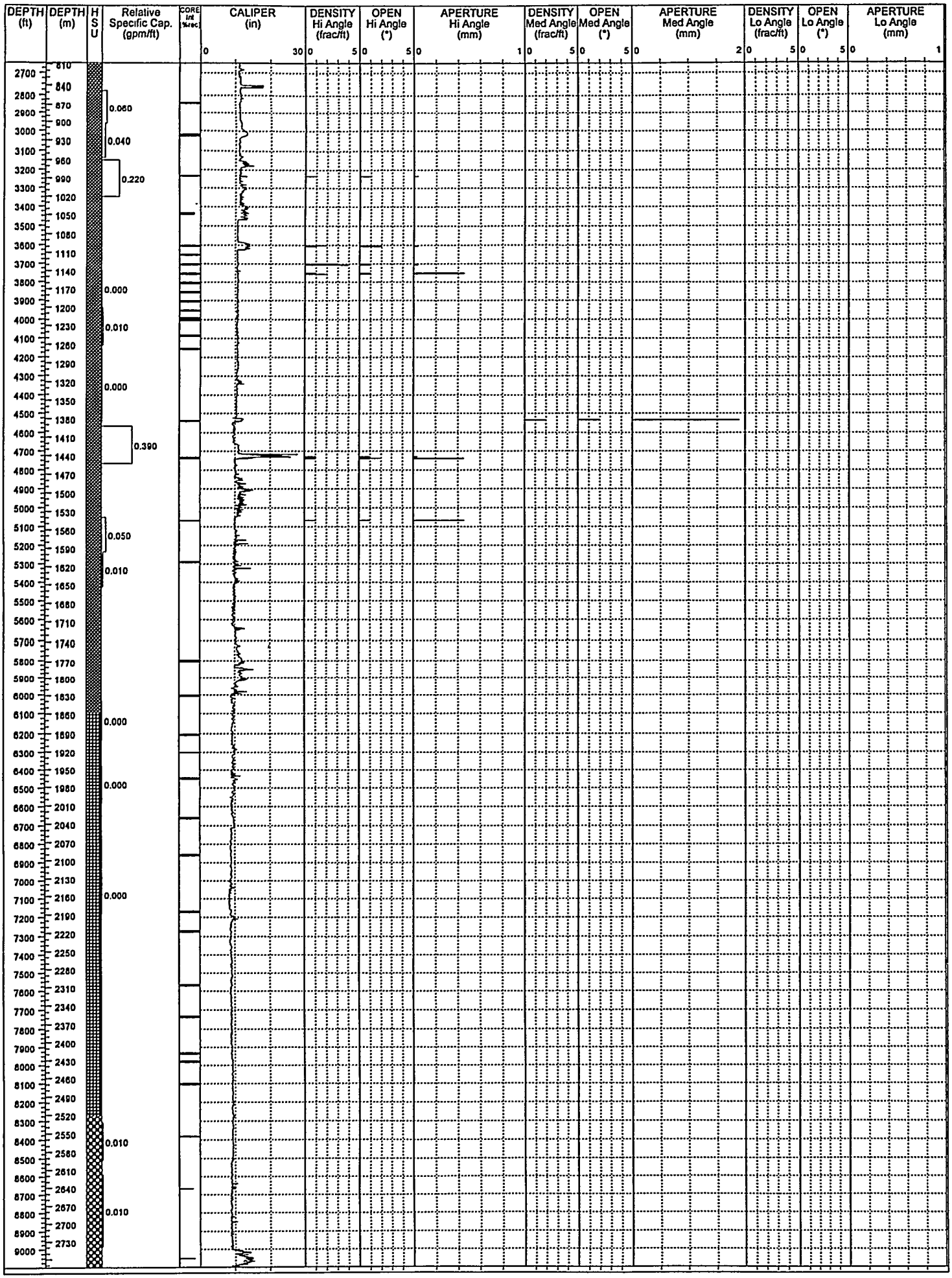
DEPTH (ft)
DEPTH (m)
H S U
Relative Specific Cap. (gpm/ft)
CORE int %rec
CALIPER (in)
DENSITY Hi Angle (frac/ft)
OPEN Hi Angle (°)
APERTURE Hi Angle (mm)
DENSITY Med Angle (frac/ft)
OPEN Med Angle (°)
APERTURE Med Angle (mm)
DENSITY Lo Angle (frac/ft)
OPEN Lo Angle (°)
APERTURE Lo Angle (mm)
0 30
0 5
0 5
0 1
0 5
0 5
0 2
0 5
0 5
0 1
2700 810
2800 840
2900 870
3000 900
3100 930
3200 960
3300 990
3400 1020
3500 1050
3600 1080
3700 1110
3800 1140
3900 1170
4000 1200
4100 1230
4200 1260
4300 1290
4400 1320
4500 1350
4600 1380
4700 1410
4800 1440
4900 1470
5000 1500
5100 1530
5200 1560
5300 1590
5400 1620
5500 1650
5600 1680
5700 1710
5800 1740
5900 1770
6000 1800
6100 1830
6200 1860
6300 1890
6400 1920
6500 1950
6600 1980
6700 2010
6800 2040
6900 2070
7000 2100
7100 2130
7200 2160
7300 2190
7400 2220
7500 2250
7600 2280
7700 2310
7800 2340
7900 2370
8000 2400
8100 2430
8200 2460
8300 2490
8400 2520
8500 2550
8600 2580
8700 2610
8800 2640
8900 2670
9000 2700
2730
0.060
0.040
0.220
0.000
0.010
0.000
0.390
0.050
0.010
0.000
0.000
0.000
0.010
0.010

LEGEND

Hydrostratigraphic Unit (HSU)

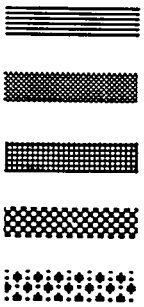

Timber Mountain Aquifer (TMA)

Tuff Cone (TC)

Bullfrog Confining Unit (TCB)

Belted Range Aquifer (TBA)

Basal Aquifer (BAQ)

(•)OPEN
(for all angles)

Number	Estimated Range of Percent Openness
0	0%
1	1 – 10%
2	10 – 50%
3	50 – 90%
4	90 – 99%
5	100%

Figure 2-26
UE-20f: Composite Log of Hydrologic Test Data, Caliper Log, and Fracture Data, 807.7 - 2,773.7 Meters

3.0 Borehole Image Log Analysis for Selected Drill Holes

Digital borehole images of both the FMS and BHTV were analyzed for fracture traces using workstation enhancement. Identified planar fracture traces were oriented using proprietary software of the logging vendor. Orientation data are displayed in this report in two formats: 1) lower hemisphere stereographic projections, and 2) rose diagrams of fracture strikes. Trend similarities associated with depth intervals are based on statistical analyses of the data prior to lithologic or stratigraphic comparisons. This was intended to prevent any preconceived biases on the part of the authors from affecting data analysis. Stratigraphy and lithology were factored in later for interpretation and reporting.

The intrinsic nature of the two borehole image logs is such that not all fractures will be imaged. The reasons for this are lack of contrast across fractures (small aperture or completely healed with secondary minerals) and imperfect borehole conditions such as breakouts or washouts. The number of fractures identified in the log data are fewer than those derived from core data. Fracture orientation (in particular, fracture strike), however, is provided by the borehole image logs. Therefore, the emphasis of this section will be fracture orientation rather than fracture density. Fractures have been categorized by level of confidence that the trace actually represents a planar fracture. Only fractures at the highest confidence level were considered.

3.1 Exploratory Hole UE-18r

A Schlumberger Formation MicroScanner log was run in the wellbore for the Underground Test Areas Project over the interval 485 m (1,590 ft) to 1504 m (4,937 ft), as illustrated in Figure 3-1. The purpose of the image log was to identify and orient natural fractures, and fracture orientations were found to vary with depth and stratigraphic unit. This section of this report is a presentation of the fracture orientations found in Exploratory Hole UE-18r.

3.1.1 Fracture Orientations

Orientations of fractures in the depth interval above 609 m (2,000 ft) in the UE-18r log are shown in Figures 3-1a and b. Fractures strike generally east-northeast. The plot of poles to fractures (line perpendicular to fracture plane, *Figure 3-1b*) show that the fractures are of medium dip, approximately 40 degrees to 60 degrees. None of the fractures are vertical. The figure also indicates both north and south-dipping fractures with the north-dipping fractures being more common.

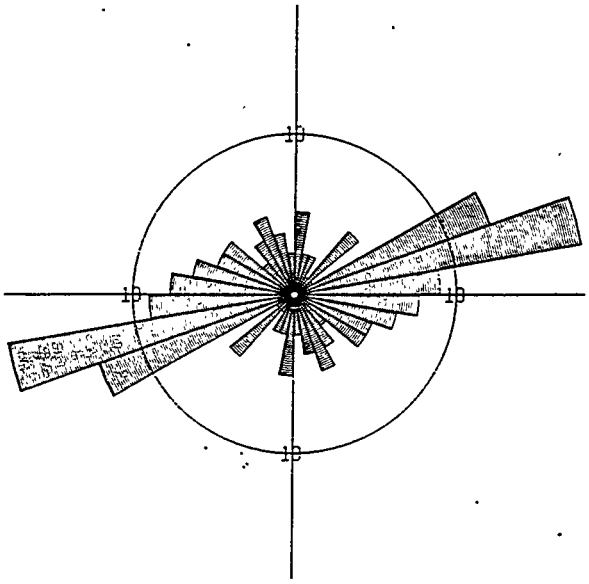

Figure 3-1a

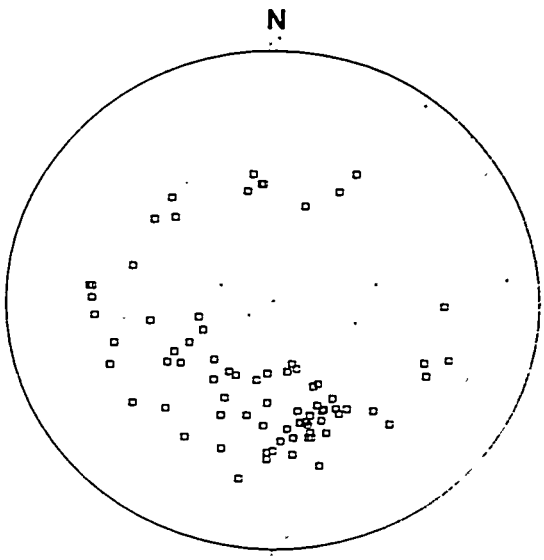

Figure 3-1b

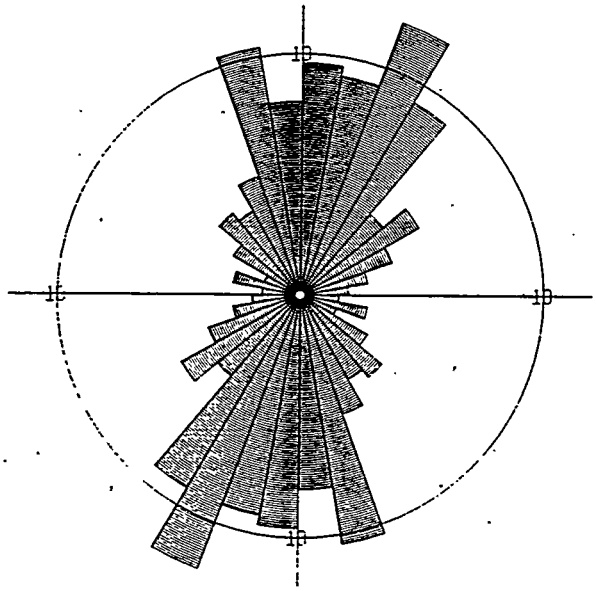

Figure 3-1c

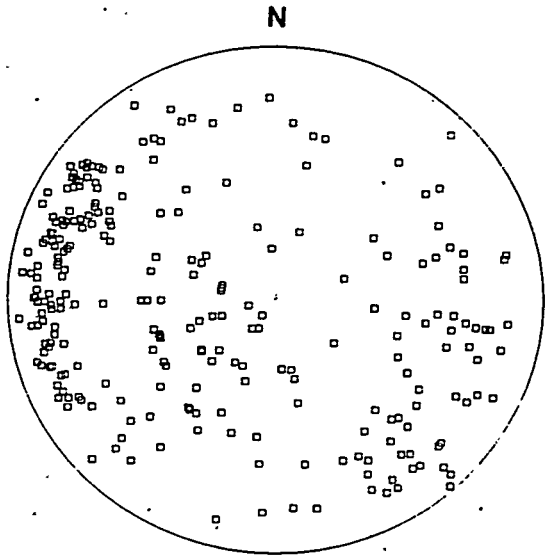

Figure 3-1d

Rose diagram petal lengths are percent of total data points in a 10-degree azimuth interval. Stereographic projections are equal area, lower hemisphere projections of poles to fracture planes. North is at the top of each figure.

3-1 a and b - Depth interval 485 meters (m) (1,590 feet [ft]) to 609 m (2,000 ft), 78 points
3-1 c and d - Depth interval 609 m (2,000 ft) to 1,097 m (3,600 ft), 250 points

Figure 3-1a-d
Diagrams Showing Fracture Orientations in Exploratory Hole UE-18r by Depth Interval
(Page 1 of 2)

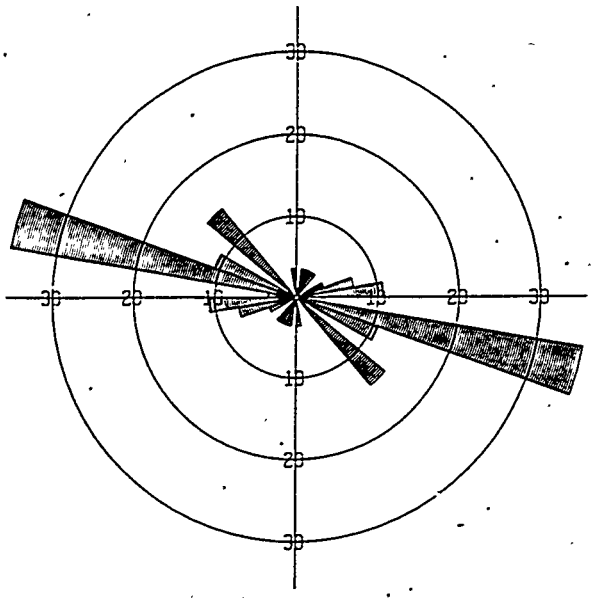

Figure 3-1e

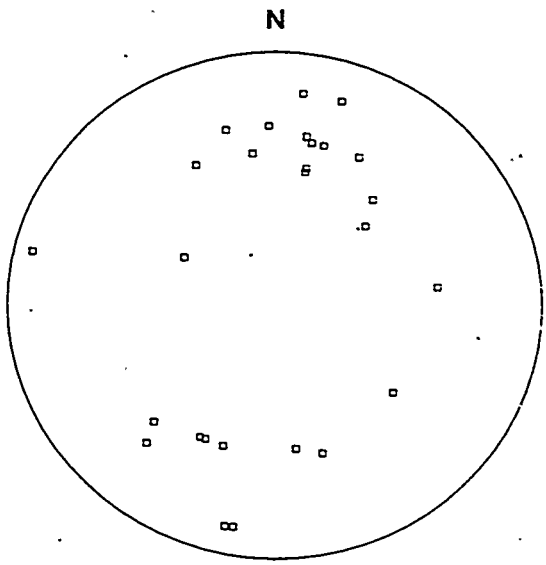

Figure 3-1f

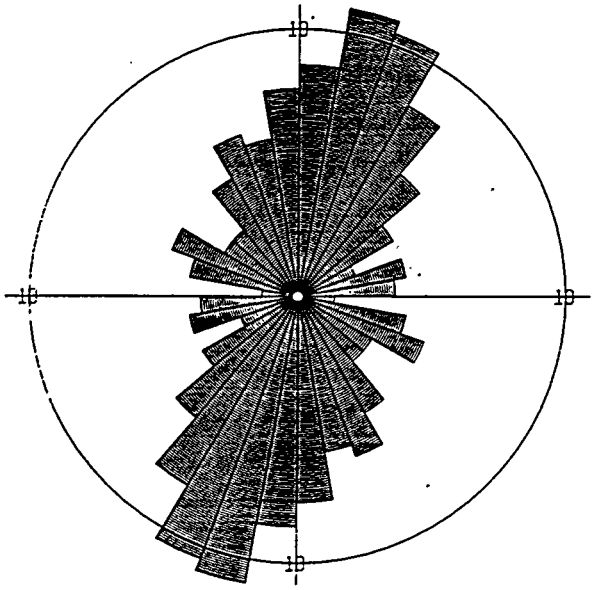

Figure 3-1g

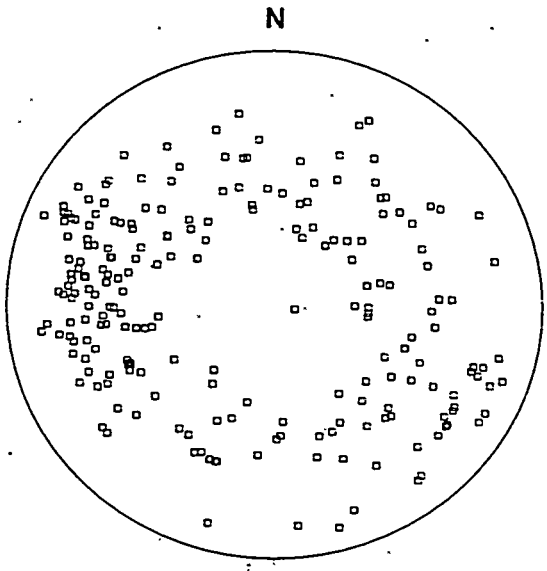

Figure 3-1h

3-1 e and f - Depth interval 1,097 m (3,600 ft) to 1,188 m (3,900 ft), 28 points
3-1 g and h - Depth interval 1,188 m (3,900 ft) to 1,504 m (4,937 ft), 220 points

Figure 3-1e-h
Diagrams Showing Fracture Orientations in Exploratory Hole UE-18r by Depth Interval
(Page 2 of 2)

Orientations of fractures in the depth interval of 609 m to 1,097 m (2,000 to 3,600 ft) are shown in *Figures 3-1c* and *3-1d*. Fractures in this interval have distinctly different orientation than those mentioned above. Fractures in this interval, in general, strike north-northeast, although there is significant scatter in strikes. Poles to fractures, shown in *Figure 3-1d*, illustrate that these fractures have steeper dips than those previously mentioned. The poles also show that fractures dip both toward the east-southeast and west-northwest.

Fractures in the depth interval of 1,097 m to 1,188 m (3,600 to 3,900 ft) have a unique orientation for the drill hole. The fairly small population of fractures in this short interval strike mostly west-northwest. These strike orientations are shown in *Figure 3-1e*. *Figure 3-1f* shows that these fractures dip steeply both toward the north and toward the south. These fractures are mostly in the rhyolite of Tannenbaum Hill.

Below the rhyolite of Tannenbaum Hill, fractures have similar orientations to the interval above the rhyolite. Orientations of fractures in the interval from 1,188 m to 1,504 m (3,900 to 4,937 ft) are shown in *Figures 3-1g* and *3-1h*. Most of the fractures strike north-northeast and dip steeply both toward the west and east, although there is a scatter of orientations.

3.1.2 Comparison of the FMS Image with Core

Fifteen intermittent cores were taken in Exploratory Hole UE-18r. There is not a good correlation of fractures visible in the core with those identified on the FMS. This may be because the FMS is an image of the wellbore wall and is not of the same piece of rock as the core. Also the FMS image does not provide full wellbore coverage. Some of the cores were taken in intervals where the wellbore is washed out.

3.2 Monitoring Well UE-20bh #1

Monitoring Well UE-20bh#1 was logged with both the FMS and the Schlumberger BHTV for a comparison of the two types of image logs. The saturated depth interval between 675 m (2,213 ft) and 856 m (2,808 ft) was logged with both tools. A thorough comparison of the two logs is not within the scope of this fracture analysis task; however, data from both are shown in Figure 3-2.

3.2.1 Fracture Orientations in UE-20bh #1

Orientations of fractures in the entire interval logged with the FMS are shown in *Figures 3-2a* and *3-2b*. The greatest majority of fractures strike north-northeast; however, there is a scatter of

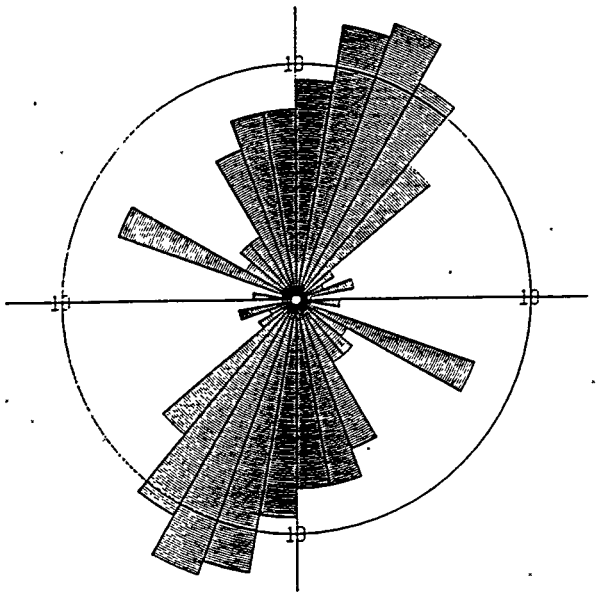

Figure 3-2a

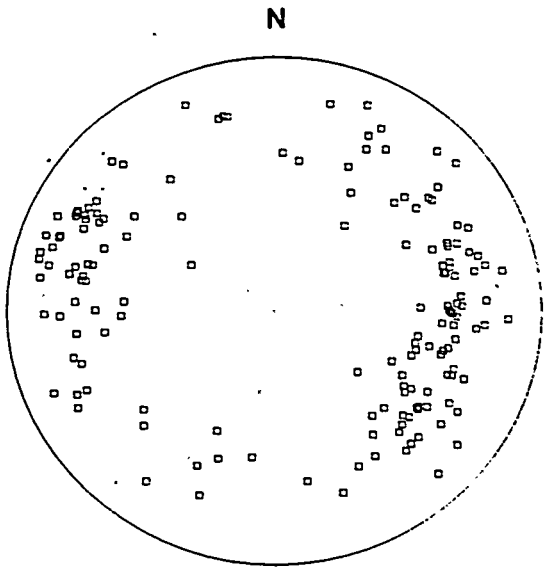

Figure 3-2b

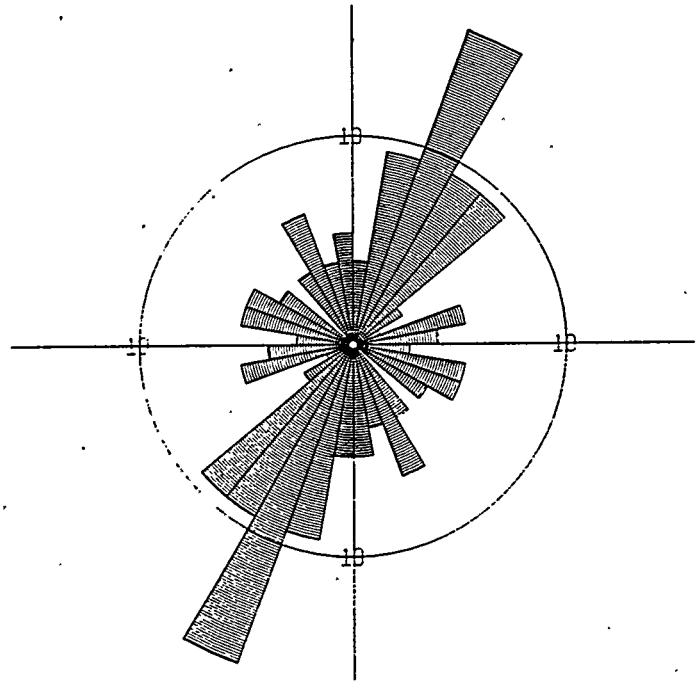

Figure 3-2c

Diagrams showing fracture orientations in Monitoring Well UE-20bh #1 for the entire logged interval. 3-2a) Rose diagram of 161 strikes identified in the FMS log. Petal lengths are percent of total data points in a 10-degree azimuth interval. 3-2b) Lower hemisphere, equal area stereographic projection of 161 poles to fracture planes in the FMS log. 3-2c) Rose diagram of 75 poles to fractures identified in the BHTV. Petal lengths are percent of total data points within a 10-degree azimuth interval. North is at the top of each figure.

Figure 3-2a-c
Diagrams Showing Fracture Orientations in Monitoring Well UE-20bh #1

strikes over a 60 to 80 degree range. A distinct subset of 13 fractures strikes perpendicular to the majority trend between 60 and 70 degrees west. *Figure 3-2b* shows that both sets of fractures have steep dips. For comparison, strikes of fractures identified with the BHTV are indicated in *Figure 3-2c*.

Although the data set is smaller for the BHTV, strikes determined with the BHTV are very similar to those in the FMS.

3.2.2 Comparison of the UE-20bh #1 Wellbore Images with Core

The short core interval from 726 m (2,382 ft) to 735 m (2,412 ft) contained several fractures, both closed and open (*Figure 2-15*). Open fractures were identified in core at 726 m (2,382 ft) depth. Other fractures present in the core were closed. The BHTV image shows several irregular fractures at 726 m (2,382 ft) depth. No other fractures are identifiable on the BHTV over the cored interval. In this example, the BHTV did not image all fractures but did image the open, more significant fractures. In the FMS analysis of the same core interval, no fractures were identified in the interval containing the open fractures at 726 m (2,382 ft). However, questionable fractures were identified at 731 m (2,398 ft) on the FMS in which healed and closed fractures were identified in core.

3.3 Well ER-20-5 #1

The location of Well ER-20-5 #1 is shown in *Figure 1-1*. The well was logged with a BHTV over the depth interval of 626 m (2,053 ft) to 826 m (2,710 ft), all within the Topopah Spring Tuff. Because of poor borehole conditions within nonwelded tuff intervals, the BHTV image is poor, and fractures are not easily identifiable. The moderately welded tuff between 704 m (2,310 ft) and 786 m (2,580 ft) yielded a good image on the BHTV, and most of the fractures selected from the log are from within that interval.

3.3.1 Fracture orientations in Well ER-20-5 #1

Orientations of fractures identified on the BHTV log from Well ER-20-5 #1 are shown in Figure 3-3. The stereographic projection in *Figure 3-3a* illustrates that the fractures from the entire logged interval are generally of steep dip because their poles plot near the rim of the circle. The clustering of poles onto several groups suggests the presence of multiple fracture sets.

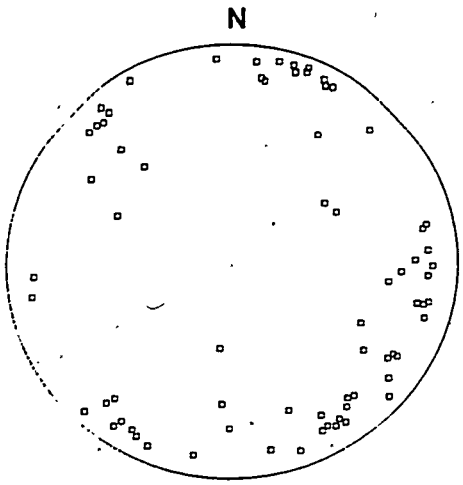

Figure 3-3a

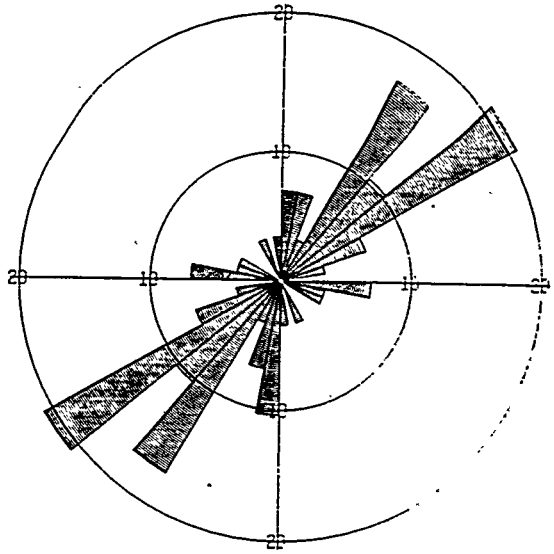

Figure 3-3b

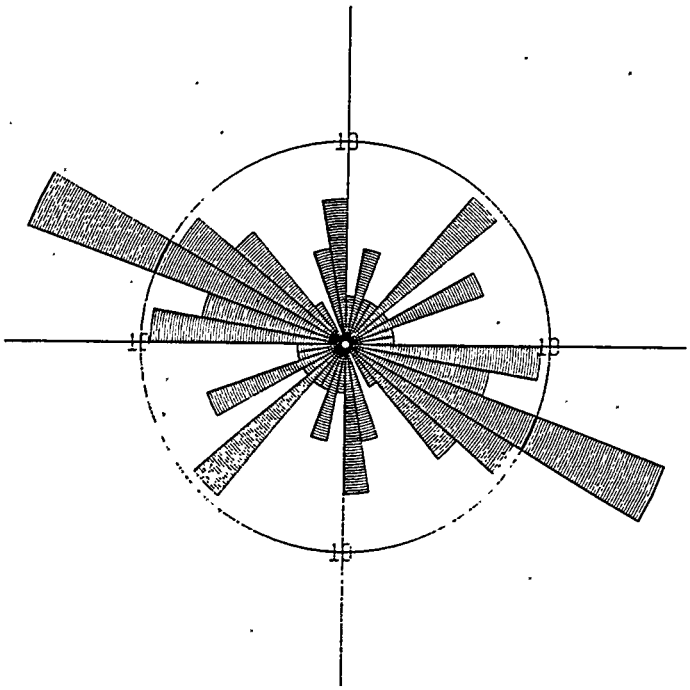

Figure 3-3c

Fracture orientation diagrams for Well ER-20-5 #1. North is to the top of each figure. 3-3a) Equal area, lower hemisphere stereographic projection of 71 poles to fracture planes from the entire logged interval. 3-3b) Rose diagram of 29 fracture strikes from the depth interval 626 meters (m) (2,053 feet [ft]) to 734 m (2,408 ft). Petal lengths are percent of points in a 10-degree azimuth interval. 3-3c) Rose diagram of 42 fracture strikes from the depth interval below 734 m (2,408 ft).

Figure 3-3a-c
Fracture Orientation Diagrams for Well ER-20-5 #1

Orientations were further differentiated by depth interval. *Figure 3-3b* shows orientations of a small set of fractures identified in the depth interval 626 m (2,053 ft) to 734 m (2,408 ft). Fractures in this upper interval strike generally northeast. Orientations of fractures in the depth interval below 734 m (2,408 ft) in *Figure 3-2c* have markedly different strikes. In this lower interval, most fractures strike west-northwest; however, the northeast strike is present. The change in fracture strikes happens at about 734 m (2,408 ft) depth, within the moderately welded tuff. There is an overlap of the two fracture orientation sets with both sets occurring locally at the same depth.

3.4 Well ER-20-2 #1

The location of well ER-20-2 #1 is shown in *Figure 1-1*. A BHTV log was run in this hole from 690 m (2,264 ft) to 770 m (2,525 ft).

3.4.1 Fracture Orientations in Well ER-20-2 #1

Orientations of fractures in Well ER-20-2 #1 are shown in Figure 3-4a. Only 17 fractures were described from this log. The stereographic projection in Figure 3-4b illustrates that fractures from the entire logged interval are generally steeply dipping. Fractures in this well generally trend northeast-southwest with one minor, perpendicular fracture set.

3.5 Synopsis of the Fracture Orientation of the Data Sets

Composite fracture orientation diagrams for each well are shown on Figure 3-5. These composite figures contain all fractures described in each log. The dominant fracture set described through orientation analysis generally trends north-northeast to south-southwest. These fractures generally are parallel to the north-northeast-trending normal faults of the area. In some wells there is a distinctly different fracture orientation with increase in depth. The shallow fractures of Exploratory Hole UE-18r trend east-northeast and are located in younger volcanic units that do not contain major north-northeast-trending normal faults. The lower fractures of this well trend more north-northeast, parallel to the regional fault system. This well is located in volcanic units within the moat of the Timber Mountain Caldera, which is structurally different than the wells on Pahute mesa. Well ER-20-5 #1 also exhibited separate fracture sets with depth.

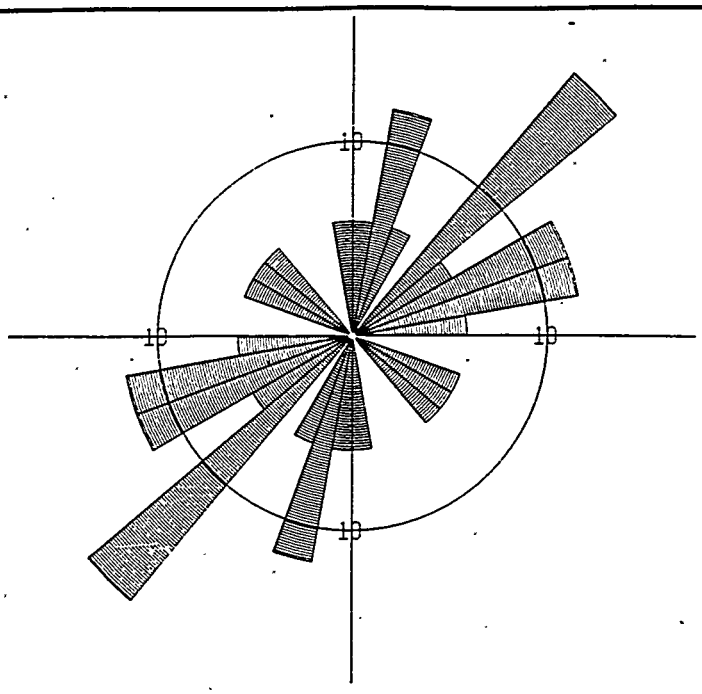

Figure 3-4a

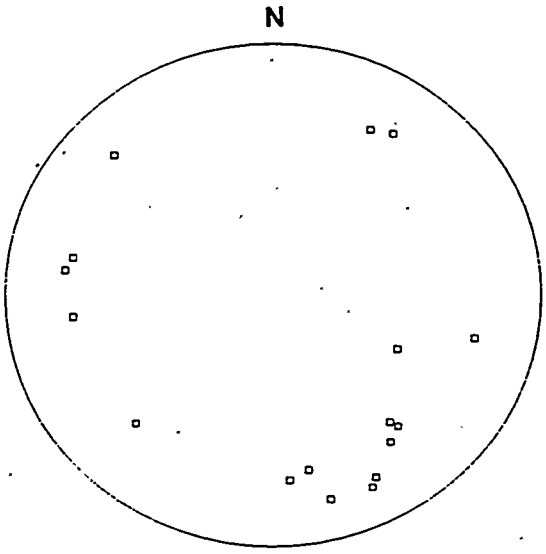

Figure 3-4b

Fracture orientation diagrams for Well ER-20-2 #1. North is to the top of each diagram. 3-4a) Rose diagram of 17 fracture strikes from the entire logged interval. 3-4b) Equal area, lower hemisphere projection of 17 poles to fracture planes in the entire logged interval.

Figure 3-4a-b
Fracture Orientation Diagrams for Well ER-20-2 #1

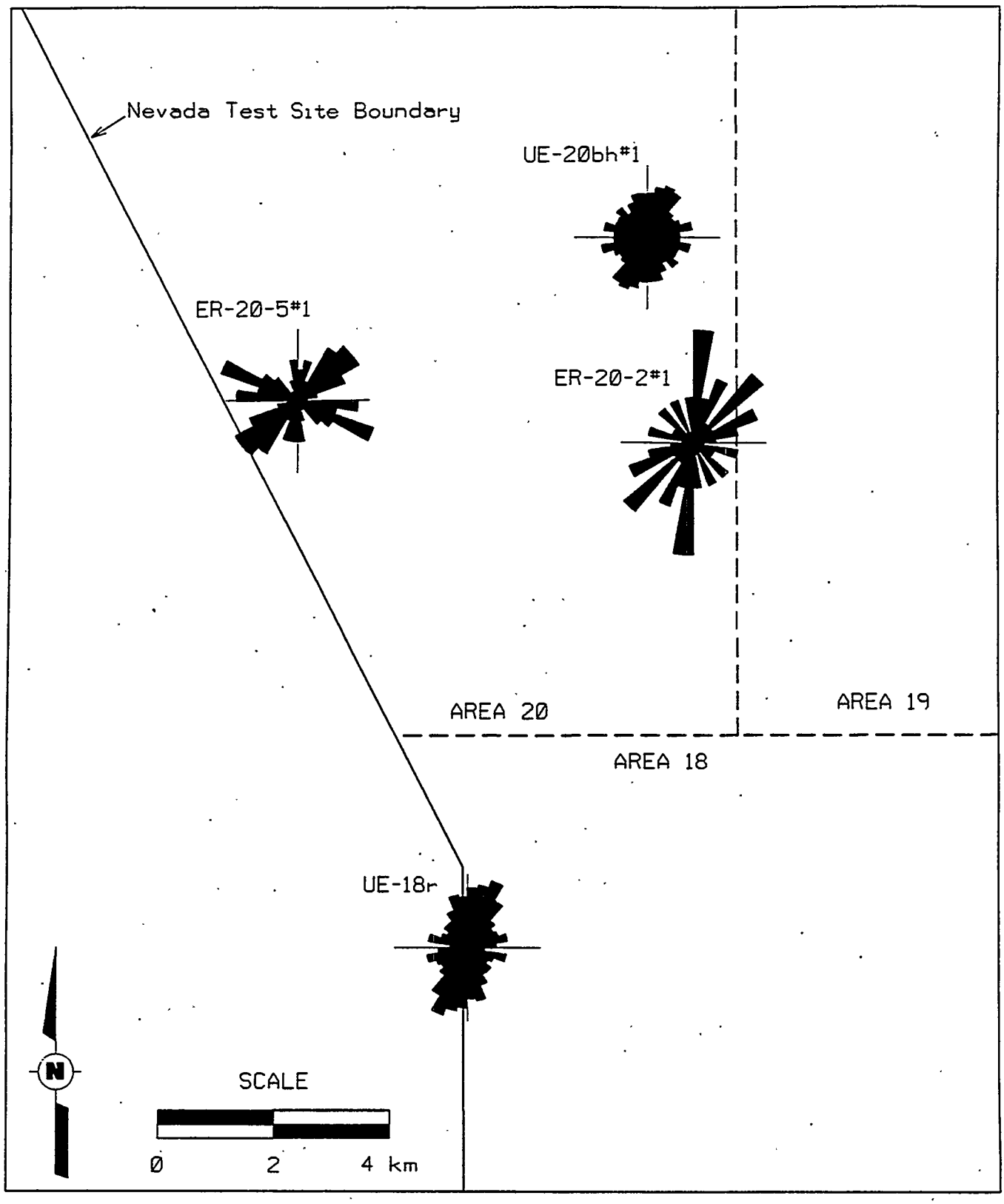

Figure 3-5
Composite Fracture Strikes for the Pahute Mesa Area

4.0 Cumulative Analysis of Fracture Data

Previous analyses and discussions of fracture attributes in this study were based on fracture data sets from individual holes. However, in order to acquire information on the regional aspects of these attributes it was necessary to analyze the fracture attributes based on a single cumulative data set comprised of fracture data from all the holes examined. Observations of fracture attributes based on the results of this analysis are discussed in the following text. General observations of fracture attributes will be discussed as well as attributes relative to HSU and HGU.

4.1 General Observations of Fracture Attributes

The following are general observations of fracture attributes based on cumulative data from all the holes. As will be shown, data from the Area 18 holes have a significant influence on the cumulative analysis of the data. Therefore, some attributes were also analyzed using the following two data subsets:

- Data from the Pahute Mesa holes only (i.e., UE-19x, U-20c/UE-20c, UE-20e#1, UE-20f, and UE-20bh#1)
- Data from the Area 18 holes only (i.e., UE-18r and UE-18t)

4.1.1 Fracture Density

The density of open and closed fractures, incorporating data from all drill holes in the study, is approximately one fracture every 0.6 m (2 ft) vertically (Figure 4-1). However, because fractures from Area 18 holes represent 75 percent of the fractures recorded, fracture data from Area 18 holes, particularly UE-18t, have a significant influence on the cumulative analysis of the data. This becomes apparent when comparing the density of open and closed fractures based on data from all holes with data from Pahute Mesa holes or Area 18 holes separately (*Figure 4-1*).

4.1.2 Orientation

Approximately 50 percent of all the fractures observed and 73 percent of the open fractures observed are high-angle (Figure 4-2a). This corresponds fairly close to what other researchers have found at the NTS Yucca Mountain site where approximately 60 percent of fractures range from 40° to 90° (Maldonado and Koether, 1983). The percentage of closed fractures exceeds the percentage of open fractures with respect to all orientations when data from all the holes are considered. However, the influence of the abundance of closed fractures in the Area 18 holes is

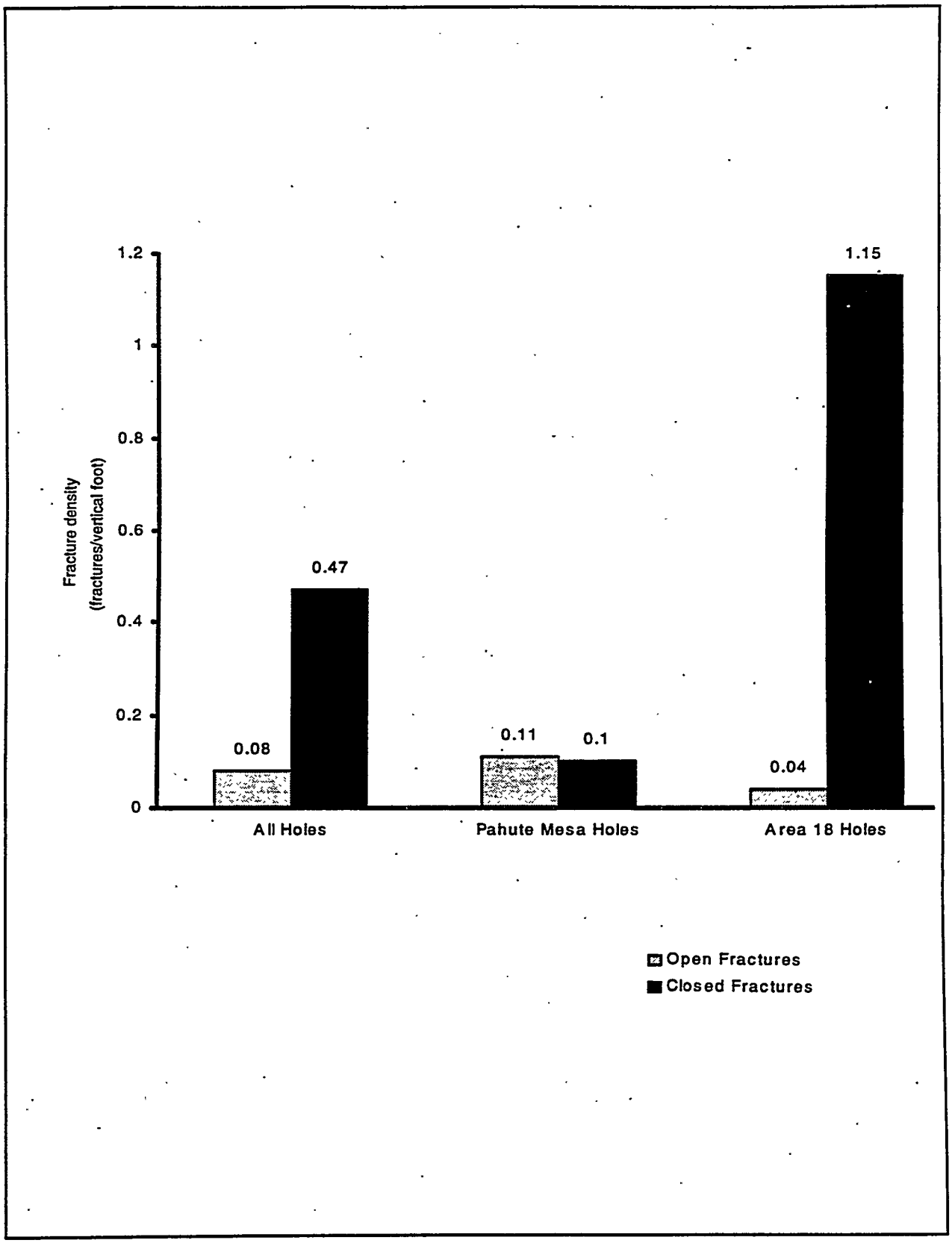

Figure 4-1
Summary of Fracture Density

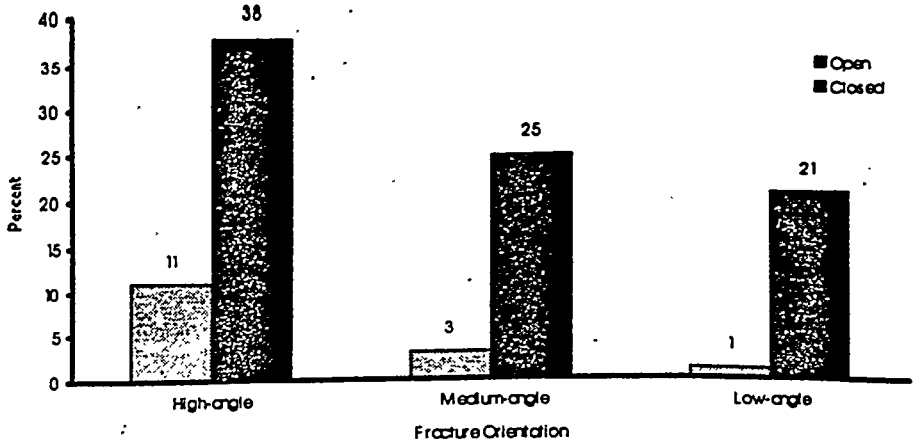

Figure 4-2a
Distribution of Open and Closed Fractures Relative to Orientation for All Holes

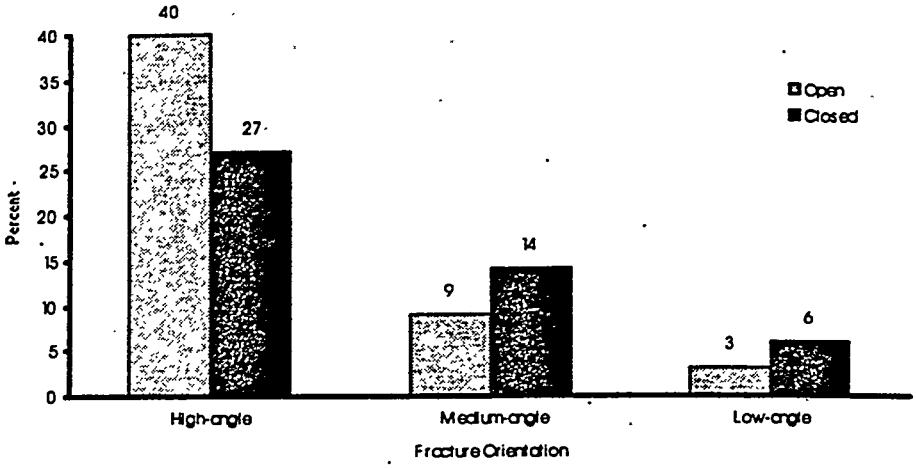

Figure 4-2b
Distribution of Open and Closed Fractures Relative to Orientation for Pahute Mesa Holes Only

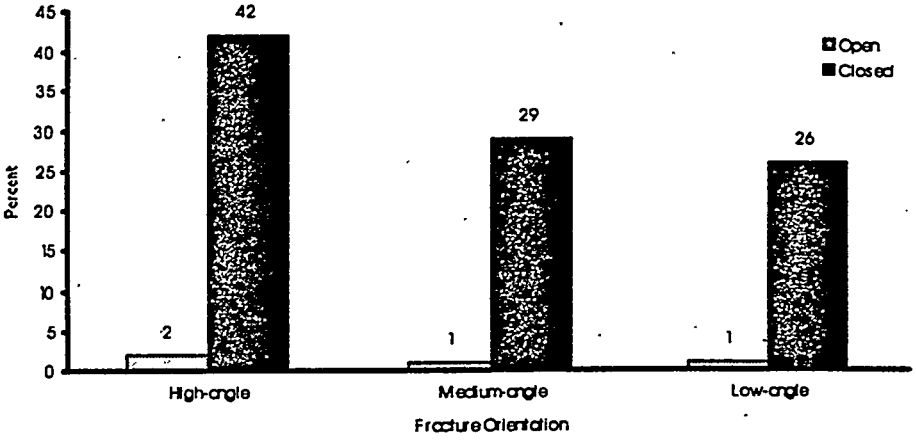

Figure 4-2c
Distribution of Open and Closed Fractures Relative to Orientation for Area 18 Holes Only

Figure 4-2a-c
Summary of Fracture Distribution Relative to Orientation

readily apparent when comparing Figures *4-2a*, 4-2b, and 4-2c. Based on data from the Pahute Mesa holes, only the percentage of high-angle open fractures exceeds that for high-angle closed fractures.

4.1.3 Aperture and Openness

Few of the open fractures examined were 100 percent open. Instead, the vast majority were partially closed with secondary mineral fillings. When aperture was observed along fracture traces, it usually averaged less than 1 mm (0.04 in.) in width.

4.1.4 Mineralogy of Fracture Coatings

The majority of the open fractures examined appeared to be 90 - 100 percent coated with secondary minerals. The minerals most often observed as secondary mineral coatings were chalcedony, euhedral quartz, calcite, zeolite, clay, and Fe/Mn oxides (Figure 4-3a). These were also the common fracture-coating minerals observed at Yucca Mountain Core Holes USW G-1 and USW G-2 (Maldonado and Koether, 1983; Carlos, 1990). Similar changes in relative abundances of these minerals were noted at both study areas. Zeolite and chalcedony occurred more often in fractures from the Pahute Mesa holes, while clay and calcite occurred more often in fractures from the Area 18 holes (Figures 4-3b and 4-3c).

4.2 Fracture Attributes Within Hydrostratigraphic Units

The following is an analysis and discussion of the fracture attributes relative to the hydrostratigraphy of Pahute Mesa/Timber Mountain area. Fracture attributes are analyzed and discussed for each of the following hydrostratigraphic units: TMA, TC, TCB, TBA, and BAQ. Due to the influence of data from Area 18 holes on the analysis of particular fracture attributes, data for these attributes are presented in three sets:

- For all holes
- Pahute Mesa holes
- Area 18 holes

4.2.1 Fracture Density

Figure 4-4a indicates that, with respect to all the holes, the TBA and BAQ have the highest density of fractures. However, it should be noted that only a limited amount of core from holes UE-20e #1 and UE-20f was available from the TBA and BAQ.

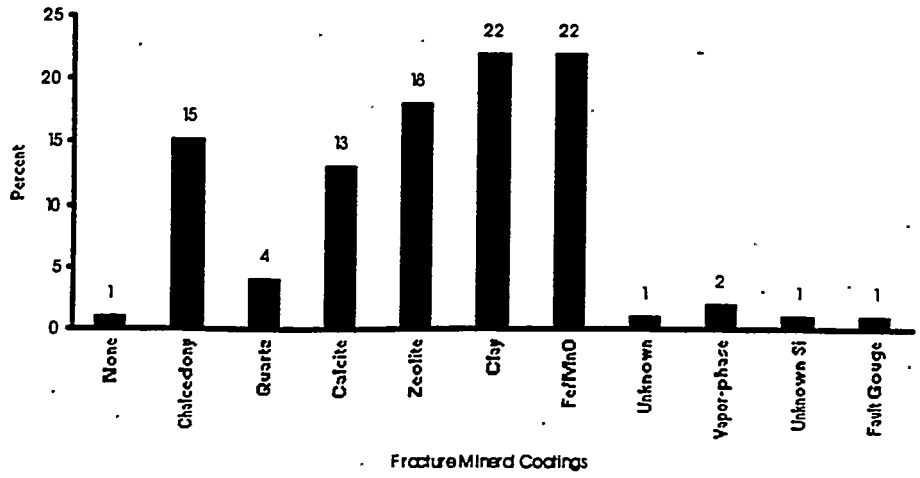

Figure 4-3a
Distribution of Fracture Mineral Coatings for All Holes

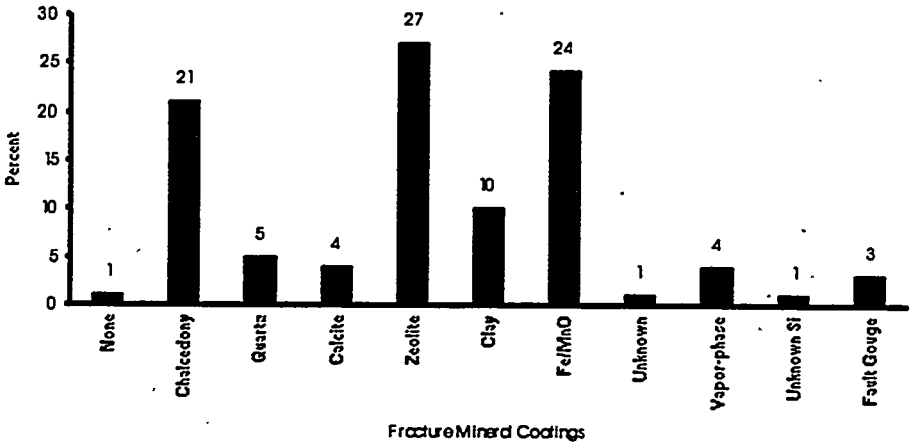

Figure 4-3b
Distribution of Fracture Mineral Coatings for Pahute Mesa Holes Only

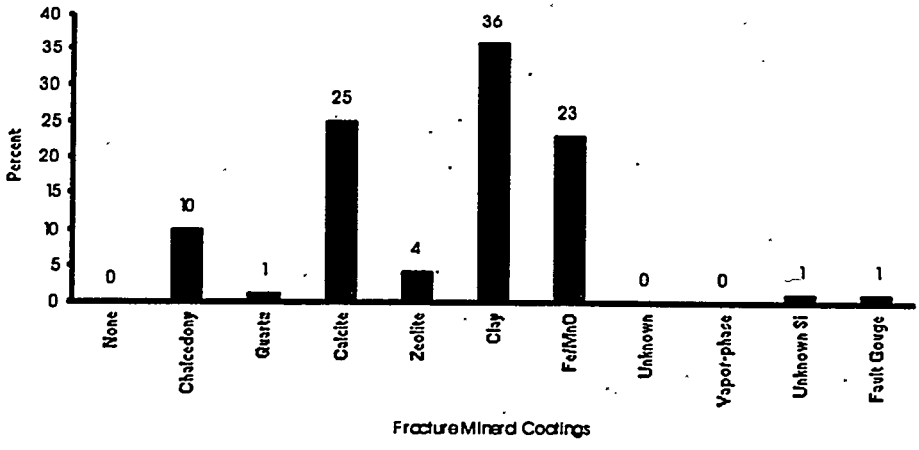

Figure 4-3c
Distribution of Fracture Mineral Coatings for Area 18 Holes Only

Figure 4-3a-c
Summary of the Distribution of Fracture-Mineral Coatings

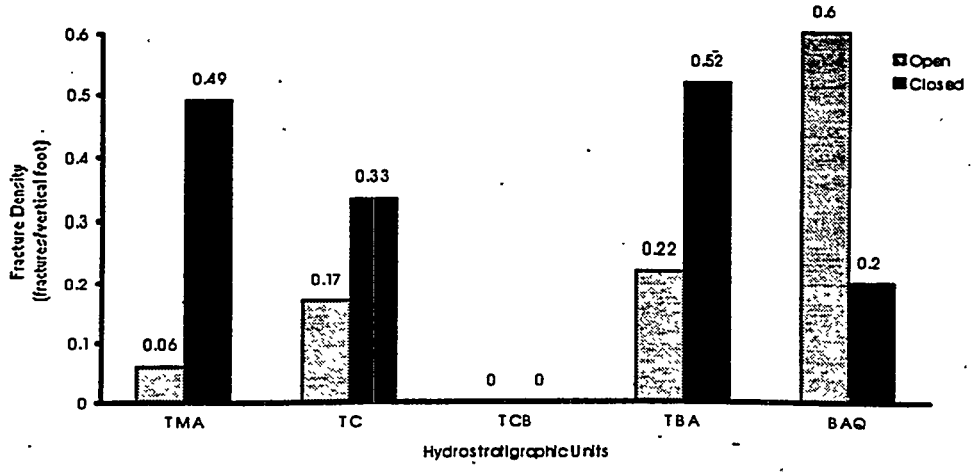

Figure 4-4a
Density of Open and Closed Fractures Relative to Hydrostratigraphy for All Holes

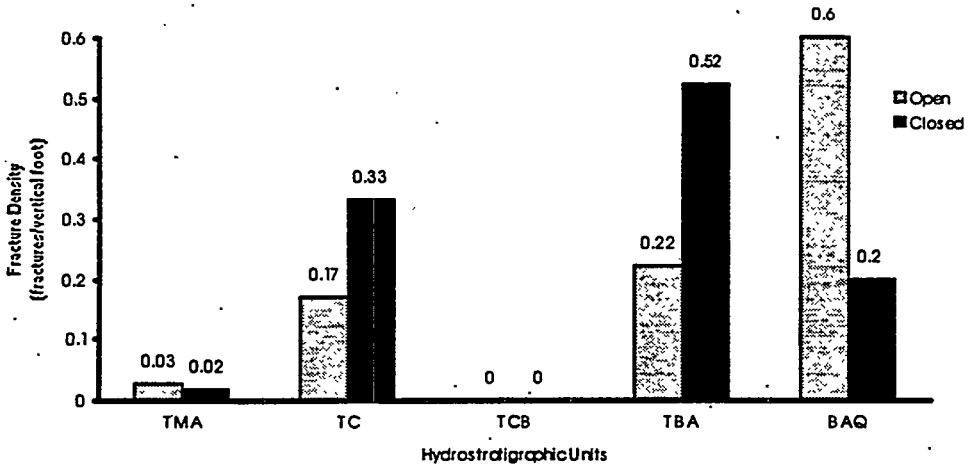

Figure 4-4b
Density of Open and Closed Fractures Relative to Hydrostratigraphy for Pahute Mesa Holes Only

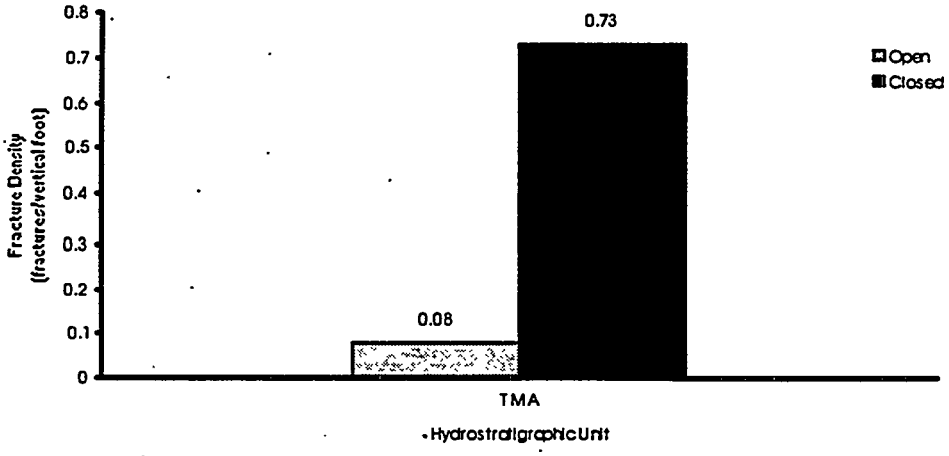

Figure 4-4c
Density of Open and Closed Fractures Relative to Hydrostratigraphy for Area 18 Holes Only

Figure 4-4a-c
Summary of Fracture Density Relative to Hydrostratigraphy

The fracture densities for TMA and TC are approximately equal with respect to data from all the holes, with the density of closed fractures exceeding that for open fractures in both holes (*Figure 4-4a*). The much higher density of closed fractures versus open fractures within the TMA appears to be the result of the influence of the Area 18 holes which have a much higher density of closed fractures than open fractures within the TMA (Figure 4-4c). With respect to Pahute Mesa holes, the TC has a much higher density of fractures than TMA (Figure 4-4b). This is probably due to the high percentage of poorly fractured vitric-tuff aquifer that comprises the TMA in the holes examined. No fractures were observed within the TCB, which is not surprising since poorly fractured TCU comprises much of the TCB.

4.2.2 Aperture and Openness

Table 4-1 shows that open fractures in the TMA were observed to have the largest average apertures, averaging 0.72 mm (0.03 in.). Open fractures within the TC were observed to have the second largest average apertures at 0.53 mm (0.02 in.), followed by open fractures within the BAQ at 0.3 mm (0.01 in.) and fractures within the TBA at 0.08 mm (0.003 in.).

Although the TBA and BAQ were observed to have the highest density of fractures, *Table 4-1* shows that not only do they have the smallest average apertures, but they also are almost completely closed, averaging less than 10 percent open. Fractures in the TC were observed to average generally less than 50 percent open, whereas fractures in the TMA showed a wide variability in the average percent open ranging from 10 - 100 percent open.

4.2.3 Mineralogy of Fracture Coatings

Because chalcedony, quartz, calcite, zeolite, clay, and iron and manganese oxides are the most commonly occurring fracture-coating minerals observed in this study (*Figure 4-3a*), all other minerals observed are grouped together for the remaining analyses and discussions.

Three secondary mineral coatings were observed to occur most often in fractures within the TMA (Figure 4-5a). These minerals were calcite, clay, and iron and manganese oxides. However, a comparison of Figures *4-5a*, 4-5b, and 4-5c shows that this distribution is strongly influenced by data from the Area 18 holes. Data from Pahute Mesa holes only show the occurrence of secondary minerals within the TMA more evenly distributed among all the minerals observed.

Table 4-1
Fracture Aperture and Percent Open Data Summary
(Data Grouped by Hydrostratigraphic Units)

	Average Aperture (millimeters)								Percent Open Category							
HSU	UE-18r	UE-18t	UE-19x	UE-20 bh #1	UE-20c U-20c	UE-20 e#1	UE-20f	Average of Data	UE-18r	UE-18t	UE-19x	UE-20 bh#1	UE-20c U-20c	UE-20 e#1	UE-20f	Average of Data
Timber Mountain Aquifer (TMA)	1.09	0.78	0.39	---	---	---	---	0.72	50-90	10-50	50-100	---	---	---	---	10 - 100[1]
Tuff Cone (TC)	---	---	0.78	0.84	0.42	0.03	0.19	0.53	---	---	1-50	1-50	1-50	1-10	1-10	1-50
Bullfrog Confining Unit (TCB)	---	---	---	---	---	---	*[2]	*	---	---	---	---	---	---	*[2]	*
Belted Range Aquifer (TBA)	---	---	---	---	---	0.08	*[3]	0.08	---	---	---	---	---	1-10	*[3]	1-10
Basal Confining Unit (BCU)	---	---	---	---	---	---	---	---	---	---	---	---	---	---	---	---
Basal Aquifer (BAQ)	---	---	---	---	---	---	0.3	0.3	---	---	---	---	---	---	1-10	1-10

1 Percent open range expanded toward low end by the UE-18t data.
--- Core representing unit either not available or not logged.
2 33.2 m (109 ft) of TCB logged, but no open fractures observed.
3 Only 4 m (13 ft) of TBA logged, no open fracture observed.

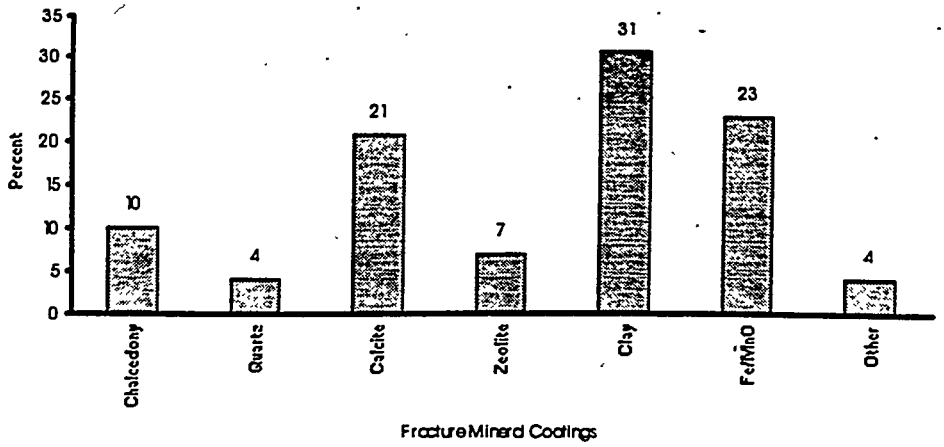

Figure 4-5a
Distribution of Fracture Mineral Coatings Within the Timber Mountain Aquifer for All Holes

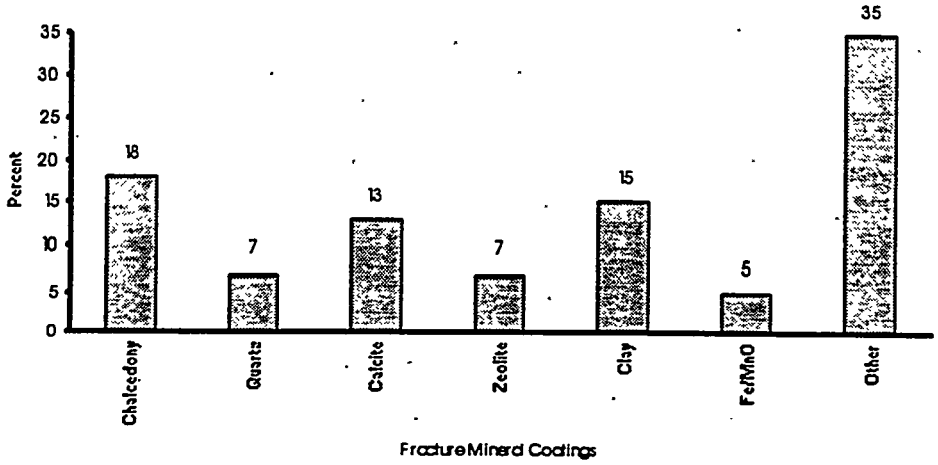

Figure 4-5b
Distribution of Fracture Mineral Coatings Within the Timber Mountain Aquifer for Pahute Mesa Holes Only

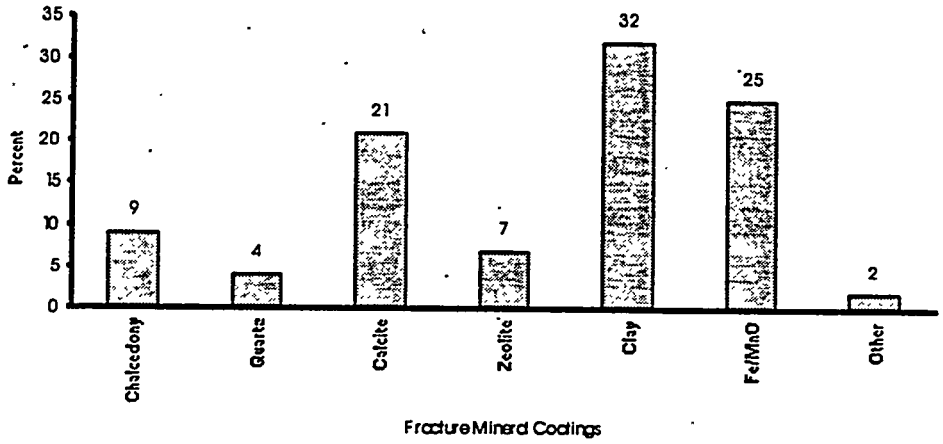

Figure 4-5c
Distribution of Fracture Mineral Coatings Within the Timber Mountain Aquifer for Area 18 Holes Only

Figure 4-5a-c
Summary of the Distribution of Fracture Mineral Coatings Within the TMA

Although a wide variety of secondary mineral coatings were observed in fractures within the TC, chalcedony, zeolite, and iron and manganese oxides occurred most often (Figure 4-6a). Euhedral quartz, zeolite, clay, and iron and manganese oxides were the only secondary minerals observed in fractures within the TBA, with iron and manganese oxides occurring most often (Figure 4-6b). Only calcite and zeolite were observed in fractures within the BAQ (Figure 4-6c).

4.3 Fracture Attributes Within Hydrogeologic Units

The following is an analysis and discussion of the fracture attributes relative to the hydrogeology of Pahute Mesa. Fracture attributes are analyzed and discussed for each of the following hydrogeologic units: (1) WTA, (2) LFA, (3) TCU, and (4) VTA. Because of the influence of data from Area 18 holes on the analysis of particular fracture attributes, data for these attributes are presented in three sets: for all holes, Pahute Mesa holes, and Area 18 holes.

4.3.1 Fracture Density

The highest density of fractures was observed within the WTA with a higher density of open fractures observed than closed fractures (Figure 4-7a). The LFA has the second highest fracture density, but closed fractures have a considerably higher density than open fractures. As expected, the TCU has a relatively low fracture density due to the less brittle nature of incorporated lithologies. The VTA has the lowest fracture density of all the hydrogeologic units because, like the TCU, the lithologies present within the VTA are much less brittle. In general, fracture densities derived in this study are consistent with similar data reported by Blankennagel and Weir (1973).

Comparison of Figures *4-7a*, 4-7b, and 4-7c shows that although the data from Area 18 holes do have a significant influence, it is mainly with respect to the density of closed fractures.

4.3.2 Aperture and Openness

Table 4-2 illustrates that fractures within the VTA and LFA have the largest apertures, averaging just under 1 mm. Fractures in the WTA and TCU have apertures averaging less than 0.5 mm.

Open fractures in the WTA were generally greater than 50 percent open, whereas open fractures in the VTA, LFA, and TCU were generally less than 50 percent open.

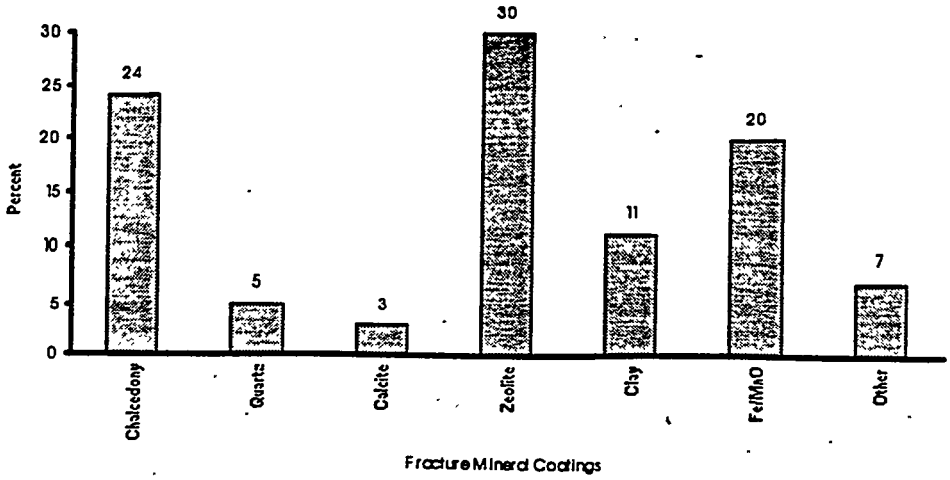

Figure 4-6a
Distribution of Fracture Mineral Coatings Within the Tuff Cone Aquifer for All Holes

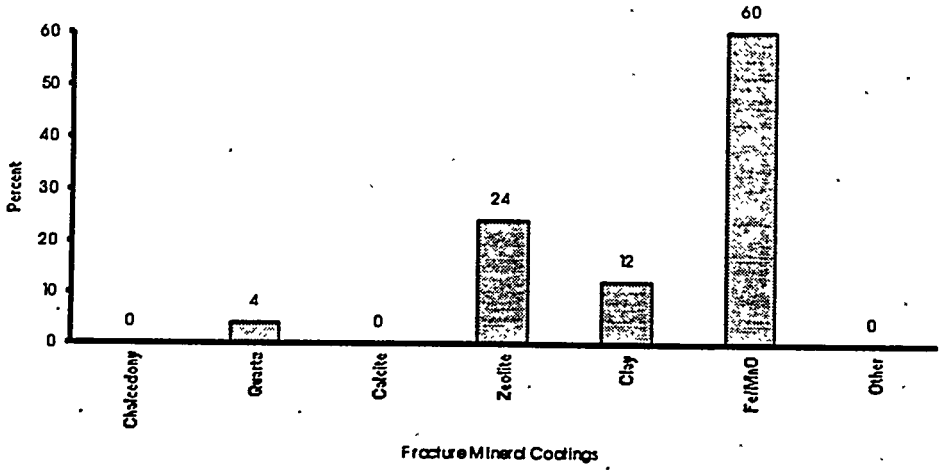

Figure 4-6b
Distribution of Fracture Mineral Coatings Within the Belted Range Aquifer for Pahute Mesa Holes Only

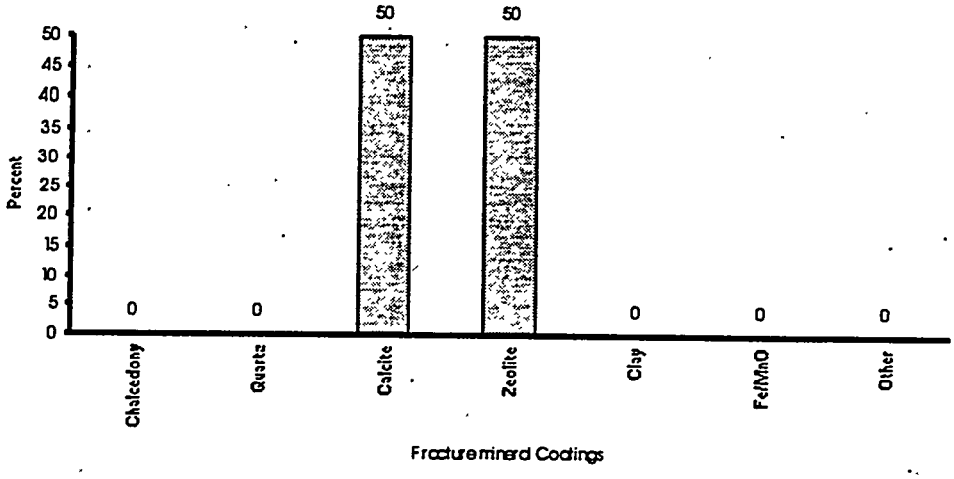

Figure 4-6c
Distribution of Fracture Mineral Coatings Within the Basal Aquifer for Area 18 Holes Only

Figure 4-6a-c
Summary of the Distribution of Fracture Mineral Coatings Relative to Hydrostratigraphy

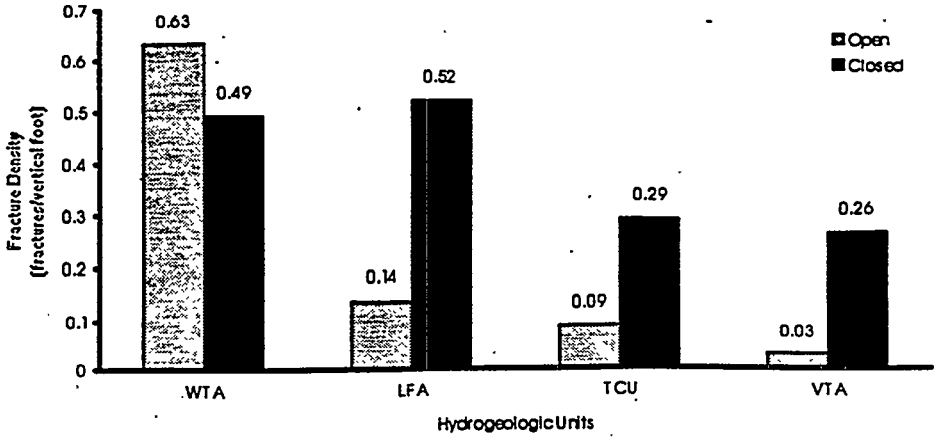

Figure 4-7a
Density of Open and Closed Fractures Relative to Hydrogeology for All Holes

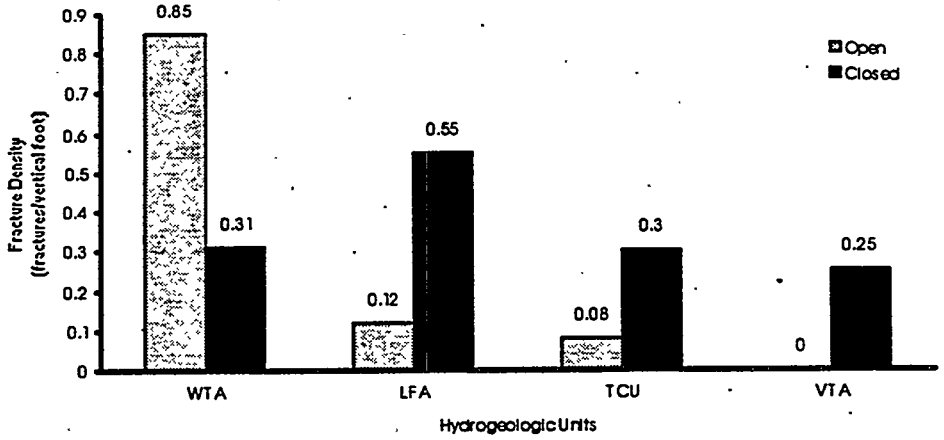

Figure 4-7b
Density of Open and Closed Fractures Relative to Hydrogeology for Pahute Mesa Holes Only

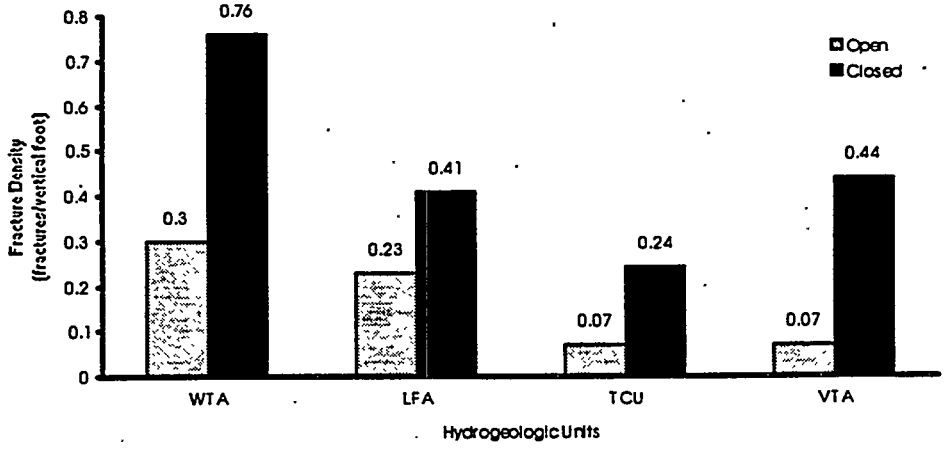

Figure 4-7c
Density of Open and Closed Fractures Relative to Hydrogeology for Area 18 Holes Only

Figure 4-7a-c
Summary of Fracture Density Relative to Hydrogeology

Table 4-2
Fracture Aperture and Percent Open Data Summary
(Data Grouped by Hydrogeologic Units)

	Average Aperture (millimeters)								Percent Open Category							
Hydrogeo-logic Units	UE-18r	UE-18t	UE-19x	UE-20 bh #1	UE-20c U-20c	UE-20 e#1	UE-20f	Average of Data[1]	UE-18r	UE-18t	UE-19x	UE-20 bh#1	UE-20c U-20c	UE-20 e#1	UE-20f	Average of Data[1]
Vitric-Tuff Aquifer (VTA)	*	0.95	*	---	---	---	---	0.95	*	10-50	*	---	---	---	---	10-50
Welded-Tuff Aquifer (WTA)	0.04	2.19	0.21	---	0.42	---	0.17	0.34	1-10 and 50-90	1-10	50-100	---	1-50	---	50-99	50-99
Lava-Flow Aquifer (LFA)	2.09	---	0.98	*	*	0.08	0.53	0.91	50-90	---	1-50	*	*	1-10	1-50	1-50
Tuff Confining Unit (TCU)	1.51	---	0.57	0.84	0.14	0.03	0.09	0.47	50-90 and 1-10	---	1-50	1-50	1-10	1-10	1-10	1-50

1 UE-18t skews data set.
* Core representing unit was logged, but no open fractures recognized.
--- Core representing unit not available from drill hole.

4.3.3 Mineralogy of Fracture Coatings

Clay, iron and manganese oxides, calcite, and chalcedony occur most often in fractures within the WTA (Figure 4-8a). Interestingly, the LFA and TCU have very similar distributions of secondary minerals with zeolite, chalcedony, and iron and manganese oxides occurring most often (Figures 4-8b and 4-8c). Fractures within the VTA were observed to be coated most often with iron and manganese oxides, zeolite, clay, and euhedral quartz (Figure 4-8d). As mentioned previously, this fracture filling/coating mineral assemblage is similar to that observed at Yucca Mountain (Maldonado and Koether, 1983).

4.4 Borehole Image Log Summary

Many fractures cannot be discerned with either of the two borehole image logs (the FMS or the BHTV) analyzed for this fracture study. Fractures with very small apertures or those completely sealed with secondary minerals (i.e., closed fractures) may not present sufficient contrast to be imaged by these logging tools. Also, borehole rugosity due to breakouts or washouts may further impede interpretation. Absolute fracture density statistics from these logs will, therefore, not be valid. However, fracture orientation data are credible and are an important hydrologic parameter for the modelers. Because oriented core was not available for this study, fracture strike information from the borehole image logs could not be compared to core data. Fracture dip information was compared and was found to correlate very well.

4.5 Comparison of Fracture Data, Available Hydrologic Test Data, and Caliper Logs

Direct comparisons between available aquifer hydrologic tests and core fracture data is not straightforward. Typically only a small percentage of the borehole was cored, and the intermittent locations did not always correlate to the hydrologic test intervals. Where core and hydrologic test intervals did overlap, comparisons were generally good. Correlations were best in the TCUs where low fracture density and apertures seemed to correlate well with low test-derived relative specific capacity values. Intervals found to be transmissive based on well aquifer tests typically correlated to LFA or WTA with higher fracture densities. Correlating high fracture density data from cores to hydrologic predictions was somewhat more difficult. Larger scale, *in situ* characteristics such as fracture interconnectivity and aquifer extent, which are not easily inferred from core alone, must be considered.

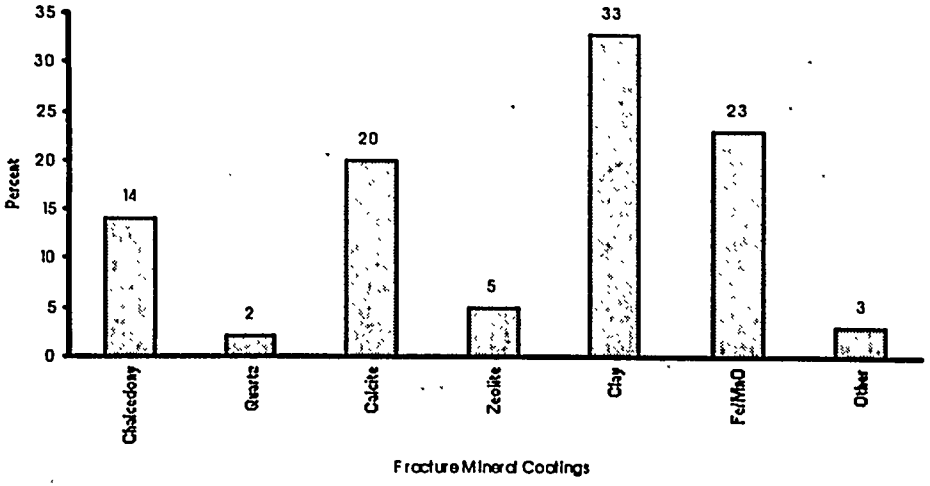

Figure 4-8a
Distribution of Fracture Mineral Coatings Within the Welded Tuff Aquifer for All Holes

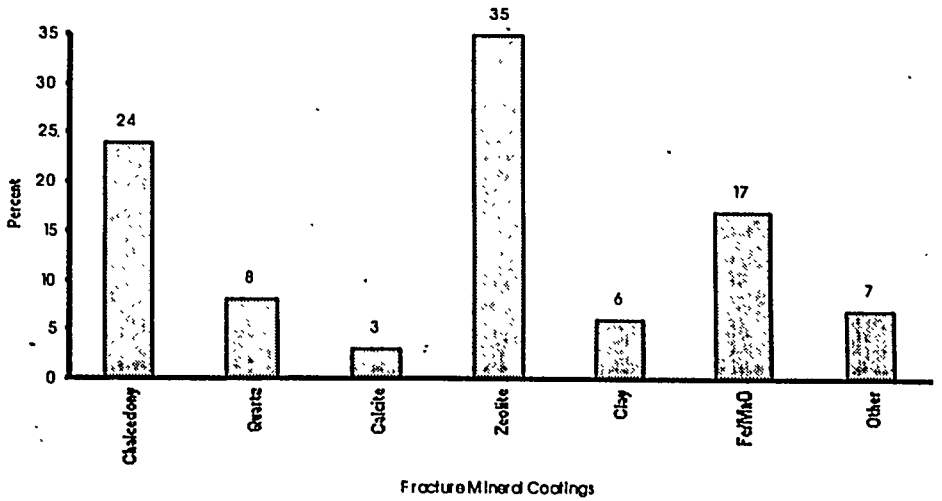

Figure 4-8b
Distribution of Fracture Mineral Coatings Within the Lava Flow Aquifer for All Holes

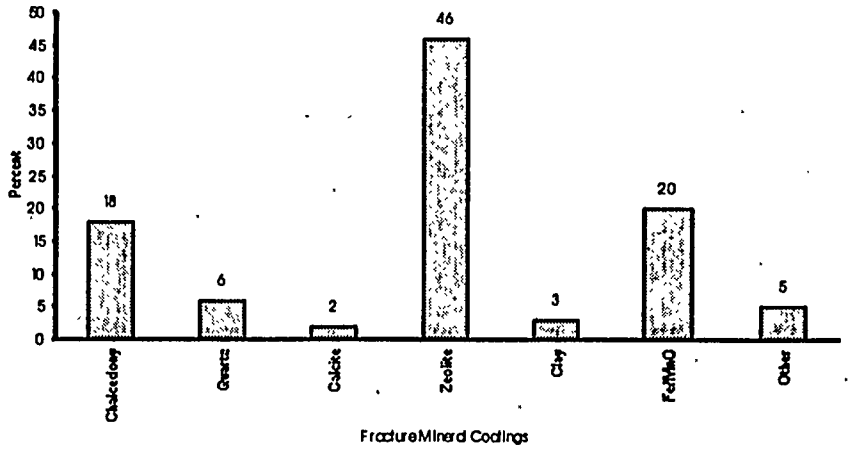

Figure 4-8c
Distribution of Fracture Mineral Coatings Within the Tuff Confining Unit for All Holes

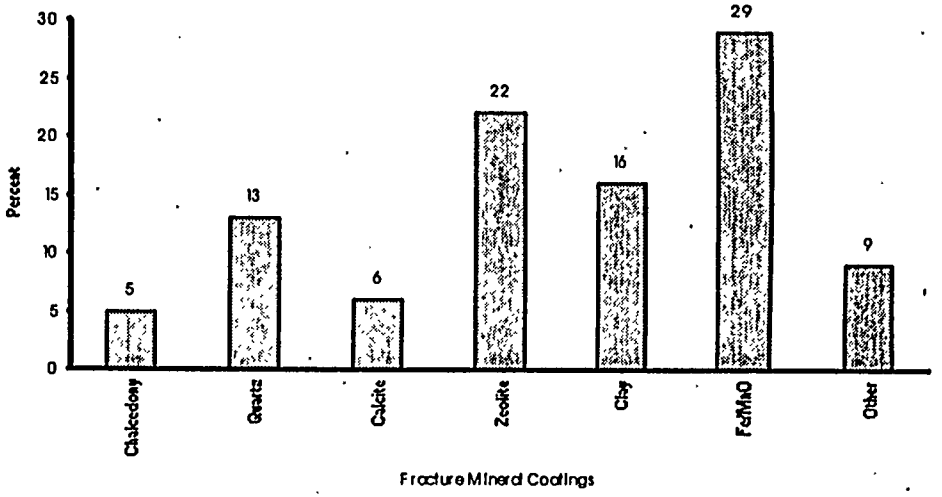

Figure 4-8d
Distribution of Fracture Mineral Coatings Within the Vitric Tuff Aquifer for All Holes

Figure 4-8a-d
Summary of the Distribution of Fracture-Coating Minerals Relative to Hydrogeology

The caliper logs from each hole were compared with the corresponding fracture data. In general, there is an inconsistent correlation between fracture density and borehole irregularities, as indicated by the caliper logs. This finding emphasizes the complex relationships among the formation character, the borehole condition (effects on the *in situ* stress field, interaction between rock and drilling mud, etc.), and geophysical log tools such as the imaging and caliper tools. Though inconsistent, these logs are useful, but must be viewed from this broader, more all-encompassing perspective. Also, it should be noted that the core holes chosen for this study had data only from the older three-arm caliper tools then available. It might be possible to glean a better indication of fractures using data obtained from the six-arm caliper tools in use today.

5.0 Summary and Recommendations for Further Study

The end product of this data analysis effort is the compilation of an extensive data set for several attributes of fractures in volcanic cores from the Pahute Mesa/Timber Mountain area. These data are valuable for the assessment of hydrologic properties and other key parameters for flow and transport modeling such as diffusion, retardation, and conductivity. Other UGTA work planned for 1997 and 1998 will continue the hydrogeologic characterization of this study area, utilizing this and other data sets.

5.1 General Conclusions

The following general statements can be made concerning the data compiled and analyzed during this study:

- Most fracture attributes vary with respect to hydrogeologic unit and, consequently, with hydrostratigraphic unit.
- The mineralogy of fracture coatings was found to vary with respect to hydrogeologic unit, as well as with position relative to the water table.
- For various reasons, not all fractures are imaged by the Borehole Televiewer or the Formation Microscanner™ logs. However, most open fractures, presumably those which are hydrologically significant, are generally recorded. The imaging data, together with the orientation data, provide the hydrologist with valuable information required for modeling.
- An inconsistent correlation between fracture density and borehole irregularities, as indicated by the caliper logs, was noted.
- Comparisons between borehole aquifer tests and core fracture data were generally good. Low fracture density and low aperture, characteristic of tuff confining units, for example, correlate well with low test-derived relative specific capacity values, while intervals found to be transmissive typically correlated to lava-flow aquifers and welded-tuff aquifers with higher fracture densities. However, typically only a small percentage of each borehole was cored, and the cored intervals did not always match the hydrologic test intervals, making direct comparisons somewhat problematical.
- Because the fracture data from UE-18t is so different from that of the other Pahute Mesa drill holes, it is recommended that fracture statistics be presented in two data sets: data from the Pahute Mesa holes only, and data from the Area 18 holes only.

5.2 Recommendations for Further Study

This fracture study highlighted several areas in which our present level of understanding could be improved. Those topics on which additional studies the authors feel would benefit the UGTA program are listed below.

- A change in fracture orientation with depth was noted on the borehole image logs from Exploratory Hole UE-18r and Well ER-20-5#1. Presently, the origin of these anomalous fracture strikes is unexplained. Exploratory Hole UE-18r is located within the moat of the Timber Mountain caldera and thus could be considered to be in a different structural setting from the other holes. Well ER-20-5#1 is located within the buried Silent Canyon caldera complex, as are the other holes in this study. Well ER-20-5#1 is also located very near the locations of TYBO, an underground nuclear test, which could have affected the nearby *in situ* stress field.

- A fair amount of work has been done with regard to the mineralogy of fracture coatings, and this study adds to that body of data. Although useful preliminary observations are presented here, more detailed studies should be conducted. A better understanding of fracture-coating minerals is imperative for modeling the effects of diffusion and sorption, of radionuclides in groundwater.

- Limited amounts of core were available for the deeper hydrostratigraphic units. Additional fracture data should be obtained for these rocks in order to assemble a statistically credible data set.

- Hydrothermal alteration can drastically affect the hydraulic parameters of the geologic medium. For example, at Exploratory Hole UE-18t, located within the Timber Mountain moat, nearly all fractures in the denser volcanic rocks are completely sealed by secondary minerals, and the softer, originally more porous volcanic rocks are altered to clays. Such large-scale alteration could have profound effects on groundwater flow from the testing areas on Pahute Mesa. Although the general location for this hydrothermal alteration is presumably related to caldera structures, highly altered areas are presently not well defined. Further studies could greatly improve our confidence in predicting the nature and extent of this type of alteration.

6.0 References

Adams, P.S. 1994. Written communication summarizing fractures, geology, and hydrogeologic tests at Exploratory hole UE-18r. Las Vegas, NV: IT Corporation.

Allen, Jim. 1993. Personal communication to IT Corp. regarding hydraulic test in Monitoring Well UE-20bh #1, Las Vegas, NV.

Bechtel Nevada. 1996. "Well-site Core Handling," department procedure NTS-GEO-004. Las Vegas, NV.

Blankennagel, R.K., R.A. Young, J.B. Cooper, and H.A. Whitcomb. 1964. *Summary of Ground Water Data Pertinent to Underground Construction and to Water-Supply Development, Pahute Mesa, Nevada Test Site*, U.S. Geological Survey Technical Letter, Special Studies I–27. Denver, CO.

Blankennagel, R.K., and J.E. Weir, Jr. 1966. *Summary of Ground Water Data Pertinent to Underground Construction and to Water-Supply Development, Pahute Mesa, Nevada Test Site,* U.S. Geological Survey Technical Letter, Special Studies I-27., Supplement 2. Denver, CO.

Blankennagel, R.K., and J.E. Weir, Jr. 1973. *Geohydrology of the Eastern Part of Pahute Mesa, Nevada Test Site, Nye County, Nevada*, U.S. Geological Survey Professional Paper 712-B. Denver, CO.

Boyd, O.S., J.L. Wagoner, and R.C. Carlson. 1992. *Site Characterization Report for HRMP Monitoring Well UE20bh-1, Nye County, Nevada Test Site.* Livermore, CA: Lawrence Livermore National Laboratory.

Brikowski, T.J. 1991. *The Hydrology of Underground Nuclear Tests: The Effect of Collapse-Chimney Formation,* Desert Research Institute Publication No. 45090. Las Vegas, NV.

Byers, F.M., Jr., W.L. Hawkins, and D.C. Muller. 1981. *Geology of Drill Hole UE18t and Area 18, Timber Mountain Caldera Moat, Nevada Test Site,* U.S. Geological Survey Report USGS-474-312. Available only from U.S. Department of Commerce, National Technical Information Service, Springfield, VA 22161.

Carlos, B.A., D.L. Bish, and S.J. Chipera. 1990. *Manganese Oxide Minerals in Fractures of the Crater Flat Tuff in Drill Core USW G-4, Yucca Mountain, Nevada*, Los Alamos National Laboratory Report, LA-11787-MS. Los Alamos, NM.

Carr, W.J., F.M. Byers, and E.C. Jenkins. 1968. *Geology of Drill Hole UE18r, Timber Mountain Caldera, Nevada Test Site*, U.S. Geological Survey Technical Letter Special Studies-69. Denver, CO.

Carr, W.J., F.M. Byers, Jr., and E.C. Jenkins. 1981. *Geology of Drill Hole UE18r, Timber Mountain Caldera, Nevada Test Site*, U.S. Geological Survey Report USGS-474-313. Available only from U.S. Department of Commerce, National Technical Information Service, Springfield, VA 22161.

Carroll, R.D. 1966. *Preliminary Interpretation of Geophysical Logs, UE-20f, Pahute Mesa, Nevada Test Site,* U.S. Geological Survey Technical Letter, Special Studies I-37, Supplement 1. Denver, CO.

DOE, see U.S. Department of Energy

Drellack, S.L., Jr, and L.B. Prothro. 1997. *Descriptive Narrative for the Hydrogeologic Model of Western and Central Pahute Mesa Corrective Action Units.* Interim documentation report for the UGTA project, submitted in support of the FY 1997 Pahute Mesa hydrogeological modeling effort. Las Vegas, NV: Bechtel Nevada.

Ekren, E.B., R.E. Anderson, P.P. Orkild, and E.N. Minrichs. 1966. "Geologic map for the Silent Butte, Quadrangle, Nye County, Nevada," U.S. Geological Survey Geologic Quadrangle Map GQ-493 Scale - 1:24,000. Denver, CO.

Ferguson, J.R., A.H. Cogbill, and R.G. Warren. 1994. "A Geophysical-Geological Transect of the Silent Canyon Caldera Complex, Pahute Mesa, Nevada." *Journal of Geophysical Research, v. 99, no. 33: 4323-4339.*

GeoTrans, Inc. 1995. *A Fractured/Porous Media Model of Tritium Transport in the Underground Weapons Testing Areas, Nevada Test Site.* Boulder, CO: GeoTrans, Inc.

Hoover, D.L. 1964. *Preliminary Report on the Lithology, Hydrology and Physical Properties of the UE20e and the UE20e-1 Drill Holes, Area 20, Pahute Mesa, Nevada Test Site,* U.S. Geological Survey Report, Special Studies I-25. Denver, CO.

IT, see IT Corp.

IT Corp. 1995a. "Chain of custody," ITLV Standard Quality Practice No. ITLV-0402. Las Vegas, NV.

IT Corp. 1995b. "Sample handling, packaging and shipping," ITLV Standard Quality Practice No. ITLV-0403. Las Vegas, NV.

IT Corp. 1996a. *Underground Test Area Fracture Analysis Report: Analysis of Fractures in Volcanic Cores from Pahute Mesa, Nevada Test Site.* Draft. Las Vegas, NV.

IT Corp. 1996b. *Regional Geologic Model Data Documentation Package (Phase I Data Analysis Documentation, Volume 1, Parts 1 and 2)*, ITLV/10972-181. Las Vegas, NV.

Iyengar, Sam. 1996. "Fracture Mineralogy of Core Fragments from Nevada Test Site." Letter to K. Roberson, IT Corp., from Analytical Materials Laboratory, Santa Barbara, CA.

Laczniak, R.J., J.C. Cole, D.A. Sawyer, and D.A. Trudeau. 1996. *Summary of Hydrogeologic Controls on Ground-Water Flow at the Nevada Test Site, Nye County, Nevada,* U.S. Geological Survey Open-File Report 96-4109. Carson City, NV.

Maldonado, F. And S.L. Koether. 1983. *Stratigraphy, Structure, and Some Petrographic Features of Tertiary Volcanic Rocks at the USW G-2 Drill Hole, Yucca Mountain, Nye County, Nevada,* U.S. Geological Survey Open File Report 83-732. Denver, CO.

Paillet, F.L. 1991. "Flowmeter and Other Log Data for Borehole Ue-18r." U.S. Geological Survey Memorandum.

Paillet, F.L. U.S. Geological Survey. February 23, 1994. Letter to Pamela Adams, IT Corp, regarding reinterpretation of 1990 flowmeter data from Well UE18r. Denver, CO.

Prothro, L.B., and S.L. Drellack, Jr. 1997. *Nature and Extent of Lava-Flow Aquifers Beneath Pahute Mesa, Nevada Test Site.* DOE/NV/11718-156. Las Vegas, NV: Bechtel Nevada.

Reiner, S.R., G.L. Locke, and L.S. Robie. 1995. *Ground-Water Data for the Nevada Test Site and Selected Other Areas in South-Central Nevada, 1992-93,* U.S. Geological Survey Open File Report 95-160. Carson City, NV.

Santos, E.S. 1964. *Preliminary Report on the Lithology of Drill Hole UE20c, Pahute Mesa, Nevada Test Site,* U.S. Geological Survey Technical Letter Special Studies I-26. Denver, CO.

U.S. Department of Energy, Nevada Operations Office. 1995. "Underground Test Area Operable Unit Geologic Cuttings and Core Collection and Management," DOE/NV Environmental Restoration Division Procedure No. ERD-UGTA-05-303, Rev. 0. Las Vegas, NV.

U.S. Department of Energy. 1994. *United States Nuclear Tests, July 1945 through September 1992,* DOE/NV-209 (Rev. 14). Las Vegas, NV.

Waddell, R.K, J.H. Robison, and R.K. Blankennagel. 1984. *Hydrology of Yucca Mountain and Vicinity, Nevada-California Investigative Results Through Mid-1983,* U.S. Geological Survey Water-Resources Investigation Report 84-4267. Denver, CO.

Warren, R.G. 1994. Informal document, *Structural Elements and Hydrogeologic Units of the Southwestern Nevada Volcanic Field.* Los Alamos, NM: Los Alamos National Laboratory.

Winograd, I.J. and William Thordarson. 1975. *Hydrogeologic and Hydrochemical Framework, South-Central Great Basin, Nevada-California with Special Reference to the Nevada Test Site,* U.S. Geological Survey Professional Paper 712-C. Denver, CO

This page intentionally left blank.

Appendix A
Mineralogy Information

A1.0 Fracture Mineralogy Sample Descriptions

A total of twenty core-fragment samples was collected from Nevada Test Site drill holes UE-19x, UE-18r, UE-18t, UE-20f, UE-20e#1, UE-20bh#1, and UE-20c. The samples were collected for laboratory analysis of the mineral phases that coat fracture surfaces on the core fragments (Table A-1). In most cases, two or more mineral species are present on the fracture surface. Qualitative descriptions of the mineral phases on each sample, based on microscopic analysis of the fracture surfaces, are provided in the following log, which also includes instructions for the analytical laboratory. The descriptions present an initial hypothesis concerning the identity of each mineral and a rough estimate of the percentage of the fracture surface that is covered by each mineral phase. These crude identifications and estimates were intended to be used as guidelines by the analytical laboratory to aid in locating and/or differentiating between the minerals.

Section A2 contains an explanation of fracture-coating categories, and the results of mineralogical analyses by Analytical Materials Laboratory are presented in Section A3.

Sample Collection Log

UE-19x

Eleven core fragment samples from core UE-19x were collected on January 18, 1996, by Sig Drellack (Bechtel Nevada [BN]), Lance Prothro (BN), Keith Roberson (IT Corp. [IT]), and Brad Schier (Daniel B. Stephens & Assoc. [DBS&A]).

Depth	Description of Material to be Analyzed/Notes
266 ft	Identify (ID) soft, waxy, white mineral with desiccation cracks, botryoidal in part (i/p) (zeolite?), covers 100% of fracture surface.
459 ft	ID cream-colored, cryptocrystalline mineral covering 90% of surface; and very finely crystalline, white, opaque, hard (>5) crystals distributed across ~60% of surface (vapor-phase silicate?)
781 ft	ID microcrystalline, clear, euhedral crystals covering entire fracture surface (Vapor-phase silicate?); plus larger colorless euhedral crystals (quartz?) (~20% coverage); plus flat, clear, colorless, striated rhombic crystals (sanidine ?) (~20% coverage); plus cream-colored, chalky mineral (zeolite?).
901 ft	ID hard (>6), white, opaque, microcrystalline (silicate ?) coating ~35% of surface; and reddish-brown, soft zeolite (?) that covers ~15% of the white mineral.
911 ft	ID milky white, hard (>6), opaque, euhedral, striated crystals (as in 907') that cover ~30% of surface; plus dark olive/gray, opaque, hard (>6), striated crystals (poss. same as white mineral; plagioclase?) (~10% surface coverage); plus any zeolites present. Also, if possible, ID the *very* fine specs of dark crystals (pyrite or other sulfide?) disseminated across fracture surface (~5% surface coverage).
1,020 ft	ID translucent, botryoidal, hard (~7) silicate (chalcedony?) that covers 90% of surface; plus overlying orange-brown, soft, waxy material (zeolite?) that overlies 70% of the chalcedony.
1,241 ft	Sample contains at least seven mineral phases for ID: white translucent calcite (10%); gray translucent chalcedony (30%); white & cream-colored zeolites (15%); hard black manganese oxide (?) (10%); very soft black clay (5%); & brownish anhedral quartz (40%).
2,041 ft	ID thin, moderately hard (~5), translucent, milky white film coating ~80% of fracture surface (one surface only).

2,142 ft ID basal fracture coating (covers ~80% of surface) of waxy, translucent, gray, moderately soft (<4) zeolite or clay (contains desiccation cracks); plus overlying harder (5 to 6), cream-colored, opaque to translucent zeolite (?) that covers 40%.

2,148 ft ID moderately hard (5 to 6), cream-colored, translucent zeolite (?) covering entire surface.

2,349 ft ID dark green/gray, waxy mineral (zeolite ?) coating entire fracture surface.

UE-20f

Two core fragment samples from core UE-20f were collected on January 18, 1996, by Sig Drellack (BN), Lance Prothro (BN), and Keith Roberson (IT).

Depth Description of Material to be Analyzed/Notes

2,628 ft ID finely sucrosic, hard, cream-colored mineral (chalcedony ?) coating 100% of surface; plus grayish brown, finely sucrosic quartz (?) coating 40% of first mineral's surface; plus tan powder zeolite (?) that covers 30% of surface (on top of first 2 minerals).

3,704 ft ID white zeolite (?) coating ~90% of both fracture surfaces.

UE-20e#1

One core fragment sample from core UE-20e#1 was collected on January 31, 1996, by Lance Prothro (BN) and Keith Roberson (IT).

Depth Description of Material to be Analyzed/Notes

4,501 ft ID 2 mineral phases: cream-colored soft powder (zeolite?) covering ~60% of fracture surface; plus white to colorless, translucent, hard (>6), equant, euhedral crystals (quartz or other silicate?) covering ~40% of surface.

UE-20bh#1

One core fragment sample from core UE-20bh#1 was collected on January 31, 1996, by Lance Prothro (BN) and Keith Roberson (IT).

Depth	Description of Material to be Analyzed/Notes
2,410 ft	ID 2 mineral phases: white, soft powder (zeolite?)that covers 100% of fracture surface and forms coherent crusts, fibrous "spider webs", and snowy masses; plus black dendrites (manganese oxide; pyrolusite?) that occur sporadically throughout the white powder.

UE-18r

One core fragment sample from core UE-18r was collected on January 31, 1996, by Lance Prothro (BN) and Keith Roberson (IT).

Depth	Description of Material to be Analyzed/Notes
3,901 ft	ID 4 mineral phases: black to dark gray, soft, fibrous, metallic mineral (resembles "steel wool") that covers ~20% of surface; brown to gray, hard, crystalline silicate (?) with bladed to honeycomb morphology (covers ~50% of surface); very fine, euhedral crystals (quartz?) covering bladed mineral (~30% surface coverage); and light pink zeolite (?) covering ~15% of surface.

UE-18t

Two core fragment samples from core UE-18t were collected on January 31, 1996, by Lance Prothro (BN) and Keith Roberson (IT).

Depth	Description of Material to be Analyzed/Notes
1,066 ft	ID 2 mineral phases: thick (8 to 10 mm) white, soft, powdery clay or zeolite (?) that covers 100% of surface; and soft black/dark gray Mn oxide (?) interspersed within the white powder (coverage undetermined).
1,251 ft	Sample contains 5 recognized mineral phases: thin black Mn-oxide (?) underlying all other mineral coatings; white to gray blades of chalcedony (?) covering ~100% of surface; dark brown to colorless, very finely sucrosic, very hard (~7), euhedral crystals (quartz?) precipitated on the chalcedony, also covering almost entire surface; soft white powdery mineral (zeolite?) covering ~10% of surface; and a second phase of amorphous white/gray chalcedony (?) covering ~30 of surface.

UE-20c

Two core fragment samples were collected from core UE-20c on February 5, 1996, by Sig Drellack (BN), Lance Prothro (BN.), and Brad Schier (DBS&A).

Depth	Description of Material to be Analyzed/Notes
2,851 ft	ID 2 mineral phases: 75% of surface is coated with tan to light brown very finely crystalline mineral (?) that appears to have been altered in places to a cream-colored clay or zeolite (?); 25% of the first mineral surface is coated by a soft, brownish black mineral (Mn oxide?) with a "splattered" distribution.
2,907 ft	ID 2 mineral phases: thin coating or crust of light reddish tan, hard cryptocrystalline material (chalcedony?) covering ~100% of surface; ~75% of that material is covered by a gray/black, hard, crystalline mineral with a "micro-botryoidal" appearance (chalcedony stained by Mn-oxide or Fe-oxide?).

A2.0 Explanation of Fracture-Coating Categories

Table A-1
Explanation of Fracture-Coating Categories
Used for Initial Visual Observation in this Study

FRACTURE COATING I.D. NUMBER	SHORT NAME	DESCRIPTION
0	None	No visible mineral coating along any portion of the fracture surface(s).
1	Chalcedony	Typical cryptocrystalline variety of quartz. May occur as a thin coating or in thicker botryoidal forms.
2	Euhedral Quartz	Typically as a sucrosic, finely crystalline coating. Less common as relatively large, > 1 mm in size, well formed quartz crystals. May occur as individual crystals scattered along a fracture face, or as clusters partially or completely lining vugs.
3	Calcite	Several varieties possible: from microcrystalline coatings to clusters of "sparry" euhedral crystals.
4	Zeolites	Soft, massive; clay-like, commonly cream to tan or green in color.
5	Clay	Typical clay properties including small desiccation cracks; may include some zeolites. White to brown, massive, soft.
6	a. Fe Oxides b. Mn Oxides	a. Reddish-brown to black (with reddish streak) to less common yellowish (limonite), usually occurs as a stain or thin veneer. b. Black, varies from spots to dendrites, to thin coating.
7	Unknown mineral(s)	Could not determine identity by visual observation.
8	Vapor phase	Vapor-phase mineralization; product of late-stage cooling and degassing. High-temperature quartz and feldspar mineralogy. Commonly exhibits a sucrosic texture. Also included is a clear, flat, tubular, striated variety.
9	Unknown silicate	Includes white, opaque, hard, massive variety; sometimes grading into larger striated microcrystalline crystals.
10	Fault gouge	Soft, pulverized material. Although clay-like, may be differentiated from the clay or zeolite categories by coarser texture, often with matrix inclusions.

A3.0 Fracture Mineralogy of Core Fragments from Nevada Test Sites

The following pages present the results of mineralogical analyses conducted by Analytical Materials Laboratory on twenty samples from Pahute Mesa core holes (see sample descriptions in Section A1.0).

This page intentionally left blank.

ANALYTICAL MATERIALS LABORATORY

Experts in X-Ray Analysis

3463 State Street, #349 • Santa Barbara, CA 93105
Phone: (805) 682-0051 • Fax: (805) 687-2297

Sam Iyengar, Ph.D
Technical Director

March 1, 1996

Mr. Keith Roberson
IT Corporation
4330 South Valley View
Suite 114
Las Vegas, Nevada 89103 - 4047

Dear Keith

Enclosed please find a report on the mineralogy of 20 samples you submitted. Please review this and call me if you have any questions or concerns

Sincerely,

S Iyengar

Sam Iyengar

This page intentionally left blank.

Fracture Mineralogy of Core Fragments from Nevada Test Sites

Introduction:

Twenty core samples from Nevada Test Site were submitted for mineralogical analysis. Mineralogy of materials on the fracture surfaces were characterized using X-ray powder diffraction (XRD), electron microprobe and polarizing microscope. The following report summarizes the findings:

Materials:

The fracture surfaces from the following twenty core samples were characterized:

Core #	Depth (ft.)
UE - 19x	266
	459
	781
	901
	911
	1020
	1241
	2041
	2142
	2148
	2349
UE - 20f	2628
	3704
UE - 20e#1	4501
UE - 20bh#1	2410
UE - 18r	3901
UE - 18t	1066
	1251
UE - 20c	2851
	2907

Methods:

Materials on the fracture surfaces were scrapped or hand picked for the analysis. *For XRD analysis,* they were ground in an agate mortor and pestle, and were loaded in a sample holder. They were examined using a Scintag diffractometer and were scanned from 5 to 65 degrees two-theta using Cu K-alpha radiation at 45 kV and 40 ma. The resulting patterns collected on a computer were matched with the reference standards for various inorganic and organic materials stored in the JCPDS data base

For Microprobe analysis, materials were applied to a spectrographically pure carbon black and vacuum coated with about 300 A carbon. They were bombarded with 20 kV electrons in a Cameca Electron beam Microprobe Analyzer causing the emission of characteristic X-rays for each element. These X-rays were detected and identified by the integral energy dispersive optics of the X-ray spectrometer. The counts were collected simultaneously for 1000 seconds and quantified with the aid of the associated Sun computer using a fundamental parameters iteration and comparison to known standards. The unknowns and the standards were run under identical conditions at a take-off angle of 42 degrees.

For Clay analysis, the powder samples were suspended and shaken in distilled water to promote dispersion. The time required to separate <2 uM fraction was calculated from the Stocks law and the suspensions were allowed to stand for appropriate time. The supernatant (with colloids) solution was decanted into a separate beaker. The process of adding water and settling was continued till the supernatant became clear.

A portion of the clay suspension in the beaker was used to make oriented clay mounts on a Millipore filter. The suspensions were filtered through a 45 uM filter paper on a Millipore filter set-up using vacuum. They were then washed thoroughly with distilled water to remove excess salts. The clay cake on the filter paper was transferred, while still wet, onto a glass slide and kept in an ethylene glycol chamber for 24 hours. A drop of glycol was placed on the edge of each slide before placing them in the chamber. The oriented mounts were heated to 150 C and 550 C in a muffle furnace to confirm the presence of smectite and chlorite, respectively.

Oriented and glycolated clay mounts were scanned from 2 to 45 degrees two-theta on a Scintag diffractometer using Cu K-alpha radiation at 40 kV and 45 ma. The heated clay mounts were scanned from 3 to 17 degrees two theta using the same setup described above

For petrographic work, grain mounts of powders were prepared in canadabalsam. They were examined using a Leitz petrographic microscope with an image processor. Thermal images of interested samples were prepared.

Results and Discussion:
The powder XRD patterns for the samples are shown in attached figures and the mineralogy is summarized in table 1. In most cases, the minerals are arranged in decreasing abundance. A NIST **silicon standard** was also analyzed and is shown in figure 21 along with a stick pattern for the reference standard (PDF # 27 - 1402) from the JCPDS data base. A certificate is also enclosed.

The non-clay minerals found are **quartz** (chert, chalcedony), **cristobalite, tridymite, feldspars (both K- and plagioclase), calcite** and **Ilmenite** In most of the figures, a stick pattern for quartz (PDF # 33 – 1161) from the Joint committee for Powder Diffraction Standards (JCPDS) data base is shown.

Two major zeolite minerals – **Clinoptilolite** (PDF # 39 - 1383) and **Mordenite** (PDF # 29 - 1257) – are present in some of the samples. Stick patterns for these two are shown in the XRD patterns for the samples that contain them.

The major clay mineral components are **smectite,** followed by small amounts of **mica (or illite).** One sample (UE - 19x @ 2349 ft.) contained a clay mineral, **palygorskite.** Another sample (UE - 18r @ 3901 ft.) contained an **Interstratified smectite-mica** mineral called **rectorite.** Its presence is evident from the appearance of integral super-lattice "d" spacings.

The presence of smectite is confirmed by analyzing oriented mounts of clay fraction (< 2 or 5 microns) that has been glycolated. An increase (expansion) in "d" spacing confirms its presence. In most of the figures, the clay XRD scan is superimposed on the corresponding scans for the whole (powdered) rock. In sample UE - 19x @ 911 ft, grains were picked from the wide "holes" on the fracture surface and analyzed. It was mostly smectite.

For microprobe analysis, selected grains were hand picked under a stereo-microscope and mounted on a carbon tape. They were analyzed using a 2 - 3 microns electron beam. When Mn oxides coatings was suspected, the same procedure was followed and confirmed its presence.

Table 1

Core #	Depth (ft)	Mineralogy		
		Minerals present	comments	Figures
UE - 19x	266	• Smectite	Expands on glycolation	Figure 1
	459	• Quartz • Na and K - Feldspars • Mica • Smectite	*Creamy and white crystals* are Si rich	Figs. 2 & 2a (XRD) Fig. 2b (probe)
	781	• Quartz • Na and K - Feldspars • Clinoptilolite • Smectite & mica	*Microcrystalline grains* were chert and Si rich. *Creamy* - clinop.	Figs 3 & 3a (XRD) Figs 3b & 3c (probe)
	901	• Quartz • Tridymite • Smectite • Feldspars	Mostly Si rich	Fig 4 (XRD) Fig 4a (probe)
	911	• Quartz • Feldspars – Ca & Na • Smectite • Clinoptilolite (trace) • Ilmenite (trace)	*Milky white & olive gray grains* are Si rich with Al, Mg – zeolite & clay. *Dark crystals* – Ilmenite	Figs. 5 & 5a (XRD) Figs 5b & 5c (probe)
	1020	• Smectite • Cristobalite • Quartz (chert) • Feldspars	*Chert grains* coated with clay	Figs 6 & 6a (XRD) Fig 6b (probe) Fig 6c (petro.)
	1241	• Cristobalite • Smectite • Clinoptilolite • Feldspars • Calcite • Mica	*White translucent, chalcedony grains* are Si rich crist. grains *White & cream colored grains* - zeolite *Black clay* – smectite with Mn coating	Figs 7 & 7a (XRD) Figs 7b, 7c & 7d (probe) Fig 7e - (petro)

Table 1 (Contd.)

Core #	Depth (ft)	Mineralogy		
		minerals present	comments	Figures
UE - 19x	2041	• Clinoptilolite • Mica		Figure 8 (XRD)
	2142	• Clinoptilolite • Smectite • Mica (trace) • Tridymite	*Waxy crystals* are Clinoptilolite *Creamy grains*– clay	Figs. 9 & 9a (XRD)
	2148	• Clinoptilolite • Quartz • Tridymite • Mica		Figs 10 (XRD)
	2349	• Clinoptilolite • Palygorskite		Fig 11 & 11a (XRD)
UE - 20f	2628	• Clinoptilolite • Cristobalite • Quartz • Tridymite • Mica	*Grayish white & tan grains* are Si rich with Al and K - - zeolite & Fd	Figs. 12 (XRD) Figs 12a (probe)
	3704	• Mordenite		Figs 13 (XRD)
UE - 20e#1	4501	• Clinoptilolite • Quartz • Feldspars • Mica		Figs 14 (XRD)
UE - 20bh#1	2410	• Mordenite • Quartz	*Black dendrites* are Mn oxide coatings	Figs 15 & 15a (XRD Fig 15b (probe)
UE - 18r	3901	• Interstratified Smectite-mica (Rectorite) • Quartz	*Honeycomb and pink materials* are same - clay *Steel wool* – clay & cherts coated with Mn oxides	Figs 16 & 16a (XRD) Figs 16b, 16c (probe) Fig 16d (petro.)

Table 1 (Contd.)

Core #	Depth (ft)	Mineralogy		
		minerals present	comments	Figures
UE - 18t	**1066**	• Smectite • Quartz	*Black* - clay coated with Mn oxides	Figs. 17 & 17a (XRD) Figs 17b & 17c (probe)
	1251	• Quartz • Smectite • Mica (trace)	*Underlying black vein* -- Chalcedony coated with Mn oxides *Euhedral grains* -- Qtz. *White powdery* -- clay	Figs. 18 & 18a (XRD) Fig 18b (probe)
UE - 20c	**2851**	• Quartz • Smectite	*Tan to light brown grains* -- Qtz or chert coated with clay & Mn oxides.	Figs 19 & 19a (XRD) Fig 19b (probe)
	2907	• Quartz • K-, Na- and Ca Feldspars • Mica	*Light reddish brown grains* -- Qtz or chert coated with fine grained mica clay *"micro-botryoidal" looking grains* -- Si grains coated with Mn oxides	Fig 20 & 20a (XRD) Fig 20b (petro.) Probe figures not shown.

Appendix B

Annotated Bibliography of Nevada Test Site Fracture Data

B1.0 Introduction

Table B-1 is an annotated bibliography that lists (alphabetically by author) pertinent documents published by the Yucca Mountain Project and the Nevada Test Site (NTS) Containment Program regarding fracture characteristics in volcanic rocks. These documents contain fracture data for saturated and unsaturated volcanic rocks at Yucca Mountain and Pahute Mesa, and generally address field- and laboratory-derived fracture parameter data that are relevant to groundwater flow and contaminant transport modeling.

These references were compiled in 1996 from the libraries of four NTS organizations: the Yucca Mountain Project (YMP), U.S. Department of Energy (DOE/NV), Bechtel Nevada (BN), and IT Corporation (IT). Key words used in the searches included aperture, conductivity, core, fracture, geohydrologic, geomechanic, hydrogeologic, hydrologic, orientation, porosity, permeability, rock mechanics, spacing, televiewer, Yucca Mountain, and various Area 25 well names.

In addition to library database key word and well name searches, the following bibliographies identified pertinent documents:

Glanzman, V.M. 1991. *Bibliography of Publications Related to the Yucca Mountain Site Characterization Project prepared by U.S. Geological Survey Personnel Through April 1991*, USGS Open-File Report 91-341. Denver, CO.

Glanzman, V.M. 1992. *Bibliography of Publications Prepared by U.S. Geological Survey Personnel Under Cooperative Programs with the U.S. Department of Energy and Predecessor Agencies, 1957-1991, with Emphasis on Nuclear Testing Programs*, USGS Open-File Report 92-502. Denver, CO.

Office of Scientific and Technical Information. 1992. *Yucca Mountain Site Characterization Project Bibliography, January-June 1992, An Update*, U.S. Department of Energy, DOE/OSTI--3406 (Suppl.3) (Add.1), DE92016339.

Russell, C.E. 1988. *Annotated Bibliography of the Physical Data of Rainier Mesa and Yucca Mountain*, NWPO-TR-012089. Las Vegas, NV: Desert Research Institute.

Documents that appraise special situations and focus on validating measurement methodologies or developing flow models are not included here. As a result, the amount of raw data presented in the reports is frequently limited. Nonetheless, this bibliography lists each report containing raw fracture data even where the data are scant. Documents without raw fracture data have generally been omitted.

Table B-1
Annotated Bibliography of Nevada Test Site Fracture Data
(Page 1 of 19)

Source	Tracking Number	Reference	Summary of Relevant Data
IT Library	4682	Anderson, L.A. 1994. *Water Permeability and Related Rock Properties Measured on Core Samples from the Yucca Mountain* USW GU-3/G-3 and USW G-4, USGS Open-File Report 92-201.	Porosity and permeability values compared with volcanic stratigraphy for 226 core samples
IT Library	0154	Anderson, L.A. 1991. *Results of Rock Property Measurements Made on Core Samples from Yucca Mountain Boreholes, Nevada Test Site, Nevada, Part 1. Boreholes UE25A-4, -5, -6, and -7, Part 2. Borehole UE25P#1*, USGS Open-File Report 90-474.	Porosity and permeability values reported for volcanic and carbonate core samples
IT Library	1175	Anderson, L.A. 1984. *Rock Property Measurements on Large-Volume Core Samples from Yucca Mountain USW GU-3/G-3 and USW G-4 Boreholes, Nevada Test Site, Nevada*, USGS Open-File Report 84-552.	Porosity values compared with rock density and volcanic stratigraphy for 144 core samples
IT Library	1174	Anderson, L.A. 1981. *Rock Property Analysis of Core Samples from the Yucca Mountain UE25a-1 Borehole, Nevada Test Site, Nevada*, USGS Open-File Report 81-1338.	Porosities and hydraulic conductivities compared with volcanic stratigraphy for 58 core samples
IT Library	0891.01	Barton, C.C. 1991. Abstract: *Fractal Scaling of Fracture Networks in Rock*, USGS Open-File Report 91-125	Spatial distributions of outcrop fracture traces quantified to establish fractal dimension
IT Library	0819	Barton, C.C., W.R. Page, and T.L. Morgan. 1989. *Fractures in Outcrops in the Vicinity of Drill Hole USW G-4, Yucca Mountain, Nevada*, USGS Open-File Report 89-92.	Strike, dip, and surface roughness of 5,000 outcrop fractures reported

Table B-1
Annotated Bibliography of Nevada Test Site Fracture Data
(Page 2 of 19)

Source	Tracking Number	Reference	Summary of Relevant Data
IT Library	4735	Barton, C.C. and P.A. Hsieh. 1989.. "Physical and Hydrologic-Flow Properties of Fractures," In the *Field Trip Guidebook T385 0-87590-650-8*, Presented at the 28th International Geological Congress, Las Vegas, Nevada; Zion Canyon, Utah; Grand Canyon, Arizona; and Yucca Mountain, Nevada. Washington, DC: American Geophysical Union.	Fracture characteristics discussed generally and mapping of Yucca Mountain pavements described
DOE/NV Library	Journal	Barton, C.C. and E. Larsen. 1985. "Fractal Geometry of Two-Dimensional Fracture Networks at Yucca Mountain, Southwestern Nevada," In *Proceedings of the International Symposium on Fundamentals of Rock Joints*, Bjorkliden, Lapland, Sweden, September 15-20.	Fracture orientation, trace lengths, and networks presented
IT Library	0012	Bentley, C.B. 1984. *Geohydrologic Data for Test Well USW G-4, Yucca Mountain Area, Nye County, Nevada*, USGS Open-File Report 84-063.	Borehole flow survey, packer test, and pump test results reported
IT Library	0013	Bentley, C. B., J.H. Robison, and R.W. Spengler. 1983. *Geohydrologic Data for Test Well USW H-5, Yucca Mountain Area, Nye County, Nevada*, USGS Open-File Report 83-853.	Pump test, borehole flow survey, and packer-injection test results reported
IT Library	0018	Blankennagel, R.K. and J.E. Weir, Jr. 1973. *Geohydrology of the Eastern Part of Pahute Mesa, Nevada Test Site, Nye County, Nevada*, Geological Survey Professional Paper 712-B.	Fracture frequency in ash-fall, nonwelded ash-fall, and welded tuffs reported
DOE/NV Library	LA-UR-86-1413	Broxton, D.E. and B.A. Carlos. 1986. "Zeolitic Alteration and Fracture Fillings," In *Silicic Tuffs at a Potential Nuclear Waste Repository, Yucca Mountain, Nevada, USA LA-UR-86-1413*, Presented at the Fifth International Water-Rock Interaction Symposium, Reykjavik, Iceland, August.	Fracture fillings discussed

Table B-1
Annotated Bibliography of Nevada Test Site Fracture Data
(Page 3 of 19)

Source	Tracking Number	Reference	Summary of Relevant Data
IT Library	4689	Buscheck, T.A. and J.J. Nitao. 1988. *Estimates of the Width of the Wetting Zone Along a Fracture Subjected to an Episodic Infiltration Event in Variably Saturated, Densely Welded Tuff*, Lawrence Livermore National Laboratory, UCID-21579.	Fracture aperture values reported
IT Library	0891.07	Carlos, B., D. Bish, and S. Chipera. 1991. Abstract: *Distribution of Fracture Lining Minerals at Yucca Mountain*, USGS Open-File Report 91-125.	Fracture coating minerals and abundance discussed
IT Library	2559	Carlos, B., D. Bish, and S. Chipera, 1990, *Manganese-Oxide Minerals in Fractures of the Crater Flat Tuff in Drill Core USW G-4, Yucca Mountain, Nevada*, LA-11787-MS. Los Alamos, NM: Los Alamos National Laboratory.	Fracture coating minerals and abundance discussed
IT Library	2557	Carlos, B. 1989. *Fracture-Coating Minerals in the Topopah Spring Member and Upper Tuff of Calico Hills from Drill Hole J-13,* LA-11504-MS. Los Alamos, NM: Los Alamos National Laboratory.	Fracture coating minerals in J-13 compared to those in USW G-4
YMP Library	LA-10415-MS	Carlos, B.A. 1985. *Minerals in Fractures of the Unsaturated Zone from Drill Core USW G-4, Yucca Mountain, Nye County, Nevada*, LA-10415-MS. Los Alamos, NM: Los Alamos National Laboratory.	Fracture coatings and fillings discussed
YMP Library	LA-UR-86-1412	Carlos, B.A. 1986. *Occurrence of Fracture-Lining Manganese Minerals in Silicic Tuffs, Yucca Mountain, Nevada*, LA-UR-86-1412. Los Alamos, NM: Los Alamos National Laboratory.	Fracture coatings and fillings discussed
DOE/NV Library	LA-10927-MS	Carlos, B.A. 1987. *Minerals in Fractures of the Saturated Zone from Drill Core USW G-4, Yucca Mountain, Nye County, Nevada*, LA-10927-MS, UC-70. Los Alamos, NM: Los Alamos National Laboratory.	Fracture coating minerals and abundance discussed

Table B-1
Annotated Bibliography of Nevada Test Site Fracture Data
(Page 4 of 19)

Source	Tracking Number	Reference	Summary of Relevant Data
IT Library	1234	Carlson, R.C. and J.L. Wagoner. 1991. *U20be Site Characteristics Report*, CP 91-18. Lawrence Livermore National Laboratory.	Fracture frequency reported
IT Library	1177	Carr, M.D., S.J. Waddell, G.S. Vick, J.M. Stock, S.A. Monsen, A.G. Harris, B.W. Cork, and F.M. Byers, Jr. 1986. *Geology of Drill Hole UE25p#1: A Test Hole Into Pre-Tertiary Rocks Near Yucca Mountain, Southern Nevada*, USGS Open-File Report 86-175.	Fracture data from oriented core (Paleozoic section) and acoustic borehole televiewer log results (Tertiary and Paleozoic sections) reported. Fractures described
BN Library	USGS Tech. Letter SS I-37, Supp. 1.	Carroll, R.D. 1966. *Preliminary Interpretation of Geophysical Logs, UE-20f, Pahute Mesa, Nevada Test Site*, U.S. Geological Survey Technical Letter, Special Studies I-37, Supplement 1. Denver, CO.	Rock properties at UE-20f, including, log response, hydrology and inferred fracture zones
IT Library	1309	Clark, S. and D. McArthur. 1986. *U20av 624.8-m Site Characteristics Report*, CP 86-55. Lawrence Livermore National Laboratory.	Location of cooling joints indicated
IT Library	1312	Clark, S., R. Newmark, and D. McArthur. 1987. *U20ar 544.7-m Site Characteristics Report*, CP 87-26. Lawrence Livermore National Laboratory.	Location of cooling joints indicated
IT Library	1310	Clark, S. and G. Pawloski. 1986. *U20at 544.1-m Site Characteristics Report*, CP 86-56. Lawrence Livermore National Laboratory.	Fracture frequency and fault attitude indicated
IT Library	1376	Clark, S. and G. Pawloski. 1985. *U20aq 549-m Preliminary Site Characteristics Summary*, CP 85-114. Lawrence Livermore National Laboratory.	Location of cooling joints indicated and cross-referenced with cooling joints at U20al
IT Library	1375	Clark, S. and C. Schmidt. 1986. *U20ap 635-m Site Characteristics Report*, CP 86-48. Lawrence Livermore National Laboratory.	Location and attitude of faults and fractures indicated

Table B-1
Annotated Bibliography of Nevada Test Site Fracture Data
(Page 5 of 19)

Source	Tracking Number	Reference	Summary of Relevant Data
IT Library	1211	Clark, S. and J. Wagoner. 1986. *U19an 615.7-m Preliminary Site Characteristics Summary*, CP 86-13. Lawrence Livermore National Laboratory.	Location of cooling joints indicated
IT Library	0011	Craig, R.W. and K.A. Johnson. 1984. *Geohydrologic Data for Test Well UE-25p#1, Yucca Mountain Area, Nye County, Nevada*, USGS Open-File Report 84-450.	Borehole flow survey, pump test, and packer-injection test results reported
IT Library	1548	Craig, R.W. and R.L. Reed. 1991. *Geohydrology of Rocks Penetrated by Test Well USW H-6, Yucca Mountain, Nye County, Nevada*, USGS Water-Resources Investigations Report 89-4025.	Borehole flow survey, pump test, and packer-injection test results reported
IT Library	0014	Craig, R.W., R.L. Reed, and R.W. Spengler. 1983. *Geohydrologic Data for Test Well USW H-6, Yucca Mountain Area, Nye County, Nevada*, USGS Open-File Report 83-856.	Pump test results reported
IT Library	0064	Craig, R.W. and J.H. Robison. 1984. *Geohydrology of Rocks Penetrated by Test Well UE-25p#1, Yucca Mountain, Nye County, Nevada*, USGS Water-Resources Investigations Report 84-4248.	Borehole flow survey, pump test, and packer-injection test reported
IT Library	0891.06	Diehl, S.F., M.P. Chornack, H.S. Swolfs, and J.K. Odum. 1991. Abstract: *Fracture Studies in the Welded Grouse Canyon Tuff: Laser Drift of the G-Tunnel Underground Facility, Rainier Mesa, Nevada Test Site, Nevada*, USGS Open-File Report 91-125.	Orientation of prominent fractures and microfractures for Laser Drift presented
IT Library	4686	Ellis, W.L. and H.S. Swolfs. 1983. *Preliminary Assessment of In-Situ Geomechanical Characteristics in Drill Hole USW G-1, Yucca Mountain, Nevada*, USGS Open-File Report 83-401.	Fracture frequency identified

Table B-1
Annotated Bibliography of Nevada Test Site Fracture Data
(Page 6 of 19)

Source	Tracking Number	Reference	Summary of Relevant Data
IT Library	0176	Erickson, J.R. and R.K. Waddell. 1985. *Identification and Characterization of Hydrologic Properties of Fractured Tuff Using Hydraulic and Tracer Tests -- Test Well USW H-4, Yucca Mountain, Nye County, Nevada*, USGS Water-Resources Investigations Report 85-4066.	USW H-4 televiewer log results reported, including fracture frequency and orientation and an estimation of fracture porosity
IT Library	0159	Flint, L.E. and A.L. Flint. 1990. *Preliminary Permeability and Water-Retention Data for Nonwelded and Bedded Tuff Samples, Yucca Mountain Area, Nye County, Nevada*, USGS Open-File Report 90-569.	Saturated permeability, relative permeability, water retention properties, grain density, bulk density, and porosity data reported for 73 core samples
IT Library	2730	Geldon, A.L. 1992. *Preliminary Hydrogeologic Assessment of Boreholes UE-25c #1, UE-25c #2, and UE-25c #3, Yucca Mountain, Nye County, Nevada*, USGS Water-Resources Investigations Report 92-4016.	Fracture density and orientation reported
IT Library	4579	GeoTrans, Inc. 1995. *A Fracture/Porous Media Model of Tritium Transport in the Underground Weapons Testing Areas, Nevada Test Site,* Boulder, Colorado.	Values used in the model for matrix porosity, aperture width, fracture spacing, fracture frequency, hydraulic conductivity, and velocity reported
BN Library	SAND82-1043	Hadley, G.R. 1984. *Water Transport through Welded Tuff*, SAND82-1043. Sandia National Laboratories.	Laboratory experiments on welded tuff core imbibing and drying, capillary action
IT Library	0441	Haldeman, W.R., Y. Chuang, T.C. Rasmussen, and D.D. Evans. 1991. "Laboratory Analysis of Fluid Flow and Solute Transport Through a Fracture Embedded in Porous Tuff, In *Water Resources Research*, Volume 27, No. 1, pp. 53-65. Tucson, AZ: University of Arizona, Department of Hydrology and Water Resources.	Laboratory experiments conducted to determine flow and transport properties of a block of fractured porous tuff described

Table B-1
Annotated Bibliography of Nevada Test Site Fracture Data
(Page 7 of 19)

Source	Tracking Number	Reference	Summary of Relevant Data
IT Library	1176	Healy, J.H., S.H. Hickman, M.D. Zoback, and W.L. Ellis. 1984. *Report on Televiewer Log and Stress Measurements in Core Hole USW-G1, Nevada Test Site, December 13-22, 1981*, USGS Open-File Report 84-15.	Fracture occurrence and orientation reported
IT Library	1374	Howard, N.W. and J.L. Wagoner. 1985. *U20ao 548.6-m Preliminary Site Characteristics Summary*, CP 85-74. Lawrence Livermore National Laboratory.	Location of cooling joints indicated
BN Library		Howard, T.M. and E. Larsen. 1984. Preliminary Study of Joints in the Upper Lithophysical Subunit of the Tiva Canyon Member of the Paintbrush Tuff Formation Near USW-G4, Yucca Mountain, Nevada. Fenix & Scisson, Inc.	Fracture occurrence, orientation, and attributes reported
IT Library		IT Corporation. 1995. *Wells ER-6-1 and ER-6-2 Core Fracture Analyses and Geophysical Log Comparisons*, DOE/NV/10972--XX.	Fracture occurrence, orientation, and attributes in carbonate and argillite rocks at Southern Yucca Flat
IT Library	4685	Janecky, D.R., R.S. Rundberg, M. Ott, and A. Mitchell. 1990. *Update Report on Fracture Flow in Saturated Tuff: Dynamic Transport Task for the Nevada Nuclear Waste Investigations*, LA-11957-MS. Los Alamos, NM: Los Alamos National Laboratory.	Porosity, roughness, fractal dimension, and aperture values presented for a block of fractured tuff removed from the surface of Yucca Mountain
YMP Library	SAND84-2642	Klavetter, E.A. and R.R. Peters. 1986. *Estimation of Hydrologic Properties of An Unsaturated, Fractured Rock Mass*, SAND84-2642. Sandia National Laboratory.	Fracture aperture, conductivity, density, porosity, compressibility, and bulk conductivity reported
IT Library	0805	Klavetter, E.A. and R.R. Peters. 1986. *Fluid Flow in a Fractured Rock Mass*, SAND85-0855C. Sandia National Laboratory.	Continuum model to evaluate water movement through fractured rock developed

Table B-1
Annotated Bibliography of Nevada Test Site Fracture Data
(Page 8 of 19)

Source	Tracking Number	Reference	Summary of Relevant Data
IT Library	0157	Kume, J. and D. Hammermeister. 1990. *Geohydrologic Data from Test Hole USW UZ-7, Yucca Mountain Area, Nye County, Nevada*, USGS Open-File Report 88-465.	Porosity data for drive core samples reported
IT Library	0158	Kume, J. and D. Hammermeister. 1991. *Geohydrologic Data from Drill-Bit Cuttings and Rotary Cores from Test Hole USW UZ-13, Yucca Mountain Area, Nye County, Nevada*, USGS Open-File Report 90-362.	Water content values reported for core samples
IT Library	0019	Lahoud, R.G., D.H. Lobmeyer, and M.S. Whitfield, Jr. 1984. *Geohydrology of Volcanic Tuff Penetrated by Test Well UE-25b#1, Yucca Mountain, Nye County, Nevada*, USGS Water-Resources Investigations Report 84-4253.	Shear fracture frequency and aquifer test results reported
IT Library	4679	Lin, M., M.P. Hardy, and S.J. Bauer, J.F.T. 1992. *Fracture Analysis and Rock Quality Designation Estimation for the Yucca Mountain Site Characterization Project*, SAND92-0449.	Fracture frequency, orientation, roughness, fillings, and coatings reported
IT Library	4678	Lin, W. and W. Daily. 1984. *Transport Properties of Topopah Spring Tuff*, UCRL-53602. Lawrence Livermore National Laboratory.	Permeability of fractured Topopah Spring tuff measured during dehydration - rehydration experiments
BN Library	SAND85-2701	Lin, Y.T., M.S. Tierney, S. Sinnock, editors. 1986. *Preliminary Estimates of Groundwater Travel Time and Radionuclide Transport at the Yucca Mountain Repository Site*, SAND85-2701. Albuquerque, NM: Sandia National Laboratories.	Addresses vertical groundwater flow, effective porosity and hydraulic conductivity.
IT Library	0195	Lobmeyer, D.H. 1986. *Geohydrology of Rocks Penetrated by Test Well USW G-4, Yucca Mountain, Nye County, Nevada*, USGS Water-Resources Investigations Report 86-4015.	Flow survey, packer-injection, and pump test results reported

Table B-1
Annotated Bibliography of Nevada Test Site Fracture Data
(Page 9 of 19)

Source	Tracking Number	Reference	Summary of Relevant Data
IT Library	0010	Lobmeyer, D.H., M.S. Whitfield, Jr., R.R. Lahoud, and L. Bruckheimer. 1983. *Geohydrologic Data for Test Well UE-25b#1, Nevada Test Site, Nye County, Nevada*, USGS Open-File Report 83-855.	Matrix porosity, pore saturation, matrix hydraulic conductivity, shear fracture frequency, and aquifer test results reported
IT Library	4684	Loskot, C.L. and D.P. Hammermeister. 1992. *Geohydrologic Data from Test Holes UE-25 UZ#4 and UE-25 UZ#5, Yucca Mountain Area, Nye County, Nevada*, USGS Open-File Report 90-369.	Water content values reported for core and cuttings samples
IT Library	0789	Maldonado, F. and S.L. Koether. 1983. *Stratigraphy, Structure, and Some Petrographic Features of Tertiary Volcanic Rocks at the USW G-2 Drill Hole, Yucca Mountain, Nye County, Nevada*, USGS Open-File Report 83-732.	Fracture frequency, dip, fillings, coatings, and fracture zones reported
BN Library	SAND84-1697	Martinez, M.J. 1988. *Capillary-Driven Flow in a Fracture Located in a Porous Medium*, SAND84-1697. Albuquerque, NM: Sandia National Laboratories.	Hydraulic lab experiments with several rock units common at Yucca Mountain
IT Library	1233	McKague, H.L. and J.R. Hearst. 1991. *U20ax Site Characteristics Report 21st Anniversary Issue*, CP 91-121. Lawrence Livermore National Laboratory	Fracture frequency reported
IT Library	1304	McKague, L., J. Hearst, and B. McKinnis. 1989. *U20bc Site Characteristics Report*, CP 89-48. Lawrence Livermore National Laboratory.	Fracture frequency reported
IT Library	0759	McKague, H.L. and R.L. Newmark. 1989. *U20bd Site Characteristics Report*, CP 89-167. Lawrence Livermore National Laboratory.	Fracture frequency reported

Table B-1
Annotated Bibliography of Nevada Test Site Fracture Data
(Page 10 of 19)

Source	Tracking Number	Reference	Summary of Relevant Data
IT Library	0004	Montazer, P. and W.E. Wilson. 1984. *Conceptual Hydrologic Model of Flow in the Unsaturated Zone, Yucca Mountain, Nevada*, USGS Water-Resources Investigations Report 84-4345.	Hypothetical model for flow-through layers of fractured volcanics presented
IT Library	0787	Moore, D.E., C.A. Morrow, and J.D. Byerlee. 1984. *Permeability and Fluid Chemistry Studies of the Topopah Spring Member of the Paintbrush Tuff, Nevada Test Site: Part II*, USGS Open-File Report 84-848.	The effect of pore pressure, sample orientation, and flow direction on permeability and pore fluid chemistry evaluated
IT Library	4738	Morgan, T.L. 1984. "Fracture Characterization of the Tiva Canyon Member, Paintbrush Tuff, Nevada," Masters Thesis, Colorado State University, Fort Collins, Colorado.	ORDERED FROM CSU COPY CENTER ON FEBRUARY 8, 1996. PHONE: 1-970-491-1828
IT Library	0891.05	Nelson, P.H., R. Snyder, and J.E. Kibler. 1991. Abstract: *Fracture Counts from Borehole Logs*, USGS Open-File Report 91-125.	Fractures in H-4 counted using sonic waveform, televiewer, and television tools. Median dip angle reported
IT Library	1308	Newmark, R.L. and L. McKague. 1988. *U20aw Site Characteristics Report*, CP 88-201. Lawrence Livermore National Laboratory.	Fracture frequency reported
IT Library	1235	Newmark, R.L. and W.B. McKinnis. 1990. *U20bf Site Characteristics Report*, CP 90-216. Lawrence Livermore National Laboratory.	Fracture frequency reported
IT Library	1212	Newmark, R.L. and J.L. Wagoner. 1988. *U19ax 615.7-m Site Characteristics Report*, CP 88-73. Lawrence Livermore National Laboratory.	Location of cooling joints indicated
IT Library	4736	Newmark, R.L. and J.L. Wagoner. 1990. *U20bb Site Characteristics Report*, CP 90-72. Lawrence Livermore National Laboratory.	Fracture frequency reported

Table B-1
Annotated Bibliography of Nevada Test Site Fracture Data
(Page 11 of 19)

Source	Tracking Number	Reference	Summary of Relevant Data
IT Library	0470	Niemi, A. and G.S. Bodvarsson. 1988. "Preliminary Capillary Hysteresis Simulations in Fractured Rocks, Yucca Mountain, Nevada," In *Journal of Contaminant Hydrology*, Vol. 3. Amsterdam: Elsevier Science Publishers B.V.	Affects of hysteretic capillary pressure - liquid saturation on flow and liquid saturation in fractured tuff simulated
DOE/NV Library	LA-10859-MS	Norris, A.E., F.M. Byers, Jr., and T.J. Merson. 1986. *Fran Ridge Horizontal Coring Summary Report, Hole UE-25h#1, Yucca Mountain Area, Nye County, Nevada*, LA-10859-MS. Los Alamos, NM: Los Alamos National Laboratory.	Fracture frequency and fillings reported
IT Library	0850.09	Novakowski, K.S. 1988. "Comparison of Fracture Aperture Widths Determined from Hydraulic Measurements and Tracer Experiments." Paper presented at the Fourth Canadian/American Conference on Hydrogeology, Banff, Alberta, Canada, June 21-24, National Water Well Association, Dublin, Ohio.	Fracture aperture widths calculated using cubic law equation
IT Library	2445	Paillet, F. 1993. "Using Borehole Geophysics and Cross-Borehole Flow Testing to Define Hydraulic Connections Between Fracture Zones in Bedrock Aquifers." In *Journal of Applied Geophysics:* Amsterdam: Elsevier Science Publishers, B.V.	Geophysical fracture logging techniques discussed
IT Library	2451	Paillet, F. 1994. *Application of Borehole Geophysics in the Characterization of Flow in Fractured Rocks*, USGS Water-Resources Investigations Report 93-4214.	Geophysical fracture logging techniques discussed
IT Library	1370	Pawloski, G.A. 1985. *U20ak 608-m Preliminary Site Characteristics Summary*, CP 85-19. Lawrence Livermore National Laboratory.	Location of cooling cracks indicated
IT Library	1307	Pawloski, G. 1987. *U20ay 620.3-m Site Characteristic Report*, CP 87-63. Lawrence Livermore National Laboratory.	Fracture frequency reported

Table B-1
Annotated Bibliography of Nevada Test Site Fracture Data
(Page 12 of 19)

Source	Tracking Number	Reference	Summary of Relevant Data
IT Library	0460	Peters, R.R. and E.A. Klavetter. 1988. "A Continuum Model for Water Movement in an Unsaturated Fractured Rock Mass." In *Water Resources Research*, Vol. 24, No. 3: 416-430.	Continuum model used to model flow in the unsaturated zone at Yucca Mountain presented
IT Library	0087	Peters, R.R., E.A. Klavetter, I.J. Hall, S.C. Blair, P.R. Heller, and G.W. Gee. 1984. *Fracture and Matrix Hydrologic Characteristics of Tuffaceous Materials from Yucca Mountain, Nye County, Nevada*, SAND84-1471.	Porosities and hydraulic conductivities for 48 different locations at Yucca Mountain reported. Aperture values derived using cubic law equation
IT Library	4688	Rautman, C.A., L.E. Flint, A.L. Flint, and J.D. Istok. 1995. *Physical and Hydrologic Properties of Outcrop Samples from a Nonwelded to Welded Tuff Transition, Yucca Mountain, Nevada*, USGS Water-Resources Investigations Report 95-4061.	Saturated hydraulic conductivity of Tiva Canyon Tuff samples reported
IT Library	1454	Raytheon Services Nevada. 1993. *Yucca Mountain Project, Wet and Dry Drilling Project, Rock Core Properties, Porosity Measurement Methods and Lithium Bromide Analyses*, Volume 1 of 3. Mercury, NV.	Water contents, saturations, porosities, and permeabilities for 40 core samples from the G-Tunnel reported
IT Library	1456	Raytheon Services Nevada. 1993. *Yucca Mountain Project, Wet and Dry Drilling Project, Rock Core Properties and Mercury Porosimetry*, Volume 3 of 3. Mercury, NV.	Rock moisture, density, and porosity data for 40 core samples from the G-Tunnel wet and dry drilling program reported
IT Library	1137.307	Reimus, P.W., B.A. Robinson, and R.J. Glass. 1983. "Aperture Characteristics, Saturated Fluid-Flow, and Tracer-Transport Calculations for a Natural Fracture, High Level Radioactive Waste Management." *Proceedings of the Fourth Annual International Conference*, April 26-30, Sponsored by the University of Nevada, Las Vegas.	Aperture distribution within a natural fracture discussed
IT Library	4681	Roberts, J.J. and W. Lin. 1994. *Permeability of Fractured Tuff as Functions of Temperature and Confining Pressure*, UCRL-JC-119116. Lawrence Livermore National Laboratory.	Permeability of Topopah Spring Tuff sample with a single fracture measured

Table B-1
Annotated Bibliography of Nevada Test Site Fracture Data
(Page 13 of 19)

Source	Tracking Number	Reference	Summary of Relevant Data
IT Library	0175	Robison, J.H. and R.W. Craig. 1991. *Geohydrology of Rocks Penetrated by Test Well USW H-5, Yucca Mountain, Nye County, Nevada*, USGS Open-File Report 88-4168.	Borehole flow survey and pump test results reported. Finite-conductivity-vertical-fracture model used to calculate fracture conductivities
IT Library	0036	Rulon, J., G.S. Bodvarsson, and P. Montazer. 1986. *Preliminary Numerical Simulations of Groundwater Flow in the Unsaturated Zone, Yucca Mountain, Nevada*, USGS Water-Resources Investigations Report.	Fracture density, porosity, permeability, and saturated horizontal hydraulic conductivity reported; Theoretical aperture widths presented
IT Library	0827	Rush, F.E., W. Thordarson, and L. Bruckheimer. 1983. *Geohydrologic and Drill-Hole Data for Test Well USW H-1, Adjacent to Nevada Test Site, Nye County, Nevada*, USGS Open-File Report 83-141.	Porosity, pore saturation, and pore-water content reported for 48 core samples. Horizontal and vertical matrix hydraulic conductivities for saturated-zone samples presented; Televiewer log summarized. Borehole flow, pump test and injection test results reported
IT Library	0016	Rush, F.E., W. Thordarson, and D.G. Pyles. 1984. *Geohydrology of Test Well USW H-1, Yucca Mountain, Nye County, Nevada*, USGS Water-Resources Investigations Report 84-4032.	Matrix porosity, matrix hydraulic conductivity, pore-water content, distribution of porous rock based on geophysical logs, occurrence, and orientation of lineations observed with acoustic-televiewer log in water-filled portion of hole, and aquifer test data reported
IT Library	0090	Russell, C.E. 1987. "Hydrogeologic Investigations of Flow in Fractured Tuffs, Rainier Mesa, Nevada Test Site," Thesis, Desert Research Institute, University of Nevada System, Las Vegas, Nevada.	Groundwater travel time through fractured tuff reported for Rainier Mesa U12n Tunnel

Table B-1
Annotated Bibliography of Nevada Test Site Fracture Data
(Page 14 of 19)

Source	Tracking Number	Reference	Summary of Relevant Data
IT Library	0310	Russell, C.E., J.W. Hess, and S.W. Tyler. 1987. *Hydrogeologic Investigations of Flow in Fractured Tuffs, Rainier Mesa, Nevada Test Site.* American Geophysical Union.	Groundwater travel time through fractured tuff reported for Rainier Mesa U12n Tunnel
IT Library	4687	Schwartz, B.M. 1990. *SNL Yucca Mountain Project Data Report: Density and Porosity Data for Tuffs from the Unsaturated Zone at Yucca Mountain, Nevada*, SAND88-0811. Sandia National Laboratory.	Porosity values reported
IT Library	1184	Scott, R.B. and M. Castellanos. 1984. *Stratigraphic and Structural Relations of Volcanic Rocks in Drill Holes USW GU-3 and USW G-3, Yucca Mountain, Nye County, Nevada*, USGS Open-File Report 84-491.	Fracture frequency, orientation, and coatings reported
IT Library	0781	Scott, R.B., R.W. Spengler, S. Diehl, A.R. Lappin, and M.P. Chornack. 1983. "Geologic Character of Tuffs in the Unsaturated Zone at Yucca Mountain, Southern Nevada." In *Role of the Unsaturated Zone in Radioactive and Hazardous Waste Disposal*, pp. 289-335, J.W. Mercer, ed. Ann Arbor, MI: Ann Arbor Science Publishers.	Fracture frequency and orientation discussed; Hydrologic conceptual model for Yucca Mountain presented
IT Library	0891.14	Smoot, J.L., 1991, Flow Through Variable Aperture Fractures, USGS Open-File Report 91-125 [ABSTRACT].	Flow through a vertical fracture in the Topopah Spring welded tuff modeled; Assumed aperture values reported
IT Library	1162	Spengler, R.W. and M.P. Chornack. 1984. *Stratigraphic and Structural Characteristics of Volcanic Rocks in Core Hole USW G-4, Yucca Mountain, Nye County, Nevada*, USGS Open-File Report 84-789.	Detailed report of fracture frequency, orientation, filling, and occurrence in volcanics with varying degrees of welding

Table B-1
Annotated Bibliography of Nevada Test Site Fracture Data
(Page 15 of 19)

Source	Tracking Number	Reference	Summary of Relevant Data
IT Library	0831	Spengler, R.W. and J.G. Rosenbaum. 1980. *Preliminary Interpretations of Geologic Results Obtained from Boreholes UE25a-4, -5, -6, and -7, Yucca Mountain, Nevada Test Site*, USGS Open-File Report 80-929.	Fracture frequency and orientation plotted and discussed
IT Library	4683	Spengler, R.W., F.M. Byers, Jr. and J.B. Warner. 1981. *Stratigraphy and Structure of Volcanic Rocks in Drill Hole USW-G1, Yucca Mountain, Nye County, Nevada*, USGS Open-File Report 81-1349.	Fracture coatings, frequency, and orientation identified
IT Library	1599	Spengler, R.W., D.C. Muller, and R.B. Livermore. *Preliminary Report on the Geology and Geophysics of Drill Hole UE25a-1, Yucca Mountain, Nevada Test Site*, USGS Open-File Report 79-1244.	Joint frequency, orientation and filling minerals reported based on a continuous core sample from 0 to 2,500 feet (95.3 percent recovery)
IT Library	1137	Spengler, R.W., C.A. Braun, R.M. Linden, L.G. Martin, D.M. Ross-Brown, and R.L. Blackburn. 1993. "Structural Character of the Ghost Dance Fault, Yucca Mountain, Nevada, High Level Radioactive Waste Management." *Proceedings of the Fourth Annual International Conference*, Las Vegas, Nevada, April 26-30, Volume I: 653-659, hosted by the University of Nevada, Las Vegas.	Attributes of 745 fractures studied. Length, strike, and dip summarized
IT Library	4690	Stock, J.M., J.H. Healy, and S.H. Hickman. 1984. *Report on Televiewer Log and Stress Measurements in Core Hole USW G-2, Nevada Test Site, October-November 1982*, USGS Open-File Report 84-172.	Fracture occurrence and orientation discussed
IT Library	0872	Stock, J.M., J.H. Healy, J. Svitek, and L. Masten. 1986. *Report on Televiewer Log and Stress Measurements in Holes USW G-3 and UE-25p1, Yucca Mountain, Nye County, Nevada*, USGS Open-File Report 86-369.	Fracture occurrence and orientation discussed

Table B-1
Annotated Bibliography of Nevada Test Site Fracture Data
(Page 16 of 19)

Source	Tracking Number	Reference	Summary of Relevant Data
IT Library	0009	Thordarson, W. 1983. *Geohydrologic Data and Test Results from Well J-13, Nevada Test Site, Nye County, Nevada*, USGS Water-Resources Investigations Report 83-4171.	Porosities, hydraulic conductivities, and aquifer test results reported
IT Library	0017	Thordarson, W., F.E. Rush, and S.J. Waddell. 1985. *Geohydrology of Test Well USW H-3, Yucca Mountain, Nye County, Nevada*, USGS Water-Resources Investigations Report 84-4272.	Distribution of porous rock based on geophysical logs, borehole-flow survey, and pump test results reported
IT Library	0172	Thordarson, W., F.E. Rush, R.W. Spengler, and S.J. Waddell. 1984. *Geohydrologic and Drill-Hole Data for Test Well USW H-3, Yucca Mountain, Nye County, Nevada*, USGS Open-File Report 84-149.	Fracture frequency versus depth qualitatively described based on televiewer log
IT Library	4691	Throckmorton, C.K. U.S. Geological Survey and U.S. Department of Energy. 1987. *Photogeologic Study of Small-Scale Linear Features Near a Potential Nuclear-Waste Repository Site at Yucca Mountain, Southern Nye County, Nevada*, USGS Open-File Report 87-409.	Fracture traces recorded on photogeologic map compared with field fracture patterns
IT Library	1137	Tsang, Y.W., K. Pruess, and J.S.Y. Wang. 1993. "The Role of Fault Zone in Affecting Multiphase Flow at Yucca Mountain, High Level Radioactive Waste." *Proceedings of the Fourth Annual Conference*, Las Vegas, Nevada, April 26-30, Volume I: 660-666, hosted by the University of Nevada, Las Vegas.	Fracture permeabilities used in model reported
IT Library	0435	Tsang, Y.W. and P.A. Witherspoon. 1985. "Effects of Fracture Roughness on Fluid Flow Through a Single Deformable Fracture, International Association of Hydrogeologists Memoirs." In Volume XVII, Part 2 Proceedings, *Hydrogeology of Rocks of Low Permeability.*	Effects of fracture surface roughness on fluid flow through a single deformable fracture discussed

Table B-1
Annotated Bibliography of Nevada Test Site Fracture Data
(Page 17 of 19)

Source	Tracking Number	Reference	Summary of Relevant Data
IT Library	0891.02	Verbeek, E.R. and M.A. Grout, 1991, Some General Properties of Joints and Joint Networks in Horizontally Layered Sedimentary and Volcanic Rocks -- An Overview, USGS Open-File Report 91-125 [ABSTRACT].	Joint properties discussed
IT Library	0031	Waddell, R.K., J.H. Robison, and R.K. Blankennagel. 1984. *Hydrology of Yucca Mountain and Vicinity, Nevada-California -- Investigative Results through Mid-1983*, USGS Water-Resources Investigations Reports 84-4267.	Matrix hydraulic conductivities, fracture porosity, and pump test data reported
IT Library	1369	Wagoner, J.L. 1985. *U20ai 609-m Preliminary Site Characteristics Summary*, CP 85-86. Lawrence Livermore National Laboratory.	Location of cooling joints indicated
IT Library	1311	Wagoner, J. and S. Clark. 1986. *U20as 605-m Site Characteristics Report*, CP 86-32. Lawrence Livermore National Laboratory.	Location of cooling joints indicated
DOE/NV Library	LBL-18473	Wang, J.S.Y. and T.N. Narasimhan. Lawrence Berkeley Laboratory. 1984. *Hydrologic Mechanisms Governing Fluid Flow in Partially Saturated, Fractured, Porous Tuff at Yucca Mountain*, LBL-18473, UC-70. Lawrence Berkeley Laboratory, Earth Sciences.	Fracture spacing and orientation from core analyses presented
IT Library	0109	Wang, J.S.Y. and T.N. Narasimhan. Lawrence Berkeley Laboratory. 1985. *Hydrologic Mechanisms Governing Fluid Flow in Partially Saturated, Fractured, Porous Tuff at Yucca Mountain*, SAND84-7202. Prepared for Sandia National Laboratory.	Fracture frequency, inclination, permeability, and saturated conductivity reported

Table B-1
Annotated Bibliography of Nevada Test Site Fracture Data
(Page 18 of 19)

Source	Tracking Number	Reference	Summary of Relevant Data
IT Library	4680	Wang, J.S.Y. and T.N. Narasimhan. Lawrence Berkeley Laboratory. 1986. *Hydrologic Mechanisms Governing Partially Saturated Fluid Flow in Fractured Welded Units and Porous Non-Welded Units at Yucca Mountain*, SAND85-7114. Sandia National Laboratory.	Fracture frequency, orientation, and calculated values for fracture permeability and aperture for 5 unsaturated tuff samples from USW G-4 presented and used in a flow model
DOE/NV Library	SAND87-7070	Wang, J.S. Y. and T.N. Narasimhan. Lawrence Berkeley Laboratory. 1988. *Hydrologic Modeling of Vertical and Lateral Movement of Partially Saturated Fluid Flow Near a Fault Zone at Yucca Mountain*, SAND87-7070, Unlimited Release, UC-70. Prepared for Sandia National Laboratory.	Tuff matrix and fracture data compared with model parameters; Correlations between saturated conductivity and unsaturated parameters for tuff matrix, fractures, and faults reported
IT Library	0171	Weeks, E.P. and W.E. Wilson. 1984. *Preliminary Evaluation of Hydrologic Properties of Cores of Unsaturated Tuff, Test Well USW H-1, Yucca Mountain, Nevada*, USGS Water-Resources Investigations Report 84-4193.	Moisture characteristics curves relating saturation and moisture tension developed
IT Library	0108	Whitfield, M.S., E.P. Eshom, W. Thordarson, and D.H. Schaefer. 1985. *Geohydrology of Rocks Penetrated by Test Well USW H-4, Yucca Mountain, Nye County, Nevada*, USGS Water-Resources Investigations Report 85-4030.	Borehole flow survey and pump test results reported
IT Library	0178	Whitfield, M.S., W. Thordarson, and E.P. Eshom. 1984. *Geohydrologic and Drill-Hole Data for Test Well USW H-4, Yucca Mountain, Nye County, Nevada*, USGS Open-File Report 84-449.	Pump test results reported
IT Library	0173	Whitfield, W.S., W. Thordarson, and D.P. Hammermeister. 1990. *Drilling Geohydrologic Data for Test Hole USW UZ-1, Yucca Mountain, Nye County, Nevada*, USGS Open-File Report 90-354.	Fracture distribution and orientation presented based on four television videotapes

Table B-1
Annotated Bibliography of Nevada Test Site Fracture Data

Source	Tracking Number	Reference	Summary of Relevant Data
IT Library	1137	Wittwer, C.S., G. Chen, and G.S. Bodvarsson. 1993. "Studies of the Role of Fault Zones on Fluid Flow Using the Site-Scale Numerical Model of Yucca Mountain, High Level Radioactive Waste Management." *Proceedings of the Fourth Annual Conference*, Las Vegas, Nevada, April 26-30, 1993, Volume I: 667-674, hosted by the University of Nevada, Las Vegas.	Combined fracture and matrix characteristic curves for welded tuffs presented showing saturated permeability versus capillary pressure
YMP Library	SAND86-1015	Zimmerman, R.M. and R.E. Finley. 1987. *Summary of Geomechanical Measurements Taken In and Around the G-Tunnel Underground Facility, NTS*, Sandia National Laboratory, SAND86-1015, Unlimited Release, UC-70.	Fracture permeabilities and aperture widths presented
YMP Library	SAND81-1971	Zimmerman, R.M. and W.C. Vollendorf. 1982. *Geotechnical Field Measurements, G-Tunnel, Nevada Test Site*, SAND81-1971, Unlimited Release, UC-70.	Fracture permeabilities reported

Appendix C
Drill Hole Data

Table C-1
Abridged Drill Hole Statistics for Exploratory Hole UE-19x

Location Data:

Coordinates:	Central Nevada State Planar:	N 904,108 feet (ft) E 586,810 ft
	Universal Transverse Mercator:	N 4,120,739.0 meters (m) E 555,962.4 m
	Ground elevation:	2,065.3 m (6,776 ft)
	Static water level:	674.8 m (2.214 ft) depth

Drilling Data:

Spud date:	09/28/77
Total depth (TD):	762.9 m (2,503 ft)
Drilling technique(s):	This hole was continuously cored from 4.6 m (15 ft) to total depth using mud.

Coring Data:

Number of cores:	278 continuous core runs
Total core recovered:	Approximately 743 m (2,438 ft) (~98%)
Percent of hole cored:	99.4%
Cored interval(s):	4.6 m (15 ft) to total depth (TD)
Core size:	6.03-centimeters (cm) (2 ⅜-inch [in.]) diameter

Table C-2
Condensed Stratigraphic and Lithologic Log for Exploratory Hole UE-19x
(Page 1 of 2)

Depth		Stratigraphic Unit	Lithology	Stratigraphic Symbol	Thickness	
Meters	Feet				Meters	Feet
0.0 - 5.3	0 - 17.5	Rhyolite of Beatty Wash, Volcanics of Fortymile Canyon	Nonwelded tuff, vitric	Tfbw	5.3	17.5
5.3 - 29.3	17.5 - 96	Mafic-rich, Ammonia Tanks Tuff, Timber Mountain Group	Moderately to densely welded ash-flow tuff, vitric, bedded tuff upper portion	Tmar	24.0	78.5
29.3 - 56.3	96 - 185	Mafic-poor, Ammonia Tanks Tuff, Timber Mountain Group	Partially to moderately welded ash-flow tuff, vitric to devitrified	Tmap	27.0	89
56.3 - 68.9	185 - 226	Bedded, Ammonia Tanks Tuff, Timber Mountain Group	Bedded tuff, vitric	Tmab	12.6	41.3
68.9 - 73.4	226 - 241	Bedded, Rainier Mesa Tuff, Timber Mountain Group	Bedded tuff, vitric	Tmrb	4.5	14.8
73.4 - 115.2	241 - 378	Mafic-rich, Rainier Mesa Tuff, Timber Mountain Group	Nonwelded to densely welded ash-flow tuff, devitrified	Tmrr	41.8	137.1
115.2 - 291.8	378 - 957	Mafic-poor, Rainier Mesa Tuff, Timber Mountain Group	Partially to moderately welded ash-flow tuff, generally devitrified	Tmrp	176.6	579.4
291.8 - 291.9	957 - 958	Andesite tephra, Rainier Mesa Tuff, Timber Mountain Group	Bedded tuff, vitric	Tmra	0.1	1
291.9 - 299.4	958 - 982	Tuff of Holmes Road, Timber Mountain Group	Bedded tuff, vitric	Tmrh	7.5	24.6
299.4 - 326.3	982 - 1,071	Pahute Mesa lobe, Tiva Canyon Tuff, Paintbrush Group	Nonwelded to densely welded ash-flow tuff, vitric to devitrified	Tpcm	26.9	88.3
326.3 - 344.0	1,071 - 1,129	Rhyolite of Delirium Canyon, Paintbrush Group	Bedded tuff	Tpd	17.7	58

Table C-2
Condensed Stratigraphic and Lithologic Log for Exploratory Hole UE-19x
(Page 2 of 2)

Depth		Stratigraphic Unit	Lithology	Stratigraphic Symbol	Thickness	
Meters	Feet				Meters	Feet
344.0 - 579.9	1,129 - 1,903	Rhyolite of Echo Peak, Paintbrush Group	Rhyolite lava flow (upper portion), and nonwelded to densely welded ash-flow tuff, generally devitrified with vitric upper part and zeolitized lower portion	Tpe	545.9	1,791.1
579.9 - 687.5	1,903 - 2,256	Rhyolite of Silent Canyon, Paintbrush Group	Mostly rhyolite lava flow, minor flow breccia and nonwelded tuff; denser lava portion is vitric, while top and bottom of interval are zeolitized	Tpr	107.6	353.0
687.5 - 696.1	2,256 - 2,284	Bedded Topopah Spring Tuff, Paintbrush Group	Bedded tuff, zeolitized	Tptb	8.6	28.2
696.1 - 758.4	2,284 - 2,488	Mafic-poor, Calico Hills Formation, Volcanics of Area 20	Bedded tuff, zeolitized	Tacp	62.3	204.4
758.4 - 762.9 TD	2,488 - 2,503 TD	Rhyolite of Inlet, Volcanics of Area 20	Nonwelded tuff, zeolitized	Tai	4.5	14.8

Source: Ferguson, *et al.*, 1994.

Table C-3
Abridged Drill Hole Statistics for Exploratory Hole UE-18t

Location Data:

Coordinates:	Central Nevada State Planar:	N 865,793 ft E 598,394 ft
	Universal Transverse Mercator:	N 4,109,094.59 m E 559,591.08 m
	Ground elevation:	1,585.3 m (5,201 ft)
	Static water level:	278.9 m (915 ft) depth on 06/02/93

Drilling Data:

Spud date:	07/23/78
Total depth:	792.5 m (2,600 ft)
Drilling technique(s):	A 66-cm (26-in.) hole was drilled to 36.6 m (120.1 ft). The hole was continuously cored from 36.6 m (120 ft) to its total depth of 792.5 m (2,600 ft) using bentonite mud with a liquid polymer as a lubricant. Lost circulation material was utilized as needed. Completed with a string of 6.03-cm (2 ⅜-in.) diameter tubing set at 577.9 m (1,896 ft).

Coring Data:

Number of cores:	278 continuous core runs
Total core recovered:	733.2 m (2,405.6 ft); 97% recovery
Percent of hole cored:	95.4%
Cored interval(s):	36.6 - 792.5 m (120 - 2,600 ft)
Core size:	HQ (2 ⅜-in. diameter) and NQ (1 ⅞-in. diameter)

Table C-4
Condensed Stratigraphic and Lithologic Log for Exploratory Hole UE-18t

Depth		Stratigraphic Unit	Lithology	Stratigraphic Symbol	Thickness	
Meters	Feet				Meters	Feet
0.0 - 91.7	0 - 301	Alluvium	Tuffaceous alluvium	QTa	91.7	301
91.7 - 108.1	301 - 355	Trail Ridge Tuff, Thirsty Canyon Group	Mostly moderately welded ash-flow tuff with bedded tuff at base	Ttt	16.4	53.8
108.1 - 131.9	355 - 433	Pahute Mesa Tuff, Thirsty Canyon Group	Nonwelded to moderately welded ash-flow tuff	Ttp	23.8	78.1
131.9 - 258.5	433 - 848	Rhyolite of Chukar Canyon, Volcanics of Fortymile Canyon	Bedded tuff	Tfbr	126.6	415.4
258.5 - 286.1	848 - 939	Rhyolite of Beatty Wash, Volcanics of Fortymile Canyon	Bedded tuff	Tfbw	27.6	90.6
286.1 - 288.0	939 - 945	Tuff of Crooked Canyon, Timber Mountain Group	Bedded tuff	Tmac	1.9	6.2
288.0 - 353.6	945 - 1,160	Mafic-rich, Ammonia Tanks Tuff, Timber Mountain Group	Partially welded to densely welded ash-flow tuff	Tmar	65.6	215.2
353.6 - 396.9	1,160 - 1,302	Mafic-poor, Ammonia Tanks Tuff, Timber Mountain Group	Nonwelded to densely welded ash-flow tuff	Tmap	43.3	142.1
396.9 - 440.7	1,302 - 1,446	Bedded, Ammonia Tanks Tuff, Timber Mountain Group	Bedded tuff	Tmab	43.8	143.7
440.7 - 498.4	1,446 - 1,635	Bedded, Rainier Mesa Tuff, Timber Mountain Tuff	Bedded tuff	Tmrb	57.7	189.3
498.4 - 792.5 (TD)	1,635 - 2,600 (TD)	Mafic-rich, Rainier Mesa Tuff, Timber Mountain Group	Moderately welded ash-flow tuff	Tmrr	294.1	964.9

Source: Ferguson, *et al.*, 1994.

Table C-5
Abridged Drill Hole Statistics for Exploratory Hole UE-18r

Location Data:

Coordinates:	Central Nevada State Planar:	N 868,100 ft E 564,700 ft
	Universal Transverse Mercator:	N 4,109,761.51 m E 549,321.53 m
	Ground Elevation:	1,688 m (5,538 ft)
	Static Water Level:	416.1 m (1,365 ft) depth on 05/18/93

Drilling Data:

Spud date:	11/29/67
Total depth:	1,525.2 m (5,004 ft)
Drilling techniques:	A 91.4-cm (36-in.) hole was drilled to 11.6 m (38 ft). A 38.1-cm (15-in.) hole was drilled to 498.7 m (1,636 ft) using direct circulation air/foam. A 25.1-cm (9 7/8-in.) hole was drilled to 1,520.3 m (4,988 ft) also using direct circulation air/foam with no apparent drilling problems. A 15.6-cm (6 1/8-in.) hole was cored using a conventional diamond core bit to a total depth of 1,525.2 m (5,004 ft). A total of fifteen cores were taken at various depths during drilling.

Coring Data:

Number of cores:	15 intermittent core runs
Total core recovered:	35.7 m (117 ft); 97% recovery
Percent of hole cored:	2.4%
Cored interval(s):	154.8 - 1,525.2 m (508 - 5,004 ft) See Table C-6 for additional coring information.
Core size:	8.9-cm (3.5-in.) diameter

Table C-6
Coring Data for Exploratory Hole UE-18r

Core Run No.	Depth Interval (feet)	Recovery (feet)	Stratigraphic Unit[1]	Lithology[2]	Hydrostratigraphic Unit[3]
#1	508 - 516	8	Tfbw	Lava	TMA
#2	839 - 847	8	Tfbw	Lava	TMA
#3	1,148 - 1,156	8	Tmac	Tuff, PW	TMA
#4	1,366 - 1,373	6	Tmac	Tuff, PW	TMA
#5	1,615 - 1,622	6	Tmac	Tuff, PW	TMA
#6	1,922 - 1,931	9	Tmacp	Tuff, PW	TMA
#7	2,228 - 2,234	6	Tmacp	Tuff, MW	TMA
#8	2,811 - 2,815	4	Tmr	Tuff, DW	TMA
#9	3,096 - 3,106	10	Tmr	Tuff, NW	TMA
#10	3,604 - 3,610	6	Tmat	Lava	TMA
#11	3,899 - 3,907	8	Tmrb	Tuff Breccia	TMA
#12	4,212 - 4,217	4	Tmrb	Tuff Breccia	TMA
#13	4,594 - 4,600	6	Tmrb	Tuff Breccia	TMA
#14	4,867 - 4,879	12	Tmrx	Tuff Breccia	TMA
#15	4,988 - 5,004	16	Tmrx	Tuff Breccia	TMA

1 Refer to Table C-22 for explanation of stratigraphic nomenclature.
2 Refer to Table C-23 for explanation of lithologic nomenclature.
3 Refer toTable 1-4 for explanation of hydrostratigraphic nomenclature.

Total core recovered: 35.7 m (117 ft); 97.5% recovery.
Amount of core logged for this fracture study: All core recovered (35.7 m), minus core samples removed (approximately 10%) for previous unrelated studies.
Static water level at 416.1 m (1,365 ft) on 11/18/93

Table C-7
Condensed Stratigraphic and Lithologic Log for Exploratory Hole UE-18r

Depth		Stratigraphic Unit	Lithology	Stratigraphic Symbol	Thickness	
Meter	Feet				Meter	Feet
0.0 - 17.1	0 - 56	Trail Ridge Tuff, Thirsty Canyon Group	Moderately welded ash-flow tuff with 3 m bedded tuff at base, generally vitric	Ttt	17.1	56
17.1 - 39.0	56 - 128	Crystal-rich, Pahute Mesa Tuff, Thirsty Canyon Group	Moderately welded ash-flow tuff	Ttpr	21.9	71.9
39.0 - 65.2	128 - 214	Crystal-poor, Pahute Mesa Tuff, Thirsty Canyon Group	Nonwelded to densely welded ash-flow tuff	Ttpp	26.2	86.0
65.2 - 103.0	214 - 338	Rocket Wash Tuff, Thirsty Canyon Group	Nonwelded ash-flow tuff	Ttr	37.8	124.0
103.0 - 324.6	338 - 1,065	Rhyolite of Beatty Wash, Volcanics of Fortymile Canyon	Rhyolite lava flow, pumiceous top and flow breccia at base	Tfbw	221.6	727.0
324.6 - 1083.3	1,065 - 3,554	Ammonia Tanks Tuff, Timber Mountain Group	Nonwelded to densely welded ash-flow tuff	Tma	758.7	2,489
1083.3 - 1184.5	3,554 - 3,886	Rhyolite of Tannenbaum Hill, Timber Mountain Group	Rhyolite lava flow, flow breccia at top	Tmat	101.2	332.0
1184.5 - 1367.0	3,886 - 4,485	Landslide or eruptive breccia, Rainier Mesa Tuff, Timber Mountain Group	Nonwelded tuff and tuff breccia	Tmrx	182.5	598.8
1367.0 - 1441.7	4,485 - 4,730	Rainier Mesa Tuff, Timber Mountain Group	Moderately welded ash-flow tuff	Tmr	74.7	245.1
1441.7 - 1525.2 (TD)	4,730 - 5,004 (TD)	Landslide or eruptive breccia, Rainier mesa Tuff, Timber Mountain Group	Tuff breccia	Tmrx	83.5	274.0

Source: Ferguson, *et al.*, 1994.

Table C-8
Abridged Drill Hole Statistics for Exploratory Hole UE-20e #1

Location Data:

Coordinates:	Central Nevada State Planar:	N 934,466 ft E 560,958 ft
	Universal Transverse Mercator:	N 4,129,966.0 m E 548,122.8 m
	Ground elevation:	1,919.3 m (6,297 ft)
	Static water level:	556.6 m (1,826 ft) depth on 04/05/75

Drilling Data:

Spud date:	03/26/64
Total depth:	1949.2 m (6,395 ft)
Drilling technique(s):	This hole was rotary drilled and cored using air-mist and soap. A 66.0-cm (26-in.) hole was drilled to 7.0 m (23 ft). A 44.5-cm (17 ½-in.) hole was drilled to 45.7 m (1,500 ft). A 31.1-cm (12 ¼-in.) hole was drilled to 502.9 m (1,650 ft). A 25.1-cm (9 ⅞-in.) hole was drilled to 1946.2 m (6,385 ft). A 15.6-cm (6 ⅛-in.) hole was cored to 1949.2 m (6,395 ft). 33 intermittent cores were cut, typically in 3 m (10 ft) runs, using a conventional diamond core bit.

Coring Data:

Number of cores:	33 intermittent core runs
Total core recovered:	80.6 m (264.5 ft); 75.8% recovery
Percent of hole cored:	5.5%
Cored interval(s):	402.3 - 1,949.2 m (1,320 - 6,395 ft). See Table C-9 in Appendix C for additional coring information.
Core size:	8.9-cm (3 ½-in.) diameter

Table C-9
Coring Data for Exploratory Hole UE-20e #1

Core Run No.	Depth Interval (feet)	Recovery (feet)	Stratigraphic Unit[1]	Lithology[2]	Hydrostratigraphic Unit[3]
#1	1,320 - 1,330	1.0	Tmr	Tuff, PW	TMA
#2	1,405 - 1,415	.5	Tacp	Rhyolite, lava flow	TC
#3	1,415 - 1,434	1.0	Tacp	Rhyolite, lava flow	TC
#4	1,652 - 1,680	00.0	Tacp	Rhyolite, lava flow	TC
#5	1,710 - 1,720	2.0	Tacp	Rhyolite, lava flow	TC
#6	1,800 - 1,810	2.5	Tacp	Rhyolite, lava flow	TC
#7	1,954 - 1,967	13.0	Tacp	Tuff, bedded	TC
#8	2,120 - 2,130	10.0	Tacp	Rhyolite, lava flow	TC
#9	2,293 - 2,303	7.0	Tacp	Rhyolite, lava flow	TC
#10	2,500 - 2,510	10.0	Tacp	Flow breccia	TC
#11	2,700 - 2,710	10.0	Tacp	Rhyolite, lava flow	TC
#12	2,950 - 2,960	10.0	Tacp	Tuff, bedded	TC
#13	3,150 - 3,160	10.0	Tacp	Tuff, NW, Z	TC
#14	3,400 - 3,410	10.0	Tacp	Rhyolite, lava flow, Z	TC
#15	3,520 - 3,530	10.0	Tacp	Rhyolite, lava flow, D	TC
#16	3,700 - 3,710	10.0	Tacp	Tuff, bedded, Z	TC
#17	3,900 - 3,910	10.0	Tacr	Tuff, NW, K	TC
#18	4,100 - 4,110	7.0	Tacr	Tuff, NW, K	TC
#19	4,150 - 4,153	3.0	Tacr	Tuff, bedded, K	TC
#20	4,200 - 4,212	12.0	Tap	Tuff, bedded, Z	TC
#21	4,250 - 4,260	8.5	Tai/Tcpj	Tuff, NW, Z	TC
#22	4,300 - 4,310	10.0	Tcpj	Tuff, NW, Z	TC
#23	4,350 - 4,360	10.0	Tcpj	Tuff, NW, Z	TC
#24	4,400 - 4,410	10.0	Tcpj	Tuff, bedded, Z	TC
#25	4,450 - 4,460	10.0	Tcpj	Tuff, bedded, Z	TC
#26	4,490 - 4,506	16.0	Tcpj	Tuff, bedded, Z	TC
#27	4,680 - 4,690	10.0	Tcpj	Tuff, bedded, Z	TC
#28	4,785 - 4,795	10.0	Tcps	Rhyolite, lava flow, D	TC
#29	5,092 - 5,102	10.0	Tct	Tuff, NW, Z	TC
#30	5,298 - 5,302	3.5	Tbdl	Rhyolite lava, P	TBA
#31	5,468 - 5,472	4.0	Tcl	Tuff, nonwelded, Z	TBA
#32	5,710 - 5,720	10.0	Tbdl	Rhyolite, lava flow, D	TBA
#33	6,385 - 6,395	8.0	Tbdk	Rhyolite, lava flow, D	TBA

1 Refer to Table C-22 for explanation of stratigraphic nomenclature.
2 Refer to Table C-23 for explanation of lithologic nomenclature.
3 Refer to Table 1-4 for explanation of hydrostratigraphic nomenclature.

Total core recovered: 80.6 m (264.5 ft).
Static water level at 556.6 m (1,826 ft) depth.

Amount of core logged for this fracture study: All core recovered below 1,188.7 m (3,900 ft) depth, approximately 48 m (158 ft), minus core samples removed (~20%) for previous unrelated studies.

Table C-10
Condensed Stratigraphic and Lithologic Log for Exploratory Hole UE-20e #1
(Page 1 of 3)

Depth		Stratigraphic Unit	Lithology	Stratigraphic Symbol	Thickness	
Meters	Feet				Meters	Feet
0 - 16.8	0 - 55	Trail Ridge Tuff, Thirsty Canyon Group	Partially to moderately welded ash-flow tuff	Ttt	16.8	55
16.8 - 53.0	55 - 174	Pahute Mesa Tuff, Thirsty Canyon Group	Partially to moderately welded ash-flow tuff	Ttp	36.2	119
53.0 - 105.2	174 - 345	Rocket Wash Tuff, Thirsty Canyon Group	Partially welded ash-flow tuff	Ttr	52.2	171
105.2 - 156.4	345 - 513	Ammonia Tanks Tuff, Timber Mountain Group	Partially to moderately welded ash-flow tuff	Tma	51.2	168
156.4 - 176.8	513 - 580	Bedded Ammonia Tanks Tuff, Timber Mountain Group	Bedded tuff, vitric	Tmab	20.4	67
176.8 - 405.4	580 - 1,330	Rainier Mesa Tuff, Timber Mountain Group	Partially to densely welded ash-flow tuff	Tmr	228.6	750
405.4 - 424.6	1,330 - 1,393	Tuff of Holmes Road, Timber Mountain Group	Bedded tuff, zeolitized	Tmrh	19.2	63
424.6 - 594.6	1,393 - 1,950	Mafic-poor, Calico Hills Formation, Volcanics of Area 20	Lava flow, devitrified; pumiceous lava below 564 m	Tacp	170.0	557
594.6 - 606.6	1,950 - 1,990	Mafic-poor, Calico Hills Formation, Volcanics of Area 20	Bedded tuff, zeolitized	Tacp	12.0	40
606.6 - 885.4	1,990 - 2,905	Mafic-poor, Calico Hills Formation, Volcanics of Area 20	Lava flow, devitrified	Tacp	278.8	915
885.4 - 1,021.1	2,905 - 3,350	Mafic-poor, Calico Hills Formation, Volcanics of Area 20	Nonwelded ash-flow tuff, zeolitized	Tacp	135.7	445
1,021.1 - 1,127.8	3,350 - 3,700	Mafic-poor, Calico Hills Formation, Volcanics of Area 20	Lava flow, devitrified to zeolitized	Tacp	106.7	350

Table C-10
Condensed Stratigraphic and Lithologic Log for Exploratory Hole UE-20e #1
(Page 2 of 3)

Depth		Stratigraphic Unit	Lithology	Stratigraphic Symbol	Thickness	
Meters	Feet				Meters	Feet
1,127.8 - 1,187.5	3,700 - 3,896	Mafic-poor, Calico Hills Formation, Volcanics of Area 20	Bedded tuff, zeolitized	Tacp	59.7	196
1,187.5 - 1,269.8	3,896 - 4,166	Mafic-rich, Calico Hills Formation, Volcanics of Area 20	Bedded tuff, zeolitized	Tacr	82.3	270
1,269.8 - 1,290.8	4,166 - 4,235	Tuff of Pool, Volcanics of Area 20	Bedded tuff, zeolitized	Tap	21	69
1,290.8 - 1,296.0	4,235 - 4,252	Rhyolite of Inlet, Volcanics of Area 20	Bedded tuff, zeolitized	Tai	5.2	17
1,296.0 - 1,331.4	4,252 - 4,368	Tuff of Jorum, Crater Flat Group	Nonwelded ash-flow tuff, zeolitized	Tcpj	35.4	116
1,331.4 - 1,446.6	4,368 - 4,746	Tuff of Jorum, Crater Flat Group	Bedded tuff	Tcpj	115.2	378
1,446.6 - 1,548.4	4,746 - 5,080	Rhyolite of Sled, Crater Flat Group	Lava flow, devitrified	Tcps	101.8	334
1,548.4 - 1,558.8	5,080 - 5,114	Tram Tuff, Crater Flat Group	Nonwelded ash-flow tuff, zeolitized	Tct	10.4	34
1,558.8 - 1,561.5	5,114 - 5,123	Comendite of Lambs Canyon, Belted Range Group	Lava flow, devitrified	Tbdl	2.7	9
1,561.5 - 1,578.0	5,123 - 5,177	Comendite of Lambs Canyon, Belted Range Group	Nonwelded ash-flow tuff, devitrified	Tbdl	16.5	54
1,578.0 - 1,620.0	5,177 - 5,315	Comendite of Lambs Canyon, Belted Range Group	Lava flow, zeolitized to devitrified	Tbdl	42	138
1,620.0 - 1,668.2	5,315 - 5,473	Lower tuff, Crater Flat Group	Bedded tuff, zeolitized	Tcl	48.2	158

Table C-10
Condensed Stratigraphic and Lithologic Log for Exploratory Hole UE-20e #1
(Page 3 of 3)

Depth		Stratigraphic Unit	Lithology	Stratigraphic Symbol	Thickness	
Meters	Feet				Meters	Feet
1,668.2 - 1,817.8	5,473 - 5,964	Comendite of Lambs Canyon, Belted Range Group	Lava flow, devitrified to zeolitized	Tbdl	149.6	491
1,817.8 - 1,828.8	5,964 - 6,000	Comendite of Lambs Canyon, Belted Range Group	Bedded tuff, zeolitized	Tbdl	11	36
1,828.8 - 1,949.2 (TD)	6,000 - 6,395 (TD)	Comendite of Kaw Station, Belted Range Group	Lava flow, devitrified	Tbdk	120.4	395

Source: Ferguson, *et al.*, 1994

Table C-11
Abridged Drill Hole Statistics for Monitoring Well UE-20bh #1

Location Data:

Coordinates:	Central Nevada State Planar:	N 908,250 ft E 574,950 ft
	Universal Transverse Mercator:	N 4,122,010.0 m E 552,406.1 m
	Ground elevation:	2,022.8 m (6,636.6 ft)
	Static water level:	674.3 m (2,212 ft) depth on 06/03/93

Drilling Data:

Spud date:	08/27/91
Total depth:	856.5 m (2,810 ft)
Drilling technique(s):	A 76.2-cm (30-in.) hole was drilled to 24.4 m (80 ft) using a hammer drill with air and air foam. A 44.5-cm (17 ½-in.) hole was drilled to 591.6 m (1,941 ft) using a hammer drill with air foam to 102.1 m (335 ft), then air, water and soap. A 31.1-cm (12 ¼-in.) hole was drilled to total depth of 856.5 m (2,810 ft) using a hammer drill with air foam. Three cores were cut using a conventional 9.1-m (30-ft) core barrel and a 22.2 cm (8 ¾-in.) Christensen diamond core bit.

Coring Data:

Number of cores:	3 intermittent core runs
Total core recovered:	18.7 m (61.3 ft); 98.9% recovery
Percent of hole cored:	2.2%
Cored interval(s):	670.3 m - 800.1 m (2,199 - 2,625.1 ft) See Table C-12 in Appendix C for additional coring information.
Core size:	10.2-cm (4-in.) diameter

Table C-12
Coring Data for Monitoring Well UE-20bh #1

Core Run No.	Depth Interval (feet)	Recovery (feet)	Stratigraphic Unit[1]	Lithology	Hydrostratigraphic Unit[2]
#1	2,199 - 2,228	29.0	Tacp	Bedded Tuff, zeolitized	TC
#2	2,383 - 2,412	28.3	Tacp	Pumiceous Lava, zeolitized	TC
#3	2,621.1 - 2,625.1	4.0	Tacp	Lava	TC

1 Refer to Table C-22 for stratigraphic nomenclature.
2 Refer to Table 1-4 for hydrostratigraphic nomenclature.

Total core recovered: 18.7 m (61.3 ft); 98.9% recovery.
Amount of core logged for this fracture study: All core recovered (18.7 m) minus core samples removed (~10%) for previous unrelated studies.
Static water level at 674.7 m (2,214 ft).

Table C-13
Condensed Stratigraphic and Lithologic Log for Monitoring Well UE-20bh #1

Depth		Stratigraphic Unit	Lithology	Stratigraphic Symbol	Thickness	
Meters	Feet				Meters	Feet
0.0 - 27.4	0 - 90	No samples (behind surface casing)	---	Tmr	27.4	90
27.4 - 113.1	90 - 371	Rainier Mesa Tuff, Timber Mountain Group	Nonwelded to densely welded ash-flow tuff, vitric to devitrified	Tmr	85.7	281
113.1 - 134.1	371 - 440	No samples	---	Tm	21	69
134.1 - 137.2	440 - 450	Tuff of Holmes Road, Timber Mountain Group	Bedded tuff, vitric	Tmrh	3.1	10
137.2 - 169.2	450 - 555	Paintbrush Group, undifferentiated	Bedded tuff, vitric	Tp	32	105
169.2 - 184.4	555 - 605	Mafic-poor, Calico Hills Formation, Volcanics of Area 20	Bedded tuff, vitric	Tacp	15.2	50
184.4 - 224.0	605 - 735	Mafic-poor, Calico Hills Formation, Volcanics of Area 20	Rhyolite lava flow, pumiceous, vitric	Tacp	39.6	130
224.0 - 416.4	735 - 1,397	Mafic-poor, Calico Hills Formation, Volcanics of Area 20	Bedded tuff, zeolitized	Tacp	192.4	631
416.4 - 519.1	1,397 - 1,703	Mafic-poor, Calico Hills Formation, Volcanics of Area 20	Rhyolite lava flow, zeolitic pumiceous top, devitrified middle, and vitric base	Tacp	102.7	337
519.1 - 725.4	1,703 - 2,380	Mafic-poor, Calico Hills Formation, Volcanics of Area 20	Bedded tuff, zeolitized	Tacp	206.3	677
725.4 - 856.5 (TD)	2,380 - 2,810 (TD)	Mafic-poor, Calico Hills Formation, Volcanics of Area 20	Rhyolite lava flow, vitric to devitrified zeolitic above 783.3 m (2,570 ft)	Tacp	131.1	430

Source: Modified from Boyd, *et al.*, 1992.

Table C-14
Abridged Drill Hole Statistics for Exploratory Hole UE-20c

Location Data:

Coordinates:	Central Nevada State Planar:	N 903,204 ft E 556,763 ft
	Universal Transverse Mercator:	N 4,120,436.0 m E 546,871.4 m
	Ground elevation:	1,915.1 m (6,283 ft)
	Static water level:	648.0 m (2,126 ft)

Drilling Data:

Spud date:	02/07/64
Total depth:	1630.1 m (5,348 ft)
Drilling technique(s):	A 40-cm (17 ½-in.) diameter hole was drilled from 10.1 to 198.1 m (33 - 650 ft). A 20-cm (9 ⅝-in.) diameter hole was drilled from 198.1 - 1,630.1 m (650 - 5,348 ft). Air was used for circulation to 635.2 m (2,084 ft) and air with soap and water was used below 635.2 m (2,084 ft). Thirty-five intermittent conventional cores were taken from 137.2 to 1,573.1 m (450 - 5,161 ft).

Coring Data:

Number of cores:	35 intermittent core runs
Total core recovered:	84.7 m (278 ft); 90.4% recovery
Percent of hole cored:	5.7%
Cored interval(s):	137.2 - 1,573.1 m (450 - 5,161 ft) See Table C-15 in Appendix C for additional coring information
Core size:	8.9-cm (3 ½-in.) diameter

Table C-15
Coring Data for Exploratory Hole UE-20c

Core Run No.	Depth Interval (feet)	Recovery (feet)	Stratigraphic Unit[1]	Lithology[2]	Hydrostratigraphic Unit[3]
#1	450 - 455	3.5	Tmr	Tuff, MW	TMA
#2	650 - 655	3.0	Tmr	Tuff, DW	TMA
#3	820 - 830	0.0	Tm	Tuff, Bedded	TMA
#4	1,185 - 1,195	10.0	Tpb	Lava	TC
#5	1,350 - 1,358	6.0	Tpb	Lava	TC
#6	1,500 - 1,508	7.5	Tpb	Lava	TC
#7	1,716 - 1,724	3.0	Tpb	Lava	TC
#8	1,925 - 1,931	6.0	Tpb	Lava	TC
#9	2,125 - 2,133	6.0	Tpcm	Tuff, MW	TC
#10	2,338 - 2,348	10.0	Tpcm	Tuff, MW	TC
#11	2,550 - 2,560	10.0	Tptb	Tuff, Bedded	TC
#12	2,600 - 2,610	10.0	Tptb	Tuff, Bedded	TC
#13	2,650 - 2,676	7.5	Tptb	Tuff, Bedded	TC
#14	2,700 - 2,710	10.0	Tptm	Tuff, MW	TC
#15	2,750 - 2,760	10.0	Tptm	Tuff, MW	TC
#16	2,800 - 2,810	10.0	Tptm	Tuff, MW	TC
#17	2,850 - 2,860	10.0	Tptm	Tuff, MW	TC
#18	2,900 - 2,910	10.0	Tptm	Tuff, MW	TC
#19	2,950 - 2,960	10.0	Tptm	Tuff, MW	TC
#20	2,990 - 3,005	15.0	Tptm	Tuff, MW	TC
#21	3,100 - 3,110	10.0	Tacp	Tuff, Bedded	TC
#22	3,200 - 3,210	10.0	Tacp	Tuff, Bedded	TC
#23	3,300 - 3,310	10.0	Tacp	Tuff, Bedded	TC
#24	3,400 - 3,410	10.0	Tacp	Tuff, Bedded	TC
#25	3,503 - 3,513	10.0	Tacp	Tuff, Bedded	TC
#26	3,600 - 3,610	10.0	Tacp	Tuff, Bedded	TC
#27	3,700 - 3,710	10.0	Tacp	Lava	TC
#28	3,900 - 3,906	6.0	Tacp	Lava	TC
#29	4,105 - 4,114	1.5	Tacp	Lava	TC
#30	4,240 - 4,242	2.0	Tacp	Lava	TC
#31	4,242 - 4,247	5.0	Tacp	Lava	TC
#32	4,537 - 4,545	8.0	Tacp	Tuff, Bedded	TC
#33	4,740 - 4,748	8.0	Tacr	Tuff, Bedded	TC
#34	4,935 - 4,945	10.0	Tacr	Tuff, Bedded	TC
#35	5,151 - 5,161	10.0	Tacr	Tuff, Bedded	TC

1 Refer to Table C-22 for explanation of stratigraphic nomenclature.
2 Refer to Table C-23 for explanation of lithologic nomenclature.
3 Refer to Table 1-4 for explanation of hydrostratigraphic nomenclature.
Total core recovered: 84.7 m (278 ft).

Amount of core logged for this fracture study: All core recovered from below the static water level (72.8 m [239 ft]), minus core samples removed (~20%) for previous unrelated studies.
Static water level at 648.0 m (2,126 ft).

Table C-16
Abridged Drill Hole Statistics for Exploratory Hole U-20c

Location Data:

Coordinates:	Central Nevada State Planar:	N 903,296 ft E 556,215 ft
	Universal Transverse Mercator:	N 4,120,464.0 m E 546,704.4 m
	Ground elevation:	1,914.4 m (6,281 ft)
	Static water level:	639.2 m (2,099 ft)

Drilling Data:

Spud date:	06/26/64
Total depth:	1,463.0 m (4,800 ft)
Drilling technique(s):	A 1.8-m (72-in.) diameter emplacement hole was drilled from 3.7 to 1,463.0 m (12 - 4,800 ft) using dual string reverse circulation with air, water, and soap. Six intermittent conventional cores were center punched from 1,386.5 - 1,463.0 m (4,549 - 4,800 ft).

Coring Data:

Number of cores:	6 intermittant core runs
Total core recovered:	36.6 m (120 ft); 100% recovery
Percent of hole cored:	2.5%
Core interval(s):	1386.5 - 1,463.0 m (4,549 - 4,800 ft) See Table C-17 in Appendix C for additional coring information.
Core size:	8.9-cm (3 ½-in.) diameter

Table C-17
Coring Data for Emplacement Hole U-20c

Core Run No.	Depth Interval (feet)	Recovery (feet)	Stratigraphic Unit[1]	Lithology	Hydrostratigraphic Unit[2]
#1	4,549 - 4,572	23.0	Tacp	Zeolitized bedded tuff	TC
#2	4,591 - 4,607	16.0	Tacp	Zeolitized bedded tuff	TC
#3	4,640 - 4,661	21.0	Tacp	Zeolitized bedded tuff	TC
#4	4,690 - 4,710	20.0	Tacp	Zeolitized bedded tuff	TC
#5	4,741 - 4,761	20.0	Tacr	Zeolitized bedded tuff	TC
#6	4,780 - 4,800	20.0	Tacr	Zeolitized bedded tuff	TC

1 Refer to Table C-22 for explanation of stratigraphic nomenclature.
2 Refer to Table 1-4 for explanation of hydrostratigraphic nomenclature.

Total core recovered: 36.6 m (120 ft); 100% recovery.
Amount of core logged for this study: All core recovered (36.6 m), minus core samples removed (~10%) for previous unrelated studies.
Static water level at 639.2 m (2,097 ft).

Table C-18
Condensed Stratigraphic and Lithologic Log for Exploratory Hole UE-20c
(Page 1 of 2)

Depth		Stratigraphic Unit	Lithology	Stratigraphic Symbol	Thickness	
Meters	Feet				Meters	Feet
0.0 - 19.5	0 - 64	Trail Ridge Tuff, Thirsty Canyon Group	Partially welded ash-flow tuff, generally vitric	Ttt	19.5	64
19.5 - 48.8	64 - 160	Pahute Mesa Tuff, Thirsty Canyon Group	Partially welded ash-flow tuff, generally vitric	Ttp	29.3	96.1
48.8 - 65.8	160 - 216	Rocket Wash Tuff, Thirsty Canyon Group	Partially welded ash-flow tuff, generally vitric	Ttr	17.0	55.8
65.8 - 67.1	216 - 220	Beatty Wash Formation, Volcanics of Fortymile Canyon	Bedded tuff, vitric	Tfb	1.3	4.3
67.1 - 132.6	220 - 435	Ammonia Tanks Tuff, Timber Mountain Group	Partially welded ash-flow tuff, generally vitric	Tma	65.5	214.9
132.6 - 134.7	435 - 442	Bedded Ammonia Tanks Tuff, Timber Mountain Group	Bedded tuff, vitric	Tmab	2.1	6.9
134.7 - 246.9	442 - 810	Rainier Mesa Tuff, Timber Mountain Group	Nonwelded to densely welded ash-flow tuff, vitric to devitrified	Tmr	112.2	368.1
246.9 - 289.6	810 - 950	Timber Mountain Group, undifferentiated	Bedded tuff, vitric	Tm	42.7	140.1
289.6 - 643.1	950 - 2,110	Rhyolite of Benham, Paintbrush Group	Mostly rhyolite lava, pumiceous lava top and bottom, with thin bedded tuff at base	Tpb	353.5	1,159.8
643.1 - 749.8	2,110 - 2,460	Tiva Canyon Tuff, Paintbrush Group	Partially to densely welded ash-flow tuff, generally devitrified	Tpcm	106.7	350.1
749.8 - 768.1	2,460 - 2,520	Paintbrush Group, undifferentiated	Bedded tuff, zeolitized	Tp	18.3	60.0
768.1 - 792.5	2,520 - 2,600	Bedded Topopah Spring Tuff, Paintbrush Group	Bedded tuff, zeolitized	Tptb	24.4	80.1

Table C-18
Condensed Stratigraphic and Lithologic Log for Exploratory Hole UE-20c
(Page 2 of 2)

Depth		Stratigraphic Unit	Lithology	Stratigraphic Symbol	Thickness	
Meters	Feet				Meters	Feet
792.5 - 929.6	2,600 - 3,050	Pahute Mesa lobe, Topopah Spring Tuff, Paintbrush Group	Nonwelded to moderately welded ash-flow tuff, generally devitrified	Tptm	137.1	449.8
929.6 - 1,106.4	3,050 - 3,630	Mafic-poor, Calico Hills Formation, Volcanics of Area 20	Bedded tuff, zeolitized	Tacp	176.8	580.1
1,106.4 - 1,258.8	3,630 - 4,130	Mafic-poor, Calico Hills Formation, Volcanics of Area 20	Rhyolite lava flow	Tacp	152.4	500.0
1,258.8 - 1,261.9	4,130 - 4,140	Mafic-poor, Calico Hills Formation, Volcanics of Area 20	Bedded tuff, zeolitized	Tacp	3.1	10.2
1,261.9 - 1,368.6	4,140 - 4,490	Mafic-poor, Calico Hills Formation, Volcanics of Area 20	Rhyolite lava flow	Tacp	106.7	350.1
1,368.6 - 1,386.8	4,490 - 4,550	Mafic-poor, Calico Hills Formation, Volcanics of Area 20	Bedded tuff, zeolitized	Tacp	18.2	59.7
1,386.8 - 1,630.1 (TD)	4,550 - 5,348 (TD)	Mafic-rich, Calico Hills Formation, Volcanics of Area 20	Bedded tuff, zeolitized	Tacr	243.3	798.3

Source: Ferguson, *et al.*, 1994

Table C-19
Abridged Drill Hole Statistics for Exploratory Hole UE-20f

Location Data:

Coordinates:	Central Nevada State Planar:	N 917,825 ft E 552,007 ft
	Universal Transverse Mercator:	N 4,124,897.0 m E 545,393.3 m
	Ground elevation:	1,864.2 m (6,116 ft)
	Static water level:	595.6 m (1,954 ft) depth with hole at 1,384.7 m (4,543 ft). .537.4 m (1,763 ft) depth with hole at TD of 4,171.5 m (13,686 ft)

Drilling Data:

Spud date:	03/03/64
Total depth:	4,171.5 m (13,686 ft)
Drilling technique(s):	A 66.0-cm (26-in.) hole was rotary drilled to 9.1 m (30 ft). A 44.5-cm (17 ½-in.) hole was rotary drilled to 224.0 m (735 ft). A 31.1-cm (12 ¼-in.) hole was rotary drilled to 1,380.7 m (4,530 ft). A 22.2-cm (8 ¾-in.) hole was rotary drilled to 4,466.6 m (13,670 ft). A 15.6-cm (6 ⅛-in.) bottom hole core was obtained to total depth of 4,171.5 m (13,686 ft). This hole was drilled with air to 453.2 m (1,487 ft), then with air, soap and water from 453.2 m (1,487 ft) to TD. 50 intermittent cores were cut (typically in 8- to 10-ft runs) at various depths between 225.2 - 4,171.5 m (739 - 13,686 ft).

Coring Data:

Number of cores:	50 intermittent core runs
Total core recovered:	120.1 m (394 ft); 94.1% recovery
Percent of hole cored:	3.1%
Cored interval(s):	225.2 - 4,171.5 m (739 - 13,686 ft) See Table C-20 for additional coring information
Core size:	8.9-cm (3 ½-in.) diameter

Table C-20
Coring Data for Exploratory Hole UE-20f
(Page 1 of 2)

Core Run No.	Depth Interval (feet)	Recovery (feet)	Stratigraphic Unit[1]	Lithology[2]	Hydrostratigraphic Unit[3]
#1	739 - 747	5.0	Tmr	Tuff, MW	TMA
#2	976 - 986	8.0	Tmr	Tuff, MW	TMA
#3	1,185 - 1,195	10.0	Tmr	Tuff, MW	TMA
#4	1,400 - 1,405	5.0	Tmr	Tuff, MW	TMA
#5	1,587 - 1,597	10.0	Tmr	Tuff, NW, V	TMA
#6	1,771 - 1,781	10.0	Tmr	Tuff, NW, V	TMA
#7	1,985 - 1,995	10.0	Tmrh	Tuff, reworked, Z	TMA
#8	2,198 - 2,208	10.0	Tmrh	Tuff, reworked, Z	TMA
#9	2,413 - 2,423	10.0	Tmw	Tuff, reworked, Z	TMA
#10	2,618 - 2,628	10.0	Tpcm	Tuff, MW	TC
#11	2,838 - 2,848	10.0	Tptm	Tuff, NW, D	TC
#12	3,020 - 3,030	10.0	Tacp	Tuff, NW, Z	TC
#13	3,232 - 3,237	5.0	Tacp	Lava, D	TC
#14	3,431 - 3,441	7.0	Tacp	Lava, D	TC
#15	3,600 - 3,608	8.0	Tacr	Lava, D	TC
#16	3,647 - 3,655	8.0	Tacr	Tuff, reworked, Z	TC
#17	3,700 - 3,708	8.0	Tacr	Tuff, NW, Z	TC
#18	3,750 - 3,758	8.0	Tacr	Tuff, NW, Z	TC
#19	3,800 - 3,808	8.0	Tacr	Tuff, NW, Z	TC
#20	3,850 - 3,858	8.0	Tacr	Tuff, NW, Z	TC
#21	3,900 - 3,908	8.0	Tacr	Tuff, NW, Z	TC
#22	3,948 - 3,956	8.0	Tacr	Tuff, NW, Z	TC
#23	3,990 - 4,009	19.0	Tacr	Tuff, NW, Z	TC
#24	4,083 - 4,091	8.0	Tacr	Bedded tuff, Z	TC
#25	4,152 - 4,160	8.0	Tacr	Bedded tuff, Z	TC
#26	4,535 - 4,543	8.0	Tacr	Lava, D/gl	TC
#27	4,731 - 4,741	10.0	Tai	Flow breccia, D	TC
#28	5,066 - 5,069	3.0	Tai	Tuff, MW	TC
#29	5,287 - 5,293	6.0	Tai	Flow breccia, D	TC
#30	5,796 - 5,806	10.0	Tcpj	Tuff, bedded, Z	TC
#31	6,000 - 6,009	9.0	Tcpj	Tuff, bedded, Z	TC
#32	6,208 - 6,209	1.0	Tcblp	Tuff, NW, Z	TCB
#33	6,300 - 6,302	2.0	Tcblp	Tuff, NW, Z	TCB
#34	6,442 - 6,452	10.0	Tcblp	Tuff, NW, Z	TCB
#35	6,655 - 6,665	10.0	Tcblp	Tuff, NW, Z	TCB
#36	6,855 - 6,865	10.0	Tcblp	Tuff, NW, Z	TCB
#37	7,165 - 7,175	10.0	Tcblp	Tuff, NW, Z	TCB
#38	7,268 - 7,278	10.0	Tcblp	Tuff, NW, Z	TCB
#39	7,563 - 7,573	10.0	Tcblp	Tuff, NW, Z	TCB

Table C-20
Coring Data for Exploratory Hole UE-20f
(Page 2 of 2)

Core Run No.	Depth Interval (feet)	Recovery (feet)	Stratigraphic Unit[1]	Lithology[2]	Hydrostratigraphic Unit[3]
#40	7,731 - 7,739	8.0	Tcblp	Tuff, NW, Z	TCB
#41	7,930 - 7,940	10.0	Tcblp	Tuff, NW, Z	TCB
#42	7,975 - 7,984	9.0	Tcblp	Tuff, NW, Z	TCB
#43	8,097 - 8,107	10.0	Tcblp	Tuff, NW, Z	TCB
#44	8,380 - 8,385	5.0	Tbdl	Lava, D	TBA
#45	8,665 - 8,668	2.0	Tbdk	Flow breccia, D	TBA
#46	9,050 - 9052	1.5	Tbdk	Flow breccia, D	TBA
#47	10,195 - 10,199	4.0	Tub	Flow breccia, Z	TBA
#48	12,230 - 12,237	0.0	To	Lava, D	BAQ
#49	12,644 - 12,644.5	0.38	To	Lava, D	BAQ
#50	13,607 - 13,686	16.0	To	Tuff, MW, D	BAQ

1 Refer to Table C-22 for explanation of stratigraphic nomenclature.
2 Refer to Table C-23 for explanation of lithologic nomenclature.
3 Refer to Table 1-4 for explanation of hydrostratigraphic nomenclature.

Total core recovered: 120 m (394 ft).
Static water level at 595.6 m (1,954 ft) with TD at 1,384.7 m (4,543 ft).
Static water level at 537.4 m (1,763 ft) with TD at 4,171.5 m (13,686 ft).

Amount of core logged for this fracture study: All core recovered below 798 m (2,618 ft), approximately 95.7 m (314 ft), minus core samples removed (~20%) for previous unrelated studies.

Table C-21
Condensed Stratigraphic and Lithologic Log for Exploratory Hole UE-20f
(Page 1 of 3)

Depth		Stratigraphic Unit	Lithology	Stratigraphic Symbol	Thickness	
Meters	Feet				Meters	Feet
0.0 - 31.4	0 - 103	Trail Ridge Tuff, Thirsty Canyon Group	Partially to moderately welded ash-flow tuff, bedded interval at base	Ttt	31.4	103
31.4 - 46.9	103 - 154	Pahute Mesa Tuff, Thirsty Canyon Group	Partially to moderately welded ash-flow tuff	Ttp	15.5	51
46.9 - 100.6	154 - 330	Rocket Wash Tuff, Thirsty Canyon Group	Partially to moderately welded ash-flow tuff	Ttr	53.7	176
100.6 - 186.2	330 - 611	Ammonia Tanks Tuff, Timber Mountain Group	Nonwelded to densely welded ash-flow tuff	Tma	85.6	281
186.2 - 210.3	611 - 690	Bedded Ammonia Tanks Tuff, Timber Mountain Group	Bedded tuff, vitric	Tmab	24.1	79
210.3 - 458.1	690 - 1,503	Rainier Mesa Tuff, Timber Mountain Group	Partially to densely welded ash-flow tuff	Tmr	247.8	813
458.1 - 594.1	1,503 - 1,949	Rhyolite of Fluorspar Canyon, Timber Mountain Group	Nonwelded ash-flow tuff with bedded interval at base	Tmrf	136	446
594.1 - 730.9	1,949 - 2,398	Tuff of Holmes Road, Timber Mountain Group	Bedded tuff, zeolitized	Tmrh	136.8	449
730.9 - 752.9	2,398 - 2,470	Rhyolite of Windy Wash, Timber Mountain Group	Reworked and bedded tuff, zeolitized	Tmw	22	72
752.9 - 793.7	2,470 - 2,604	Rhyolite of Benham, Paintbrush Group	Bedded tuff	Tpb	40.8	134
793.7 - 830.0	2,604 - 2,723	Tiva Canyon Tuff, Paintbrush Group	Moderately to densely welded ash-flow tuff, devitrified	Tpcm	36.3	119
830.0 - 864.1	2,723 - 2,835	Rhyolite of Delirium Canyon, Paintbrush Group	Bedded tuff	Tpd	34.1	112
864.1 - 899.2	2,835 - 2,950	Topopah Spring Tuff, Paintbrush Group	Nonwelded ash-flow tuff, devitrified	Tptm	35.1	115
899.2 - 924.8	2,950 - 3,034	Mafic-poor, Calico Hills Formation, Volcanics of Area 20	Bedded tuff, zeolitized	Tacp	25.6	84

Table C-21
Condensed Stratigraphic and Lithologic Log for Exploratory Hole UE-20f
(Page 2 of 3)

Depth		Stratigraphic Unit	Lithology	Stratigraphic Symbol	Thickness	
Meters	Feet				Meters	Feet
924.8 - 1,066.8	3,034 - 3,500	Mafic-poor, Calico Hills Formation, Volcanics of Area 20	Lava flow, devitrified	Tacp	142	466
1,066.8 - 1,106.4	3,500 - 3,630	Mafic-rich, Calico Hills Formation, Volcanics of Area 20	Lava flow, devitrified	Tacr	39.6	130
1,106.4 - 1,116.5	3,630 - 3,663	Mafic-rich, Calico Hills Formation, Volcanics of Area 20	Reworded tuff, zeolitized	Tacr	10.1	33
1,116.5 - 1,323.8	3,663 - 4,343	Mafic-rich, Calico Hills Formation, Volcanics of Area 20	Nonwelded and bedded tuff, zeolitized, pumiceous lava at base	Tacr	207.3	680
1,323.8 - 1,450.9	4,343 - 4,760	Rhyolite of Inlet, Volcanics of Area 20	Lava flow, devitrified, with flow breccia at base	Tai	127.1	417
1,450.9 - 1,585.0	4,760 - 5,200	Rhyolite of Inlet, Volcanics of Area 20	Moderately welded ash-flow tuff	Tai	134.1	440
1,585.0 - 1,644.4	5,200 - 5,395	Rhyolite of Inlet, Volcanics of Area 20	Lava flow, devitrified, with minor flow breccias	Tai	59.4	195
1,644.4 - 1,704.8	5,395 - 5,593	Rhyolite of Inlet, Volcanics of Area 20	Nonwelded to partially welded ash-flow tuff, zeolitized	Tai	60.4	198
1,704.8 - 1,709.9	5,593 - 5,610	Basalt of Fontina, Volcanics of Area 20	Basalt lava flow	Taf	5.1	17
1,709.9 - 1,859.3	5,610 - 6,100	Tuff of Jorum, Crater Flat Group	Bedded tuff, zeolitized	Tcpj	149.4	490
1,859.3 - 2,521.6	6,100 - 8,273	Mafic-poor, lithic-rich, Bullfrog Tuff, Crater Flat Group	Nonwelded ash-flow tuff, zeolitized	Tcblp	662.3	2173
2,521.6 - 2,636.2	8,273 - 8,649	Comendite of Lambs Canyon, Belted Range Group	Lava flow, devitrified, with flow breccia at base	Tbdl	114.6	376
2,636.2 - 2,974.2	8,649 - 9,758	Comendite of Kaw Station, Belted Range Group	Flow breccia and lava flow, devitrified	Tbdk	338	1109

Table C-21
Condensed Stratigraphic and Lithologic Log for Exploratory Hole UE-20f
(Page 3 of 3)

Depth		Stratigraphic Unit	Lithology	Stratigraphic Symbol	Thickness	
Meters	Feet				Meters	Feet
2,974.2 - 3,011.1	9,758 - 9,879	Bedded Grouse Canyon Tuff, Belted Range Group	Nonwelded tuff, zeolitized	Tbgb	36.9	121
3,011.1 - 3,118.1	9,879 - 10,230	Tub Spring Tuff, Volcanics of Big Dome	Flow breccia, zeolitized	Tub	107	351
3,118.1 - 3,378.7	10,230 - 11,085	Tub Spring Tuff, Volcanics of Big Dome	Nonwelded to densely welded ash-flow tuff	Tub	260.6	855
3,378.7 - 3,542.1	11,085 - 11,621	Redrock Valley Tuff, Volcanics of Oak Spring Butte	Moderately welded ash-flow tuff, zeolitized	Tor	163.4	536
3,542.1 - 3,610.7	11,621 - 11,846	Tuff of Twin Peaks, Volcanics of Oak Spring Butte	Moderately welded ash-flow tuff	Tot	68.6	225
3,610.7 - 3,671.3	11,846 - 12,045	Tuff of Burnt Mountain, Volcanics of Oak Spring Butte	Nonwelded and/or bedded tuff, zeolitized	Tom	60.6	199
3,671.3 - 3,879.2	12,045 - 12,727	Volcanics of Oak Spring Butte, undifferentiated	Lava flow	To	207.9	682
3,879.2 - 3,953.3	12,727 - 12,970	Volcanics of Oak Spring Butte, undifferentiated	Nonwelded tuff	To	74.1	243
3,953.3 - 4,086.2	12,970 - 13,406	Volcanics of Oak Spring Butte, undifferentiated	Lava flow	To	132.9	436
4,086.2 - 4,171.5 (TD)	13,406 - 13,686 (TD)	Volcanics of Oak Spring Butte, undifferentiated	Moderately welded ash-flow tuff	To	85.3	280

Source: Ferguson, *et al.*, 1994

Table C-22
Stratigraphic Nomenclature Used In This Report (listed stratigraphically)
(Page 1 of 2)

QTa	Alluvium, undivided

Thirsty Canyon Group (Tt)

Tt	Thirsty Canyon Group, undivided
Ttt	Trail Ridge Tuff
Ttp	Pahute Mesa Tuff
Ttp	crystal-rich Pahute Mesa Tuff
Ttpp	crystal-poor Pahute Mesa Tuff
Ttr	Rocket Wash Tuff

Volcanics of Fortymile Canyon (Tf)

Tf	Volcanics of Fortymile Canyon, undivided
Tfb	Beatty Wash Formation
Tfbr	rhyolite of Chukar Canyon
Tfbw	rhyolite of Beatty Wash

Timber Mountain Group (Tm)

Tmac	tuff of Crooked Canyon
Tma	Ammonia Tanks Tuff
Tmar	mafic-rich Ammonia Tanks Tuff
Tmap	mafic-poor Ammonia Tanks Tuff
Tmab	bedded Ammonia Tanks Tuff
Tmr	Rainier Mesa Tuff
Tmrb	bedded Rainier Mesa Tuff
Tmrx	landslide or eruptive breccia
Tmrr	mafic-rich Rainier Mesa Tuff
Tmrp	mafic-poor Rainier Mesa Tuff
Tmra	andesite tephra
Tmrf	rhyolite of Fluorspar Canyon
Tmrh	tuff of Holmes Road
Tmw	rhyolite of Windy Wash

Paintbrush Group (Tp)

Tp	Paintbrush Group, undivided
Tpb	rhyolite of Benham
Tps	rhyolite of Scrugham Peak
Tpc	Tiva Canyon Tuff
Tpcm	Tiva Canyon Tuff, Pahute Mesa lobe
Tpd	rhyolite of Delirium Canyon
Tpe	rhyolite of Echo Peak
Tpr	rhyolite of Silent Canyon
Tpt	Topopah Spring Tuff
Tptm	Topopah Spring Tuff, Pahute Mesa lobe
Tptb	bedded Topopah Spring Tuff

Table C-22
Stratigraphic Nomenclature Used In This Report (listed stratigraphically)
(Page 2 of 2)

Volcanics of Area 20 (Ta)

Tacp	mafic-poor Calico Hills Formation
Tacr	mafic-rich Calico Hills Formation
Tap	tuff of Pool
Tai	rhyolite of Inlet
Taf	basalt of Fontina

Crater Flat Group (Tc)

Tcpj	tuff of Jorum
Tcps	rhyolite of Sled
Tcpk	rhyolite of Kearsarge
Tcb	Bullfrog Tuff
Tcblr	mafic-rich, lithic-rich Bullfrog Tuff
Tcblp	mafic-poor, lithic-rich Bullfrog Tuff
Tct	Tram Tuff

Belted Range Group (Tb)

Tbd	Dead Horse Flat Formation, undivided
Tbdl	comendite of Lambs Canyon
Tbdk	comendite of Kaw Station
Tbds	comendite of Saucer Mesa
Tbg	Grouse Canyon Tuff
Tbgb	bedded Grouse Canyon Tuff

Tram Ridge Group (Tr)

Tr	Tram Ridge Group, undivided

Tunnel Formation (Tn)

Tn4	Tunnel 4 Member
Tn4JK	Tunnel 4 Member, beds 4J and 4K

Volcanics of Big Dome (Tu)

Tuq	comendite of Quartet Dome
Tub	Tub Spring Tuff

Volcanics of Oak Spring Butte (To)

To	Volcanics of Oak Spring Butte, undivided
Tor	Redrock Valley Tuff
Tot	tuff of Twin Peaks
Tom	tuff of Burnt Mountain

Volcanics of Quartz Mountain

Tq	Volcanics of Quartz Mountain, undivided
Tqm	Dacite of Mt. Helen

Table C-23
Lithologic and Alteration Nomenclature
Used In This Report

Symbol	Lithology
AL	Alluvium
B	Bedded tuff
RWT	Reworked tuff
NW	Nonwelded tuff
PW	Partially welded tuff
MW	Moderately welded tuff
DW	Densely welded tuff
V	Vitrophyre
L	Lava
PL	Pumiceous lava
FB	Flow breccia
TB	Tuff breccia
Symbol	**Alteration**
A	Argillized
Z	Zeolitized
V or gl	Vitric (glassy)
D or dv	Devitrified
VP	Vapor-phase mineralization

This page intentionally left blank.

Distribution List

	Copies
DOE Office of Scientific and Technical Information, Oak Ridge, TN	2
DOE/NV Technical Information Resource Center, Las Vegas, NV	1
DOE/NV Public Reading Room, Las Vegas, NV	1
R. M. Bangerter, DOE/ERD. Las Vegas, NV	1
D. W. Duncan, DOE/ERD, Las Vegas, NV	1
R. Andricevic, DRI, Las Vegas, NV	1
C. E. Russell, DRI, Las Vegas, NV	1
C. Shirley, DRI, Las Vegas, NV	1
P. D. Rowley, USGS, Las Vegas, NV	1
J. E. Magner, USGS Geologic Data Center, Mercury, NV	1
D. A. Trudeau, USGS/WRD, Las Vegas, NV	1
A. B. Kersting, LLNL, Livermore, CA	1
G. A. Pawloski, LLNL, Livermore, CA	1
D. K. Smith, LLNL, Livermore, CA	1
A. Tompson, LLNL, Livermore, CA	1
D. L. Finnegen, LANL, Los Alamos, NM	1
W. L. Hawkins, LANL, Los Alamos, NM	1
M. A. McGraw, LANL, Los Alamos, NM	1
P. W. Reimus, LANL, Los Alamos, NM	1
R. G. Warren, LANL, Los Alamos, NM	1
A. V. Wolfsberg, LANL, Los Alamos, NM	1
Library, IT Corp., Las Vegas, NV	1
E. H. Price, HSI GeoTrans, Las Vegas, NV	1
K. R. Rehfeldt, HSI GeoTrans, Las Vegas, NV	1
R. K. Waddell, HSI GeoTrans, West Minster, CO	1
B. M. Allen, BN, Mercury, NV	1
H. S. Bensinger, BN, Las Vegas, NV	1
S. L. Drellack, BN, Las Vegas, NV	1
J. L. Gonzales, BN, Las Vegas, NV	1
P. K. Ortego, BN, Las Vegas, NV	1
L. B. Prothro, BN, Mercury, NV	1
M. J. Townsend, BN, Mercury, NV	1